R-9557

FINAL REPORT

A STUDY OF THE DURABILITY OF BERYLLIUM ROCKET ENGINES

PREPARED FOR

NATIONAL AERONAUTICS AND SPACE ADMINISTRATION
LYNDON B. JOHNSON SPACE CENTER

CONTRACT NAS9-13476

OCTOBER 1974

ROCKETDYNE DIVISION
ROCKWELL INTERNATIONAL
6633 CANOGA AVENUE
CANOGA PARK, CALIFORNIA 91304

R-9557

FINAL REPORT

A STUDY OF THE DURABILITY OF BERYLLIUM ROCKET ENGINES

PREPARED BY

R. D. Paster
G. C. French

PREPARED FOR

National Aeronautics and Space Administration
Lyndon B. Johnson Space Center
Houston, Texas

N. Chaffee, Technical Monitor

Contract NAS9-13476

October 1974

Rocketdyne Division
Rockwell International
6633 Canoga Avenue
Canoga Park, California 91304

FOREWORD

This final report presents the results of a 1-year program (June 1973-June 1974) entitled "A Study of the Durability of Beryllium Rocket Engines". The contract (NAS9-13476) was conducted by Rocketdyne Division, Rockwell International, and was administered by the Lyndon B. Johnson Space Center of the National Aeronautics and Space Administration. The NASA Technical Monitor was Mr. N. Chaffee of the Auxiliary Propulsion and Pyrotechnics Branch. The Rocketdyne Program Manager was Mr. R. W. Helsel and Project Engineer was Mr. R. D. Paster.

ABSTRACT

An experimental test program was performed to demonstrate the durability of a beryllium INTEREGEN rocket engine when operating under conditions simulating the Space Shuttle reaction control system. A Vibration Simulator was exposed to the equivalent of 100 missions of X, Y, and Z axes random vibration to demonstrate the integrity of the recently developed injector to chamber braze joint. An Off-Limits engine was hot fired under extreme conditions of mixture ratio, chamber pressure, and orifice plugging. A Durability Engine was exposed to six environmental cycles interspersed with hot fire tests.

Results from this program indicate the ability of the beryllium INTEREGEN engine concept to meet the operational requirements of the Space Shuttle reaction control system.

ACKNOWLEDGEMENTS

The Project Engineer gratefully acknowledges the valuable contributions to the program of the following people: Mr. G. C. French for direction of the development test program and thermal analysis; Mr. R. K. Kiningham for engine design; Mr. B. D. Goracke for performance analysis; Mr. N. E. Bergstresser for structural/life analysis; Mr. J. M. Haworth for vibration test coordination and analysis; the Rocketdyne Santa Susana Test personnel, particularly Mr. A. M. Norman, Jr. for their support of the hot fire test program; and the Approved Engineering Test Laboratory test personnel for their support of the environmental test program.

CONTENTS

ILLUSTRATIONS

TABLES

INTRODUCTION

The broad and aggressive spectrum of activities which has been proposed by NASA for the decade of the 70's and beyond has created the need for a family of propulsion systems and components of increased capability. The currently on-going programs, including the Space Shuttle and planetary probes, as well as potential future programs including Space Tug, Space Station, reusable satellites, deep space probes, and Mars exploration, without exception, will require reaction control system (RCS) engines where durability requirements exceed that of any engine developed to date. Typical requirements may include very long service life: 10 years or more; very high cycle life: perhaps half a million cycles in the operational lifetime; multiple reuse capability with or without refurbishment, such as in Space Shuttle; reusable satellites or replaceable Space Station propulsion modules; capability of undergoing multiple launch and re-entry cycles and surviving the range of environments associated with this, such as in the Space Shuttle.

A great deal of effort in the past several years has been devoted to the development and demonstration of beryllium rocket engines and the technology associated with the thermal and structural design is well known. Applications have included missile post-boost control systems, Mariner Mars 71, and Viking Orbiter '75. The beryllium engine concept employed on these programs and further development at Rocketdyne on Independent Research and Development Programs, have indicated the potential to meet the reusable, long life requirements of future vehicles.

The unique properties of beryllium were first employed in 1964 to demonstrate the feasibility of a new rocket engine design concept. This concept used the low-density, high thermal conductivity, strength at elevated temperature, and chemical inertness of beryllium to implement an entirely new approach to rocket engine cooling. This process is known as INTEREGEN (INTErnal REGENerative) cooling, and is covered by U.S. Patent 3,439,503. As shown in Fig. 1, INTEREGEN cooling causes the heat input to the throat and combustion zone areas to flow through the highly conductive beryllium combustion chamber walls to an internally (fuel) cooled boundary layer region near the injector. Both the sensible and latent heat of vaporization of the fuel are used to INTEREGEN cool the thrust chamber. Thermal equilibrium is possible over a wide range of operating conditions. A unique feature of INTEREGEN cooling is its three-dimensional heat-dissipation characteristic provided by the beryllium mass and its high resistance to erosive or burn-through failures. INTEREGEN cooling combined with the high conductivity of the beryllium quickly dissipates the thermal energy from local high-heat-flux areas. The impact of plugging injector orifices is minimized.

Engine operating temperatures can be controlled at appropriate levels to meet the duty cycle and mission requirements of the particular application. This is done by adjusting the fuel coolant flow into the boundary layer and by specifying the combustion chamber and beryllium wall geometry. INTEREGEN cooled beryllium thrust chambers operate at relatively low temperatures (< 1000 F).

The design concept, characterized by high thermal and structural margins of safety, has been verified by 9 years of testing a variety of beryllium engines which were subjected to more than 300,000 seconds of hot fire.

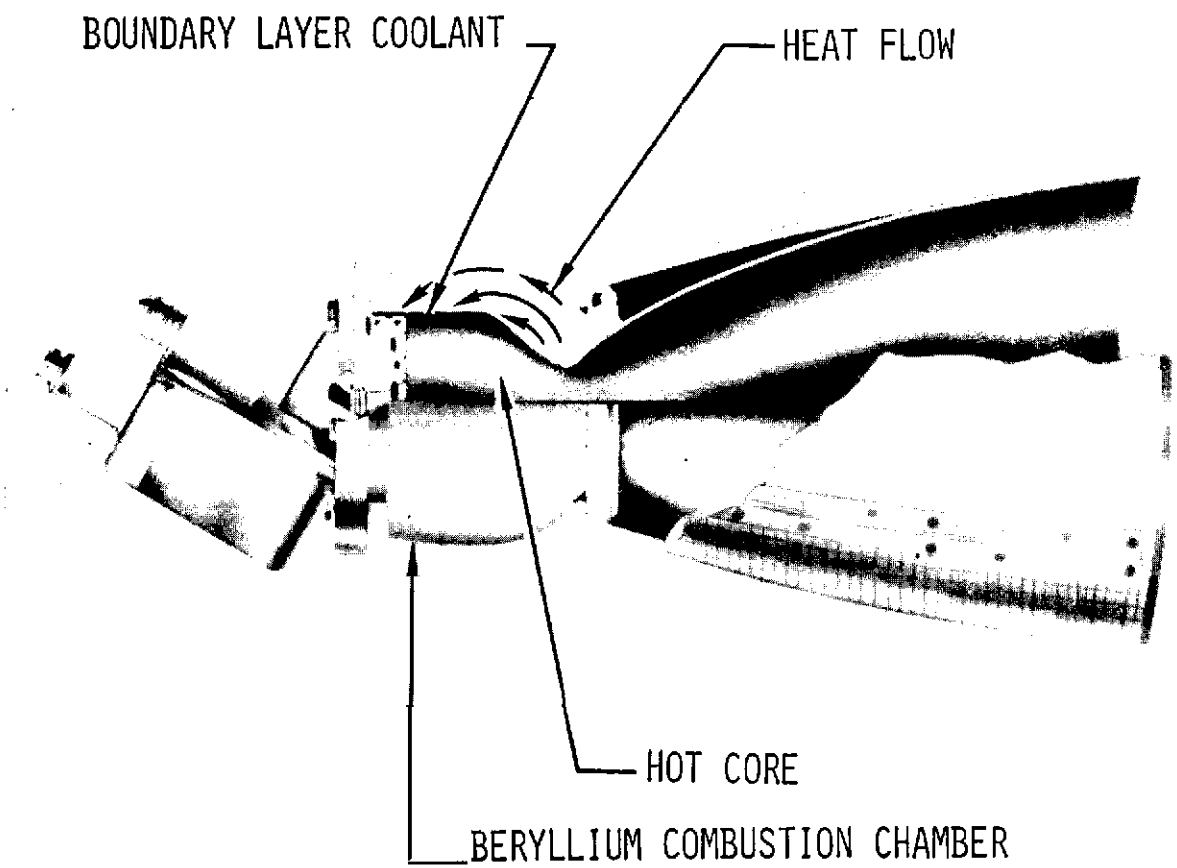

Figure 1. INTEREGEN Cooling

The objective of this program was to evaluate the potential applicability of beryllium rocket engines to reaction control systems of vehicles requiring long service life, and for multiple reuse cycles including repetitive launch-re-entry cycles. The engine design had features not previously used (i.e., brazed injector/chamber joint, insulated columbium nozzle extension) in order to achieve maximum durability and reuse capability with minimum servicing and maintenance. An objective of this program was to evaluate these new design features. The four-phase program demonstrated beryllium engine capabilities through a program of analysis, design, fabrication, and test.

Phase I was directed toward establishing the engine assembly configuration and operating characteristics through design and analysis. Fabrication of a flight engine assembly and a vibration simulator was accomplished under Phase II. Testing in Phase III was accomplished in three areas: (1) a Durability Engine was exposed to alternating sequences of simulated duty cycles and environmental tests, (2) an Off-Limits Engine was hot fired over a wide range of inlet pressures and with multiple orifice plugging, and (3) a Vibration Simulator was exposed to a 100 mission random vibration environment. Test data analysis was performed under Phase IV and the flight design was updated based on test results. The Durability Engine was delivered to NASA-JSC at the completion of the program.

SUMMARY

A 600-pound thrust (vacuum) Durability Engine, an Off-Limits Engine, and a Vibration Simulator (Fig. 2) were rigorously evaluated by hot-fire and environmental testing. The test program was conducted to establish the baseline performance and thermal characteristics of the beryllium engine, thoroughly investigate hot-fire and environmental cycle endurance capability, verify ability of beryllium engine to withstand off-limit operational conditions, and expose the brazed configuration by way of a simulated engine to vibration durations equal to 100 simulated Space Shuttle missions.

DURABILITY ENGINE

The purpose of the Durability Engine test program was to demonstrate the multiple reuse capability of a beryllium engine without cleaning, service, or maintenance. Five sequential exposures to hot-fire and environmental tests were planned, but because of valve problems, modifications to the test sequence was required. The test program consisted of exposing a flight configuration 600-pound thrust engine to five hot-fire series at simulated altitude, and six environmental test series. The first three environmental test series consisted of sequential exposure to simulated rain, humidity, salt atmosphere, sand/dust, and vibration with hot-fire between each set. The fourth, fifth and sixth environmental test series consisted of sequential exposure to simulated rain, sand/dust, and vibration with the valve pressurized with 300 psig GN_2 during vibration. GN_2 purges were carried out between the fourth, fifth and sixth environmental test series to simulate engine firing effects. A hot-fire test followed the completion of the sixth environmental test series.

The engine demonstrated 290 and 294.4 lb_f-sec/lb_m steady-state specific impulse with saturated and unsaturated propellants, respectively, at the nominal design point with a nonoptimum nozzle contour (1.4 second performance penalty). The pulse specific impulse goal of 220 lb_f-sec/lb_m with saturated propellants was demonstrated for a minimum impulse bit of 30 lb_f-sec at a pulse frequency of 5 cycles/second. An engine start transient of 0.040 seconds (on-signal to 90 percent) was demonstrated with the MOOG Inc. bipropellant valve and with a maximum pressure overshoot of 20 percent. A shutdown transient of 0.020 second (off-signal to 10 percent chamber pressure) was attained. At nominal operating conditions with a 30 psid valve and allowing a 10 psid calibration orifice, the inlet pressure is 290 psia which meets the design requirement.

The maximum single burn requirement of 600 seconds for the Durability Engine was demonstrated with steady-state performance and thermal equilibrium conditions achieved. During the pulse mission duty cycle over which 1/3 to 5 Hz frequency was demonstrated with pulse widths of 0.050 to 1.0 second operation, lower than steady-state mean operating temperatures were obtained. Cold and hot first pulse operation was demonstrated with negligible effects on performance experienced. Durability Engine thermal equilibrium was demonstrated with and without a nozzle extension insulation blanket, with and without helium saturated propellant, including tests in which four film coolant holes were plugged.

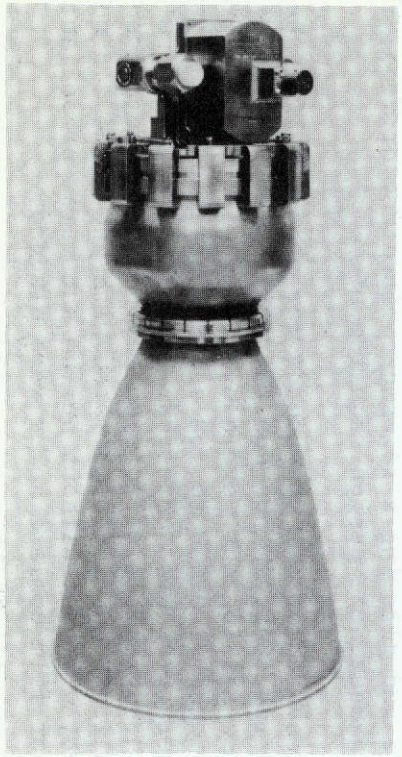

OFF-LIMITS ENGINE

- 694 STARTS - 6033 SEC
- 66-235 PC
- 1.3 - 3.0 MR
- PLUGGED ORIFICES

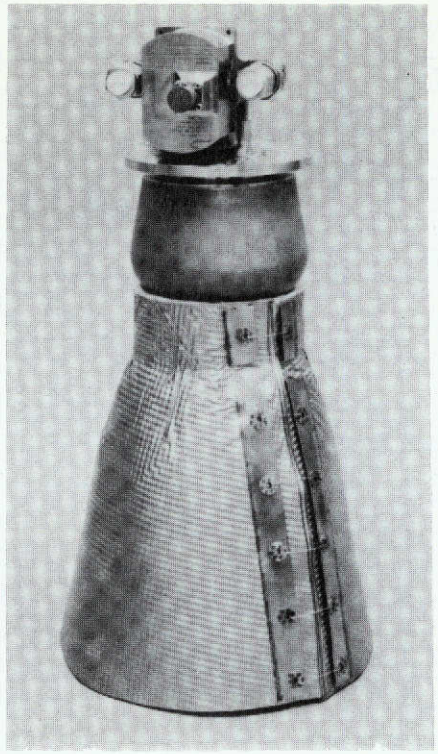

DURABILITY ENGINE

- 500 STARTS - 1451 SEC
- 6 ENVIRONMENTAL CYCLES

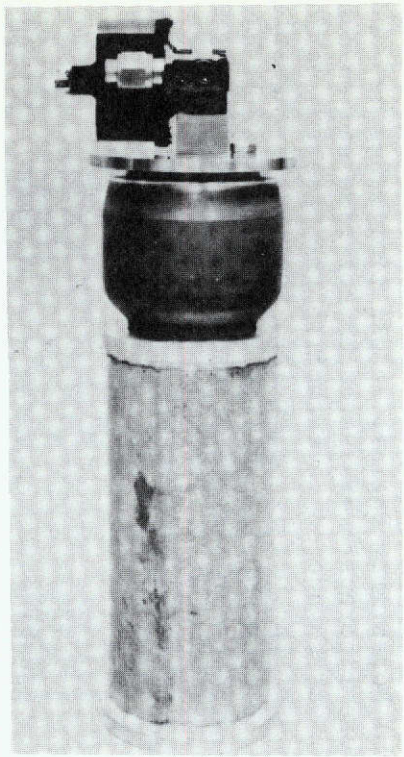

VIBRATION SIMULATOR

- 100 MISSION 3 AXIS RANDOM VIBRATION

Figure 2. SS/RCE Technology Program Engines

For the baseline performance test, thermal equilibrium was reached in 200 seconds of on time. A maximum temperature of 500 F was recorded at the throat OD. The measured peak nozzle temperature was 2000 F. The recorded beryllium temperatures were relatively unchanged by insulation of the nozzle. However, the peak nozzle temperature was increased by approximately 150 F when thermally insulated. Nozzle insulation OD peak temperature exceeded the 800 F requirement by 75 F, but this can be corrected easily by emissivity control of the outer shell or minor thickening of the insulation. The maximum valve temperature was 200 F after 30 minutes of thermal soak which presents no problem to valve integrity or restart performance.

Up to four film coolant holes were plugged in the injector during exposure to environmental conditioning. The plugging was detectable during subsequent hot-fire tests in measured beryllium temperatures since the average value was 600 F and a peak of 835 F was recorded downstream of the plugged region. The plugged coolant orifices caused only slight oxidation of the throat ID. The beryllium combustor maximum head end temperature was increased by approximately 20 F and measured nozzle temperatures were unchanged.

Posttest thermal analyses have been made of the engine and indicate that the beryllium chamber can be reduced in weight by approximately one-half pound while maintaining INTEREGEN operation. Additional weight savings can be gained by going from the present 6:1 contraction ratio to 4:1. The injector alone could be reduced by 3.8 lb_m.

The six environmental cycles of testing had no adverse effect on the engine other than slight superficial staining and pitting of the beryllium chamber. However, detrimental effects were sustained by the MOOG Inc. bipropellant torquemotor valve because of sand/dust and vibration. Severe damage was sustained by the valve seats during environmental testing from migration of sand/dust particles between the poppet and seat during vibration sequence even under specification lockup inlet pressures. The valve, which was designed to meet an inlet pressure of 300 psia, also exhibited problems opening at higher inlet pressures for certain tests.

The engine successfully completed the sinusoidal vibration testing with no evidence of detrimental effects. During random vibration testing, strain gage data indicated that low-frequency resonant modes were present in the 150 to 250 Hz frequency range. Strain values recorded in the braze transition joint between the injector and chamber were on the order of one-half that allowed in the design. Therefore, the design is capable of withstanding inertial loads greater than twice those experienced in test. Analyses have shown that the Durability Engine design exceed Space Shuttle life requirements. The success of the test program has corroborated these predictions on life.

The combustion stability characteristics of the Durability Engine injector were evaluated under a company-sponsored program. The average overpressure ranged from 574 to 882 psia. The rise rates were all greater than 1 psi/msec and average damp times were 12 msec or less. All data indicate that the tests were valid indication of the dynamic stability characteristics of the engine.

OFF LIMITS ENGINE

The purpose of the Off-Limits Engine test program was to demonstrate the ability of a beryllium INTEREGEN engine to operate over a wide range of propellant inlet pressures and with multiple orifice plugging. The Off-Limits Engine demonstrated very broad off-limits operation capability (1.43 through 2.88 o/f mixture ratio and 66 through 230 psia chamber pressure) without sustaining damage. However, during the worst case (simulated dual oxidizer regulator failure - 2.88 o/f mixture ratio with 238 psia chamber pressure) operation, high temperatures in the Haynes 25 nozzle extension caused a failure of the material. This test was repeated successfully with this same engine with a columbium nozzle extension on a company-sponsored program. The Off-Limits Engine was tested to steady-state conditions with one plugged primary fuel hole and with one and three adjacent plugged coolant holes. The engine throat OD temperatures reached predictable values which demonstrated the feasibility of reliable engine shutdown devices to allow for subsequent engine operation. The plugged coolant orifice caused only slight oxidation of the throat ID downstream of the plugging.

VIBRATION SIMULATOR

The purpose of the Vibration Simulator test program was to demonstrate the structural integrity of the chamber/injector joint by exposing a flight configuration joint to random vibration equivalent to 100 Space Shuttle missions. The measured peak strain amplitude was less than one-half the design value. Therefore, the injector/chamber braze joint can withstand inertial loads greater than twice those experienced in test. Posttest proof pressure at 500 psig and leak tests at 200 psig verified the structural integrity of the simulator and demonstrated the high reliability of the beryllium braze joint.

SUMMARY OF RESULTS

Posttest examination of all thrust chamber assembly hardware indicated it to be in excellent condition. High cycle life was demonstrated by the attainment of low beryllium chamber operating temperatures and thermal gradients. The low operating temperatures at nominal conditions provide large thermal margin which allows for operation over a wide range of inlet conditions.

The results from this program indicate the ability of the beryllium INTEREGEN engine concept to meet the operational requirements of the Space Shuttle reaction control system.

ENGINE REQUIREMENTS

The beryllium rocket engine for this program is a pressure-fed, pulse-modulated, hypergolic, bipropellant engine designed to meet the design requirements listed in Table 1 and performance goals listed in Table 2. The engine must be capable of long life and multiple reuse when sequentially exposed to launch pad and launch environment, vacuum and high altitude operation in any attitude, and landing area environment, with minimum maintenance for 100 missions. Within the constraints of the per-mission requirements of 1000 seconds total firing time, 600 seconds maximum single burn, 30 lb-sec minimum impulse bit, 5 pulses per second maximum frequency and 2000 pulses per mission, the engine should be capable of performing any combinations of burns without excessive soakback to the injector/valve assembly which could cause valve damage or propellant vaporization. The engine must be capable of safe operation over a wide range of chamber pressures and mixture ratios and with injection orifice partial or total blockage causing oxidizer spray on the wall or localized film coolant interruption.

The nominal design point is 600 pounds thrust, 200 psi chamber pressure, NTO/MMH propellants at a 1.63 o/f mixture ratio, and 40:1 nozzle extension. However, the engine concept should be scalable over a 100 to 1100 lbm thrust range and the nozzle should be capable of scarfing to fit a vehicle mold line when installed in a buried mode. The engine was designed to provide maximum performance consistent with life and thermal margin requirements.

TABLE 1. DESIGN REQUIREMENTS

Thrust, Vacuum, pounds	600
Steady-State Chamber Pressure (P_c), psia	200
Engine Steady-State Mixture Ratio, (o/f)	1.63
Exhaust Nozzle Area Ratio, (ε)	40:1
Propellants	
Oxidizer	N_2O_4 (MIL-P-26539C MON-1)
Fuel	MMH (MIL-P-27404)
Pressurant	Helium (MIL-P-27407)
Propellant Feed Conditions	
Static Pressure	300 $\pm$6 psia
Dynamic Pressure	290 $\pm$10 psia
Temperature	75 $\pm$35 F
Valve Voltage	28 $\pm$4 VDC
Installation	
Within a Vehicle Mold Line	
Maximum Outer Surface Temperature	
Engine Assembly (Environment 300 F), F	800
Engine Weight and Envelope	Minimized
Minimum Impulse Bit (Nominal Conditions), lb_f-sec	30 $\pm$10
Maximum Pulse Frequency, cps	5
Maximum Single Firing, seconds	600
Maximum Firing Time per Mission, seconds	1000
Maximum Number Pulses per Mission (Including 75 Full Thermal Cycles)	2000
Engine Life	
Missions	100
Years	10
Burn, seconds	100,000
Pulses (Including 7500 Full Thermal Cycles)	200,000
Stability	
Chamber Pressure (Nominal Steady-State), percent	$\pm$5
Chamber Pressure (Periodic or Cyclic 2000 hz), percent	$\pm$8

TABLE 1. DESIGN REQUIREMENTS (Continued)

High Frequency	Dynamically Stable, Recover in .020 sec
Thrust Vector Alignment, degree	0.5
Plume Contamination	Minimize
Thermal Soakback, any duty cycle	No Detriment to Valve, Injector, Life Performance Goals or Cause Vaporization in Valve
Engine Environment	
General	Withstand Multiple Launch, Space, Entry and Landing, Ground Handling/Service, 168 Hours/Mission
Temperature, F	
Active Portions	-20 to +200
Non-Operating, 30 Minutes	300
Launch and Entry, 5 Minutes	2000 @ Nozzle, 1500 @ Throat
Pressure	S/L to 10^{-13} Torr
Acceleration, g's (One Minute Each Axis, Twice per Mission)	3.5
Vibration, Random (One Minute Each Axis)*	20-90 hz Constant @ $0.1g^2$/hz
	90-180 hz +12 db/octave
	180-350 hz Constant @ $1.6g^2$ hz
	350-2000 hz -6 db/octave
Vibration, Random (70 seconds Each Axis) Revised 1-14-74	20-100 hz +9 db/octave
	100-300 hz Constant @ $0.70g^2$/hz
	300-2000 hz -3 db/octave
Vibration, Sinusoidal (One Minute Each Axis)	5-23 hz @ 1.0g
	23-40 hz @ 0.036 inch double amp
One Mission (One Octave/Minute, Total Sweep 6 Minutes)	5 hz to 40 hz to 5 hz
	Dwell @ Resonance for 30 sec

* Performed on vibration simulator - X-axis only

TABLE 1. DESIGN REQUIREMENTS (Concluded)

Rain (Per Mission)	0.5 In/Hr for One-Half Hour
Sand and Dust (Per Mission)	140 Mesh Silica Velocity 500 ft/min for 4 hours
Salt (Per Mission), One Percent (Revised 1-14-74)	Coastal Area @ 75± 20 F for 30 Days
Humidity (Per Mission)	0-100 Percent for 30 Days
Internal or External Leakage	None

TABLE 2. PERFORMANCE GOALS

Specific Impulse (Nominal Condition $\geq$ 1 second), lb_f-sec/lb_m	295
Pulsing Specific Impulse (MIB Nominal Conditions), lb_f-sec/lb_m	220
Specific Impulse Shift (Nominal Range Conditions)	Minimized
Mixture Ratio Shift (Nominal Range Conditions)	Minimized
Engine Start Transient (Signal "ON" to 90 Percent P_c), second	< 0.050
Engine Shutdown Transient (Signal "OFF" to 10 Percent P_c), second	< 0.050
Off-Limits Operating Capability	
Engine design capable of broad off-limits operation without sustaining damage. This includes feed pressure ranges (both common to each propellant and mismatched), feed temperature ranges, valve voltage ranges, valve opening and closing mismatch, operation with gas bubbles, blockage of injector orifices.	

PHASE I - ENGINE ANALYSIS AND DESIGN

The principal components of the beryllium INTEREGEN engine are: (1) a single stage bipropellant valve, (2) a high-performance, multielement, unlike doublet injector, (3) an INTEREGEN cooled beryllium thrust chamber, (4) a thin-wall nozzle extension, and (5) an insulation blanket. Figures 3, 4, and 5 provide assembly drawings for the flightweight brazed configuration (Durability Engine) used for durability tests, the bolted configuration (Off Limits Engine) used for off limits tests, and the Vibration Simulator used to demonstrate braze joint structural integrity. A detail discussion of the designs selected and analyses performed during this phase of the program are provided in this section.

DURABILITY ENGINE DESIGN

All components and assembly hardware on the Durability Engine (Fig. 3) are flightweight with the exception of the back side of the injector which was designed to mate with an existing MOOG valve and hot-fire test facility. Additional injector mass could be removed in a production operation through contour machining of excess material.

Thrust Chamber Design

The thrust chamber for the Durability Engine is composed of a combustion chamber (Fig. 6) fabricated of aerospace grade, hot pressed and sintered beryllium, a nozzle extension (Fig. 7) fabricated of WC103 columbium, diffusion coated with the Vac Hyd silicide coating VH-101, and an insulation blanket (Fig. 8). The nozzle is attached at an expansion ratio of 3:1. The beryllium is procured to a Rocketdyne specification tailored to rocket thruster requirements (STD170-RB01444). Fabrication methods for the engine follow state-of-the-art conventional techniques.

The chamber is cylindrical, has a 16.0-inch characteristic length, a 6:1 contraction ratio, and is contoured to optimize the INTEREGEN coolant film effectiveness.

The design of the beryllium thrust chamber was determined by the use of the INTEREGEN thermal analysis program. The model is used to optimize the heat transfer conductive path from the throat region and overturning region to the head end of the chamber. The basic design approach is one of selecting a particular shape and then determining temperatures as a function of time. The final shape selected evolved from the "conventional" cylindrical beryllium chamber.

Design improvements were made relative to previously tested INTEREGEN thrusters, i.e., Minuteman III PBPS, Mars Mariner '71, Viking Orbiter '75, RM1000; the chamber throat section and combustion section contours were modified to minimize thermal load and thereby minimize thermal stresses, and enhance the endurance limit and provide longer life. The throat section was modified to reduce the heat input by a reduction in exposure area. This was accomplished by reducing the curvature radii and increasing the expansion angle (42 degrees). These changes result in a 20- to 30-percent reduction in heat transfer.

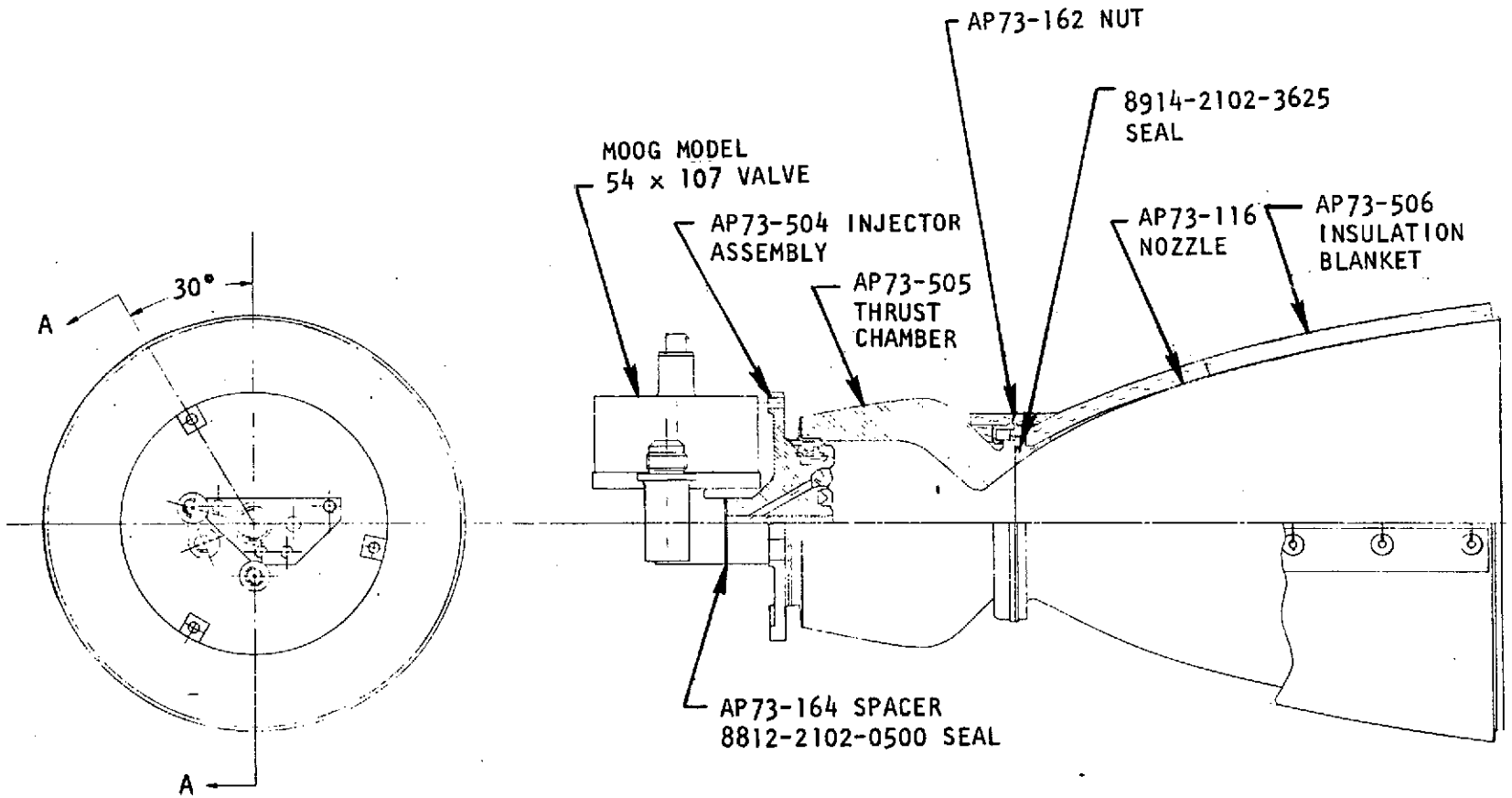

Figure 3. Durability Engine Assembly

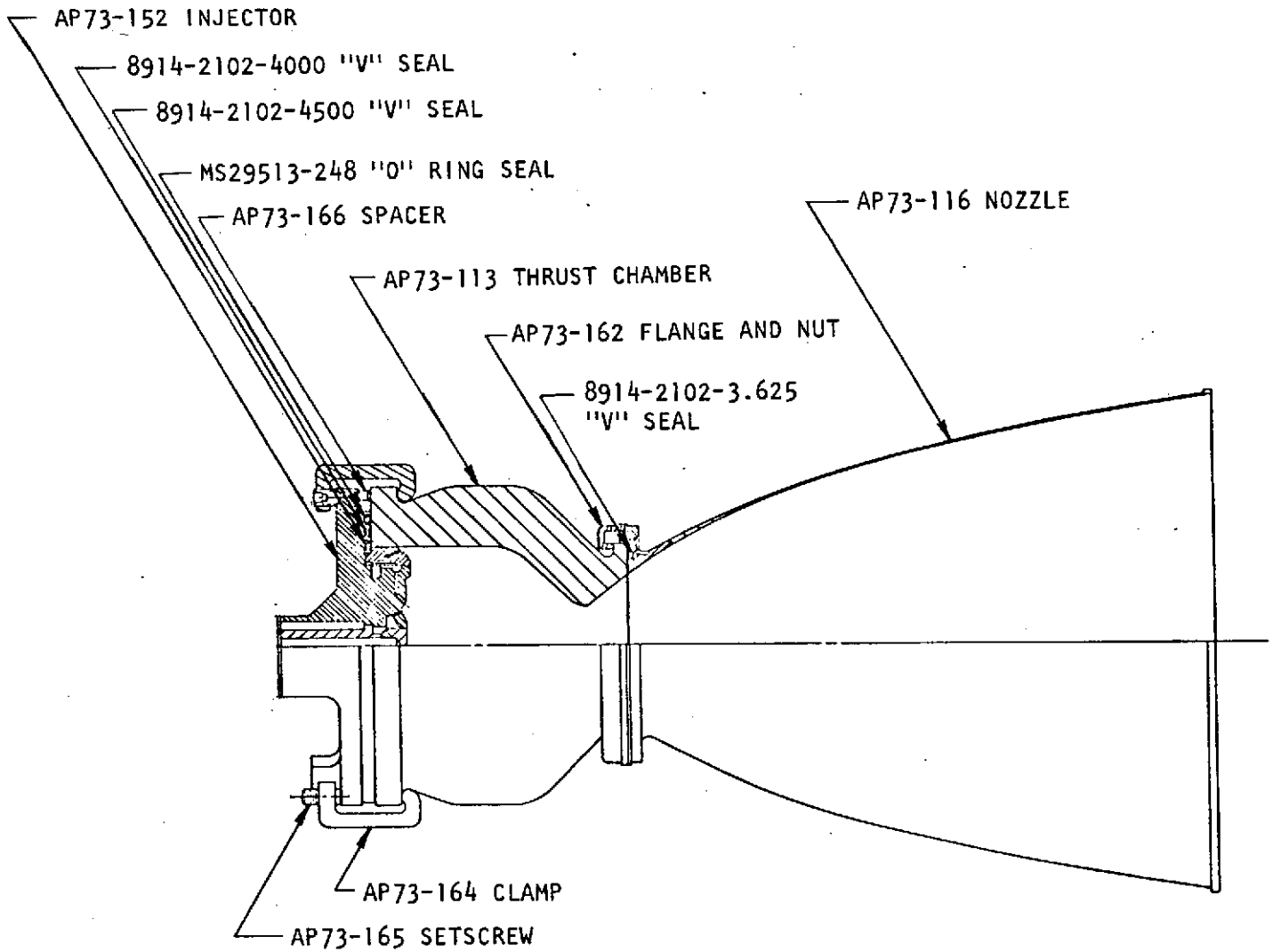

Figure 4. Off-Limits Engine Assembly

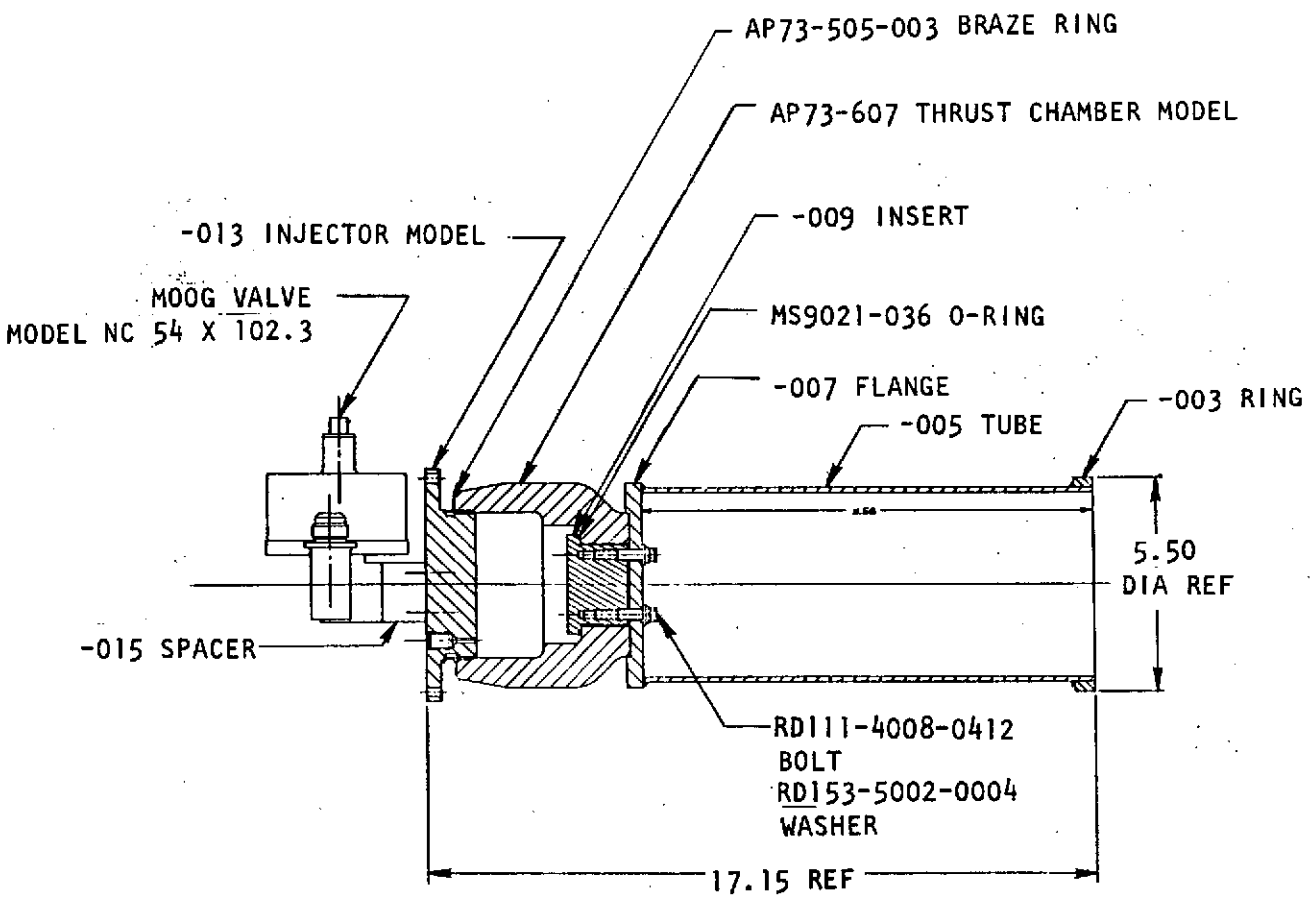

Figure 5. Vibration Simulator Assembly

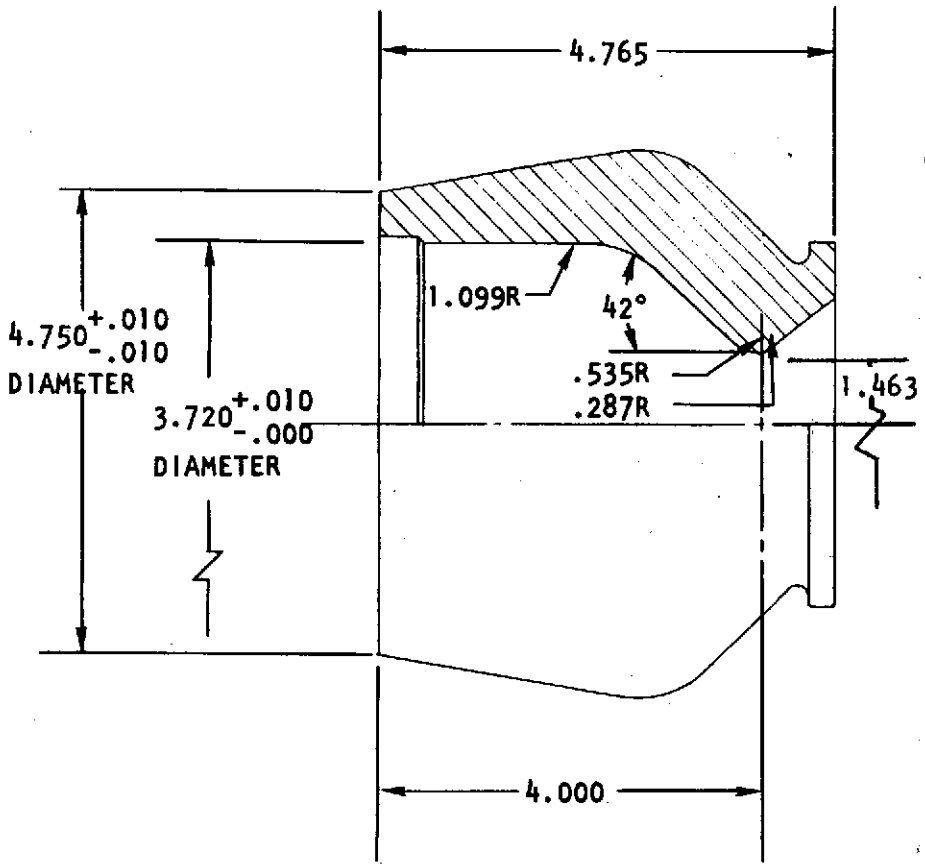

- CONTRACTION RATIO-- 6:1
- INJECTOR-TO-THROAT, IN. - 3.5
- CHARACTERISTIC LENGTH, IN. - 16
- CHAMBER/NOZZLE ATTACH, A/A_t - 3.23:1
- 42-DEGREE THROAT DOWNSTREAM EXPANSION ANGLE
- 0.10 THROAT DOWNSTREAM RADIUS RATIO

Figure 6. Beryllium Combustion Chamber

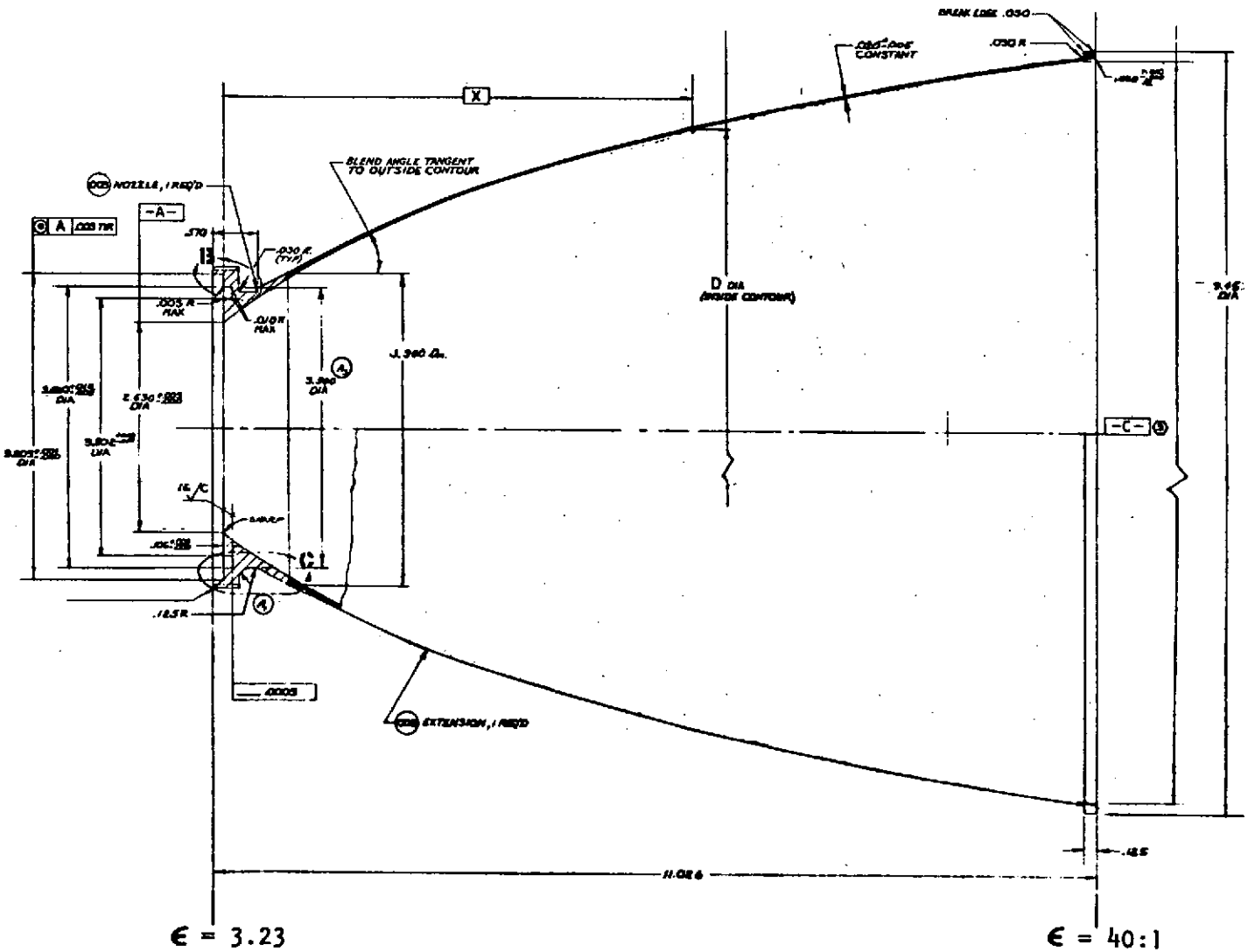

Figure 7. WC103 Nozzle Extension

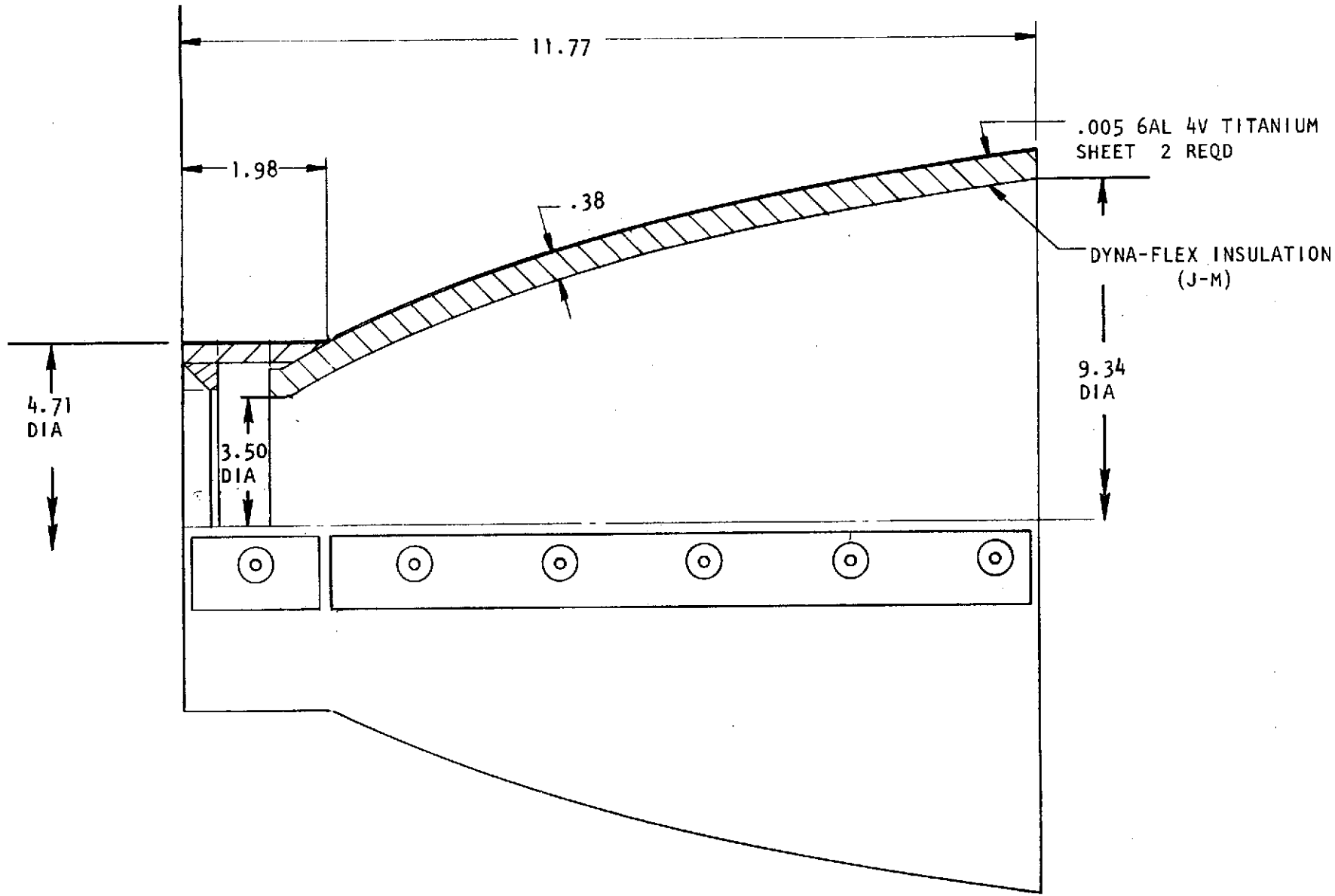

Figure 8. Insulation Blanket

A coated columbium nozzle was selected in place of the cobalt base alloy Haynes-25 configuration used on the Mars Mariner '71 and Viking Orbiter '75 engines to provide thermal margin at extreme off-limits operating conditions. A Haynes-25 nozzle would be adequate for normal engine operation but, operation with multiple orifice plugging or with feed system regulator malfunctions, could result in failure of a Haynes-25 skirt in the shuttle buried-mode application.

The nozzle incorporated an 80-percent bell and extended from the 3:1 beryllium attach point to 40:1. A special nozzle contour, originated to reduce nominal nozzle operating temperature from 2000 F to 1900 F of a Haynes-25 configuration, was used on the columbium nozzle. As shown in Fig. 9, the thermally optimized nozzle contour reduced wall pressure at the higher heat flux, higher expansion ratio. A 0.42 percent performance loss (1.4 lbf-sec/lbm specific impulse) results from this design. In the shuttle application, with the use of a coated columbium nozzle, the higher temperature, high performing nozzle contour should be employed.

The nozzles are attached to the chamber at an expansion ratio of 3:1 through a flexible Rene '41 flange and threaded nut arrangement identical in configuration to that employed in the Mars Mariner '71 and Viking Orbiter '75 engines. This design permits differential thermal growth of the beryllium chamber and the nozzle extension. Low-pressure leakage is prevented by the lapped interface joint. A Hastelloy V-seal was included in the joint for redundancy; however, experience in the Mars Mariner and Viking Orbiter engines, as well as company-sponsored programs, indicate this V-seal may not be required.

The nozzle is insulated by Dynaflex, a flexible insulation material manufactured by Johns-Manville, which is encased in a thin titanium steel jacket. This material was selected over Min-K, used on the Minuteman III PBPS beryllium engine, because of its higher operating temperature capability. Min-K usage is duration limited for use temperatures above 1600 F, whereas Dynaflex has long life capability at temperatures up to 2700 F. The Dynaflex selected has a density of 8 lb/ft^3 and conductivity of 1 $Btu\text{-}in./ft^2\text{-}sec\text{-}F$ in a vacuum. Because of the low operating temperature of the combuster, the insulation is required only in the nozzle section to maintain temperatures below the 800 F requirement.

Injector Design

The injector selected for the beryllium engine is a multiple element, unlike doublet configuration, fabricated from 321 stainless steel alloy material. This injector was designed, fabricated and characterized under a company-sponsored program. The injector (P/N AP73-504, Fig. 10) contains 56 elements impinging along three concentric rings. Injector design parameters are summarized in Table 3. The injector is patterned after a large family of unlike doublet injectors designed for use with earth-storable propellants in INTEREGEN-cooled beryllium thrust chambers.

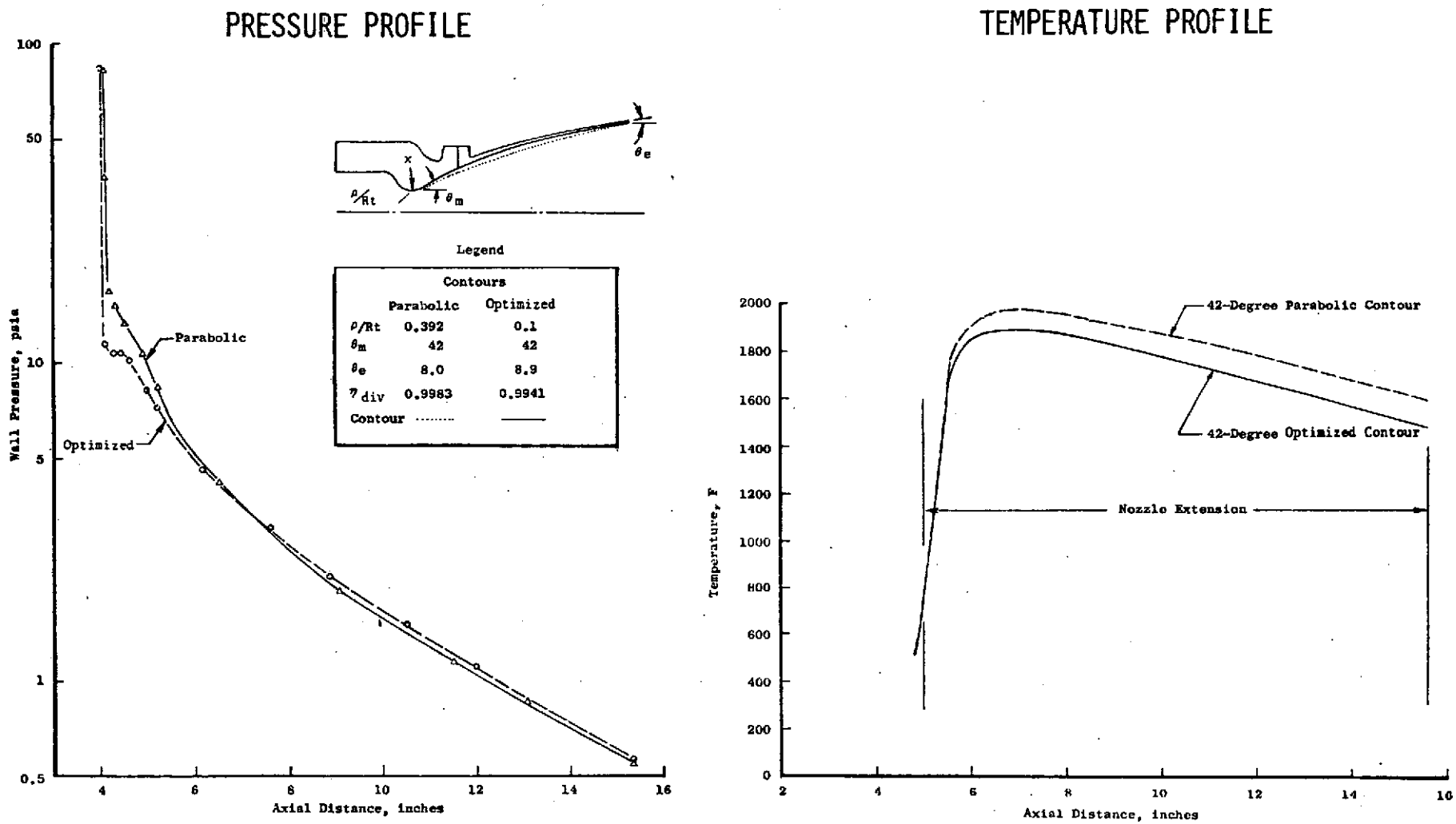

Figure 9. Optimized Nozzle Analysis

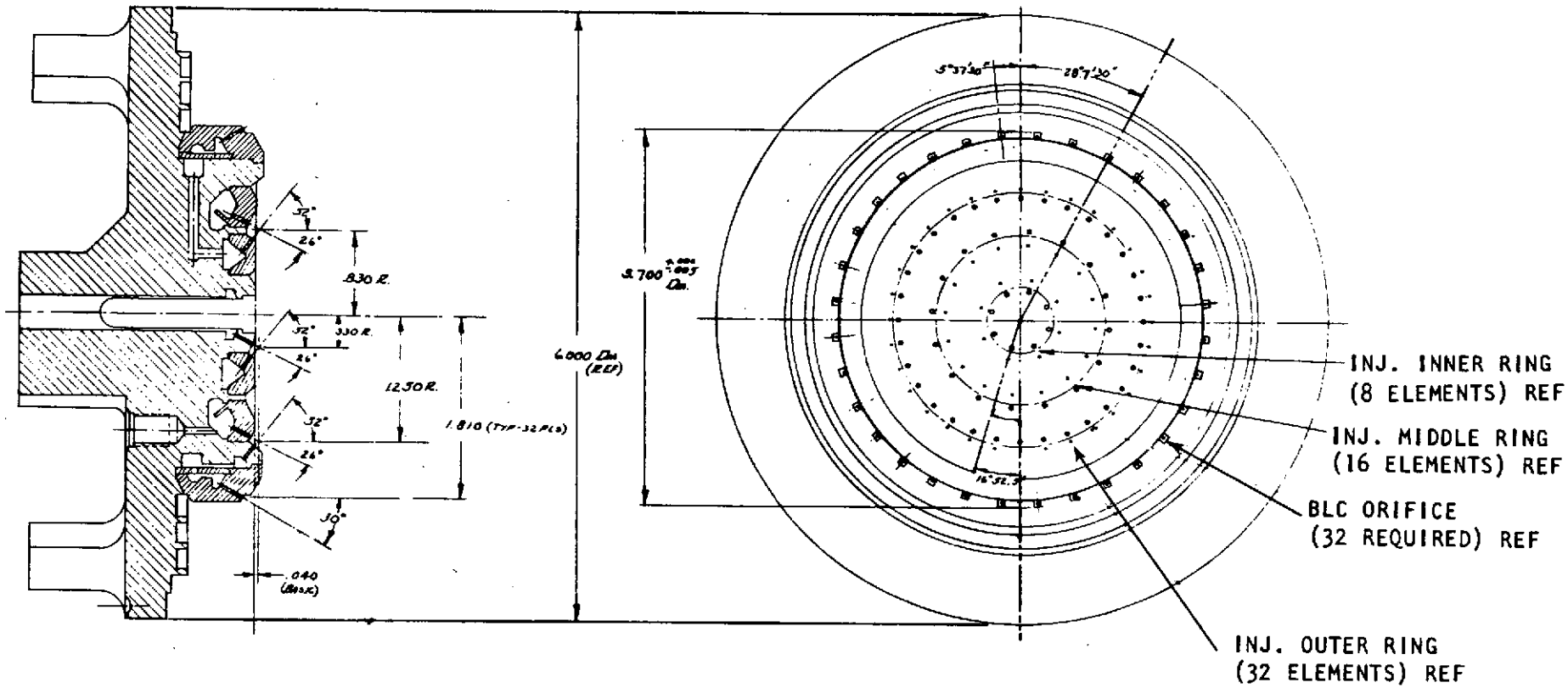

Figure 10 . Three-Ring Injector Assembly

TABLE 3. THREE RING INJECTOR DESIGN CHARACTERISTICS

MIXTURE RATIO, o/f:	OVERALL	1.63
	OUTER ROW	3.05
	MIDDLE ROW	2.30
	INNER ROW	2.30
BOUNDARY LAYER COOLING:	PERCENT OF TOTAL FUEL	40
	INJECTION VELOCITY, FT/SEC	35
	ORIFICE DELTA-P, PSID	11.3
INJECTOR DELTA-P, PSID: (MANIFOLD AND ORIFICE)	OXIDIZER	50
	FUEL	50
NUMBER OF ELEMENTS:		56
NO. HOLES/HOLE DIAMETER:	BLC	32/0.0305
	OUTER ROW FUEL	32/0.0203
	OUTER ROW OXID	32/0.0312
	MIDDLE ROW FUEL	16/0.0209
	MIDDLE ROW OXID	16/0.0279
	INNER ROW FUEL	8/0.0209
	INNER ROW OXID	8/0.0279
RUPE NO.:	OUTER ROW	0.606
	MIDDLE ROW	0.572
	INNER ROW	0.572
BETA ANGLE, DEGREES	OUTER ROW	5
	MIDDLE ROW	0
	INNER ROW	0
DOUBLET INCLUDED ANGLE, DEGREES		78

Several areas were considered in selecting the number of elements and rings in the injector. Minimum manifold volume is desirable to obtain high pulse performance and minimize contaminant generation at shutdown due to unburned residual propellant. Too low a manifold volume can cause maldistribution of propellants due to high manifold velocities and large pressure losses. In the injector design, manifold losses were limited to 10 psid with maximum manifold velocities of 20 ft/sec. These considerations resulted in a 1.63 cubic inch manifold volume (total downstream of valve seat, fuel plus oxidizer sides).

The number of elements was selected as a compromise between the desire for high performance (maximize number of elements) and for a system insensitive to contaminants (few elements, large orifice size). It was these conflicting design goals which led to the fabrication of two injector configurations during a company-sponsored program. The second injector, a 36-element, 2-ring configuration, was used on the Off-Limits Engine described later in this section. The higher performing 3-ring configuration was selected for the Durability Engine since it was more representative of that projected for the Space Shuttle whose RCS engine thrust level was baselined at 900 pounds.

At the circumference of the injector, film cooling orifices inject 40 percent of the fuel onto the combustion chamber wall, both to protect the wall and to provide INTEREGEN cooling. The injection ports are recessed into the acoustic cavity so that the liquid film is injected along the combustor wall with minimum disturbance from the combustion process. The film coolant orifices are spaced evenly and impinge on the chamber wall at a 30-degree angle to offer maximum thrust chamber wall protection. A metering ring is installed upstream of the film coolant manifold to produce an optimum coolant flow velocity. Orifice size, spacing impingement angle, and velocity were selected based on previous test experience. Acoustic cavities (0.080-in. width x 0.750-in. depth) are machined in the injector periphery and are tuned to stabilize the first tangential mode (7347 Hz). Thirty-two isolation dams are equally spaced between cavities.

To minimize performance loss with large quantities of fuel film coolant (40 percent), the injector is designed to promote mixing of the core gases with the film coolant as the cooling function is completed. This is accomplished by utilizing an oxidizer rich outer zone (outer row of elements) which has a momentum toward the combustor wall.

An injection orifice pressure drop of 40 psid was selected to provide a reasonable performance level (high velocity promotes propellant atomization), provide stability margin during low pressure operation with helium saturated propellant should blowdown operation be required, and meet the inlet pressure requirement of 290 psia when accounting for pressure losses through the injector manifold (~10 psid), valve (~30 psid), and engine calibration orifice (~10 psid).

Injector/Chamber Interface Design

The injector/chamber interface incorporates a brazed joint configuration (Fig. 11), specifically developed for the Space Shuttle RCS application under a company-sponsored program. A Haynes-25 ring is brazed directly to the beryllium and the

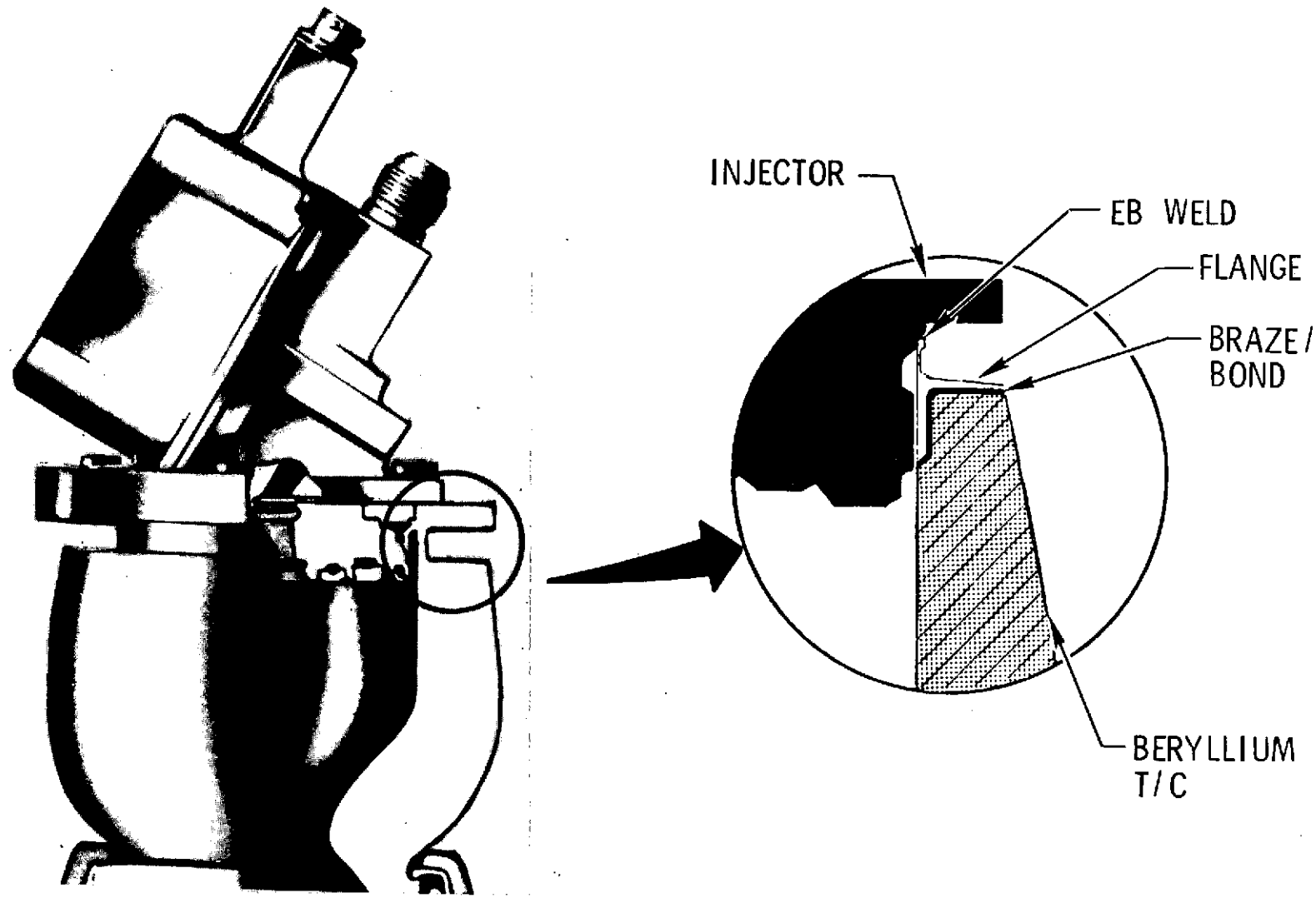

Figure 11. Injector/Chamber Interface Design

ring is then EB welded to the CRES injector. This approach replaces the complex and heavy bolted configuration employed on prior beryllium engine applications as well as the Off Limits Engine used in this program. A primary objective of the contract is to demonstrate the compatibility and structural integrity of this joint when exposed to successive cycles of hot fire and environmental conditions typical of the Space Shuttle.

Valve

A single-stage, direct-operated bipropellant valve was selected for the beryllium rocket engine. The single-stage design was considered as the most reliable concept with the minimum scheduled maintenance requirements based upon existing flight proven technology. The MOOG, Inc., torquemotor operated, staggered poppet design Model 54X107, developed by MOOG for NASA contract NAS9-12996, was selected.

The MOOG torquemotor bipropellant valve is a mechanically linked poppet design (Fig. 12). Valve poppet movement is controlled by flapper arms attached at one end to the motor armature and the opposite end to the seat poppet. The fuel and oxidizer poppets are mechanically linked by welding each flapper arm to the single armature of the motor. The flapper and valve interior is isolated from the motor by thin wall, flexure tube sleeves welded at one end of the valve body and the opposite end to the armature and flapper. The valve is made essentially of 17-7 PH and 304 CRES with Teflon seats.

A staggered seat design minimizes the valve pressure drop and the opening force requirement for the existing 55 in.-lb torquemotor used on the Minuteman III and Mars Mariner '71 rocket engine valves. The staggered seat is a poppet arrangement which seals on two parallel seat surfaces. On opening, propellant flow passes around the poppet from the first seal and through the hollow poppet center across the second seal. On closing, the first Teflon seat seals the flow around the poppet and the second Teflon seat seals the flow through the poppet center. This arrangement minimizes the ΔP for a particular design, thus minimizing the poppet and seat diameter. This arrangement also minimizes the opening force of the valve by balancing the fluid pressure across the sealing areas. Unbalance force for seal loading is provided by making the first seal slightly larger than the second seal and biasing the armature position closed. This pressure force together with the force of the permanent magnets provides the necessary force to fail-safe close.

The valve requirements are listed in Table 4. A design goal 30 psid pressure drop was specified with the projected valve response time 30 msec opening and 15 msec closing. The valve weighs 4.5 pounds. The valve is bolted to the injector with thin titanium spacers in between to insulate the valve from the engine. The insulator contains grooves for V-seals between the injector and valve.

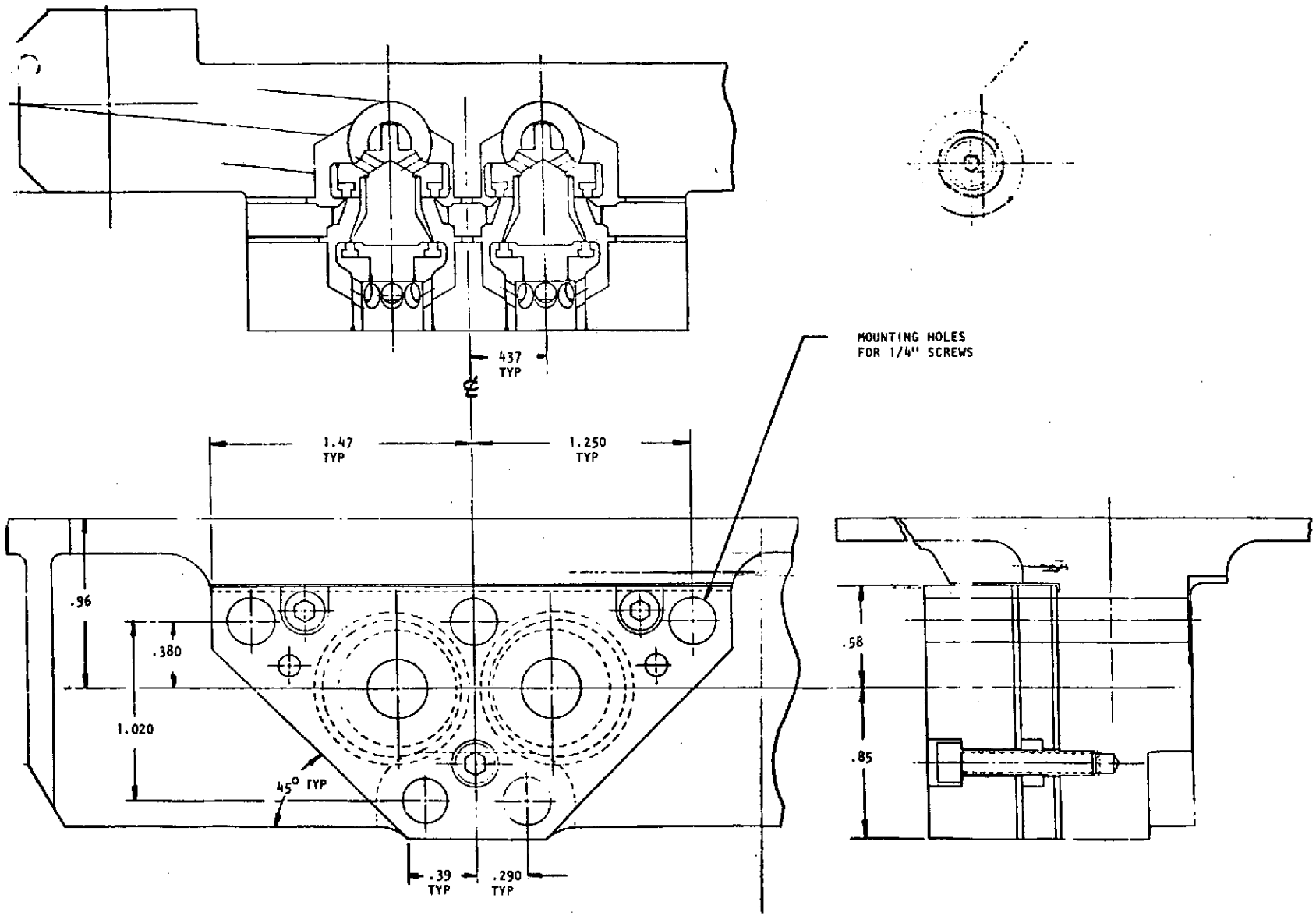

Figure 12. Mechanically Linked Bipropellant Valve
Moog Model 54X107A

TABLE 4. MOOG VALVE DESIGN REQUIREMENTS

Type	Bipropellant, mechanically linked, torque-motor operated
Fluid Handled	Nitrogen tetroxide and monomethyl hydrazine
Operating Pressure	300 psig
Flowrates	1.252 lb/sec NTO and 0.783 lb/sec MMH
Pressure Drops	30 to 40 psid
Power	Minimum at 28 ±4 energizing voltage
Response	≤30 msec open
	≤15 msec close
Temperature	+20 F to 165 F
Operating Life	250,000 on-off cycles
Leakage	≤20 cc/hr total gaseous nitrogen
Weight	≤5 pounds

OFF-LIMITS ENGINE DESIGN

The engine assembly (Fig. 4) employed for off limits tests was made available to the contract from a company-sponsored program. Differences between the Off Limits and Durability Engines are:

1. Facility valves were used in place of the MOOG valve, the latter being unable to open at the elevated inlet pressures required for off-limits testing.
2. A two-ring, 36-element injector was used in place of the three-ring 54-element configuration.
3. A bolted injector/chamber interface similar to that used on Minuteman III and Mars Mariner '71 engines was used in place of the brazed configuration (beryllium geometry at injector interface modified for bolted configuration).
4. Uninsulated Haynes-25 nozzle in place of the insulated coated columbium configuration (nozzle geometry identical for both nozzles).

The injector design employed is shown in Fig. 13 with design characteristics provided in Table 5. The injector has fewer elements and a lower manifold volume than the three-ring configuration used in the Durability Engine. The fewer elements result in larger orifices (0.025-in. minimum diameter compared to 0.020-in. on the three-ring design). This injector has lower steady-state performance due to its coarser pattern, but higher pulse performance for short pulse widths due to reduced manifold volume. The effect of lower performance on thrust chamber heat flux is negligible since the chamber wall environment (film coolant and high mixture ratio outer row of elements) is similar to the three-ring injector. Table 6 provides differences in engine operating temperatures recorded during the company-sponsored test program.

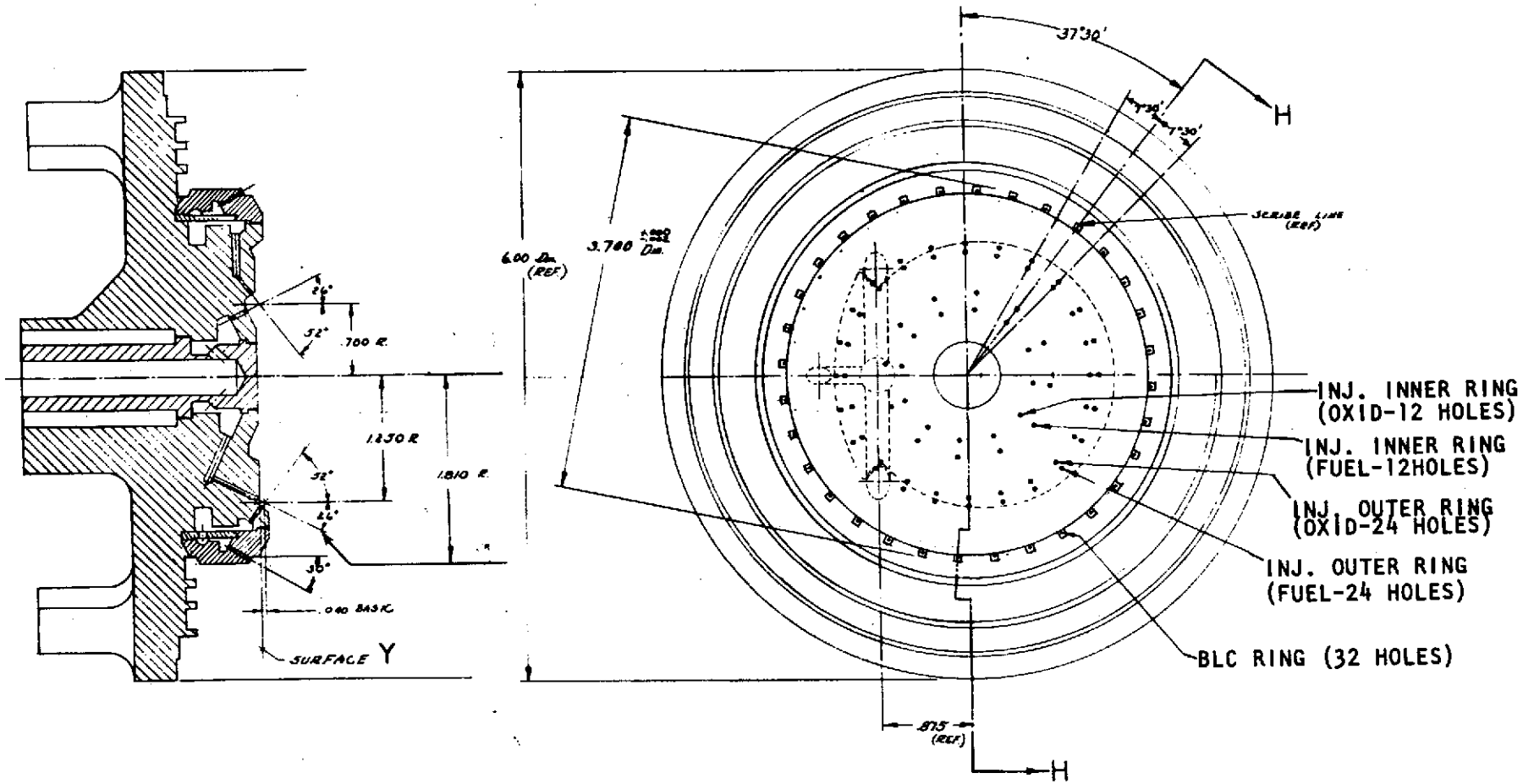

Figure 13. Two-Ring Injector Assembly

TABLE 5. TWO RING INJECTOR DESIGN CHARACTERISTICS

Mixture Ratio, o/f	Overall	1.63
	Outer Row	2.94
	Middle Row	--
	Inner Row	2.25
Boundary Layer Cooling	Percent of total fuel	40
	Injection Velocity, ft/sec	35
	Orifice ΔP, psid	11.3
Number of Elements		36
Number Holes/Hole Diameter	Boundary Layer Cooling	32/0.0305
	Outer Row Fuel	24/0.0259
	Inner Row Fuel	12/0.0251
	Inner Row Oxidizer	12/0.0332
Rupe Number	Outer Row	0.602
	Inner Row	0.569
Beta Angle, degrees	Outer Row	5
	Inner Row	0
Doublet Included Angle, degrees		78

TABLE 6. INJECTOR THERMAL COMPARISON*

Location	Temperature, F	
	Two-Ring Injector	Three-Ring Injector
Measured Beryllium OD		
Head End	198	205
Throat	450	478
Nozzle Attach	529	595
Nozzle Attach Nut	797	798
Maximum Nozzle Skirt (L-605)	1752	1804

*Tests with He saturated propellant data at 600 seconds

VIBRATION SIMULATOR DESIGN

The purpose of the Vibration Simulator (Fig. 5) is to verify the structural integrity of the brazed injector/chamber joint when subjected to 100 missions to launch vibration (X, Y, Z axes random vibrations). To meet this objective, the simulator was designed to have the same mass and moments of inertia as the flight configuration Durability Engine. Since the primary structural feature being demonstrated is the thrust chamber/injector braze joint, the simulator design in this area is identical to the flight configuration. To minimize cost, the beryllium chamber contouring is minimized and a dummy aluminum nozzle extension is used to simulate the proper mass and inertia. The injector body manifolding and orifices are not included, but again, the proper mass and inertia is simulated. An existing MOOG valve, whose mass properties are identical to the valve selected for the Durability Engine, is bolted to the injector.

DESIGN ANALYSIS

Design analyses have been performed for the Durability Engine whose operating characteristics are representative of a flight configuration. These have included evaluation of performance, thermal, structural/life, hydraulic, and stability characteristics, identification of maintainability, reliability, and safety in the space shuttle RCS application; and assessment of scalability of the beryllium engine concept over a thrust range of 100 to 1100 pounds.

Performance

The injector selected for the Durability Engine is shown in Fig. 10. This injector was previously tested using nonflightweight hardware on company-sponsored programs. Therefore, the performance predictions presented here are primarily based on empirical results. The engine configuration used in company-sponsored programs for the preliminary evaluation of injector performance allowed for bolting the injector to a beryllium combustion chamber which had contraction ratio (ϵ_c = 6:1), characteristics length (L* = 16.0), and expansion ratio (ϵ_{ex} = 40:1) identical to the Durability Engine.

Steady-State Performance. The predicted steady-state performance for the Durability Engine is presented in Fig. 14. The specific impulse is shown for operation with 100-percent helium saturated propellants and is predicted for use of unsaturated propellants and predicted for use of a performance optimized nozzle over a mixture ratio range of from 1.3 to 1.9 o/f. The data are for nominal NTO/MMH propellant temperature, 75 F, and nozzle expansion ratio of 40:1. The 290-second specific impulse at a 1.63 o/f mixture ratio is below the design goal of 295 seconds; but the goal can be achieved with minimum development effort. A value of 293 seconds was reached at 1.3 o/f mixture ratio with saturated propellants. Predictions of 292 and 293.4 seconds at 1.63 o/f mixture ratio are made for unsaturated and optimim nozzle, respectively.

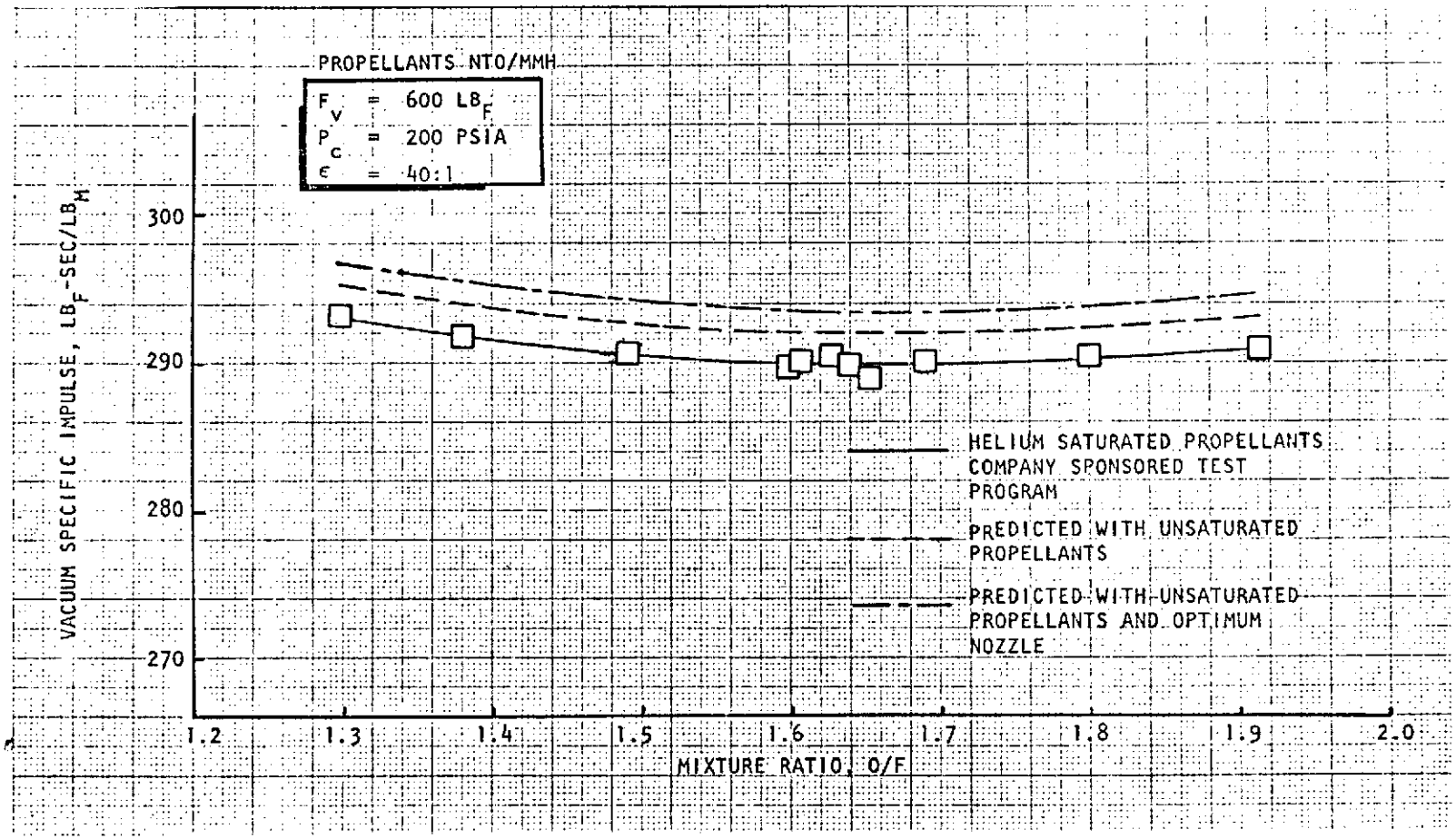

Figure 14. Durability Engine Steady-State Performance

The effect of propellant inlet pressure on engine nominal mixture ratio and thrust was established for temperatures 75 ±35 F and pressure 290 ±20 psia (Fig. 15 and 16). As shown, mixture ratio excursion from 1.46 to 1.83 can occur for the assumed maximum ±10 psia inlet pressure variations. Mixture ratio excursion from 1.59 to 1.67 can occur for variation in inlet temperature of ±35 F.

Pulse Performance. The engine is to be capable of delivering 220 lbf-sec/lbm pulse vacuum specific impulse at a minimum impulse bit of 30 lbf-sec. Constraints on the design were a 50 msec start, 50 msec shutdown, minimum chamber pressure overshoot and simplicity of manufacture.

Experience gained in the design of pulsing engines with thrust levels of 25 to 1600 lbf has resulted in a broad base of empirical data on pulse engine design relationships. Both simple and sophisticated computer models have also been developed to analyze pulse performance and this background was employed to write a program for the analysis of this engine. This model was used for preliminary design of the engine in such areas as manifold volume ratio and effect of manifold volume on performance.

Final engine design incorporated a total volume (fuel and oxidizer) downstream of the valve seat to the injector face of 1.63 $in.^3$. This volume is minimized to give maximum pulse performance while allowing a design ensuring low propellant velocities and good injector mass flow distribution for uniform heat flux on the chamber walls and for maximum steady-state mixing and vaporization efficiencies. Theoretical studies indicate a gain of about 4 seconds of pulse specific impulse at 30 lbf-sec and long off times (1 second) for a reduction of total manifold volume of 0.1 $in.^3$. It is felt that a flight design can expect a reduction of manifold volume of 10 to 15 percent over the test design due mainly to decreasing valve volume and a minor refinement of the manifold passages.

The engine dribble volume is composed of 0.84 $in.^3$ fuel volume and 0.79 $in.^3$ oxidizer volume. Theoretical studies indicated that, even though equal volumes have been traditionally employed, a 10-percent smaller oxidizer volume would minimize overshoot at start. Because of the system resistance budget and the BLC volume, equal volumes would have resulted in a significant fuel lead and accumulation in the combuster leading to an ignition flash and pressure spike. The present design employs the 10 percent smaller NTO volume which theoretically led to a maximum 50 percent overshoot using worst case assumptions. In fact, the overshoots observed were 20 percent or less. No other manifold or residual propellant explosions or pressure spikes were observed during the Durability Engine testing.

An idealized engine pulse is sketched in Fig. 17. The observed delay between on-signal and first valve movement was 17 msec. The time required to prime the fuel manfiold, the first to fill, was 17 msec also. From first fuel to the combustor, then first oxidizer, ignition delay and buildup to 90-percent thrust covered 6 msec. This 40 msec start time is faster than the engine specification of 50 msec. Valve closure requires very little time, 3 msec for de-energize and then 4 msec to move to the closed position. The time required to reach 10 percent thrust from off-signal varied from 15 to 20 msec during the testing. Zero thrust was reached

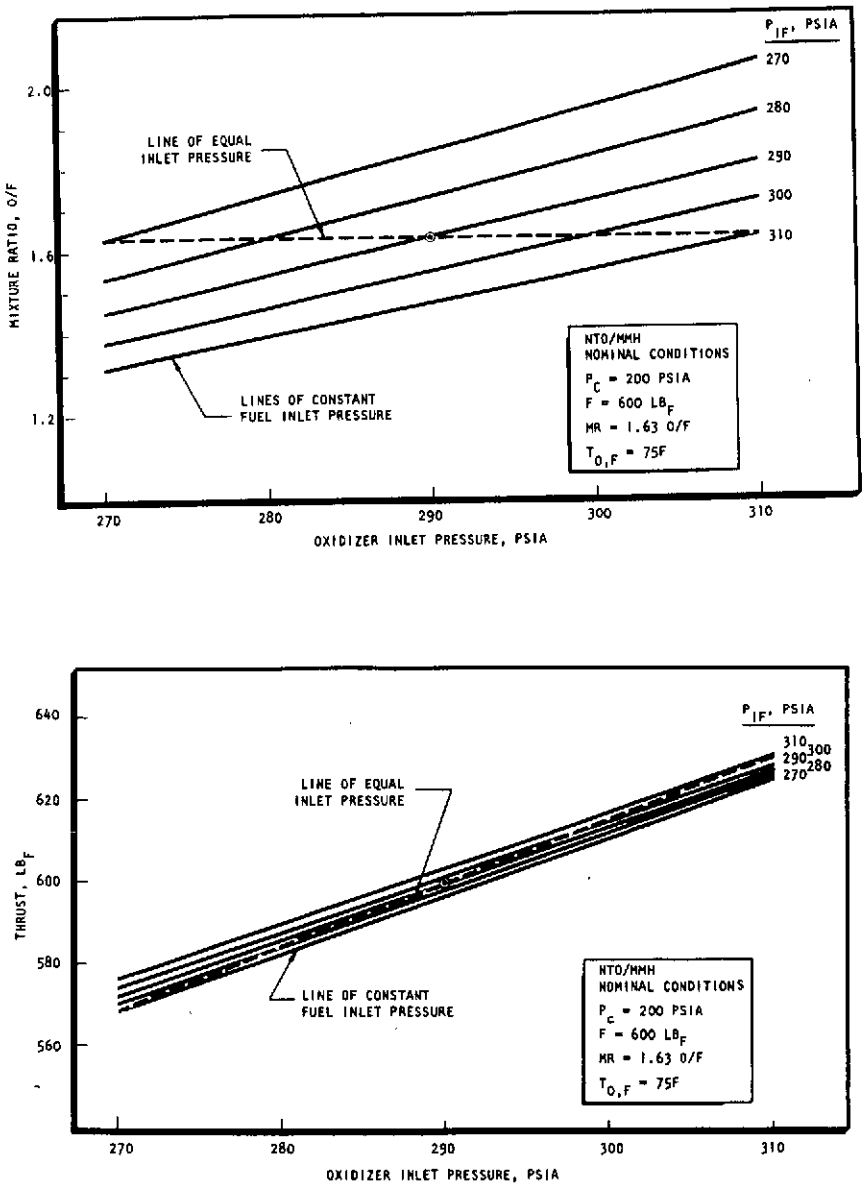

Figure 15. Effect of Propellant Inlet Pressure on Engine Thrust and Mixture Ratio at RCS Nominal Propellant Temperature

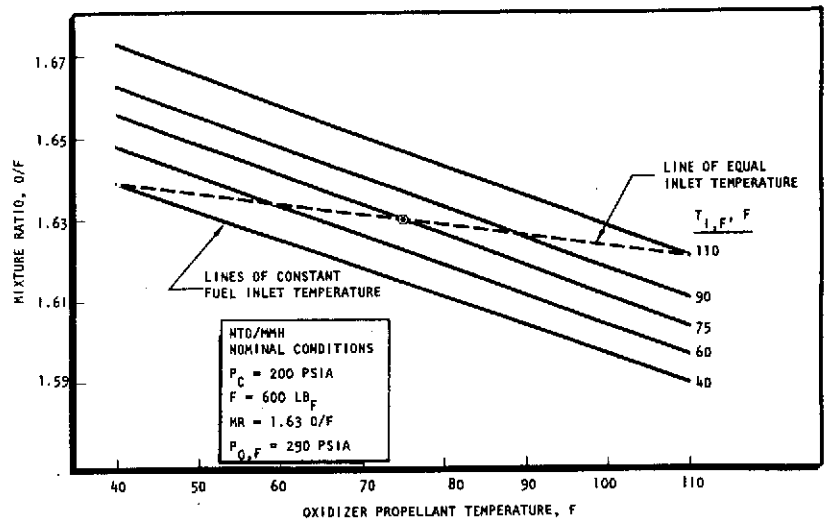

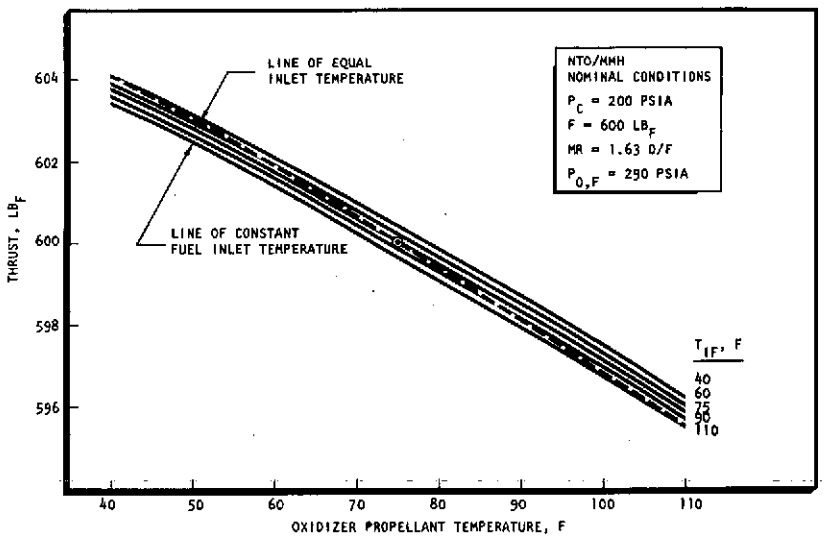

Figure 16. Effect of Propellant Temperature on Engine Thrust and Mixture Ratio at RCS Nominal and Inlet Pressure

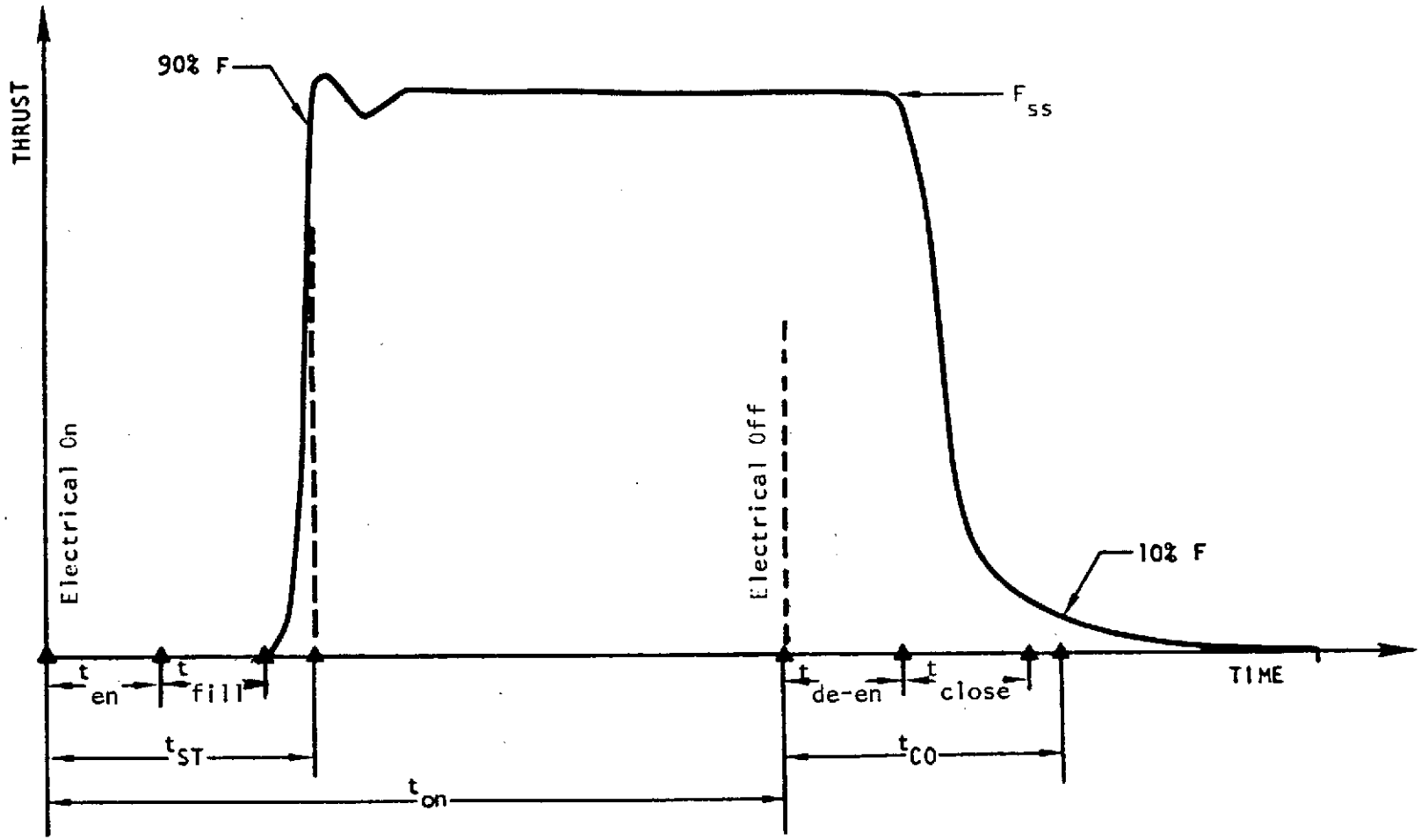

- VALVE OPENING DELAY TIME, t_{en} 17 msec
- MANIFOLD PRIME TIME, t_{fill} 17 msec
- THRUSTER START TIME, t_{st} 40 msec
- VALVE CLOSING DELAY TIME, t_{de-en} 3 msec
- VALVE CLOSING TRAVEL TIME, t_{close} 4 msec
- THRUSTER CUTOFF TIME, t_{co} 20 msec

Figure 17. Durability Engine Response Characteristics

approximately 700 msec after off-signal. Shutdown impulse averaged about 9 lbf/sec. As pulse frequency increased, manifold prime time decreased asymptotically to about 7 msec due to entrapped propellant. Hardware temperature had little effect on the pulse characterization times.

The hot-fire pulse performance study consisted of more than 300 pulses using helium saturated NTO/MMH with valve electrical on times from 50 to 1000 msec. Pulse frequencies ranged from 0.25 to 5 pulses per second. The pulses were run at 185 psia chamber pressure due to valve operating difficulties, but no significant difference running at 200 psia is theoretically predicted or was seen empirically on other engines. No significant difference was observed between pulses run with ambient hardware and with hot hardware immediately following an extended steady-state run.

The hot-fire data is presented in Fig. 18 through 21. These summarize pulse total impulse, pulse vacuum specific impulse, and pulse mixture ratio versus electrical on-time and pulse specific impulse versus pulse total impulse with pulse frequency. A summary of the data at the minimum impulse bit (MIB) is presented in Table 7. Figure 22 combines the hot-fire data on the test engine and the theoretical model to present a graph of specific impulse which can be employed as a design aid in meeting performance specifications at 30 lbf-sec MIB.

TABLE 7. DURABILITY ENGINE PULSE PERFORMANCE

(F = 565 LB, P_c = 181 PSIA, MR = 1.62 o/f)

Start Time, msec	40
Cutoff Time, msec	20
Total Impulse at 50 msec Pulse Width, lb-sec	
1/3 cps	17
1 cps	19
2 cps	20
Pulse Specific Impulse at MIB (30 lb-sec), sec	
1/3 cps	167
1 cps	183
2 cps	196
5 cps	220
Pulse Mixture Ratio at MIB (30 lb-sec), o/f	
1/3 cps	1.42
1 cps	1.48
2 cps	1.54

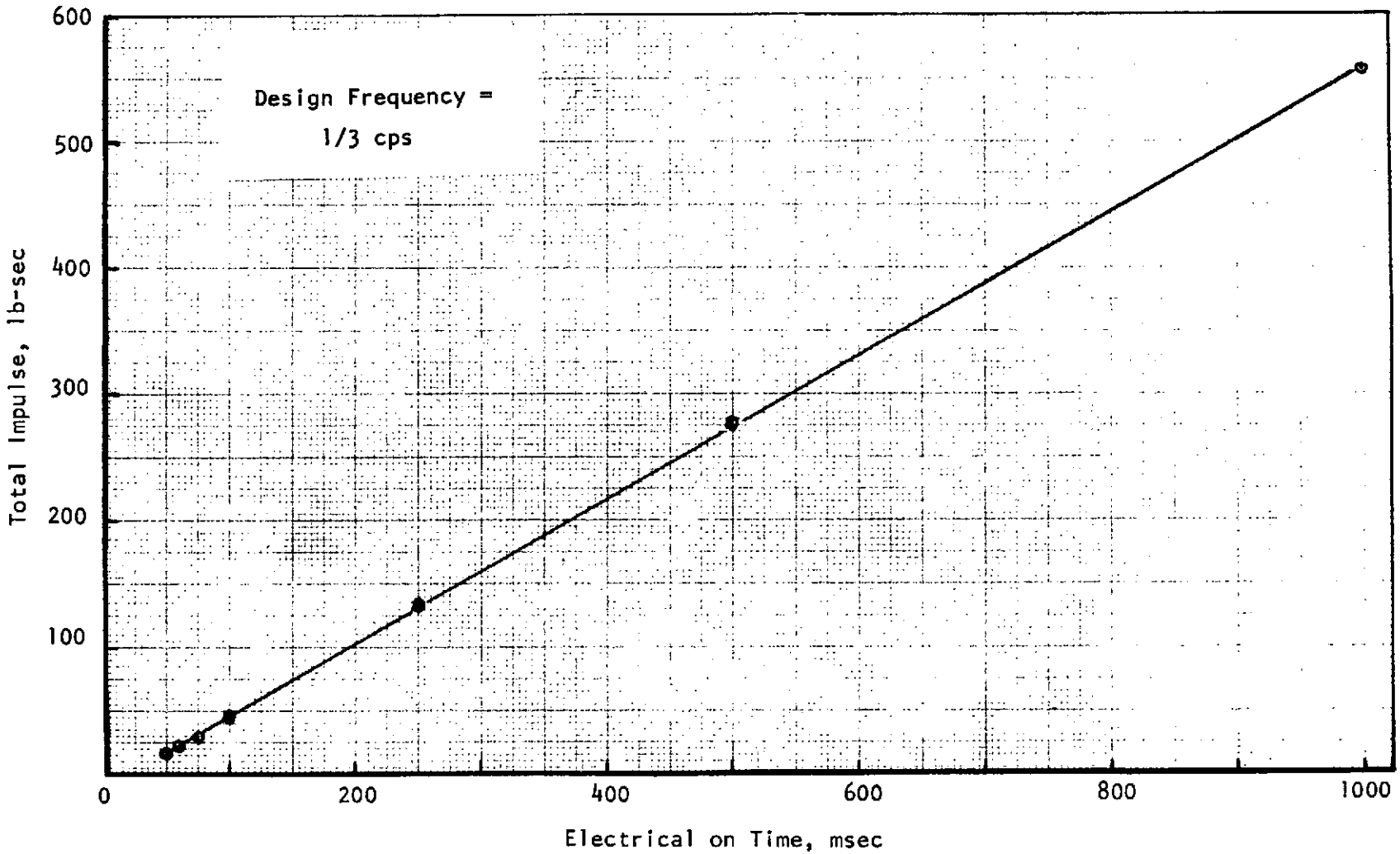

Figure 18. Total Impulse vs On-Time

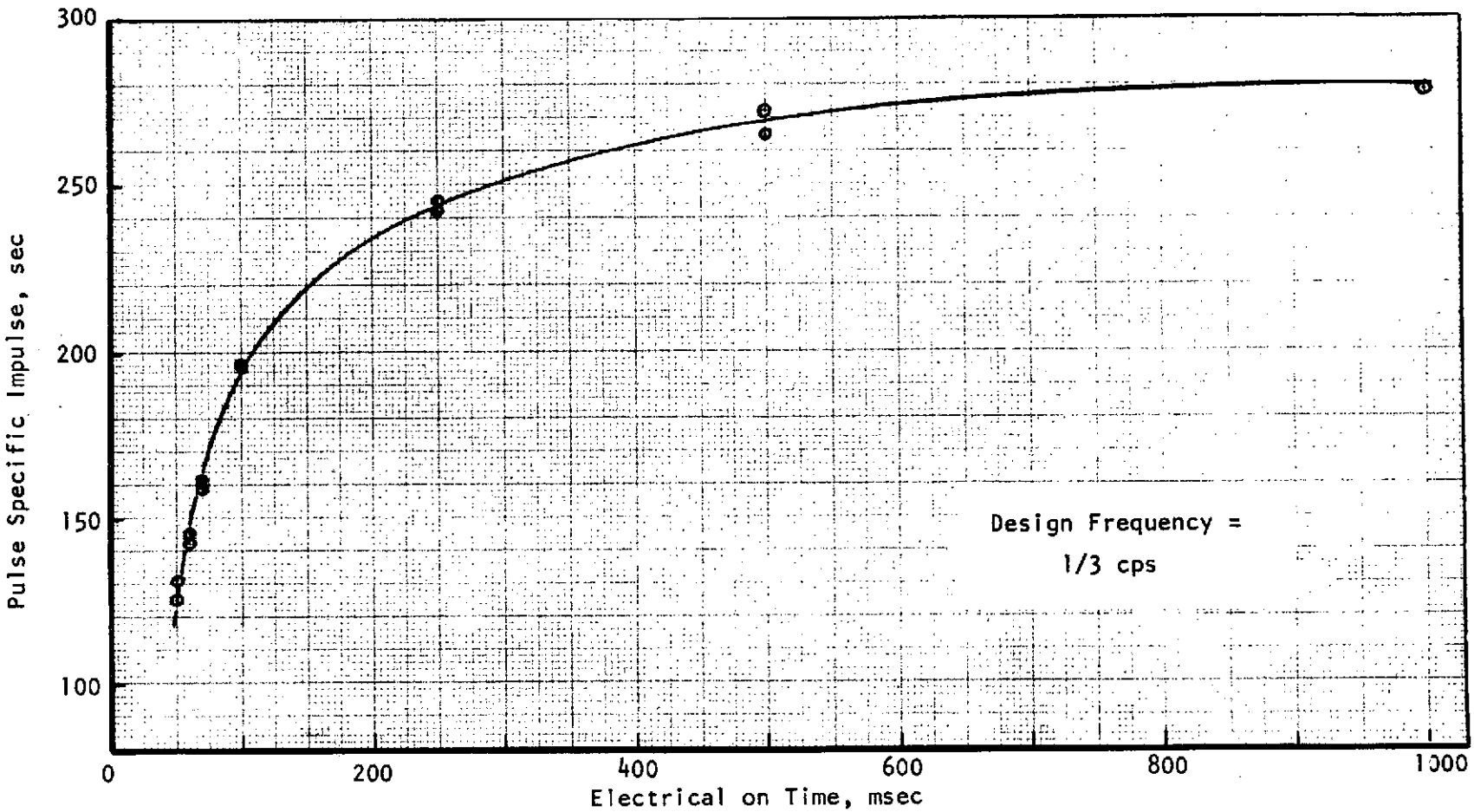

Figure 19. Pulse Specific Impulse vs On-Time

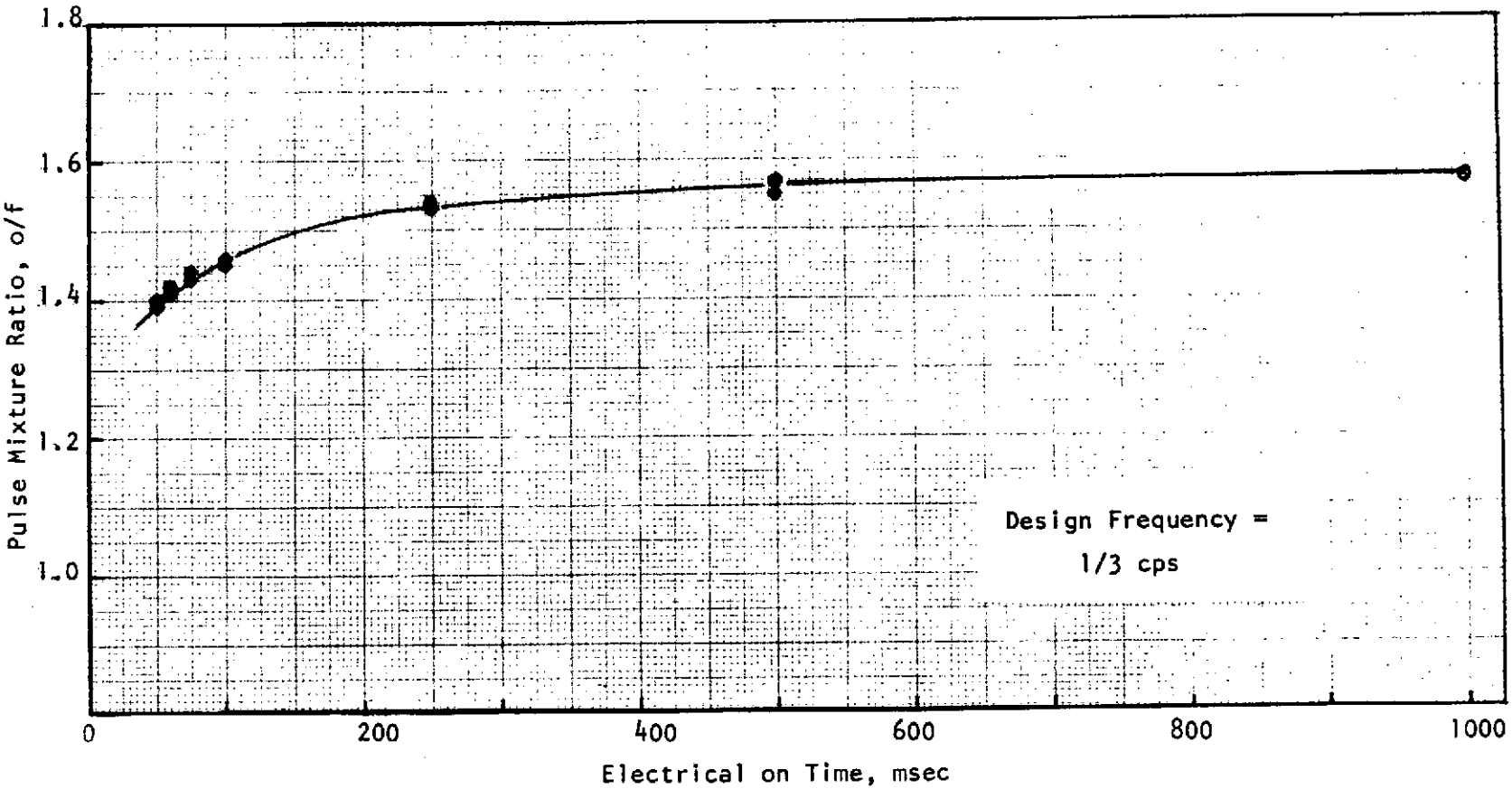

Figure 20. Pulse Mixture Ratio vs On-Time

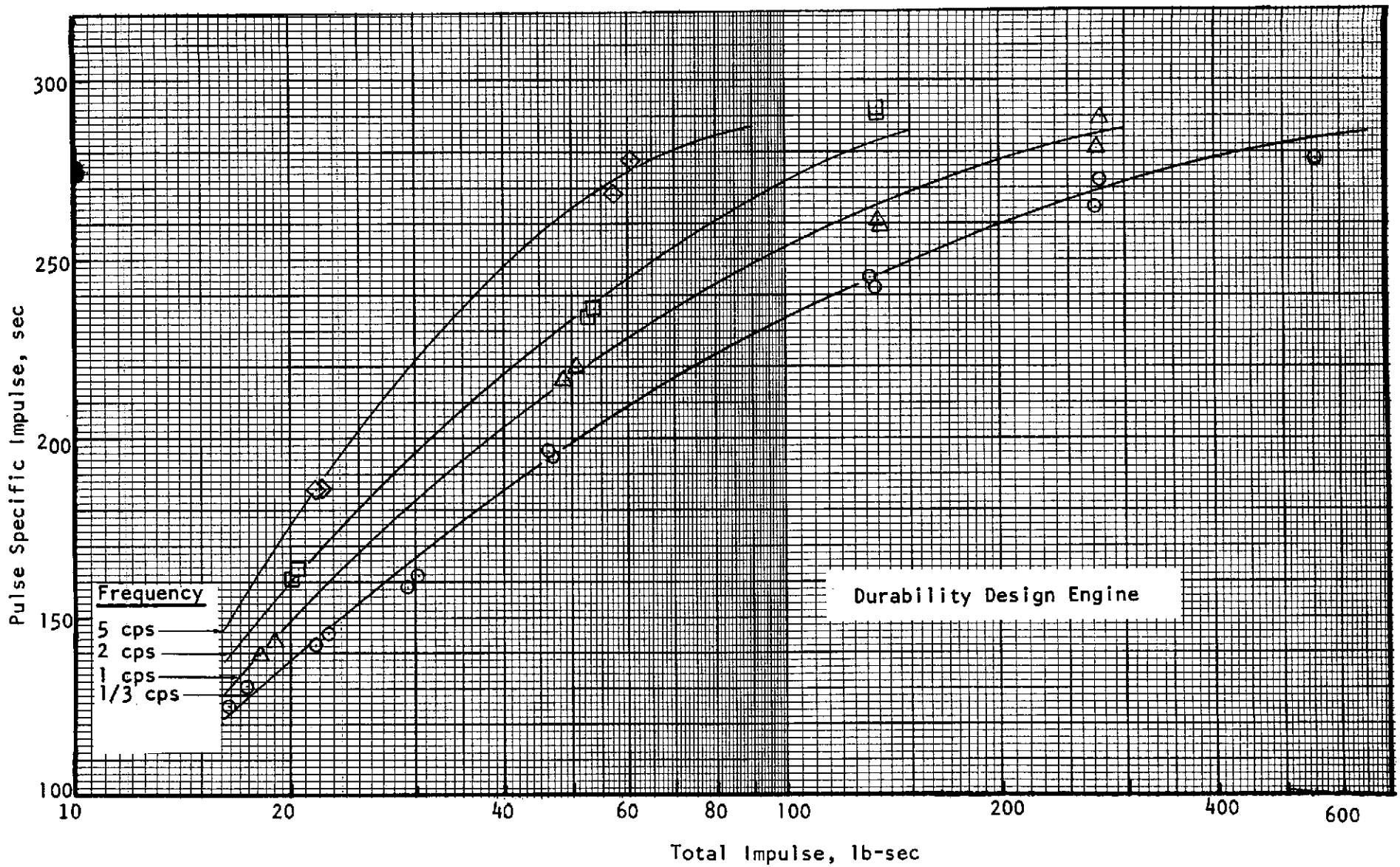

Figure 21. Pulse Specific Impulse vs Total Impulse

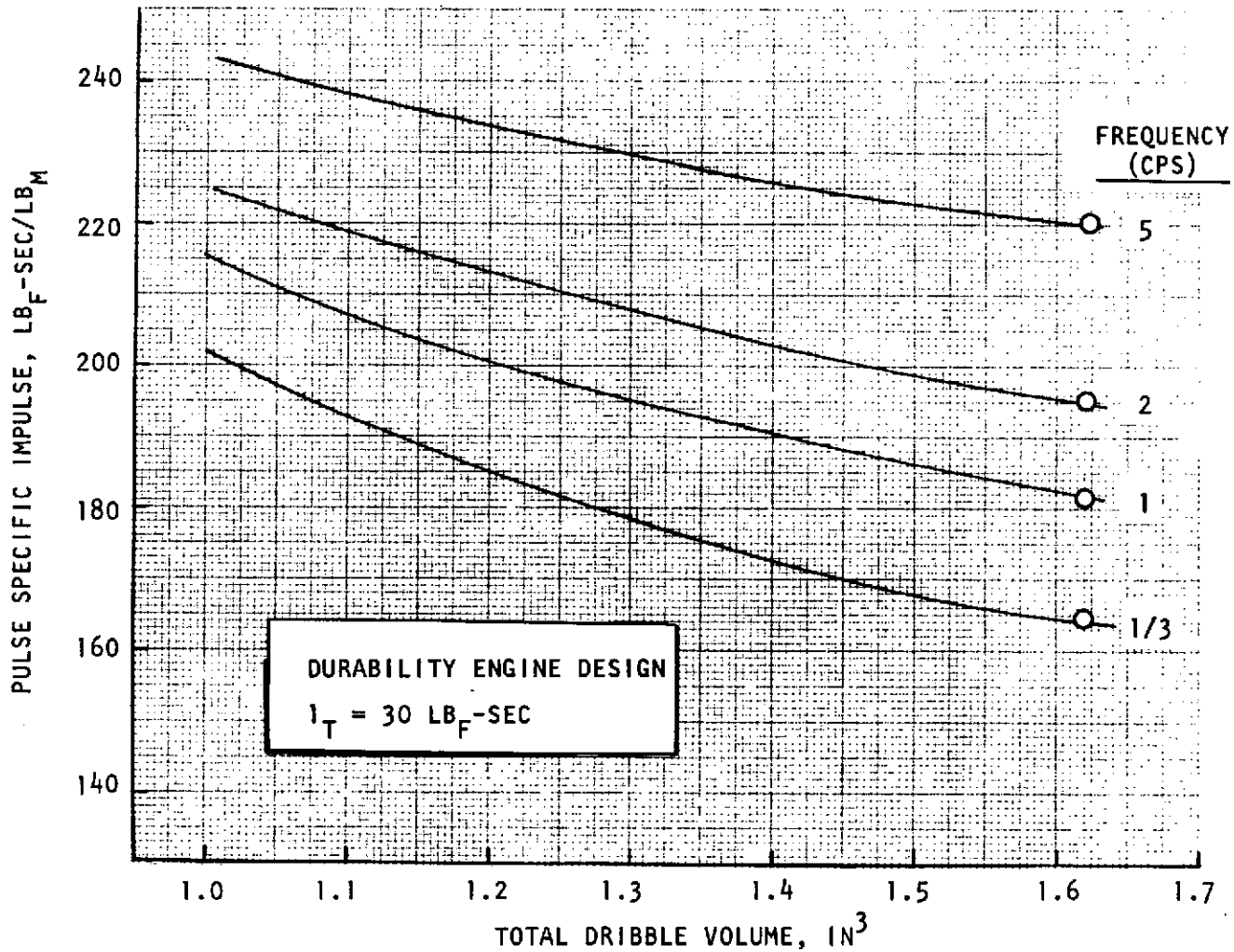

Figure 22. Pulse Specific Impulse Vs Dribble Volume

The data show that this design does meet the design pulse requirements at the 5 Hz frequency. The run-to-run repeatability observed in hot-fire testing of this engine assembly was 3 lbf-sec at the 95 percent confidence interval.

Thermal Analysis

Nominal Operation. The Durability Engine has been designed to meet the thermal requirements of the space shuttle RCS. To meet these requirements, it is essential that the thruster operate at an overall low temperature potential as well as with minimum temperature gradients.

A unique thermal analysis engine model has been developed at Rocketdyne to perform the required analyses to design optimum INTEREGEN thruster configurations. The basic design approach is one of defining internal and external contours, gas-side boundary conditions, and environmental constraints and then determining temperatures as a function of time. The nodal network representing a thrust chamber cross section is shown in Fig. 23.

Extensive analyses have been conducted of INTEREGEN cooled thrusters. To achieve the thermal margin for INTEREGEN cooling and meet the design requirements and performance goals of the RCS beryllium engine, the optimum design has been determined to be that shown in Fig. 3.

The thermal analyses have been based on using 40 percent of the fuel (15.2 percent total propellant flow).

The analysis considered insulation of the nozzle with Dynaflex material to reduce the external surface of the assembly to 800 F. The basic design analysis has been with the assumption that the vehicle environmental temperature would be 75 F; however, some analysis was made with an environmental temperature of 300 F while the engine is firing for 600 seconds. The results indicate that an increase in temperature will be on the order of 30 F over the 600 second period of firing.

The results of the thermal analysis of the optimized design are presented in Fig. 24 through 26. Figure 24 shows the steady-state isotherm distribution (600 seconds firing) through the combustor. Figure 25 depicts the predicted transient-to-steady-state temperature history. Figure 26 illustrates the internal and external steady state temperature distribution for the Durability Engine as a function of axial length.

As can be seen, the maximum beryllium operating temperature is 1020 F at the ID and 942 F at the nozzle attach point. At the throat, outside surface of 635 F is predicted. The time to steady-state temperatures is approximately 200 seconds. This long temperature transient minimizes the thermal cycle requirement of the engine. The mass average beryllium temperature is 435 F, which eliminates any restart problem and minimizes thermal soakback to the injector and valve at thruster shutdown.

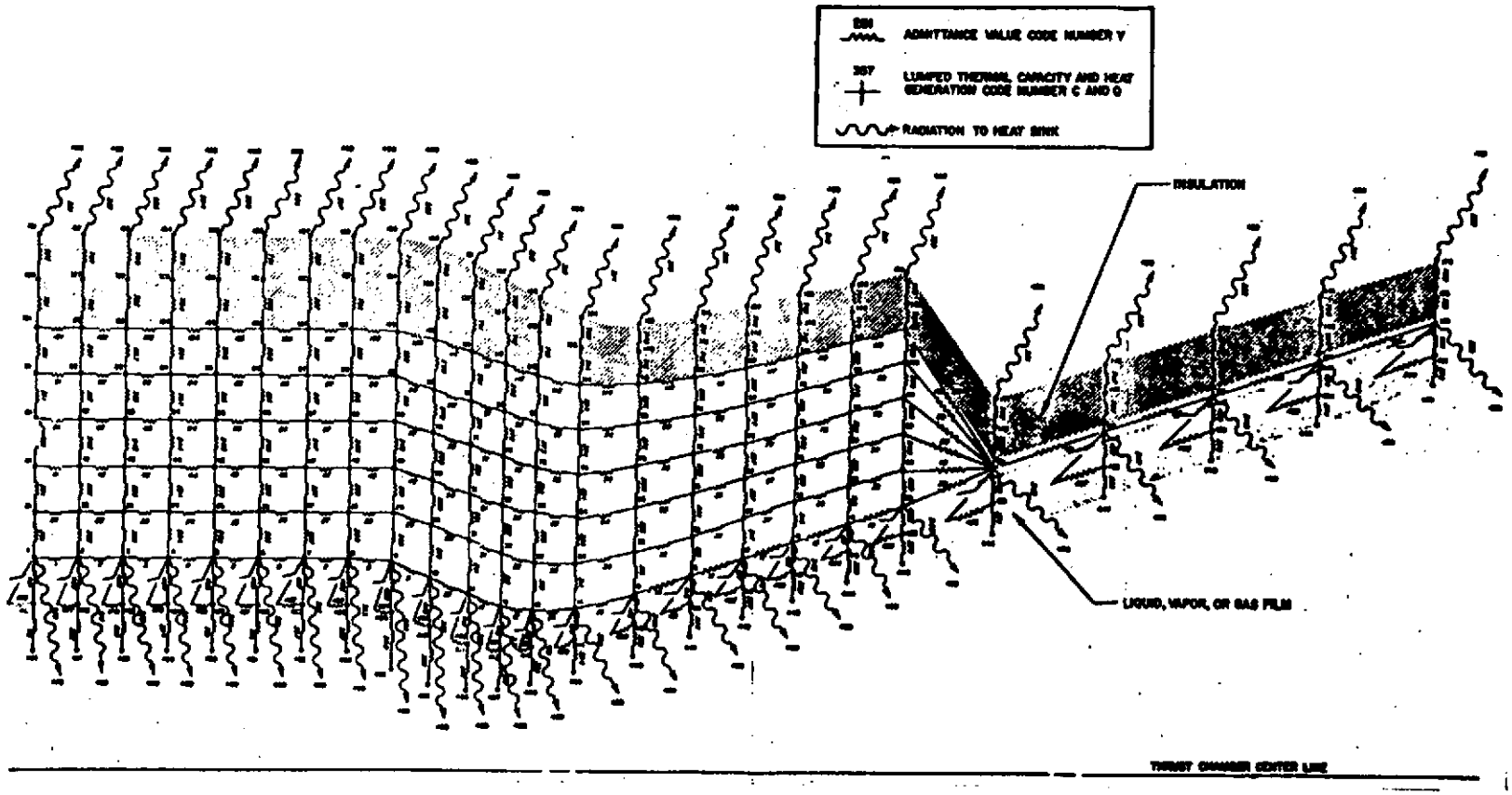

Figure 23. Nodal Network Representing a Thrust Chamber Cross-Section for Computing Axi-Symmetric Temperature Distributions by DEAP

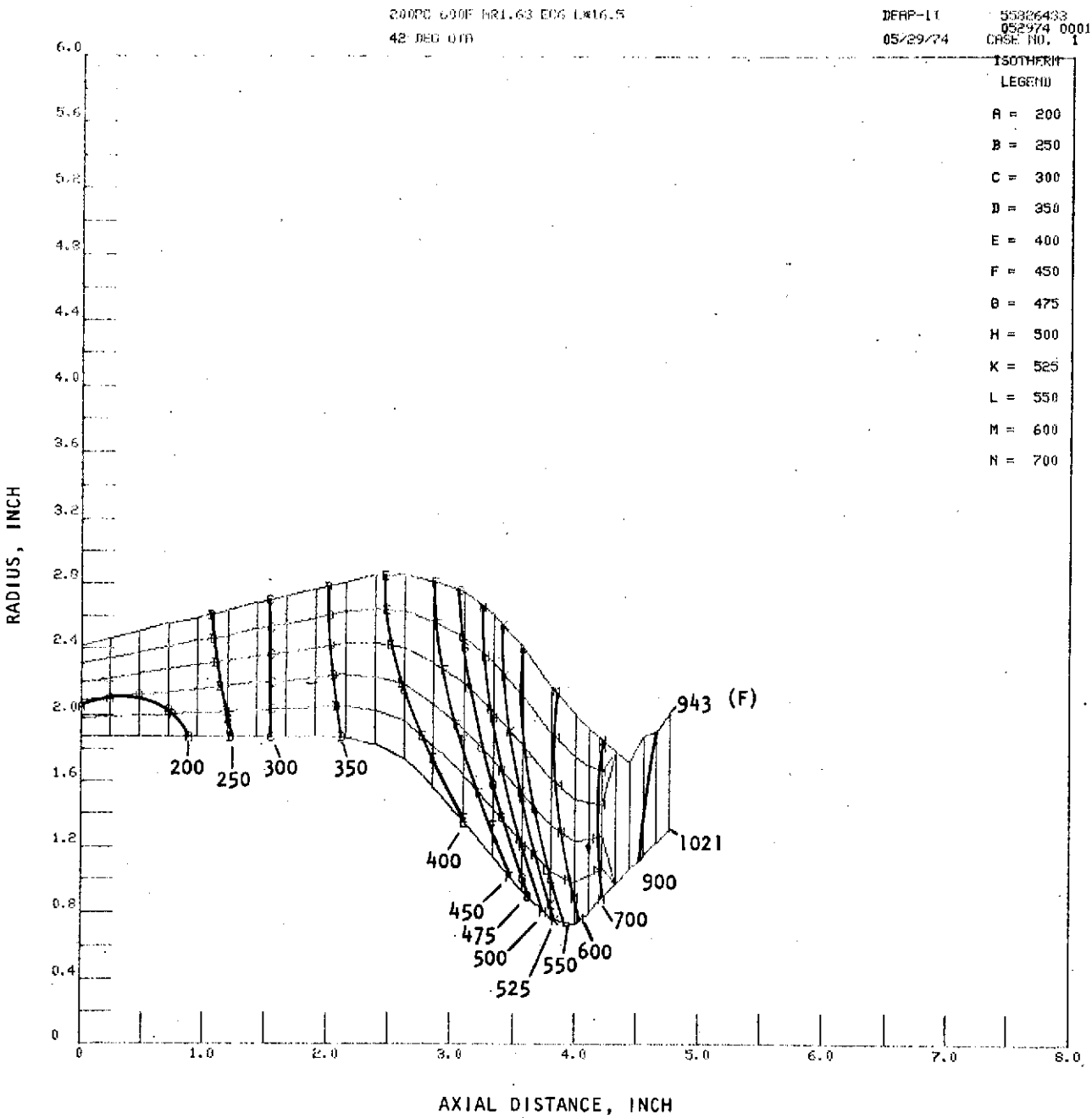

Figure 24. Durability Engine Predicted Isotherms - Steady State Condition

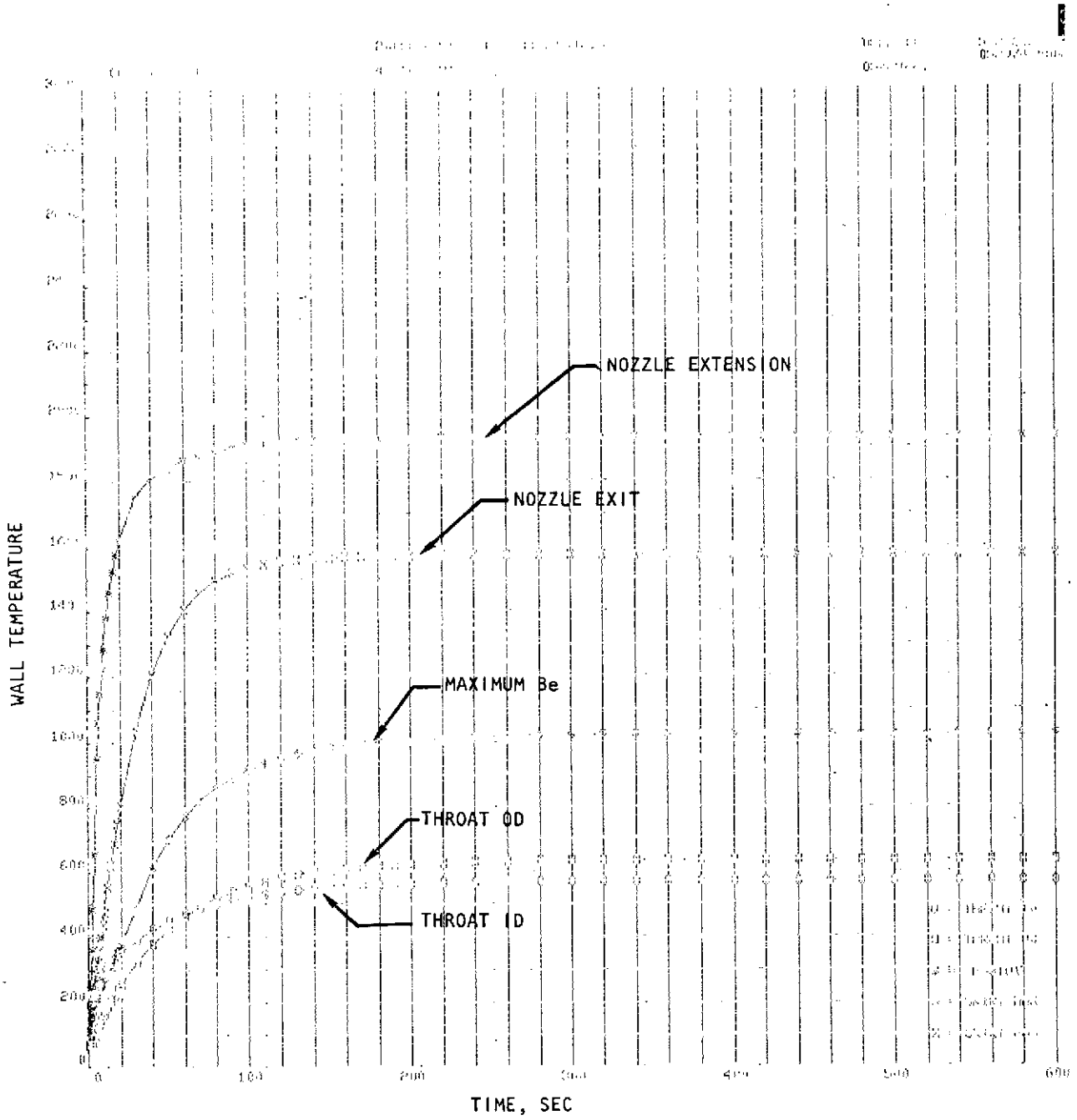

Figure 25. Durability Engine Predicted Temperature History

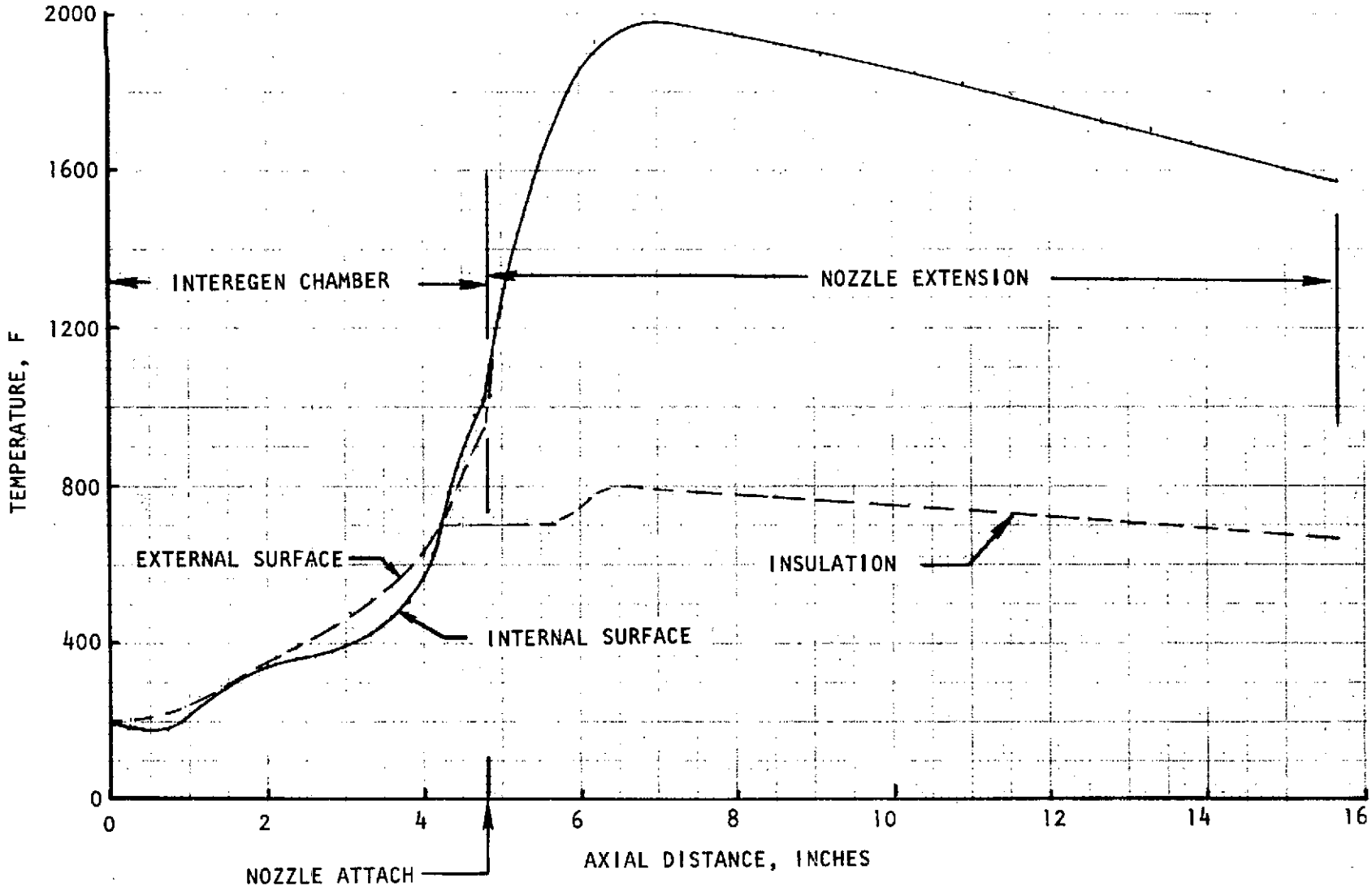

Figure 26. Durability Engine Predicted Temperature Profile Steady State Operating Conditions

The effect of saturated propellant on INTEREGEN cooling has been evaluated on the MM III, MM '71, and IR&D programs. Both He and GH_2 saturated propellants have been tested without any measurable affect on thermal characteristics.

Off-Limits Operation. Off-limits operation of the baseline advanced beryllium engine were performed for steady state operating effects. The design was analyzed for inlet propellant temperature of 75 ±35 F and inlet propellant pressure of 290 ±20 psia which produced a resultant range in mixture ratio of from 1.32 to 2.04 o/f. The results of the analysis are presented in Table 8, and it indicates a maximum beryllium temperature of 1475 F at the combined high mixture ratio and high inlet propellant temperature condition. INTEREGEN is predicted at all these off-limit conditions. The engine design was thermally analyzed to determine the effects of blowdown operation. These results are shown in Table 9.

Thermal Soakback. Thermal soakback from the thrust chamber to the injector-valve assembly by conduction, convection, and radiation was evaluated to determine maximum operating temperature. Temperatures must be maintained below 200 F at the propellant valve seat to ensure against propellant vaporization and subsequent pulse performance degradation.

A computer model of the engine assembly was developed for use with the Differential Equation Analyzer Program (DEAP) to determine thermal soakout temperature distributions. The model (shown in Fig. 27) uses 34 nodes to represent the thruster assembly and considers material thermal properties as a function of temperature and heat transfer by conduction, convection, and radiation. The predicted soakback thermal results for the baseline design are shown in Fig. 28. They illustrate the predicted soakout temperatures for the nozzle insulation, beryllium mass average, injector flange, valve seat, and valve body. The predictions show that the external temperature requirement of 800 F and 200 F maximum allowable valve seat temperature will be satisfied.

Streak Heating. Thermal analyses were conducted of the Durability Engine for a unit length section in the throat plane to determine the effects of no film cooling over a defined streak width. Thermal gradients were generated in the throat plane. The liquid and gas side film coefficient calculated at steady-state conditions in the INTEREGEN computer model used in the nominal operating conditions were used for the analysis. The fuel vapor film that covers the throat at steady-state conditions was assumed for the boundary condition except for the streak section. The boundary condition for the streak was adiabatic wall temperature, T_{AW} = 4315 F, and gas-side film coefficient, h_g = 0.0013 Btu/in.^{2}-sec-F. Since a streak could be the result of the absence of film cooling, main element fuel plugging (oxidizer on the wall), etc., various multiples of the gas-side film coefficient and streak width were considered.

The results of the analysis are presented in Fig.29 through 32. For a streak width of 0.5 inch with the nominal gas side heat transfer coefficient assumed, a radial temperature differential of 300 F is predicted at the streak location.

TABLE - 8. DURABILITY ENGINE PREDICTED OFF-LIMITS OPERATING EFFECTS

600 SECOND STEADY-STATE

CONDITION	PROPELLANT INLET TEMPERATURE, F		PROPELLANT INLET PRESSURE, PSIA		MR, O/F	TEMPERATURE THROAT OD, F	MAXIMUM BE, F	MAXIMUM NOZZLE, F
	OXIDIZER	FUEL	OXIDIZER	FUEL				
NOMINAL	75	75	290	290	1.63	635	1021	1972
HIGH TEMPERATURE	110	110	290	290	1.62	703	1114	1980
HIGH OXIDIZER, LOW FUEL PRESSURE →HIGH MR	75	74	310	270	2.05	952	1358	2019
LOW OXIDIZER, HIGH FUEL PRESSURE →LOW MR	75	75	270	310	1.32	499	696	1948
HIGH TEMPERATURE AND HIGH OXIDIZER LOW FUEL PRESSURE →HIGH MR	110	110	310	270	2.05	1064	1465	2071

TABLE 9. DURABILITY ENGINE PREDICTED BLOWDOWN OPERATING EFFECTS

600 SECOND STEADY-STATE

PROPELLANT TEMPERATURE = 75 F, MR = 1.63 O/F

CONDITION	PROPELLANT INLET PRESSURE, PSIA		TEMPERATURE, F THROAT OD	MAXIMUM BE, F	MAXIMUM NOZZLE, F
	OXIDIZER	FUEL			
NOMINAL P_C 200	290	290	635	1021	1972
P_C 150	207	207	630	982	1902
P_C 100	126	126	644	947	1793
P_C 50	57	57	376	427	1592

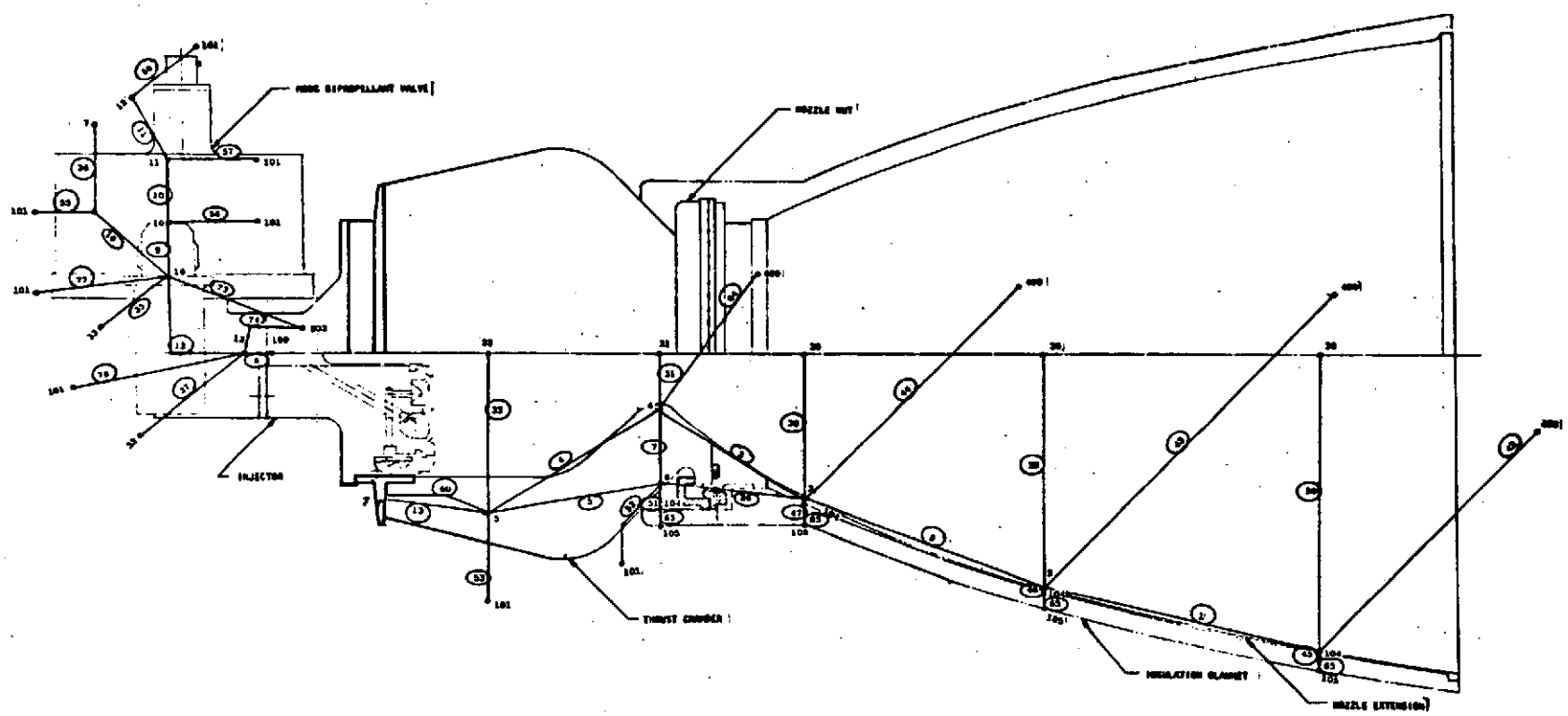

Figure 27. Thermal Soakback Model

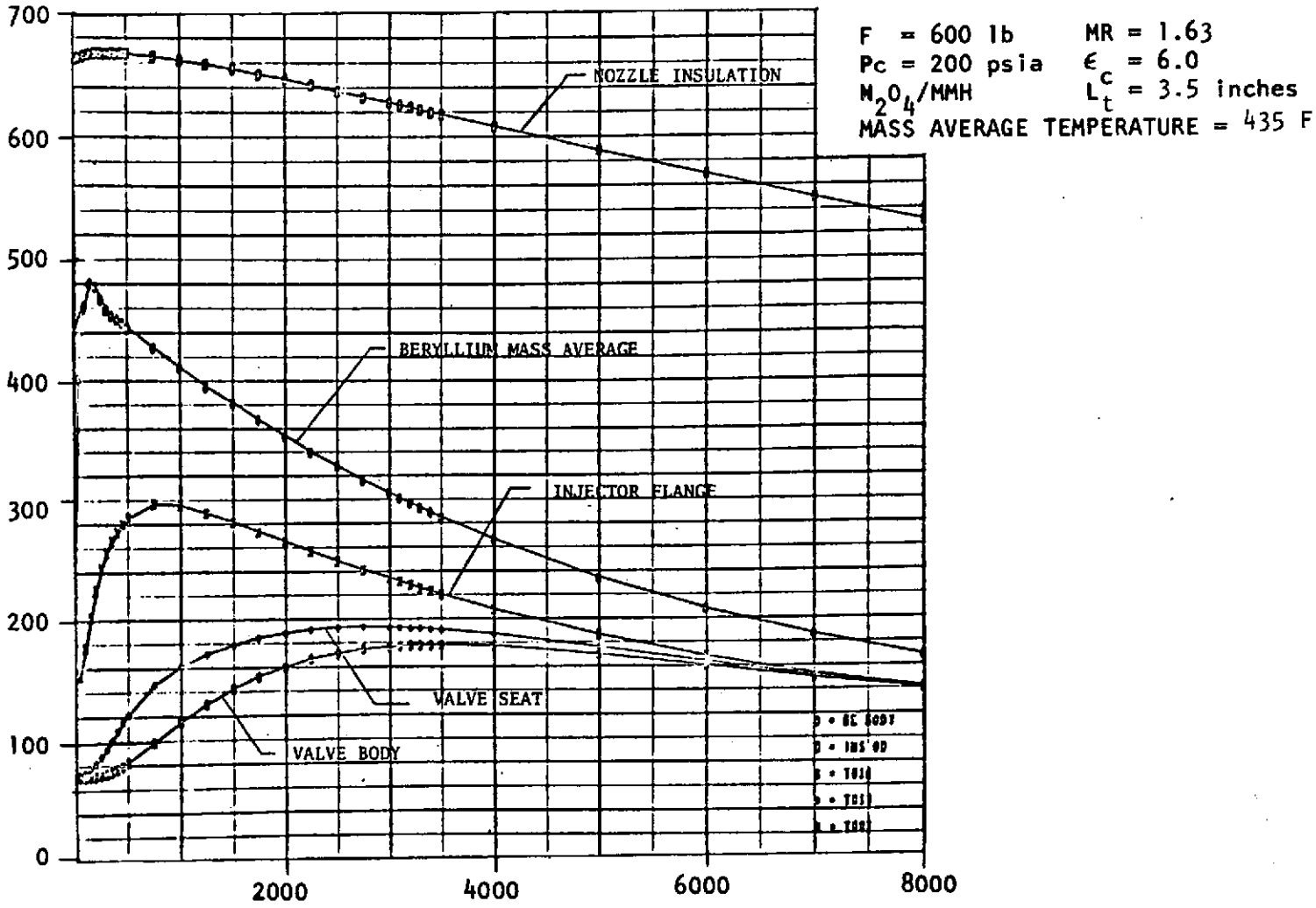

Figure 28. Soakback Analysis Predicted Temperature Response

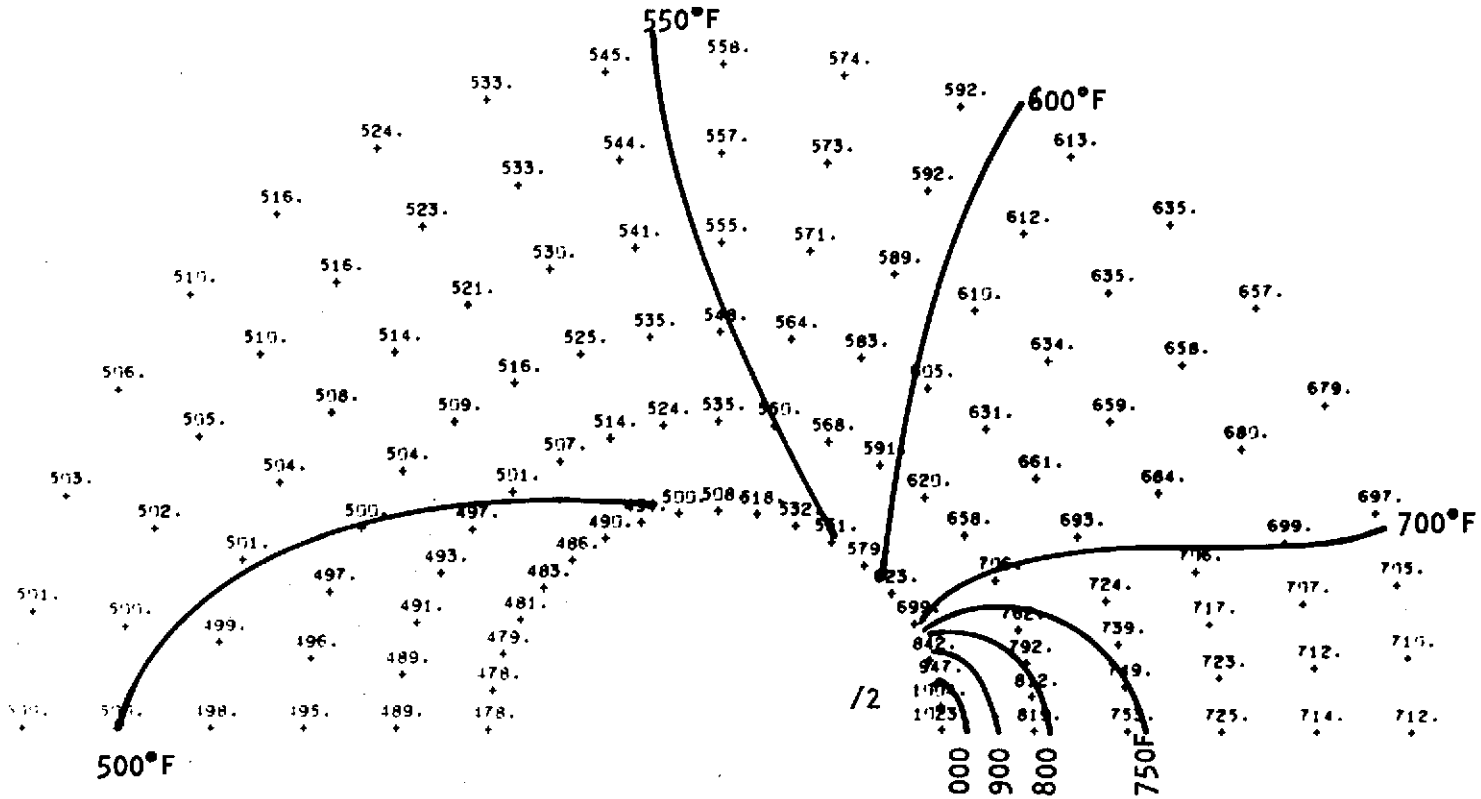

Figure 29. Temperature Distribution in Throat Section of Beryllium RCS Chamber with Film Coolant Loss

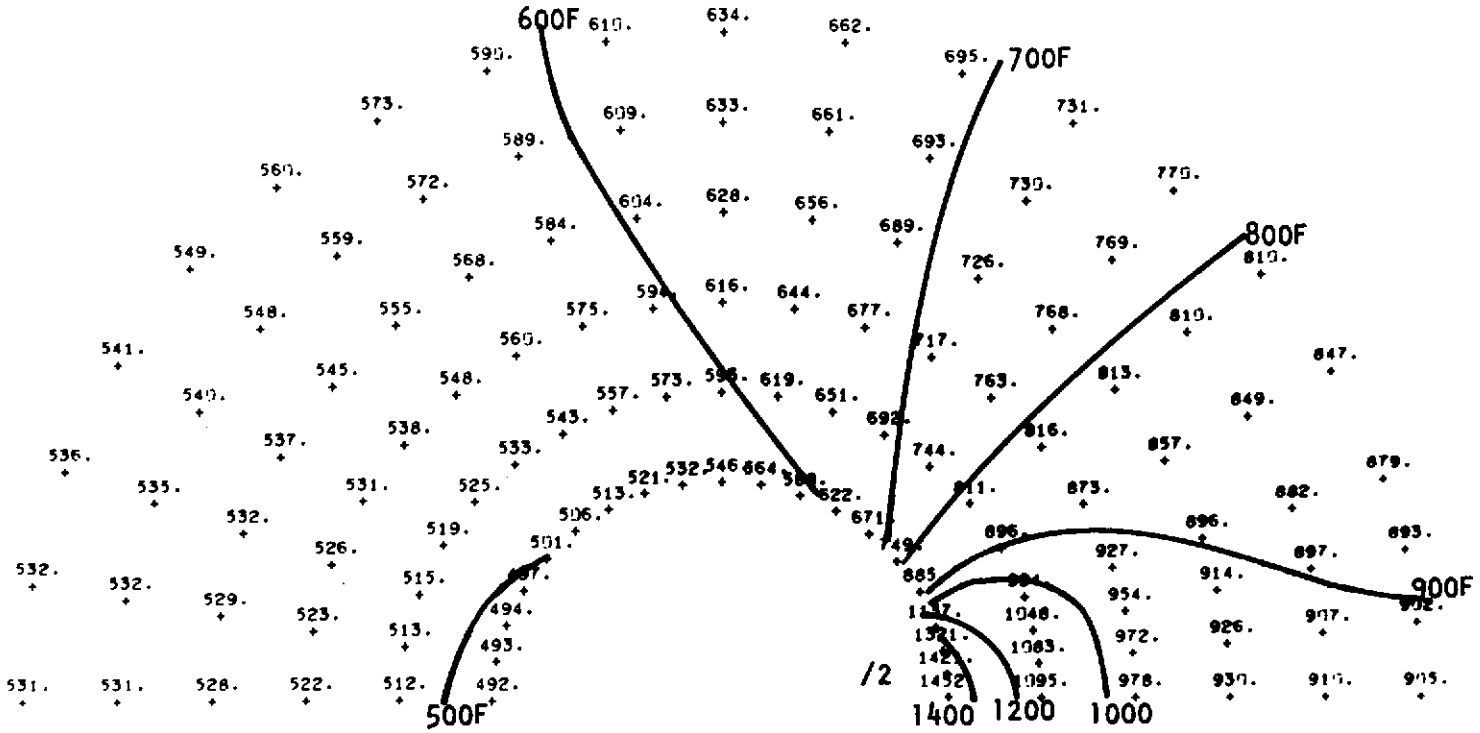

NOMINAL STREAK CONDITIONS

HEAT FLUX = TWICE NO FILM COOLING CASE

T_{AW} = 4315°F

$h_g = 0.0026 \frac{BTU}{IN^2\text{-}SEC}$

STREAK WIDTH = 0.50"

Figure 30. Temperature Distribution in Throat Section of Beryllium RCS Chamber with Hot-Streak and Film Coolant Loss

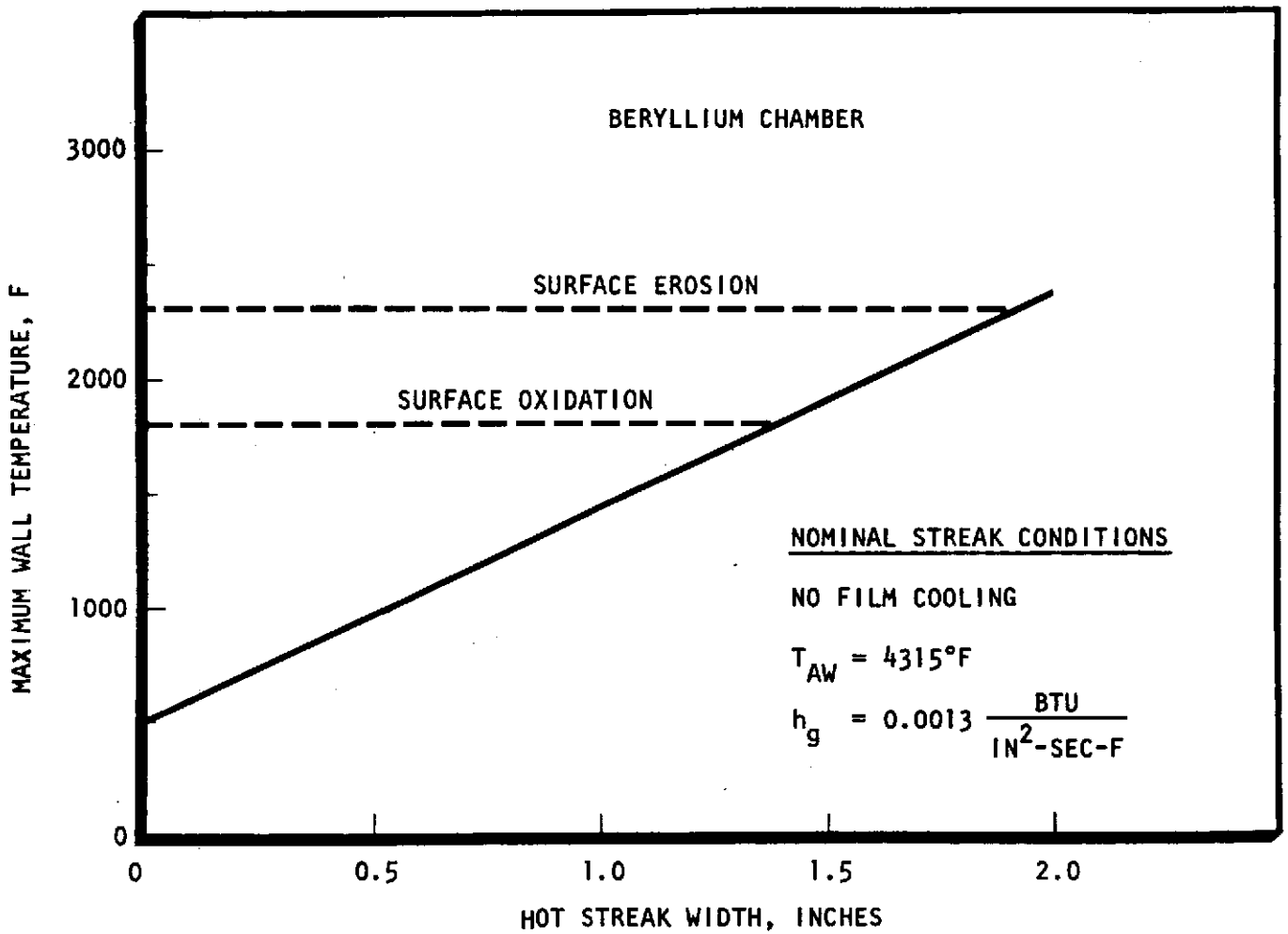

Figure 31. Effect of Hot-Streak Width on Throat Temperature

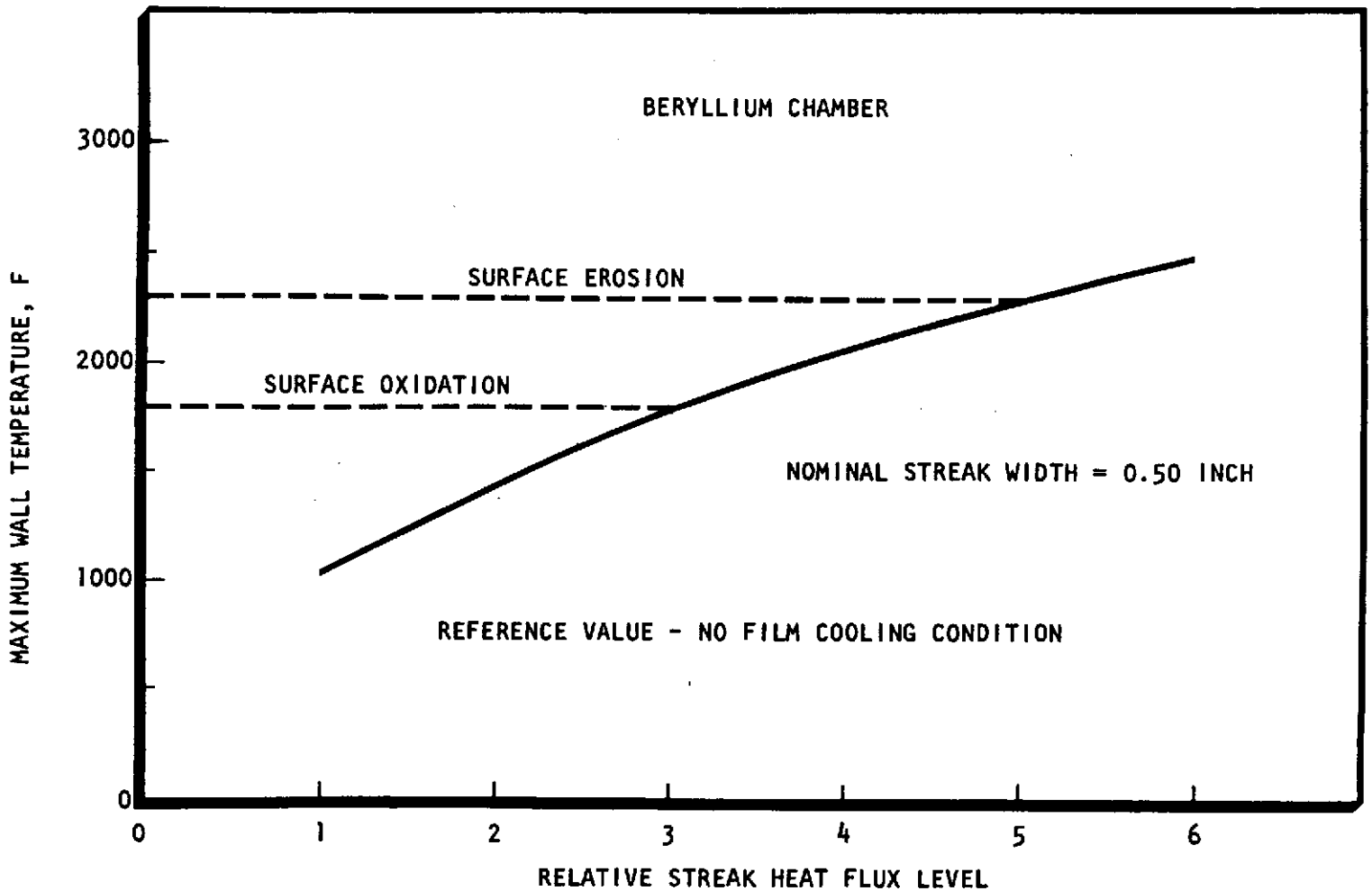

Figure 32. Effect of Relative Streak Heat Flux Level on Throat Wall Temperature

With a multiple of two on the coefficient, the differential is increased to 400 F. Beryllium throat oxidation occurs at approximately 1800 F and surface erosion at 2300 F. The results of the analysis indicate, Fig. 31, that with nominal gas-side heating, oxidation and surface erosion are predicted to occur with streak widths of 1.4 and 1.9 inch, respectively. With an assumed streak width of 0.50 inch, multiples of 3 and 5 on gas-side heat transfer coefficient are required for surface oxidation and erosion, respectively, according to Fig. 32.

Structural and Life Analysis

Pressure, thermal, and thrust loading as well as anticipated flight inertial loading were used in evaluating the structural and life requirements of the Durability Engine. Basic structural criteria consisted of maintaining a minimum yield safety factor of 1.2 and a minimum ultimate safety factor of 2.0 based on minimum guaranteed material properties and maximum primary stress with thermal, pressure, thrust, and inertia loads applied. A safety factor of 10 was used for all fatigue analyses.

Inertia Loading. The Durability Engine was analyzed to the shuttle vibration requirements shown in Table 1. These requirements were compared with vibration test values used for testing the Viking 1975 (VO '75) engine assembly. The shuttle requirements are considerably higher in magnitude at some frequencies. It was estimated that the engine may experience equivalent static inertia loads on the order of 2.5 times that found by test for the VO '75 engine. Lateral response was 57 g units for the nozzle and 40 g units for the nozzle/combustor assembly. Axial response was 144 g units. Therefore, the following inertial loading for the engine structural analysis was used:

Axial Inertia Loading	360 g units
Lateral Inertia Loading for the Nozzle	143 g units
Lateral Inertia Loading for the Combustor/Nozzle Assembly	100 g units

Injector. Structural analysis of the injector consisted primarily of a consideration of a loading condition resulting from a detonation of propellants in the manifolding. The criteria selected for this special condition was 20,000 psi burst pressure in either or both the oxidizer and fuel feed systems.

Nozzle Extension. The flight design nozzle extension was analyzed for anticipated flight inertia loading in accord with the vibration requirements. The weight of a thermal blanket was also included. The results indicate the nozzle extension wall can withstand the inertia levels.

Nozzle Extension Attach Nut. The nozzle extension attach nut joins the beryllium combustor to the nozzle extension. The nut is threaded to the nozzle extension flange and shoulders on the flange of the beryllium combustor. The thread diameter is approximately 4 inches. The nut is so designed to have a spring rate that will maintain proper clamping force on the joint under all operating conditions. The nozzle combustor joint is a flange type joint with a metallic "V" seal between the two flange faces. The joint and nut are subject to over 1000 F temperatures during operation as shown in Fig. 33.

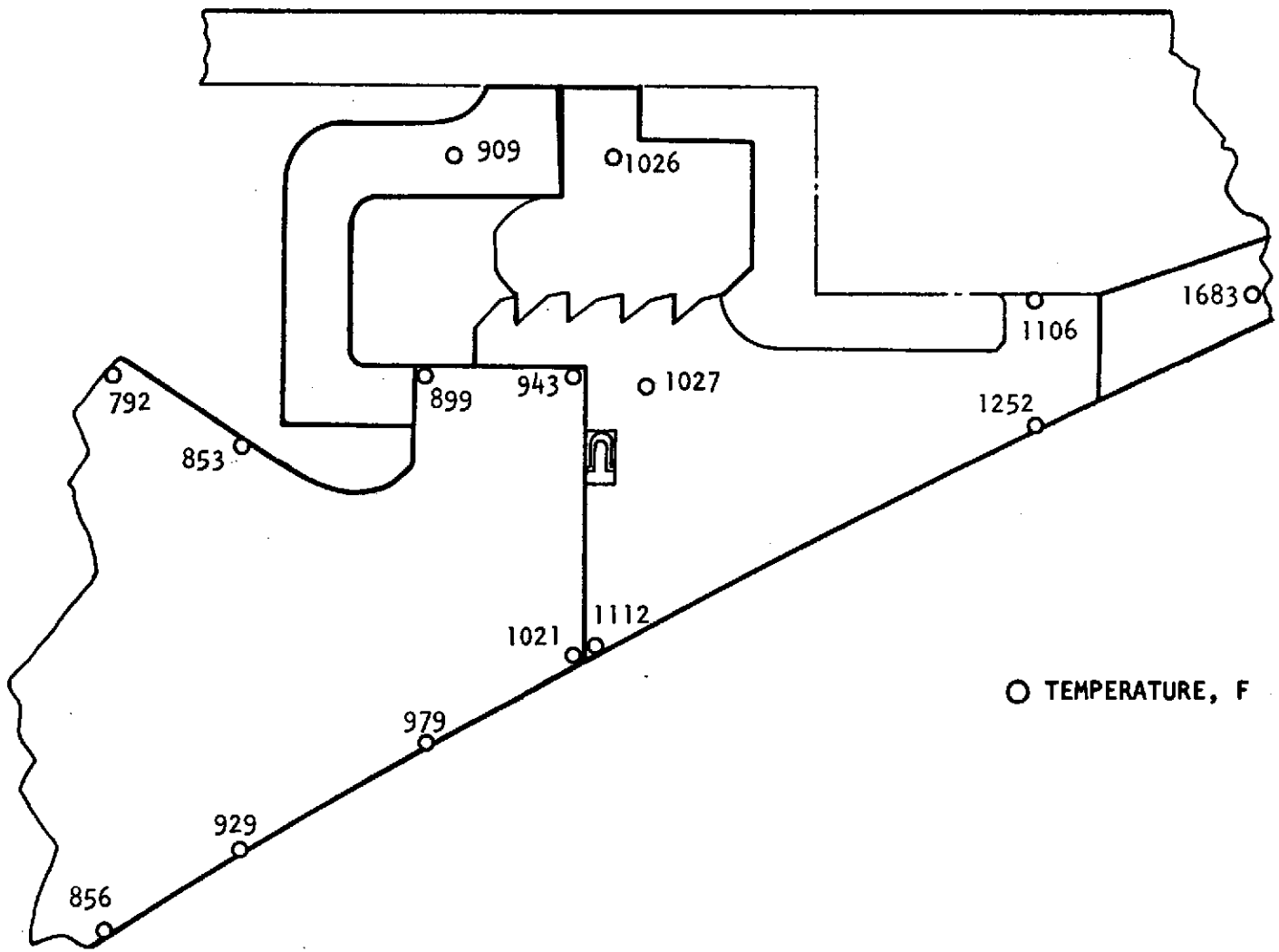

Figure 33. Beryllium Engine Chamber/Nozzle Joint Analysis

The nut and joint were designed to react to a seal load plus flight inertia loading, plus 10 percent overload for a ±5 percent tolerance preloading. The initial loading was at room temperature. At elevated temperature, the load is relieved, since the modulus of elasticity is reduced. There is an insignificant amount of stress induced because of differential thermal growth.

Rene' 41 was selected as the most suitable material to withstand 1000 F temperature and to have the most compatible thermal expansion rate with the joint flanges.

A low spring rate nut was required to attain the proper preloading of the joint within reasonable torqueing tolerance limits. The preload is controlled by rotation angle of the nut. A second need for the low spring rate is to allow for the differential thermal expansions without a large change in joint loading.

Injector to Chamber Joint. The finite element analysis method was selected for analysis of the chamber/injector braze joint. The nodal network of the joint is shown in Fig. 34. An elastic-plastic, finite element analysis was conducted for the brazed joint of Haynes-25 to the beryllium thrust chamber.

The analysis was conducted by applying increments or cycles of load that represent the sequence of condition that the joint undergoes:

1. As brazed configuration and cooling from 1650 to 70 F.
2. Final machined configuration of the brazed assembly.
3. 400 psia start transient pressure spike.
4. Steady state operation.
5. Soakback temperature.
6. 400 psia start transient pressure spike at soakback temperature.

The above load cycles were applied sequentially with the stress and strain conditions of each previous cycle carried over to the following cycle as shown in Table 10. Thus the cumulative effect was evaluated. For fatigue analysis, the stress and strain excursions that are repeated with cycles of operation are used.

These analyses have indicated the joint meets all structural and operational requirements.

Life Evaluation. A life evaluation of the beryllium combustor was conducted and the expected life found to be well within design goals.

A finite element model, Fig. 35, was prepared for the purpose of calculating thermal strain. The analysis logic is shown in Fig. 36. The property data are incorporated into the finite element model and duty cycle analyses are performed, Fig. 37, 38, and 39.

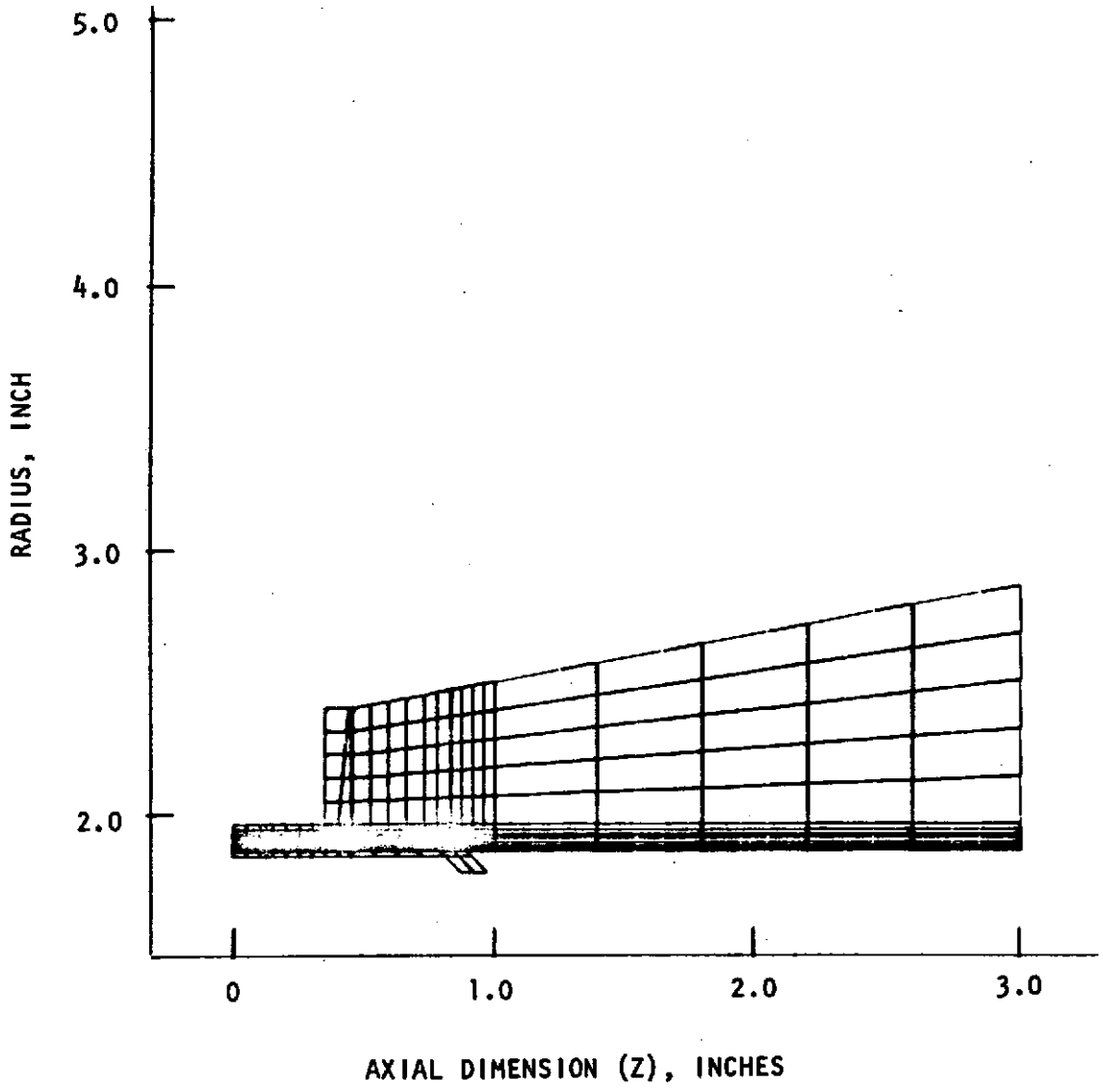

Figure 34. Injector/Chamber Braze Joint
Nodal Point Network

TABLE 10. BRAZE JOINT STRESS ANALYSIS

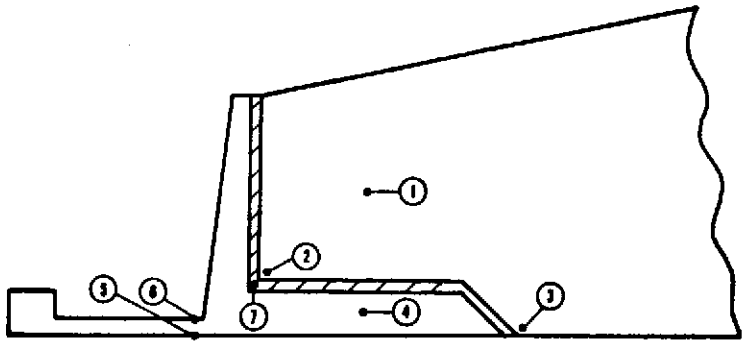

POINT	MATERIAL	AS FABRICATED STRESS, KSI	OPERATING STRESS EXCURSIONS	
			PLUS, KSI	MINUS, KSI
1(HOOP)	Be	5.97	2.01	1.80
2(MAX. PRIN.)	Be	24.83	1.86	7.21
3(MAX. PRIN.)	Be	-16.98	6.10	-
4(HOOP)	L - 605	-39.32	15.87	-
5(AXIAL)	L - 605	29.74	8.59	14.94
6(AXIAL)	L - 605	-34.58	30.49	-
7(EFF.)	BRAZE	13.61	0.34	8.90

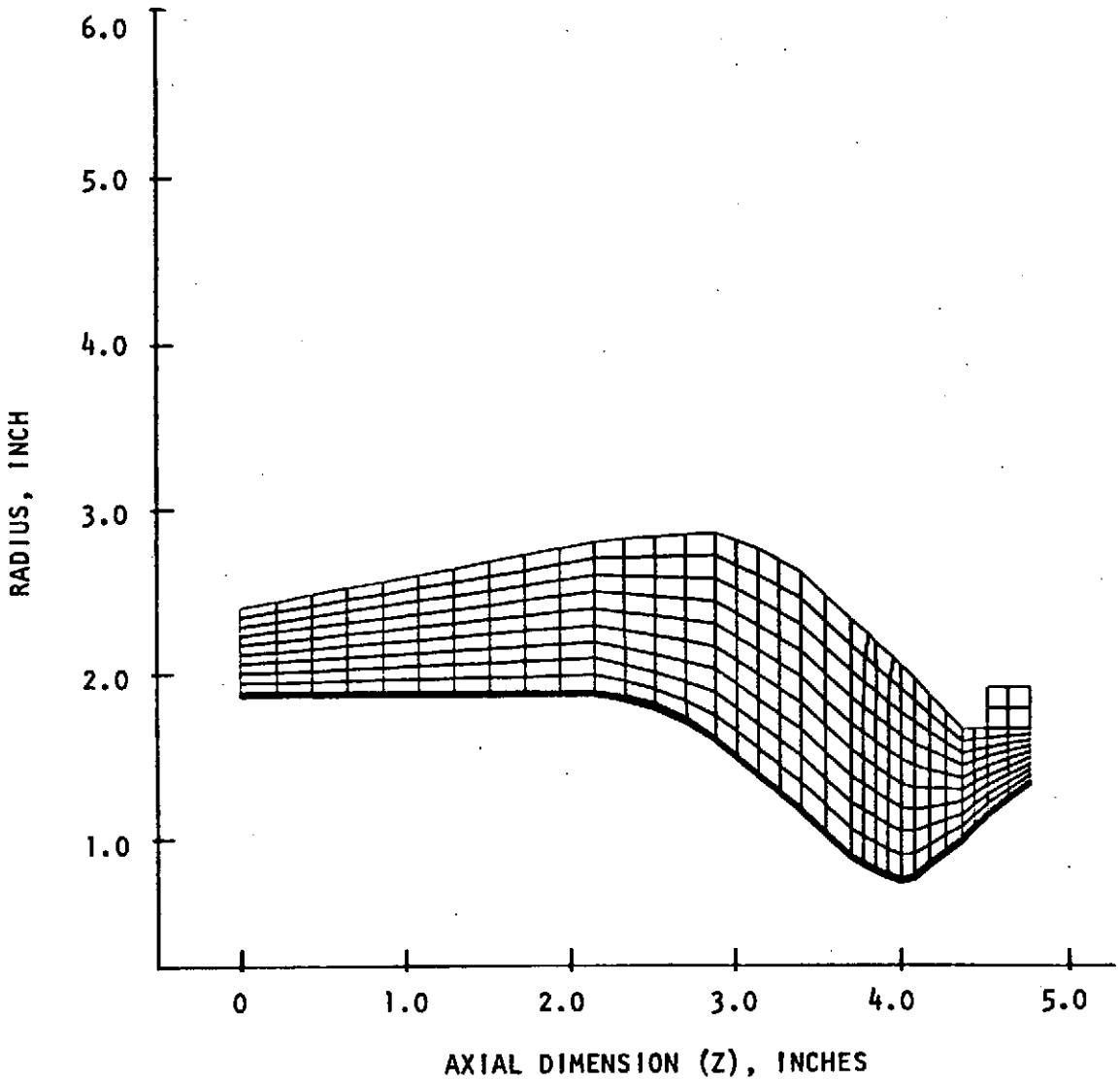

Figure 35. Beryllium Chamber Nodal Point Network

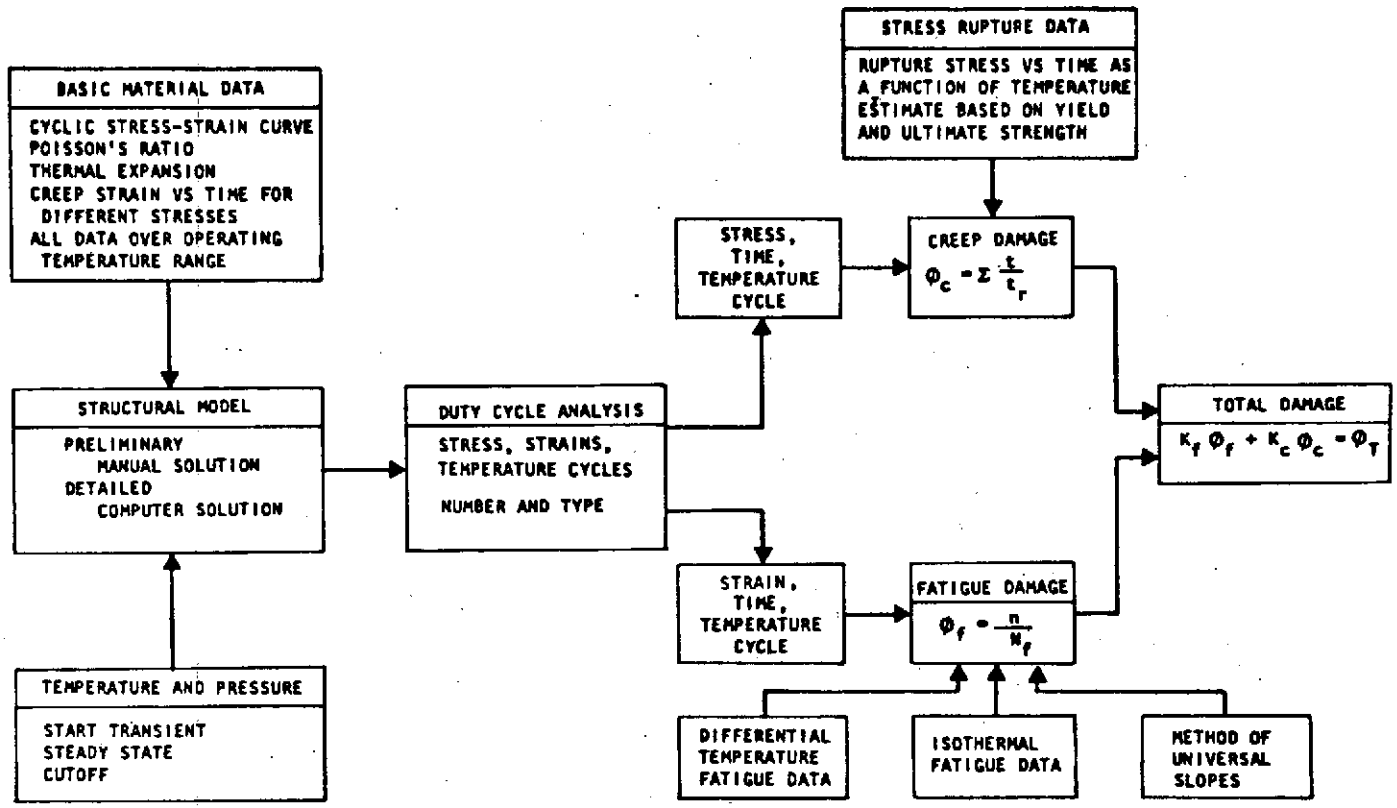

Figure 36. Life Analysis Logic

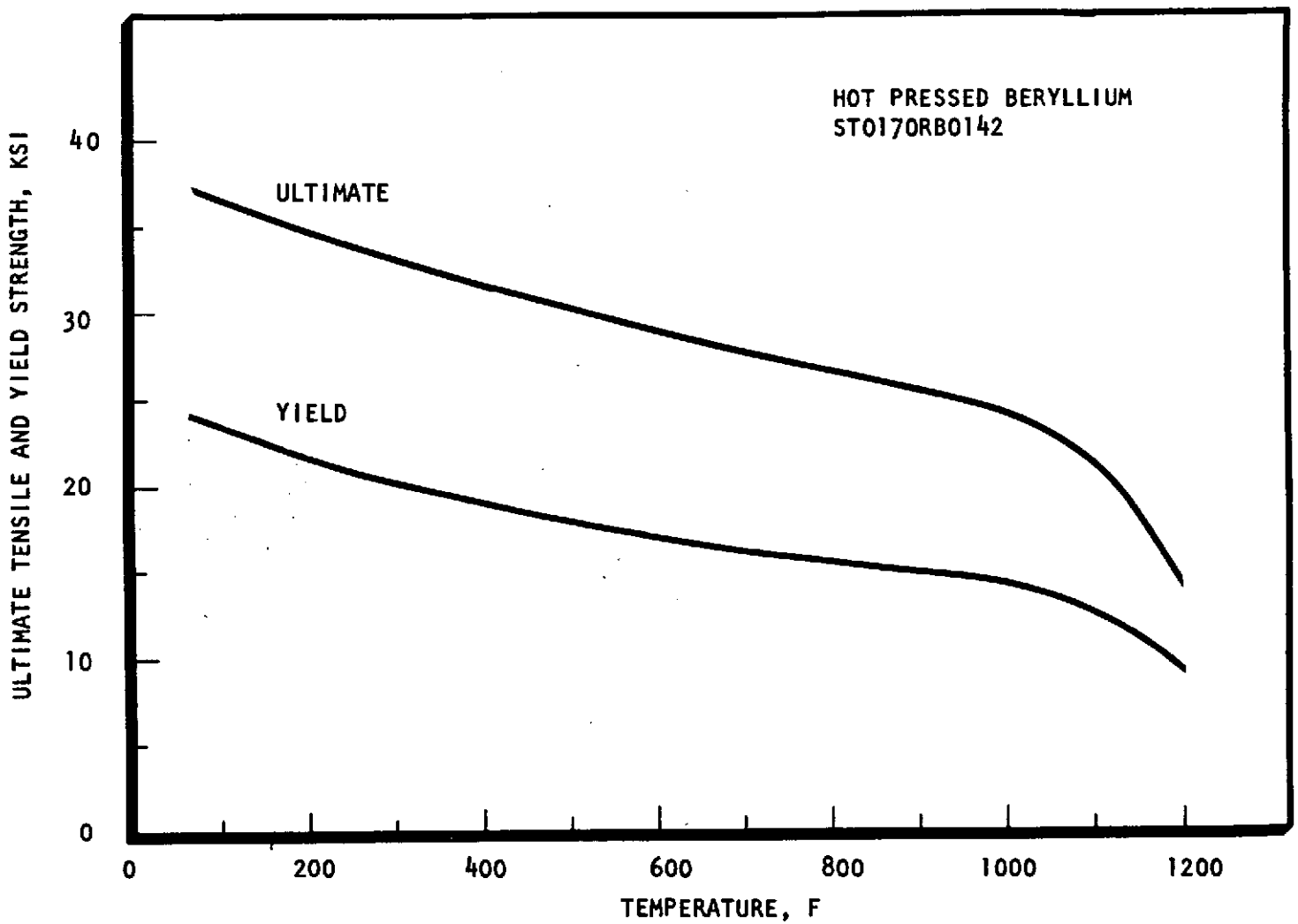

Figure 37. Beryllium Minimum Tensile Strength Properties

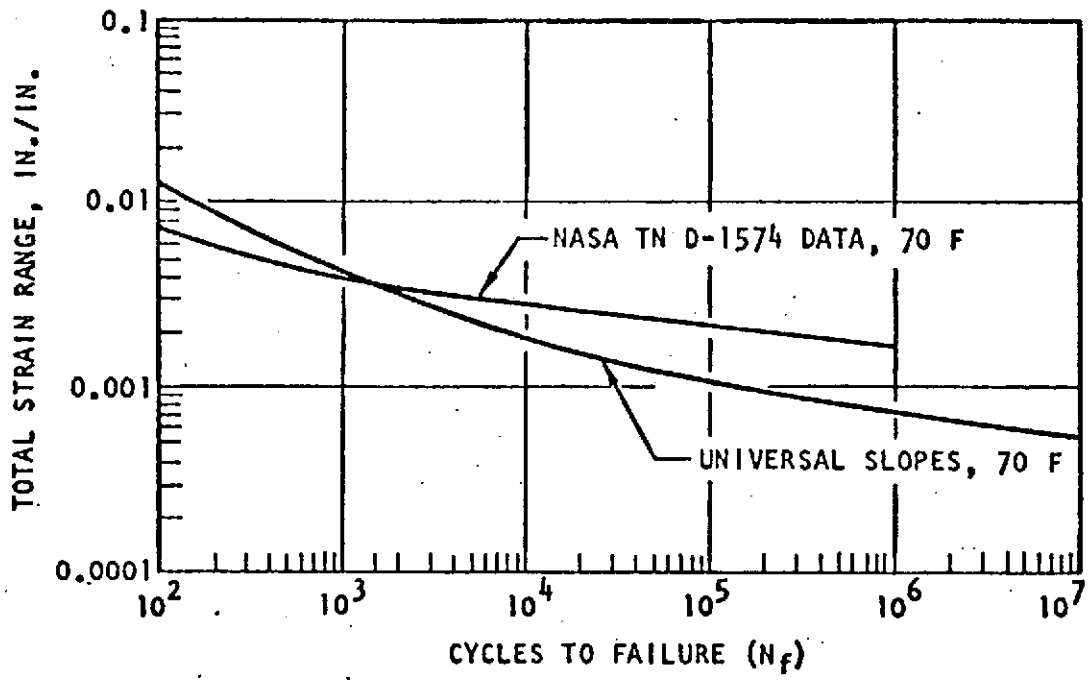

Figure 38. Beryllium Fatigue Data - Room Temperature

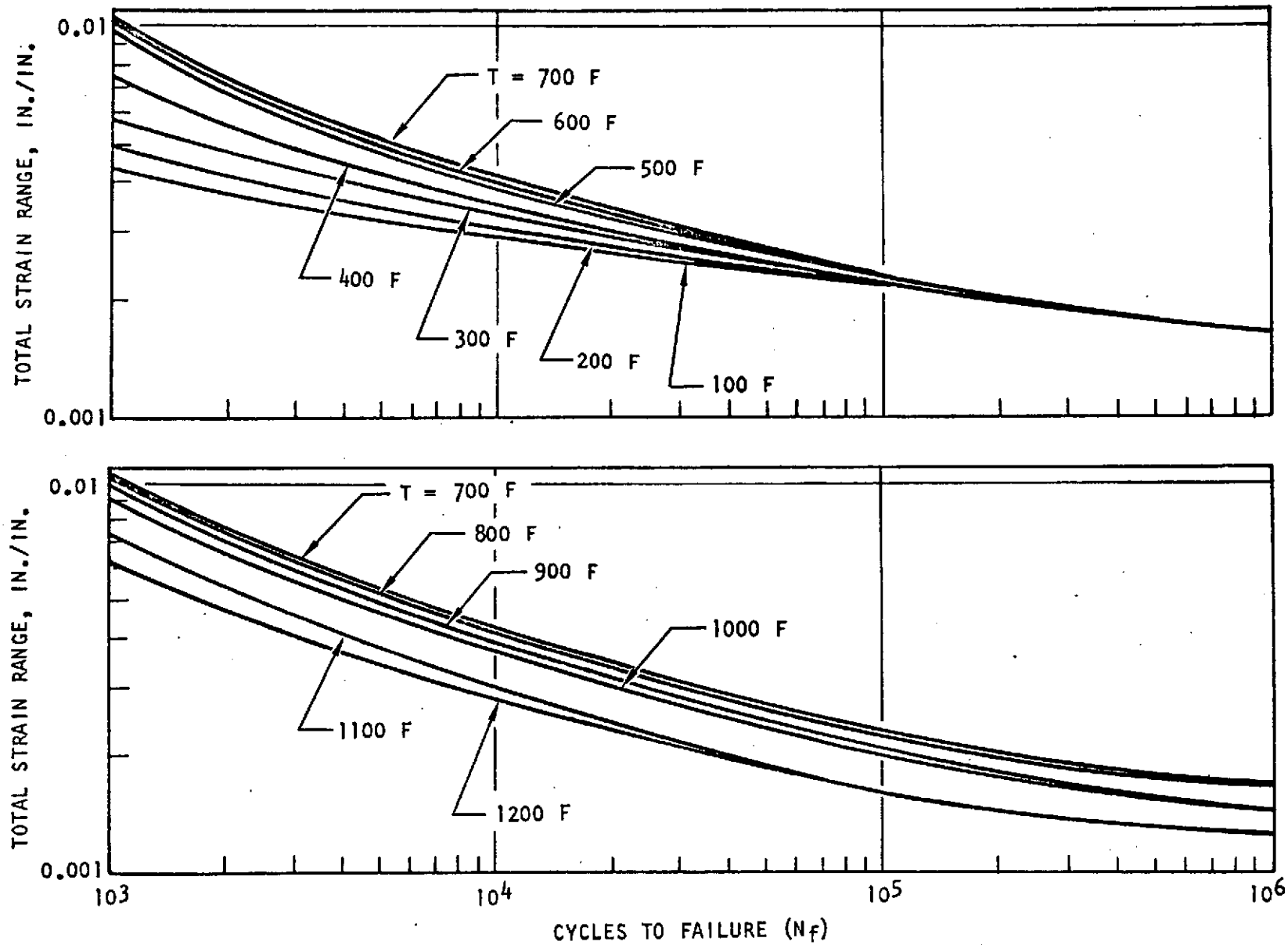

Figure 39. Beryllium Fatigue Data - Universal Slopes Data Adjusted with NASA TMD-1574 Data

The fundamental theory used in the life prediction analyses is that failure depends on the accumulation of creep damage and fatigue damage. In equation form, this is expressed as:

$$(S.F.) \times (\phi_f + \phi_c) \leq 1$$

This equation was expanded as follows to facilitate the life evaluation:

$$(S.F.)_1 (\phi_{fp} + \phi_c) + (S.F.)_2 \phi_{fF} \leq 1$$

where

$(S.F.)_1$ = 10
ϕ_c = zero (creep damage is negligible)
ϕ_{fp} = pulse cycle fatigue damage
$(S.F.)_2$ = safety factor for full thermal cycles
ϕ_{fF} = full thermal cycle fatigue damage

A study of thermal gradients developed during pulsing, Fig. 40, indicated that the strain excursions for individual pulses will be below the elastic limit of beryllium and therefore a fatigue capability on the order of the endurance limit is expected (10^7 cycles) for pulse mode operation. A train of pulses is equivalent to one full thermal cycle whose equivalent steady firing time is approximately equal to the accumulated pulse-on time. The damage fraction for pulsing is:

$$\phi_{fp} \text{ pulse} = n/N_{fp}; \; n = 200{,}000; \; N_{fp} = 10^7; \text{ and } \phi_{fp} = 0.02$$

$$(S.F.)_1 (\phi_{fp} + \phi_c) = 0.2$$

thus it is seen that

$$(S.F.)_2 \phi_{fF} \leq 0.8$$

it can further be considered that

$$(S.F.)_2 \phi_{fF} = \frac{N_F}{N_{fF}} = 0.8$$

where

N_F = number of full thermal cycles
N_{fF} = number of full thermal cycles to cause failure if no other material damage occurred

The cycles to failure plotted in Fig. 41 are N_F as defined above.

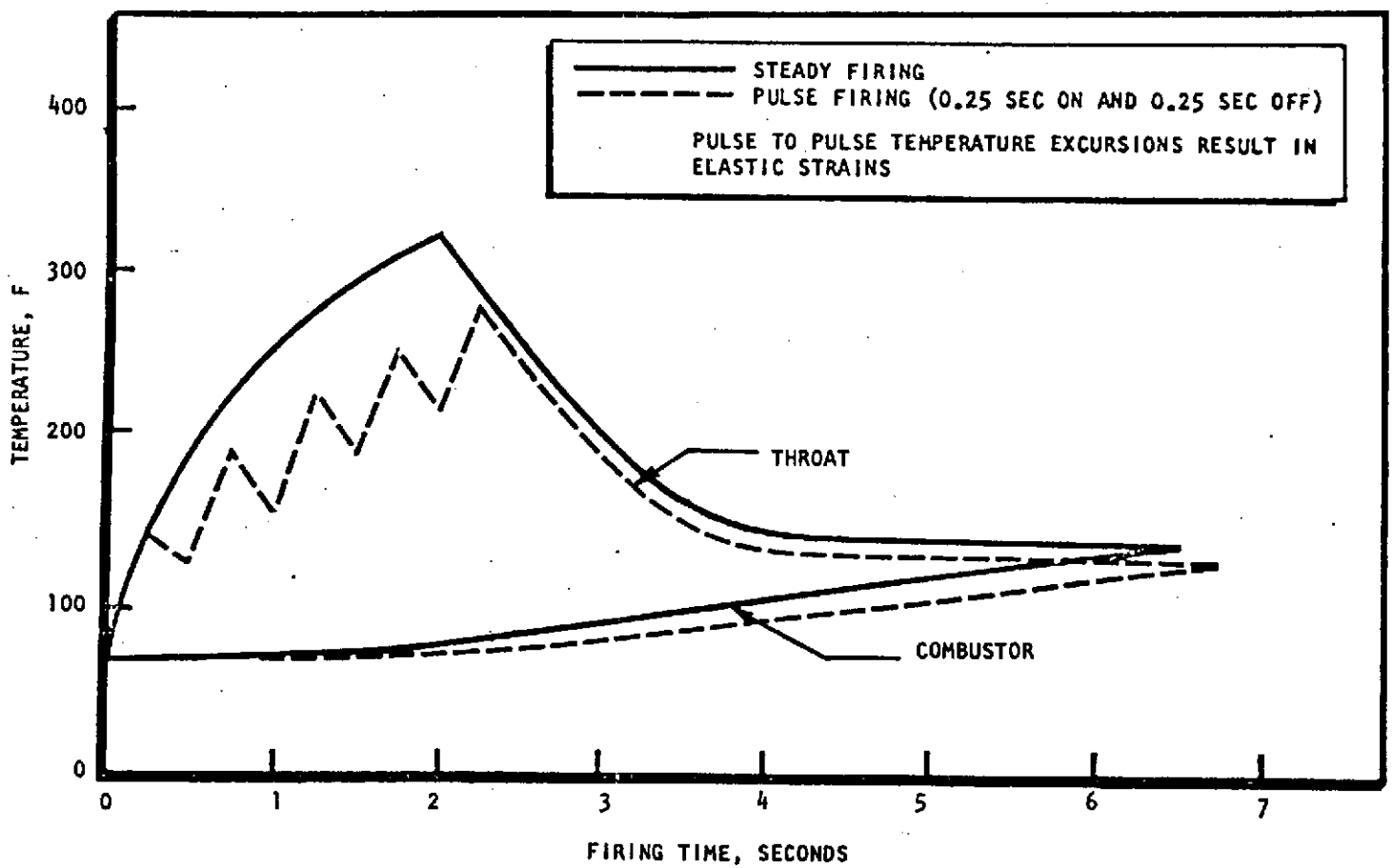

Figure 40. Duty Cycle Definition

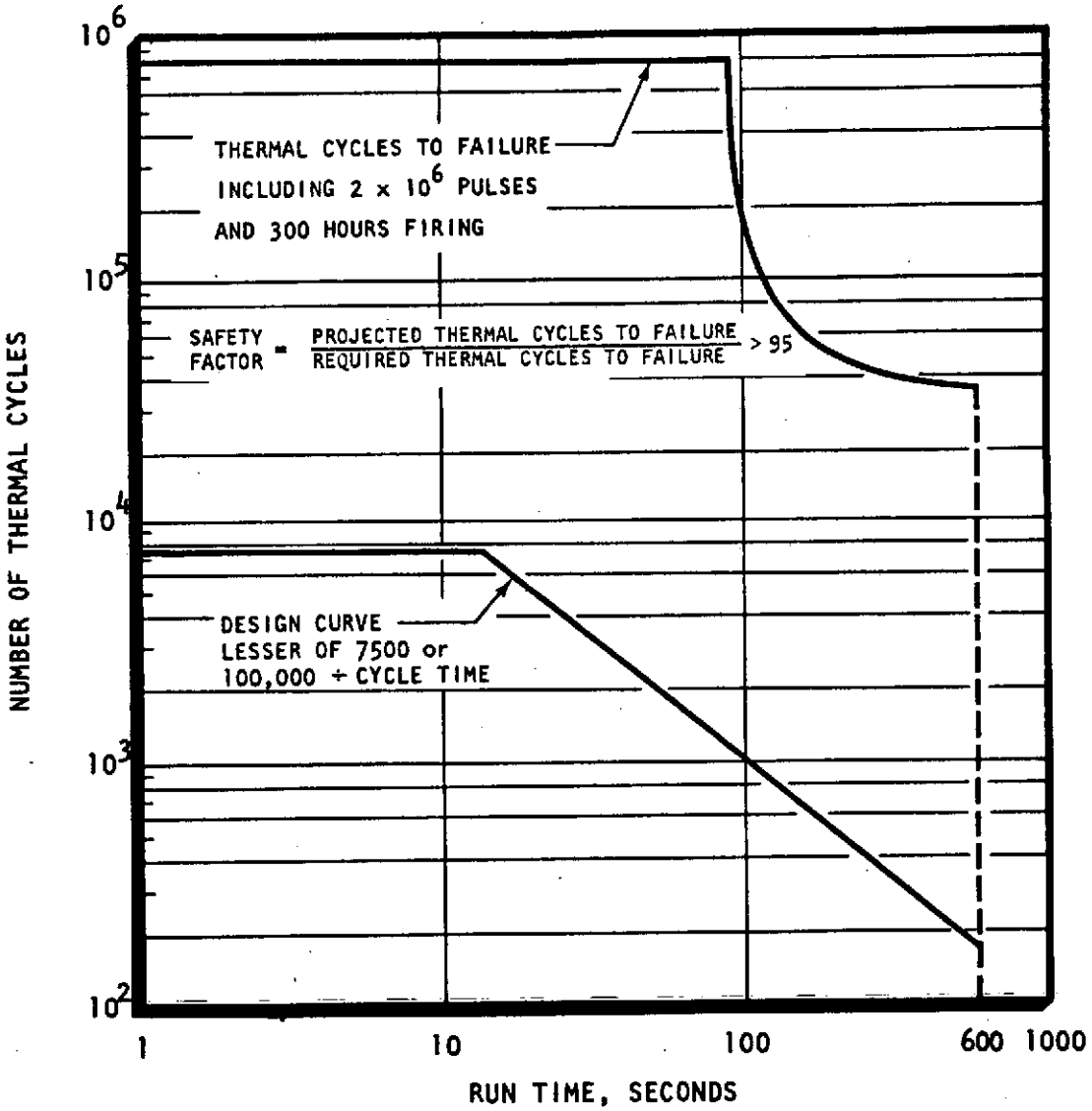

Figure 41. Durability Engine Cycle Life

The iso-strains shown in Fig. 42 are for steady-state operating conditions. It shows the highest strain for any time in the firing of the engine and maximum strain is less than 0.25 percent.

Hydraulic Analysis

A complete hydraulic analysis of the valve and injector (also effects of feed system) was conducted. The effects of system, valve and injector were included in the pulse analysis presented in a preceding section of this report. The pressure drops, flow splits, flow velocities, and passage volumes are presented here.

Each passage of the injector was analyzed for pressure drop, velocity, and volume. The passages were analyzed in sections as shown in Fig. 43(a) and (b) for nominal flow conditions; namely, 200 psia chamber pressure (nozzle stagnation), 1.63 o/f mixture ratio, 1.26 lb/sec oxidizer flowrate, 0.77 lb/sec fuel flowrate, and 75 F propellant temperature.

The results of the analysis are presented in Table 11. The analysis indicates that the injector orifice maximum oxidizer and fuel velocities of 66 and 83 ft/sec will be attained at the design orifice pressure drop of 40 psia. In the injector design, manifold losses were limited to 10 psid with maximum velocities of 22 ft/sec. The manifold total volume is 1.366 cubic inches.

A summary of the engine hydraulic characteristic is shown in Table 12.

Injector Cold Flow Calibration. Each of the injection orifices was individually calibrated. Flow through each orifice was determined as a percent of the total flow through each propellant system. The results are presented in Table 13 and shows that the distribution of flow for the BLC and injection rings are very close to the expected values. The resultant mixture ratios and BLC are shown in Table 14. The BLC flow is 40.8 percent of the fuel flow, and the outer, middle, and inner ring mixture ratios are 3.20, 2.23, and 2.18 o/f, respectively. This compares favorably to the design values of 40 percent BLC and outer, middle, and inner mixture ratios of 3.05, 2.30, and 2.31 o/f, respectively.

Design Pressure Profile. The design pressure profile for nominal conditions, 200 psia chamber pressure and 1.63 o/f mixture ratio, is shown in Fig. 44. It is based on the company sponsored hot-fire calibration pressure drops for the injector and 30 psid nominal design valve pressure drop. It includes 11.4 and 12.5 psid calibration orifices, oxidizer, and fuel sides, respectively.

Combustion Stability Analysis

The two common instability modes (1) feed system coupling, and (2) acoustic, have been considered in the engine design.

The primary consideration for feed system coupling are the available injector pressure drop (relative to chamber pressure), engine physical size, and propellant combination. Table 15 compares engine configurations, developed for use with

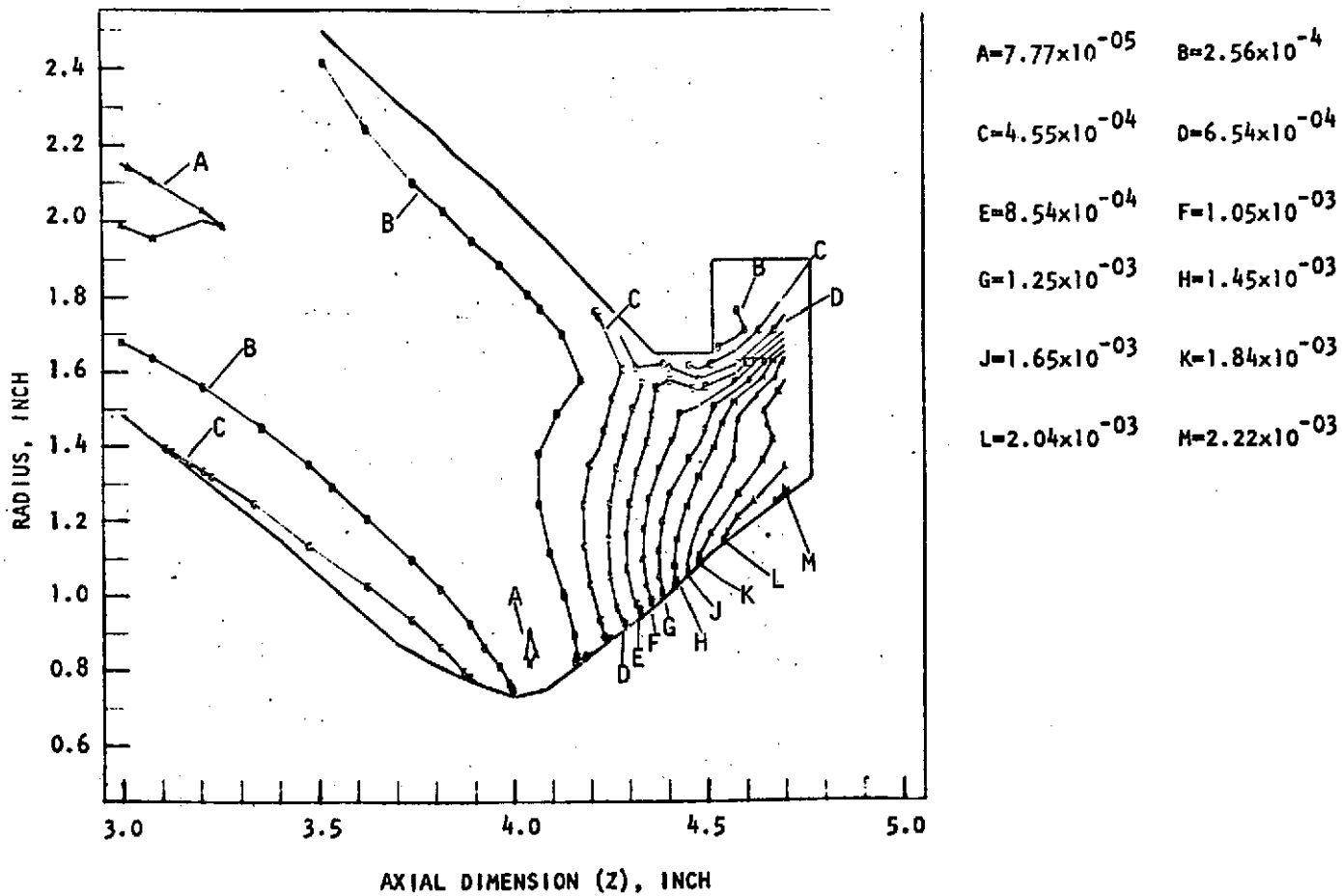

Figure 42. Effective Beryllium Steady-State Iso-Strain Plot

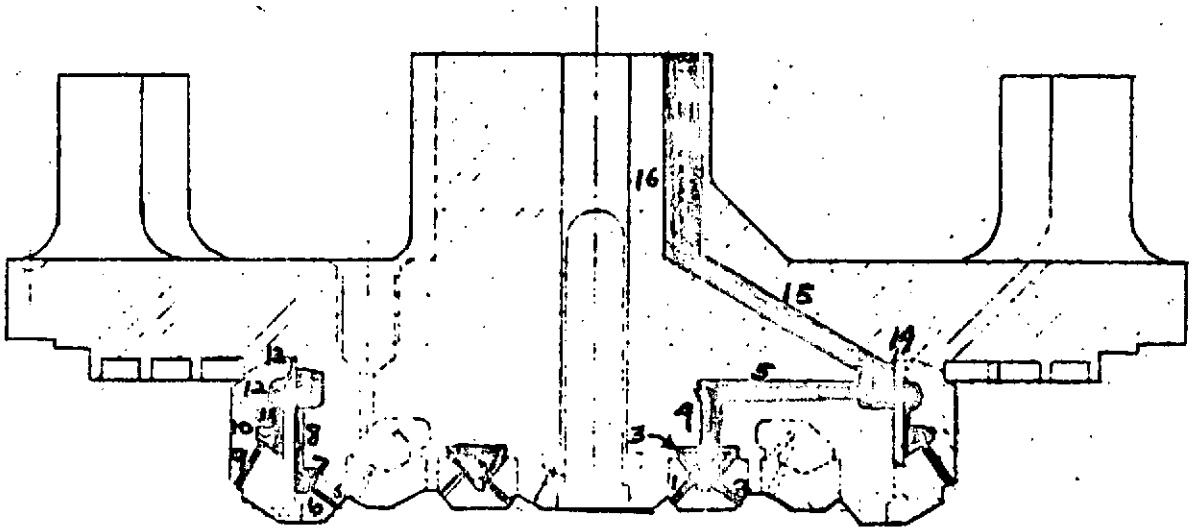

(a) Fuel Side

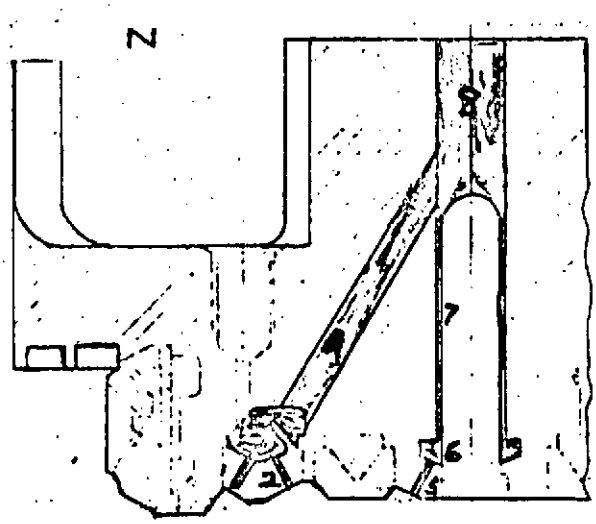

(b) Oxidizer Side

Figure 43. Durability Engine Three-Ring Injector Hydraulics

TABLE 11. DURABILITY ENGINE INJECTOR HYDRAULIC ANALYSIS SUMMARY

	Zone*	W lb/sec	ΔP Loss psi	ΔP Total psi	Velocity fps	Volume in^3
FUEL						
• Inner & Middle Elements	1 & 2	0.1995	36.6	36.6	79	0.0012
	3	"	0.1	36.7	3	0.0697
	4	"	2.2	38.9	20	0.0082
	5	"	2.1	41.0	20	0.0217
• Outer Elements	6	0.2645	40.6	40.6	83	0.0021
	7	"	0.1	40.7	3	0.0211
	8		0.3	41.0	8	0.0179
• BLC	9	0.3093	11.3	11.3	44	0.0058
	10	"	0.1	11.4	4	0.0202
	11	"	0.5	11.9	9	0.0090
	12	"	0.9	12.8	12	0.0564
	13	"	28.2	41.0	69	0.0016
• Injector Feed	14	0.7733	1.3	42.3	15	0.2610
	15	"	2.4	44.7	20	0.1182
	16	"	2.8	47.5	22	0.0986
						0.7127
OXID						
• Outer & Middle Elements	1 & 2	1.0984	39.6	39.6	64	0.0068
	3	"	0.3	39.9	6	0.2530
	4	"	3.7	43.6	20	0.1362
• Inner Elements	5	0.1575	42.4	42.4	66	0.0315
	6	"	0.1	42.4	2	0.1189
	7	"	1.2	43.6	11	0.0282
• Feed	8	1.2606	4.6	48.2	22	0.0790
						0.6536
						1.3663

* Refer to Figure 43a and 43b

TABLE 12. DURABILITY ENGINE HYDRAULIC CHARACTERISTICS

SUMMARY

MOOG Valve-54-109		
Manifold Volume, in^3		
Oxidizer		0.134
Fuel		0.134
Injector - Fuel Configuration		
Manifold Volume, in^3		
Oxidizer		0.6536
Fuel		0.7127
Maximum Velocity, ft/sec		
Manifold Oxidizer		22
Manifold Fuel		22
Injection Orifice Oxidizer		66
Injection Orifice Fuel		83
Pressure Drop, psid		
Manifold	approx	10
Orifice	approx	40

TABLE 13. DURABILITY ENGINE INJECTOR FLOW DISTRIBUTION

		PERCENT OF EACH PROPELLANT FLOW						
		ORIFICE FLOW						
SYSTEM	RING	AVE	MIN	MAX	σ	TOTAL MEASURED	HYDRAULIC ANALYSIS	DESIGN VALUE
Oxidizer	Outer	1.99	1.90	2.39	0.07	63.6	62.8	62.5
Oxidizer	Middle	1.46	1.41	1.54	0.02	23.3	24.2	24.4
Oxidizer	Inner	1.64	1.58	1.77	0.06	13.1	13.0	12.1
Fuel	BLC	1.28	1.03	1.49	0.07	40.8	-	40.0
Fuel	Outer	1.02	0.92	1.18	0.06	32.4	33.7	33.4
Fuel	Middle	1.07	0.97	1.19	0.06	17.0	17.0	17.3
Fuel	Inner	1.21	1.08	1.29	0.05	9.8	8.6	9.3

TABLE 14. DURABILITY ENGINE INJECTOR FLOW CALIBRATION

	DESIGN	WATER CALIBRATION
OUTER RING, O/F	3.05	3.20
MIDDLE RING, O/F	2.30	2.23
INNER RING, O/F	2.31	2.18
BLC, PERCENT OF FUEL	40.0	40.8
TOTAL, O/F	1.63	1.63
OUTER RING RUPE NO.	0.606	0.632
MIDDLE RING RUBE NO.	0.572	0.560
INNER RING RUPE NO.	0.572	0.549

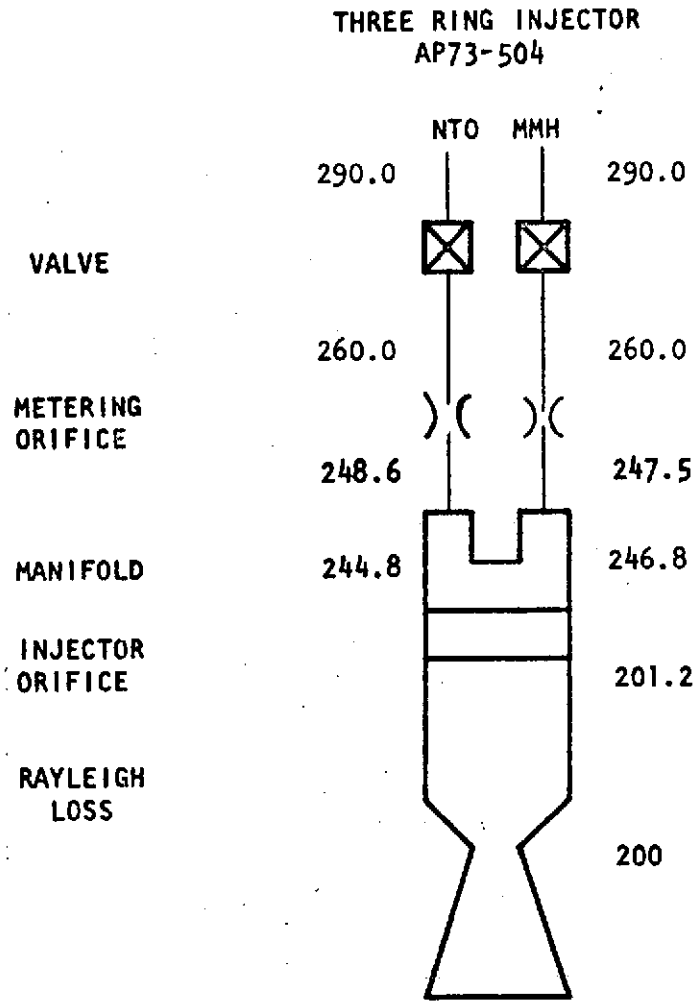

Figure 44. Durability Engine Design Pressure Profile

TABLE 15. DEMONSTRATED INJECTOR PRESSURE RATIOS FOR LOW-FREQUENCY STABILITY

ENGINE	PROPELLANT COMBINATION	CHAMBER DIAMETER, INCHES	CHAMBER PRESSURE, PSIA	INJECTOR PRESSURE DROP, PSID		PRESSURE DROP/ CHAMBER PRESSURE, PERCENT	
				OXIDIZER	FUEL	OXIDIZER	FUEL
Transtage/ RCS	N_2O_4/50-50	1.1	140	25	33	0.18	0.23
MM III	N_2O_4/MMH	3.0	125	54	47	0.43	0.37
SS/APS-IR&D	N_2O_4/50-50	5.3	150	35	50	0.23	0.33
LM-A	N_2O_4/50-50	7.8	120	32	31	0.27	0.26
Durability Engine	N_2O_4/MMH	3.72	200	50	50	0.25	0.25

N_2O_4/hydrazine-base fuel propellants, which have exhibited stable operation with the Durability Engine design. The $\Delta P/P_c$ ratio of 25 percent for this engine compares favorably with the $\Delta P/P_c$ ratios present in previously stable engine configurations. Thus, feed system coupling is not expected to occur with the Durability Engine design.

In acoustic stability, the primary considerations are injection scheme, engine size, propellant type, and the mechanism involved in interaction of the burning process with wave motions within the gas of the combustion zone (as opposed to interaction of the burning process with natural wave motions of the feed system; i.e., feed system coupling). Acoustic stability is commonly achieved with the use of a damping device or "stability aid." The primary stability aids are baffles and absorbers. Baffles are generally used in large engines with low frequencies. Absorbers have successfully provided stability in small-diameter engines with high frequencies (NAS9-7498 and NAS9-9866). The calculated frequencies for the Durability Engine are shown in Fig. 45. The lowest predicted acoustic mode is 7347 Hz.

The MM III engine, which is close in size to the Durability Engine (3.0 versus 3.72 inch diameter), uses the same injection concept and has demonstrated stable operation with acoustic cavities. The extensive MM III test program is summarized in Fig. 46. With an acoustic cavity configuration, 0.06 inch wide x 0.055 inch deep, all tests were stable; 1 percent of the tests without the cavity were unstable.

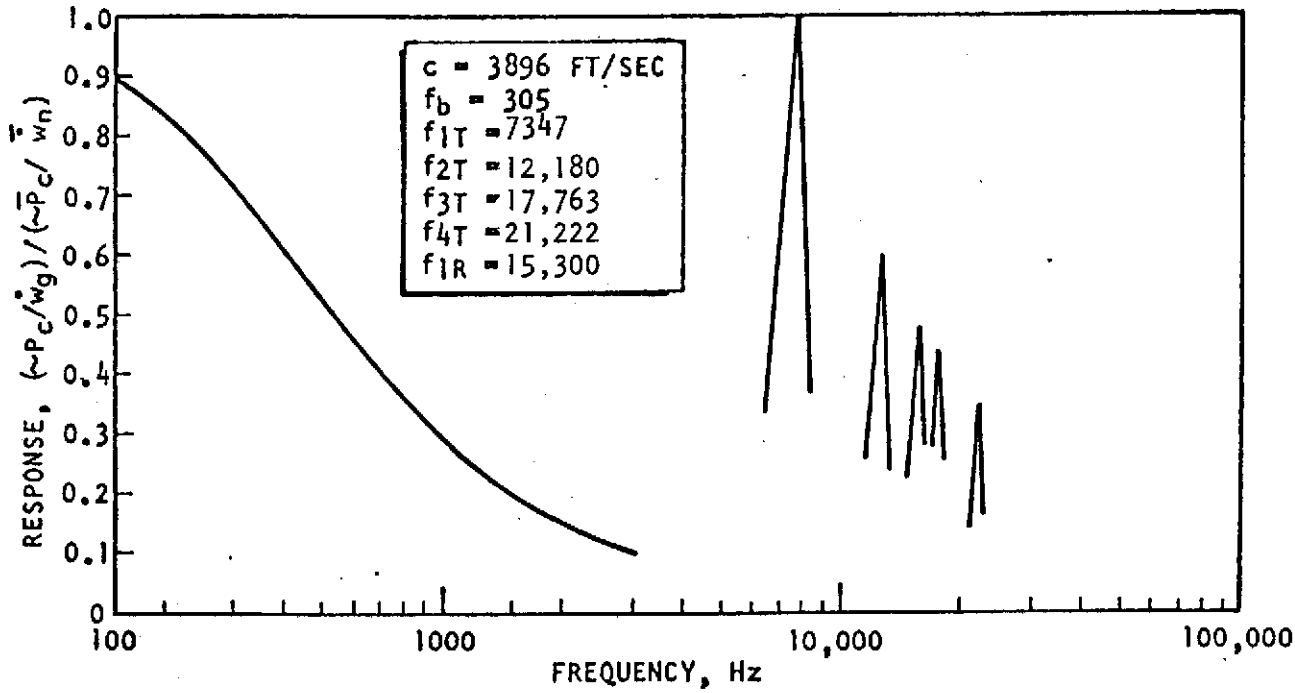

Figure 45. Chamber Response of Durability Engine

The Durability Engine design employs a straight acoustic slot (0.080 inch wide x 0.750 inch deep), which results in an absorber open area of 7.0 percent. This value places this engine design close to both the stable LM-A engine and MM III engine absorber designs. The Durability Engine design is expected to have completely satisfactory stability characteristics because of the incorporation of acoustic cavities along the injector periphery.

Combustion Stability Test. The combustion stability characteristics of the Durability Engine injector were evaluated under a company-sponsored program using a MOOG bipropellant valve. Three bomb tests were conducted using six charges (two charges set off during each test). The charges employed were high order explosives which produce detonation waves in the combustion processes as opposed to gun-type propellants which produce less severe deflagration waves. This is believed to be the most critical and valid rating of dynamic stability.

Three Photocon transducers were flush mounted in the chamber wall and the data were recorded on FM magnetic tape. The tape data were transcribed on strip chart recorders, an example of which is shown in Fig. 47. The overall frequency response of this acquisition and transcription system is approximately 15,000 Hz.

CONFIGURATION															
ENGINE	0	0	1	1	2		2	3	3	4	4	4	5		6
CHAMBER UNIT	0	0	1	1	2		2	3	3	4	4	4	4		1
INJECTOR UNIT	0	0	1	1	2	1	2	3	3	1	1	1	2	3	3
NO. OF STARTS	625	2	600	33	600	200	33	600	7	600	7	5	600	200	3
TYPE OF TEST	①	②	①	②	①	③	②	①	②	①	②	④	①	③	④
PROPELLANT TEMPERATURE, F	AMB	AMB	60	AMB	60	60	AMB	80	AMB	100	AMB	AMB	100	100	AMB
INSTABILITIES	NONE →					3	NONE →							1	NONE

① STABILITY PULSE SERIES
② MISSION DUTY CYCLE
③ STABILITY REFERENCE
④ BOMB TESTS

WITH ACOUSTIC CAVITY

WITHOUT ACOUSTIC CAVITY

Figure 46. Minuteman III Stability Verification Test

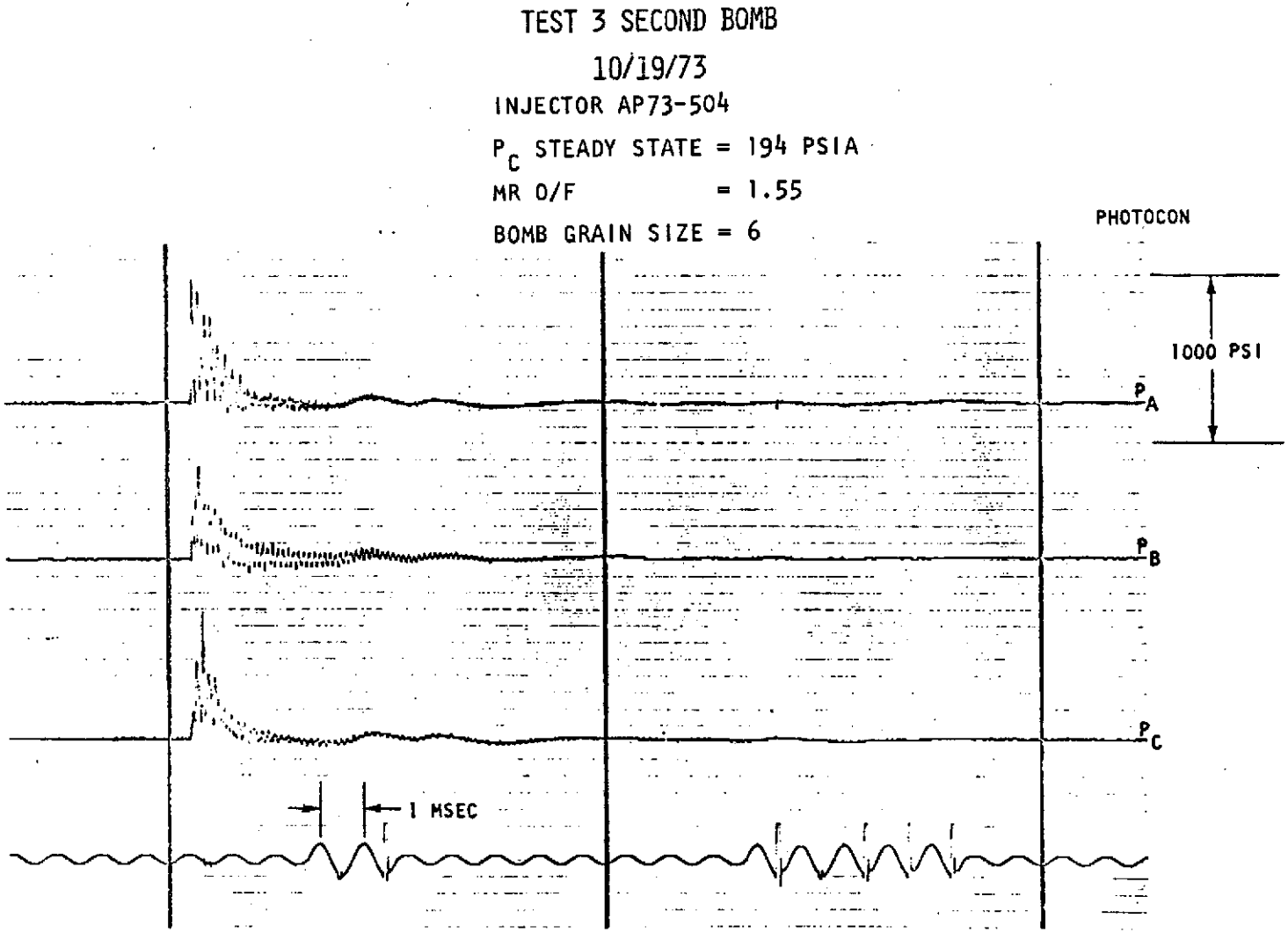

Figure 47. Stability Bomb Test

Detailed analysis of the data is tabulated in Table 16. These data were obtained directly from the transcription shown typically in Fig. 47. The example shown is the 6-grain bomb from test No. 3. Pertinent variables are the peak overpressure, rise rate or brisance, damp time and primary frequencies of the disturbance. Individual values were measured and average values were calculated for each of the six disturbances.

The average overpressure ranges from 574 to 882 psia. A linear trend of overpressure with bomb size was not noted, indicating the measurements are probably the reaction of the combustion process to the bomb.

The rise rates are all greater than 1 psi/msec and characteristic of high order detonations. There was a clearer trend to greater rise rates with larger bombs than with overpressures.

The average damp times were 12 msec or less and were governed primarily by lower frequency disturbances which are considered of little consequence. The high frequency disturbances all damped in significantly shorter times as can be seen in Fig. 47.

The frequencies in the vicinity of 8000 to 12,000 Hz correspond to the first and second tangential modes of the chamber as expected. The data indicated that the engine was adequately designed to damp these modes.

All the data indicate these tests to be a valid indication of the dynamic stability characteristics of the engine.

Scalability

The scalability of beryllium engines is illustrated by discussion of the broad range of engines built to date. The unique properties of beryllium were first employed in 1964 to demonstrate the feasibility of a new rocket engine design concept. This concept used the low-density, high-thermal conductivity, strength at elevated temperatures, and chemical inertness of beryllium to implement an entirely new approach to rocket engine cooling. Sixteen beryllium engine models (Fig. 48) which cover a chamber pressure range of 50 to 400 psia and thrust level of 1 to 1600 lbf have been developed with >420,000 starts and >500,000 seconds of burn time accumulated. Beryllium engines have been qualified and flown in the MM III PBPS (>840 units produced to date), MM '71 vehicles (10 months operation in space), and the VO '75 (~20,000 seconds accumulated on single DDT&E units).

The maturity of the beryllium engine technology is demonstrated by the following:

- Single engines have demonstrated these hot-fire capabilities with no apparent physical degradation:

  Single burn duration -- 10,000 seconds
  Total burn duration -- 25,764 seconds
  Start and pulses -- 58,000

TABLE 16. STABILITY BOMB TEST SUMMARY DURABILITY ENGINE INJECTOR

TEST DATE: 10-19-73

Test No.	Pc and MR	Bomb Size (gr)	Det Time, sec Relative to 90% Pc	Pressure Measurement, (Photocon)	Overpressure, Peak psi	Rise Time (Brisance) psi/ms	Damp Time (ms)	Predominate Frequency, (Hz)
1	194 1.52	2	0.528	A	540	.828	8	10K/500
				B	744	2.112	8	8K/500
				C	437	.644	20	12K/500
				Average	574	1.19	12	
		3	1.53	A	747	3.68	10	11K/500
				B	384	1.92	8	11K/500
				C	805	1.84	16	10K/500
				Average	645	2.48	11	
2	194 1.62	2	0.523	A	792	3.12	4	12K
				B	960	3.60	3	9K
				C	696	1.92	3	13K
				Average	816	2.88	3	
		6	1.565	A	792	4.80	3	12K
				B	312	2.40	3	10K
				C	792	3.60	3.5	13k
				Average	632	3.60	3	
3	194 1.55	3	0.510	A	532	2.16	8	9K
				B	884	6.50	7	9K
				C	528	1.44	8	10K
				Average	648	3.36	8	
		6	1.52	A	984	7.20	8	11K
				B	728	3.25	8	8.5K
				C	936	1.92	8	12K
				Average	882	4.12	8	

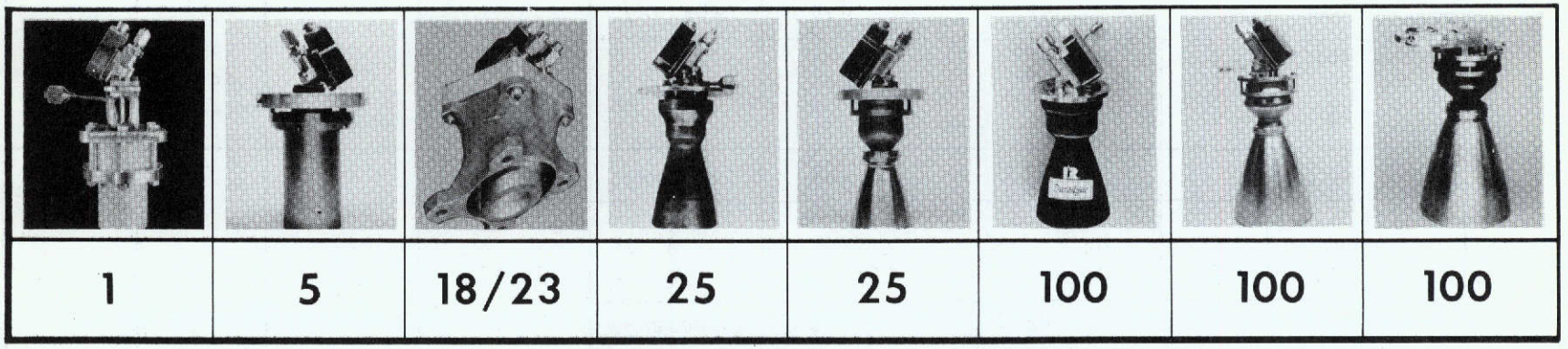

16 MODELS > 420,000 STARTS - 500,000 SECONDS

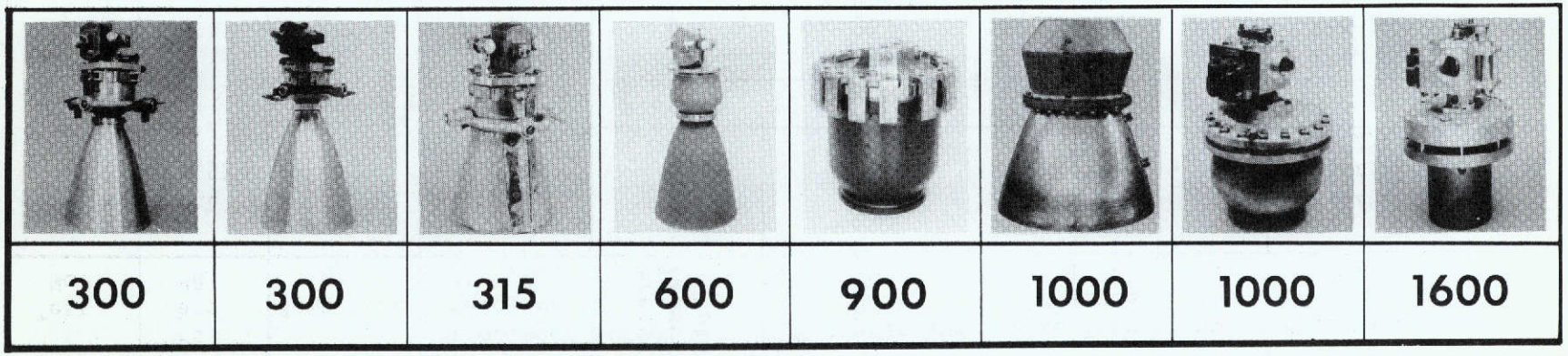

Figure 48. Beryllium Engine Models and Thrust Chambers, 1 to 1600 lb_f Thrust

- Fabrication

  961 engines produced (Durability Engine size)
  831 engines delivered

- Flights

  75 flights with 100-percent reliability
  10 months of operation in space

The beryllium INTEREGEN engine is currently in its fourth generation of development. Improvements in cooling efficiency and assembly have been introduced and demonstrated for the Durability Engine to provide an engine that meets the high-cycle life, multiple reuse requirements of the Space Shuttle.

Reliability, Safety, and Maintainability Analyses

The beryllium engine flight configuration was evaluated relative to reliability, safety, and maintainability criteria for the SS/RCS application. In performing this assessment it was assumed that the torque motor bipropellant valve would be designed specifically for the point design configuration, e.g., not a modified version of an existing valve as used on this contract's test program.

The SS/RCS beryllium engine incorporates design concepts proven to be reliable, safe and maintainable in engines designed for multiple use in single missions, and ground-tested in multiple missions. This design meets both material aging and wear-out goals of the Space Shuttle. Redundancy in cooling is inherent in the design because of the high conductivity and thermal capacity of beryllium. The engine is capable of operating safely and reliably in two firing modes: (1) INTEREGEN, cooled mode, and (2) the heat sink mode. Flight instrumentation and post flight visual inspection will provide necessary fault detection/isolation information. Key design features which lead to high reliability and fail-safe operation are:

Margin of strength
Off-limits margin
Redundancy in engine cooling
Design simplicity
All-metal construction
Flight-proven design concepts
Positive isolation of propellants
Demonstrated material compatibility
Easy decontamination
Flight instrumentation for fault detection/isolation

Reliability. Key design characteristics, included in the preliminary design, which contributed to achievement of high inherent reliability are listed in Table 17.

A Failure Mode, Effect and Criticality Analysis (FMECA) of the engine was made to assess the reliability of the baseline design (see Table 18).

TABLE 17. KEY DESIGN CHARACTERISTICS

Reliability Features	Engineering Design Features
	Rocket Engine Assembly
Simplicity	Few parts
Insensitivity to environments	Demonstrated durability
Reuseability and design marging	Demonstrated cycle life
Life and reuseability enhanced	Excellent thermal management producing super-cooled surfaces
Insensitivity to heat	Titanium insulators between valve and injector
Insensitivity to thermal and pressure cycles	Low operating temperatures and material stress levels. High margins of safety
	Bipropellant Valve
Simplicity	Few parts, single-stage, scalable, no vents
Insensitivity to Environments	Demonstrated durability and material compatibility; motor hermetically sealed; thermal isolation
Reuseability	No sliding fits, material compatibility, inlet filter
Life	Demonstrated concepts, compatible materials, welds and metal seals, durable seat, inlet filter
Fail-safe	Valve poppets biased to fail closed; welds and metal seals
Simultaneity	Mechanically linked poppets
Positive propellant isolation	Parent material, redundant seals, captive Teflon seat, inlet filters, compatible materials
Ability to clean	Inlet filters, simple contour, no sliding fits, compatible materials
Insensitivity to heat	Propellant-cooled seat, titanium space insulator, minimum Teflon volume
Valve position, flight monitoring	System instrumentation - chamber pressure, valve command signal
	Injector
Simplicity	Symmetric, uniform pattern and passages, no baffles, scalable, even distribution
Durability	Unlimited life, low face heat flux
Reuseability	Compatible materials, all-welded design
Life	Demonstrated performance, compatible with chamber, compatible materials, state-of-the-art design
Stability	Acoustic cavity demonstrated operation, positive ignition with unlike doublets, thousands of firing on variety of engine shapes, sizes, propellants and performance levels.
Positive propellant isolation	Parent material, machined; all EB welded, 100% inspectable; all EDM drilled passages in quality material bar stock.
	Thrust Chamber
Simplicity	Single piece
Durability	Compatible materials, thermally forgiving, high strength
Reuseability and Life	Compatible materials, thermally forgiving, demonstrated concept on variety of engine shapes, sizes, propellants and performance levels.
Insensitivity to heat	Thermally forgiving, INTEREGEN-cooled, radiation-cooled nozzle
Simplicity	Single piece
Durability	Compatible material, high strength, compatible with environments
Life	Demonstrated performance, compatible materials
Insensitivity to heat	Compatible, high-strength material, single piece, insulated, radiation cooled

TABLE 18. FAILURE MODE, EFFECTS AND CRITICALITY ANALYSIS

Component/Function	Failure Mode	Criticality	Failure Effect		Preventive/Corrective Measures	Detection/Isolation
			Engine	Vehicle		
Bipropellant Valve Provide simultaneous propellant flow to injector and control engine operation through an electrical signal to valve.	Slow open	Minor	Engine ignition delay	Upper correction/ nonunitform vehicle movement	No sliding fits, generous force margins, compatible materials, hermetically sealed.	Post-flight data sample; correlation of chamber pressure rate valve command.
	Fails to open	Critical	Fail to Start	No effect; engine redundancy	Same as (slow open) above In flight: No chamber pressure signal: switch to redundant engines	Chamber pressure signal
	Excessive flow resistance	Major	Engine performance low	Slower vehicle reaction acceleration	Same as (slow open) above	Condition monitor chamber pressure versus inlet pressures.
	Slow closing	Major	Slower thrust termination than normal cutoff impulse	Over correction of vehicle movement; nonuniform response	All forces tend to close valve (pressure torque tube, permanent magnet polarity); no sliding fits; compatible materials	Same as (slow open) above.
	Fails to close	Critical	No thrust termination; engine continues to operate until propellant depletion	Loss of reaction control; conti-	Pressure and permanent magnet forces tend to close valve (fail-safe closed); no sliding fits; compatible materials; hermetically sealed; in fligth: chamber pressure signal, thrust continues after valve command ceases	Chamber pressure signal.
	Internal leakage (one propellant only)	Minor to Critical	Minor Leakage; no effect to freezing of oxidizer	No effect to thrust irregularity on engine firing	Teflon seat demonstrated positive seal; inlet filter controls contamination; pressure and magnet forces hold valve closed	Pre/Post flight pressure lockup to monitor system sealing integrity, including valve
		Major to Catastrophic	Major Leakage; accumulation of propellant in chamber; potential vehicle damage and fire	Thrust irregularity on engine firing, or explosion; potential vehicle damage and fire	Pressure and magnet forces hold valve closed; Teflon seat demonstrated positive seal; inlet filter controls contamination; valve fail safe closes; vehicle switch to redundant engine	Same as above
	External Leakage (one propellant only)	Critical	Minor Leakage; no effect	Propellant vapors accumulation in pod	Parent material barrier; quality bar stock, compatible with propellants; all EB welds and metal seals	Same as above, plus visual inspection
		Critical to Catastrophic	Major leakage; off-mixture ratio at firing	Propellant liquid accumulation in pod; potential fire or explosion	In flight, skin temperature thermocouple will detect fire	Condition monitored chamber pressure correlations

TABLE 18. (Concluded)

Component/Function	Failure Mode	Criticality	Failure Effect		Preventive/Corrective Measures	Detection/Isolation
			Engine	Vehicle		
Seal, Valve to Injector Confine propellant within the defined flow passages	External leakage	Minor	No effect-Redundant seals	No effect	Redundant gold plated Inconel X omega seals on each flow passage. Bolted assembly. Titanium spacer plate.	Periodic visual inspection
Injector Assembly Injects propellants into thrust chamber in prescribed manner to ensure controlled ignition and satisfactory combustion	Poor combustion	Minor to Critical	Irregular thrust, instability	No effect to poor vehicle response	EDM precision drilled orifices; stable operation capability over wide pressure range;	Condition monitored chamber pressure correlations
	Plugging		Throat Erosion	No effect	INTEREGEN cooling combined with high thermal conductivity of beryllium automatically dissipates local heating, thermal malfunction device can be used to shut down engine prior to erosion or nozzle failure	Visual Inspection
	Instability	Major to Catastrophic	Rapid structural damage	No effect (redundant engines) to potential vehicle fire	Proven acoustic cavities for damping	Not required (failure mode not credible
	Internal leakage	Critical Catastrophic	Potential Explosion, structural damage	Explosion and fire in vehicle pod	Parent material between propellants; machined bar stock, parent material	Not required (failure mode not credible)
	External leakage	Critical	Minor leakage no effect; major leakage - off mixture ratio	Propellant vapors/liquids in vehicle pod; potential fire	Machined bar stock, quality material; all EB welds, 100 percent inspected; cool operation	Visual inspection
Injector to Chamber Braze Confine hot combustion gases within chamber	External Joint Leakage	Minor Major	Performance loss with non-uniform cooling. Potential structural damage	Propellant vapors/liquids in vehicle pod; potential fire	Stress excursions within yield; structural integrity of joint demonstrated under vibration tests equilibrium to 100 MDC.	Chamber pressure visual inspection
Thrust Chamber Receive propellants under pressure; contain burning propellants.	Fails to impart high velocity to combustion gases to produce thrust	Critical	Throat erosion (if sufficiently severe, structural failure could occur.	No effect (Engine redundancy)	Single piece, all metal, durable, high strenght beryllium, thermal forgiving. INTEREGEN cooled walls. Demonstrated cool operation.	Condition monitored chamber pressure - pressure correlations
	External leakage	Critical to Catastrophic	Crack in engine wall	Combustion gases in vehicle pod: fire	Single piece, durable, high strength beryllium, INTEREGEN cooled walls; demonstrated cool operation	Chamber pressure visual inspection
Seal, Chamber to Nozzle	External leakage	Minor	No effect Redundant sealing	No effect	Clamp nut designed so adequate clamping force is maintained at all times without yielding material; used on MM '71 and VO '75.	Visual inspection
Nozzle Contained combusted gases and impart high velocity to expelled combustion gases to produce thrust	External leakage	Critical to Catastrophic	Failure of nozzle wall	Hot combustion gases in vehicle pod: fire	Single piece durable, high-strength columbium radiation-cooled walls; thermally insulated exterior proven Technology	Visual inspection

Safety. The RCS engine is safe to operate and maintain because of the (1) fail-safe design concepts, (2) strength margins at operating pressures and temperatures, (3) life margin, (4) positive isolation of propellants, and (5) ability to operate at off-design conditions of mixture ratio, propellant temperature, combustion pressure, and boundary layer coolant (BLC) flow. These safety margins have been established through analysis and also from test data on similar engines, i.e., the Mars Mariner '71 engine which ran successfully with restricted BLC flow. The materials are thermally forgiving because of their durability and high thermal conductivity. The engine has a long time margin to failure due to its configuration, durability, high thermal conductivity, thermal capacitance and cool operation.

The cooling principal leads to low operating temperatures which result in high thermal, structural, life, and time to critical failure margins. The design is relatively insensitive to off-design operation and has no duty cycle constraints. The heat capacity of the thrust chamber permits firing durations up to 50 seconds without any coolant flow before a critical burn-through failure will occur. The highly abnormal possibility can be readily detected prior to critical failure and engine firing terminated.

A potentially hazardous condition can exist from the inhalation of beryllium metal or its compounds during fabrication. Operations such as machining, filing, grinding, polishing, etching, or other processing that may produce airborne concentration of beryllium materials are controlled at Rocketdyne by accepted industrial safety procedures. Wet machining is used for all operations except final lapping on the MM III, MM '71, and VO '75 thrust chamber/injector interface. Vacuum collectors, air sampler indicators, hoods, and face mask filters provide added protection.

More than 800 beryllium thrust chambers have been manufactured at Rocketdyne since 1964 without incident. Industrial processing of beryllium material is widespread, particularly at Rockwell International divisions. This is becuase of its attractive properties for electronic, aircraft, and space applications. Beryllium is commonly used for aircraft brake parts because of its high thermal conductivity.

Beryllium particles are not released during or after engine operation because of the extremely low operating temperature of the thrust chamber, <1000 F at all conditions, including off-limits; a temperature of 1800 F is the point at which beryllium oxidation occurs. Established safety precautions exist to cover a hazardous condition should a malfunction or accident occur which releases beryllium particles.

The subsystem hazard analysis of Table 19 identifies hazard sources and controls associated with flight operation and ground maintenance of the Durability Engine.

Maintainability. The Durability Engine has been designed so that no servicing or periodic replacement would be necessary in the 100-flight, 10-year life span; however, fault detection/isolation instrumentation and visual inspection is recommended to monitor performance degradation for unscheduled maintenance. Time and resources required for corrective maintenance have been minimized by the use

TABLE 19. SUBSYSTEM HAZARD ANALYSIS

SUBSYSTEM: DURABILITY ENGINE — DATE:
LRU: — REPORT:

HAZARD SOURCE	OPERATIONAL PHASE	HAZARD	HAZARD CLASSIFICATION	HAZARD CONTROL	REMARKS
FUEL OR OXIDIZER LEAK PAST BIPROPELLANT VALVE SEAT OR VALVE INLET INTERFACE JOINT	LAUNCH PREPARATION AND LAUNCH	TOXIC FUMES: FUEL OR OXIDIZER, PRESENTING HAZARD TO SERVICING PERSONNEL	III. CRITICAL	ISOLATE PROPELLANT FROM VALVE UNTIL LAUNCH AREA CLEARED OF PERSONNEL	VALVE AND SUBSYSTEM WILL HAVE PASSED THE PREVIOUS FLIGHT POST-OPERATIONAL AND PREFLIGHT LEAK CHECKS
	FLIGHT	INTERFACE JOINT--NONE	I: MINOR	PROPELLANT SEALS ARE ALL EXTERNAL TO VEHICLE	
	FLIGHT	SEAT LEAK--SOLIDIFICATION OF LEAKING OXIDIZER OR LEAKING FUEL INSIDE ENGINE (LOW TEMPERATURE) FOLLOWED BY INTRODUCTION OF BOTH PROPELLANTS			
	FLIGHT	EXPLOSION IN INJECTOR OR THRUST CHAMBER	III: CRITICAL	PREFLIGHT LEAK DETECTION OF BIPROPELLANT VALVE	DETECTION BY P_c MONITOR WILL ENABLE PROPELLANT ISOLATION TO PREVENT FIRE PROPAGATION
	POST-OPERATION AND RECOVERY	TOXIC FUMES: FUEL OR OXIDIZER, PRESENTING HAZARD TO SERVICING PERSONNEL	III: CRITICAL	NORMAL OPERATION: PROPELLANTS WILL BE PURGED FROM ENGINE MANIFOLDS PRIOR TO RECOVERY OPERATION. LEAK-FREE SYSTEM VERIFIED BY ON-BOARD PRESSURE DECAY TEST PRIOR TO INITIATION OF VEHICLE SAFING MALFUNCTION: IF A SYSTEM LEAK OR OTHER MALFUNCTION DETECTED IN FLIGHT, REMOVE RCS TO SERVICE AREA. SEE NORMAL OPERATION AND ALTERNATE METHOD	ALTERNATE METHOD: REMORE ENTIRE RCS TO ISOLATED SERVICE AND CHECK-OUT AREA. PERSONNEL MUST WEAR PROTECTIVE CLOTHING. AREA MUST BE ENVIRONMENTALLY CONTROLLED TO PREVENT PROPELLANT VAPOR HAZARD

TEST 19. (Concluded)

SUBSYSTEM: DURABILITY ENGINE
LRU:
DATE:
REPORT:

HAZARD SOURCE	OPERATIONAL PHASE	HAZARD	HAZARD CLASSIFICATION	HAZARD CONTROL	REMARKS
SIMULTANEOUS LEAKAGE AT BOTH FUEL AND OXIDIZER OR SPONTANEOUS COMBUSTION OF FUEL IN AIR	LAUNCH PREPARATION AND LAUNCH; POST-OPERATION AND RECOVERY; VEHICLE SERVICING	FIRE: UNCONTROLLED BURNING OF FUEL AND OXIDIZER IN VICINITY OF RCS ENGINE	III. CRITICAL	PROPELLANTS NOT NORMALLY IN ENGINE INLET MANIFOLDS EXCEPT IN FLIGHT	ALTERNATE METHOD-PROPELLANTS ARE IN MANIFOLD; THEREFORE, PERSONNEL MUST WEAR PROTECTIVE CLOTHING AND RESPIRATORY EQUIPMENT
	FLIGHT	SAME AS ABOVE	III. CRITICAL	POSITIVE PARENT MATERIAL OR DOUBLE WELD ISOLATION BETWEEN FUEL AND OXIDIZER IN THE BIPROPELLANT VALVE AND INJECTOR	
EXTERNAL HOT GAS LEAK: 1. NOZZLE-THRUST 2. INJECTOR OR THRUST CHAMBER BURN-THROUGH	FLIGHT	FIRE: BURNING EXTERNAL TO RCS ENGINE DURING THRUSTER OPERATION	III: CRITICAL	1. LOW-PRESSURE JOINT 2. HIGH THERMAL MARGINS: INJECTOR, THRUST CHAMBER AND NOZZLE, INCLUDING PROVISIONS FOR GROSS OFF-MIXTURE RATIO OPERATION. BURNTHROUGH AVOIDED DUE TO HIGH THERMAL CONDUCTIVITY, COOL OPERATION, THERMAL FORGIVENESS, MATERIAL DURABILITY, AND EXTRA WALL THICKNESS. THERMAL MALFUNCTION DEVICE CAN BE USED TO SHUTDOWN ENGINE PRIOR TO EROSION OR NOZZLE FAILURE.	NEVER OCCURRED ON MINUTEMAN III, MARS MARINER '71 OR IR&D STEADY-STATE RUNS. DEMONSTRATION OF PRIMARY INJECTOR ORIFICE PLUGGING (OXIDIZER IMPING ON WALL) OR FILM COOLANT (1 TO 4 ADJ HOLES) CONDUCTED. SATISFACTORY ENGINE OPERATION AT THERMAL EQUIL. DEMONSTRATED WITHOUT FAILURE.

of condition monitoring. On-board equipment used in flight to monitor the engine's operational status combined with visual inspection will provide the primary indication for maintenance action. This rapid malfunction detection and isolation capability is augmented by engine design features which permit ease of maintenance. Table 20 provides the maintenance design features of the engine.

TABLE 20. MAINTAINABILITY DESIGN FEATURES

Component / Design Feature \ Maintainability Design Criteria	Eliminate Need for Servicing	No Preventative Maintenance	Long-Life Design	Wearout Margins	No Deterioration Propellants	No Deterioration Corrosion	No Special Protection	No Special Cleaning/Decon.	No Alignment Required	No Adjustment Required	No Calibration Required
Valve, Bipropellant											
• Single-stage, linked poppet for simultaniety, simplification (no pilot stages to adjust); easy to purge	X	X	X		X				X	X	X
• No sliding surfaces or critical fits				X							
• Propellant compatible metals and non-metals						X		X			
• In-line filtration					X						
• Hermetically sealed torque motor						X	X				
• Minimum static seals		X									
Injector											
• Easily purged clean of residual propellants (in-flight operations)	X	X						X			
• Propellant and moisture compatible material (Inconel or CRES)					X	X	X				
• Thermal margins prevent burning and impingement orifice enlargement										X	X

TABLE 20. (Continued)

Maintainability Design Criteria / Component / Design Feature	Eliminate Need for Servicing	No Preventative Maintenance	Long-Life Design	Wearout Margins	No Deterioration Propellants	No Deterioriation Corrosion	No Special Protection	No Special Cleaning/Decon.	No Alignment Required	No Adjustment Required	No Calibration Required
• Stable combustion			X	X	X						
• Filtration prevents contaminants from reaching injector					X						X
• One piece injector face; welded assembly			X	X					X	X	
Thrust Chamber											
• One piece thru the combustion zone, solid wall	X	X	X		X				X	X	X
• INTEREGEN thermal margins against erosion				X					X	X	X
• Minimum susceptibility to thermal distortion (throat, nozzle)									X		
• Beryllium insensitivity to storage and use environments					X	X	X	X			
Nozzle											
• Coated WC103 Columbium provides excellent oxidation resistance	X	X			X	X	X	X			
• Adequate operational thermal margin				X					X	X	X

TABLE 20. (Concluded)

Maintainability Design Criteria / Component / Design Feature	Eliminate Need for Servicing	No Preventative Maintenance	Long-Life Design	Wearout Margins	No Deterioration Propellants	No Deterioration Corrosion	No Special Protection	No Special Cleaning/Decon.	No Alignment Required	No Adjustment Required	No Calibration Required
Insulation											
• Titanium jacket encased	X	X	X		X	X	X	X			
• Usable to 2700 F; has good thermal margin			X	X							
• Not critical to engine function									X	X	X
Attach Injector Brazed to Thrust Chamber											
• Provision for axial and radial growth	X	X	X		X			X	X	X	X
• Provision for thermal isolation	X	X	X		X			X	X	X	X
Attach - Nozzle/Thrust Chamber											
• Flexible flange-nut allows thermal growth while maintaining alignment	X	X	X	X				X	X	X	X
• V-seal is all metal			X	X	X			X			

PHASE II - HARDWARE FABRICATION

During this program, three test configurations were assembled from components purchased and fabricated under the contract or available from prior company-sponsored programs. The three test units were the Durability Engine, Off-Limits Engine, and Vibration Simulator.

DURABILITY ENGINE FABRICATION

A complete engine parts list for the Durability Engine is provided in Table 21. As noted, the injector and columbium nozzle were supplied from a Rocketdyne company-sponsored program. The MOOG valve model 54X107A (Fig. 49) was provided by NASA/JSC from Contract NAS9-12996. This valve (S/N 003) failed during the test program and a second valve (S/N 005) was provided. Characteristics of the valve are given in Table 22.

Figure 50 describes the injector fabrication sequence and Fig. 51 shows the injector at various points during fabrication. The injector is an all EB welded assembly with parent material between fuel and oxidizer manifolds. The orifices are EDM'd. Figure 52 shows the injector being cold flow calibrated. The flow characteristics of the injector are listed in Tables 13 and 14.

Figure 53 describes the fabrication sequence of the thrust chamber assembly which includes machining of the beryllium combustor, injector/chamber transition ring and nozzle nut; brazing the chamber and transition ring together; final machining the brazed transition ring; and EB welding on the nozzle nut and the injector to the chamber. Figure 54 shows the thrust chamber during fabrication.

The nozzles were fabricated by CS Industries. The columbium nozzle was coated locally by Vac-Hyd (VH-101 silicide coating). Figure 55 shows the two nozzles. The dynaflex insulation blanket was purchased from Johns-Manville.

Figures 56 and 57 show the Durability Engine Assembly with and without the insulation blanket installed.

OFF LIMITS ENGINE FABRICATION

The Off Limits Engine was available to the contract from a prior company sponsored program. Figure 58 shows the engine assembly.

VIBRATION SIMULATOR FABRICATION

The Vibration Simulator assembly is shown in Fig. 59. As previously discussed the purpose of the simulator was to demonstrate the durability of the brazed joint. The injector/transition ring/beryllium combustor assembly was therefore identical to that employed in the durability engine. An aluminum cylinder was used for the nozzle which was clamped to the beryllium as previously shown in Fig. 5. A MOOG valve available from another Rocketdyne program where mass is equivalent to that used on the Durability Engine, was bolted to the injector as a mass/center of gravity simulator.

TABLE 21. DURABILITY ENGINE PARTS LIST

PART NO.	NAME	QUANTITY	
Model 54x107	Propellant Valve	1	MOOG
8812-2102-0050	Parker V Seal	2	INCO X750 Gold Plated
AP73-164-009	Valve Spacer	1	6AL 4V Titanium
AP73-504*	Injector	1	321 CRES
AP73-505-001	TCA	1	--
-003	Thrust Chamber	1	Beryllium
-005	Ring	1	Haynes 25
8914-2102-3625	Parker V Seal	1	INCO 718 Gold Plated
AP73-116-001	Nozzle	1	Haynes 25
AP73-116-011*	Nozzle	1	C103, VH-101 Coating
AP73-162	Nut and Flange	1	Rene 41
AP73-506-001	Blanket Assembly	1	--
-003	Insulation	1	Dynaflex (JM)
-005	Shell	1	6AL 4V Titanium

*Available from Rocketdyne company sponsored program

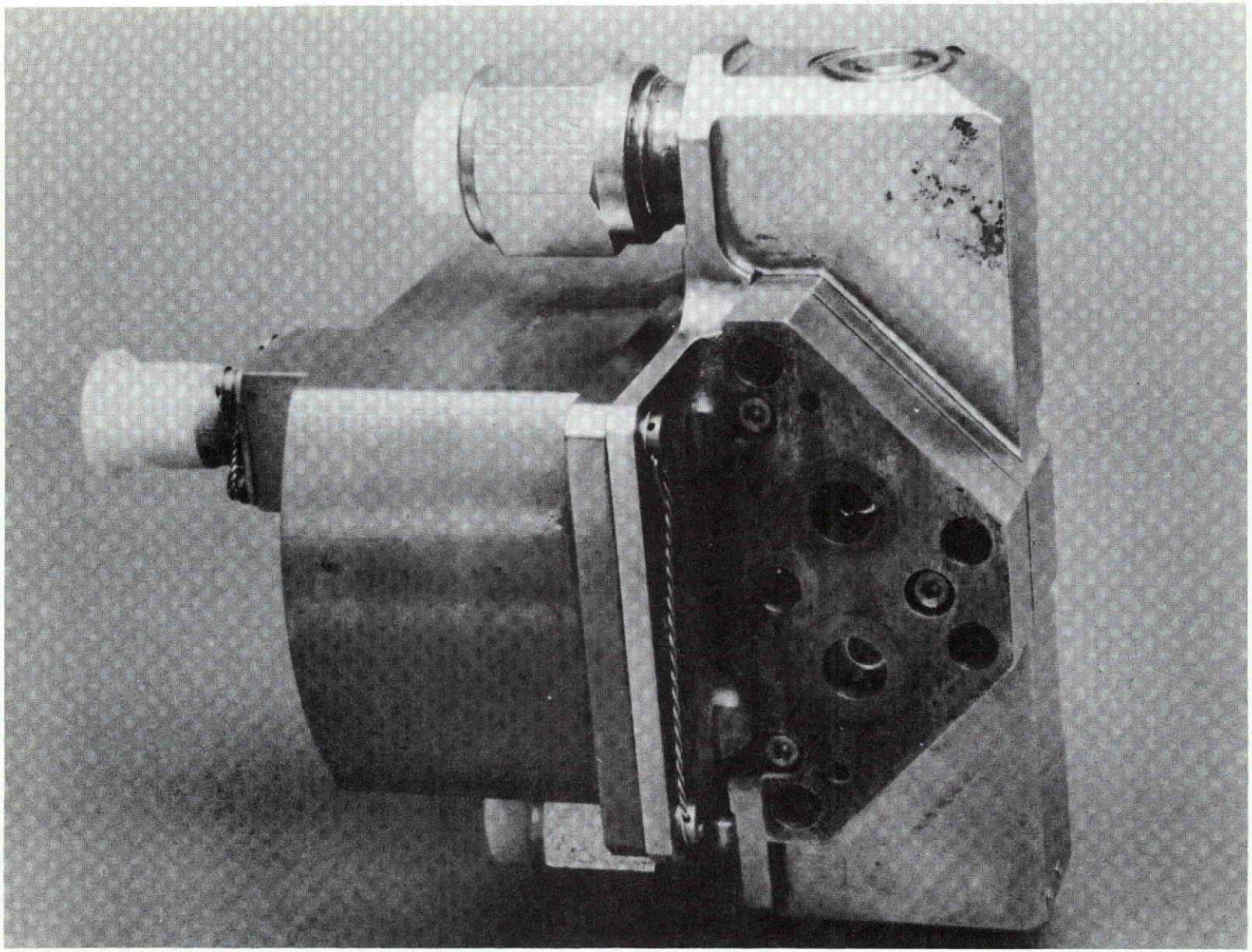

1SA22-12/14/73-C1H*

Figure 49. Moog Valve Model 54X107A

TABLE 22. MOOG MODEL 54X107A BIPROPELLANT VALVE CHARACTERISTICS

	S/N 003	S/N 005
Pressures		
Supply, psig	300	300
Proof, psig	450	450
ΔP_{fu}, psid @ 0.783 lb/sec	23.5	27.9
ΔP_{ox}, psid @ 1.252 lb/sec	37.5	41.5
Power, watts (at 28 vdc)	25.4	27.8
Voltage Supply, VDC	24-32	24-32
Response @ 28 VDC, msec		
Open	38	37
Close	5	7
Pull-in Current @ 300 psig, amps	0.378	0.349
Weight, lb	4.55	4.54
Electrical		
Coil Resistance @70F	30.9	31.8
Insulation Resistance @ 500 VDC, megohms	>15.000	500.000
Dielectric Strength @ 1000 VAC, microamps	1	1

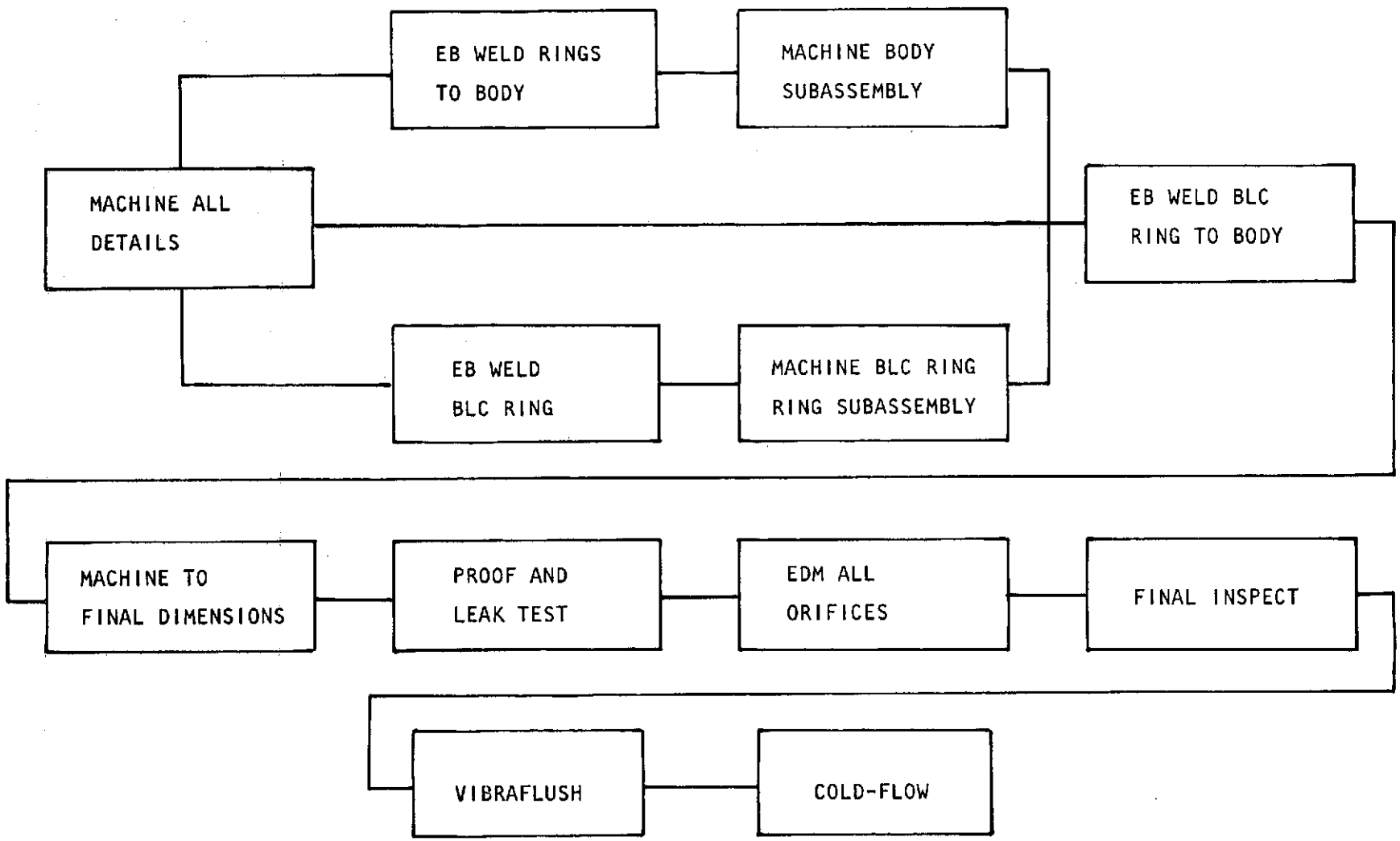

Figure 50. Injector Fabrication Sequence

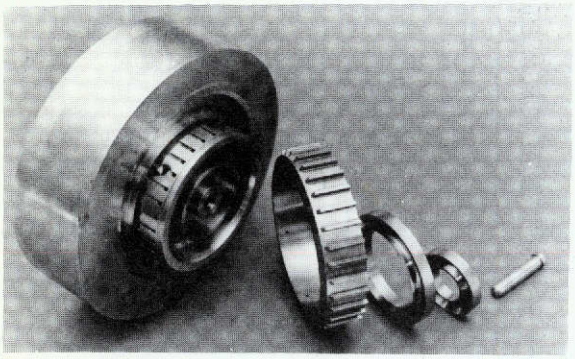

5AJ33-7/27/73-C1A

INJECTOR DETAILS

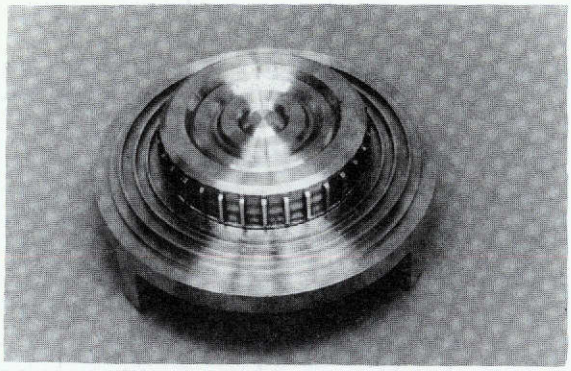

5AJ33-8/15/73-C1C

WELDED INJECTOR

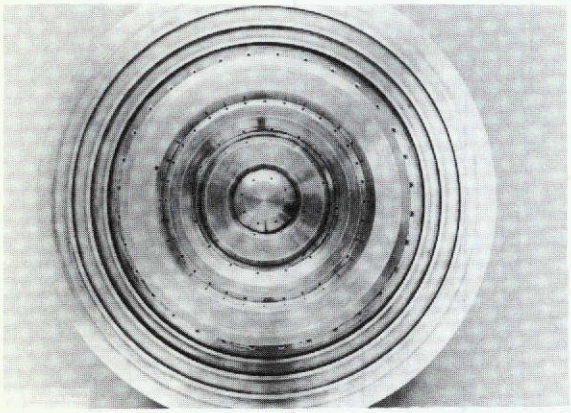

5AD33-9/10/73-C1

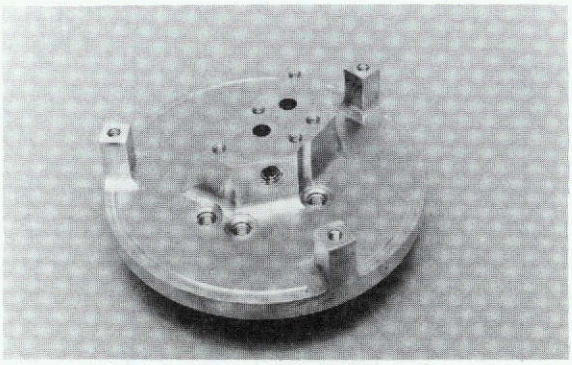

5AJ33-8/15/73-C1D

COMPLETED INJECTOR

Figure 51. Fabricated Injector

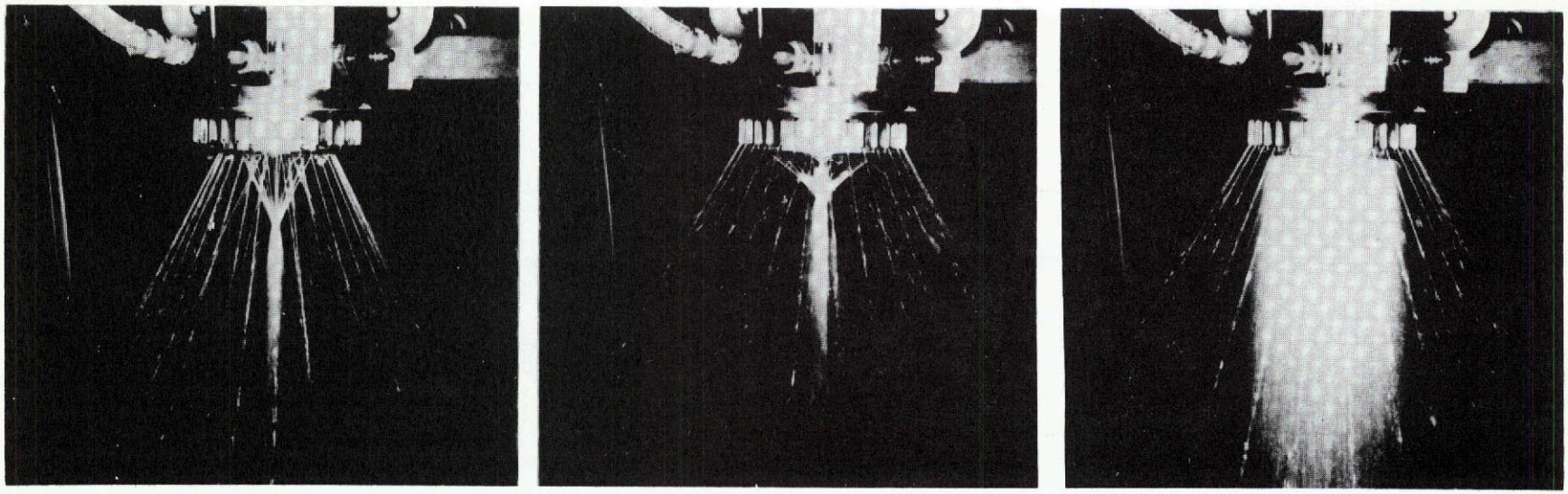

Figure 52. Three-Ring Injector Cold Flow

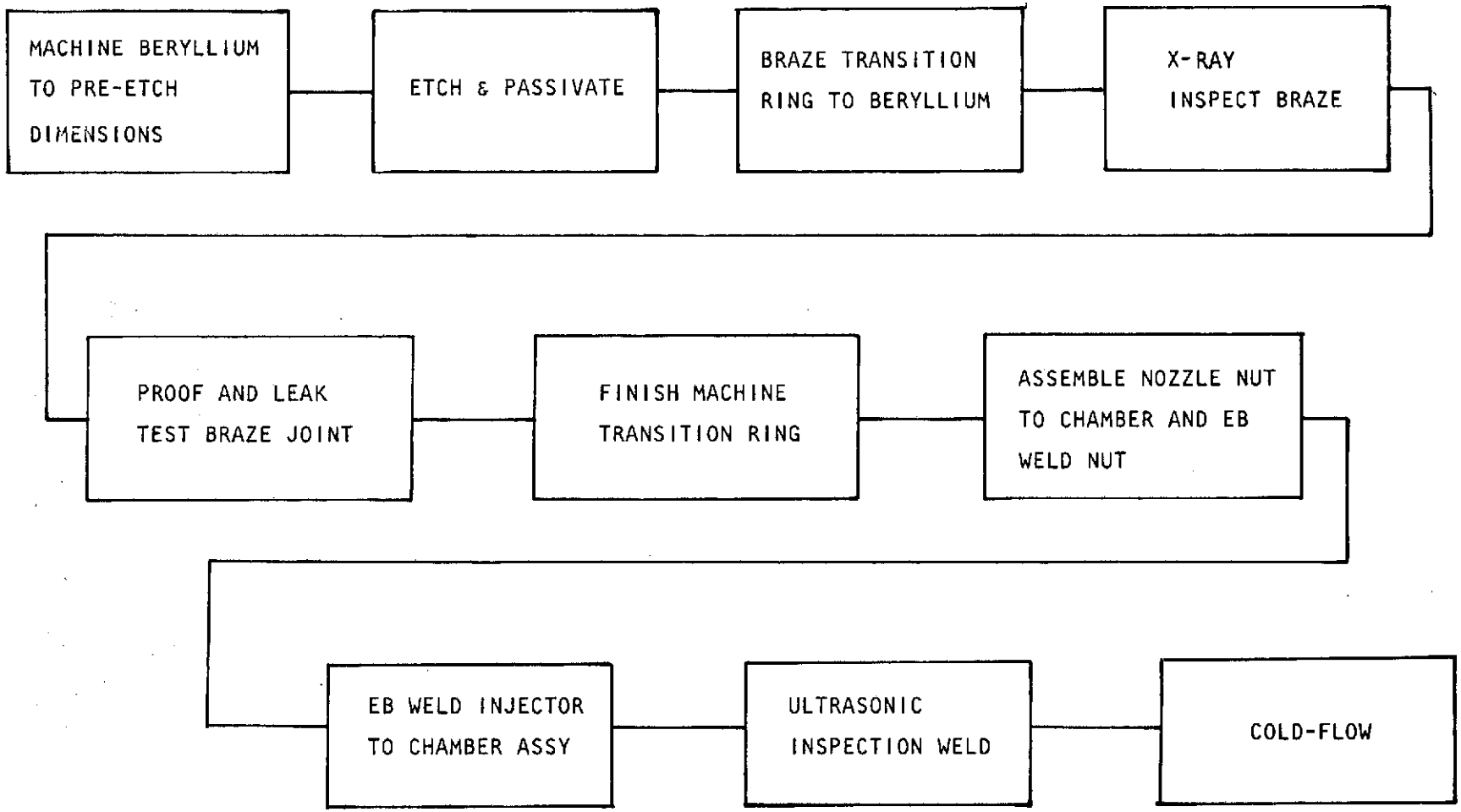

Figure 53. Thrust Chamber Assembly Fabrication Sequence

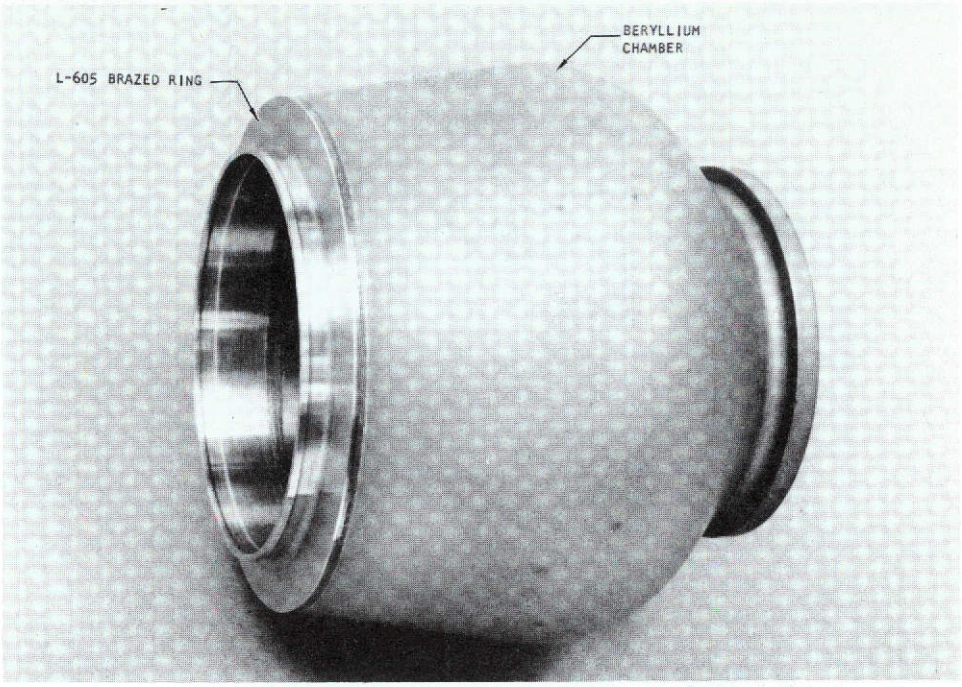

1SA22-12/13/73-C1F

COMBUSTION CHAMBER

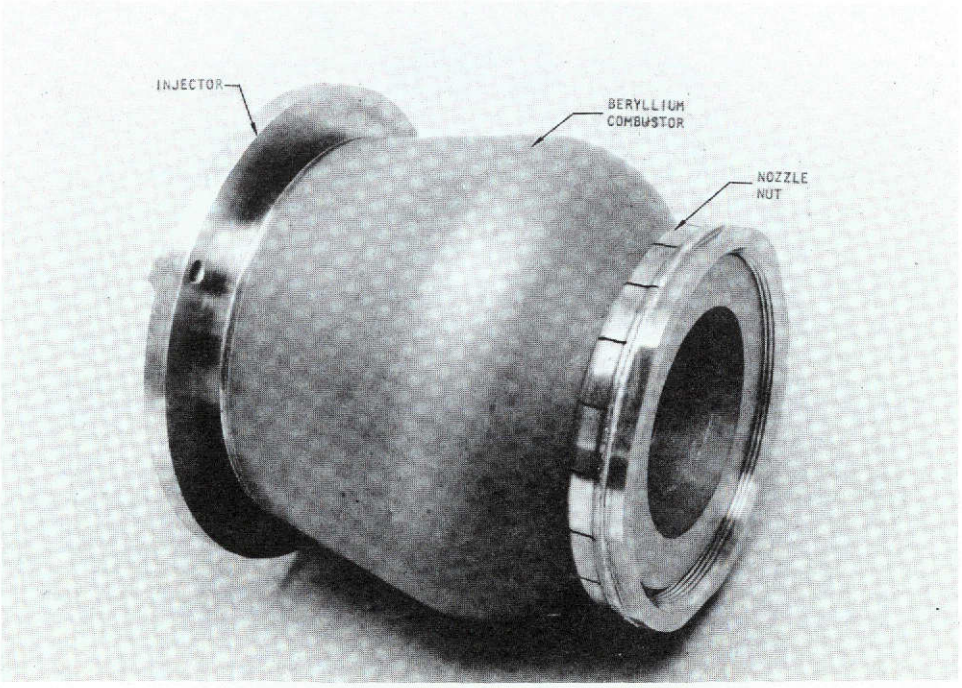

1SA22-12/14/73-C1G

COMBUSTION CHAMBER/INJECTOR ASSEMBLY

Figure 54. Fabricated Combustion Chamber Asembly

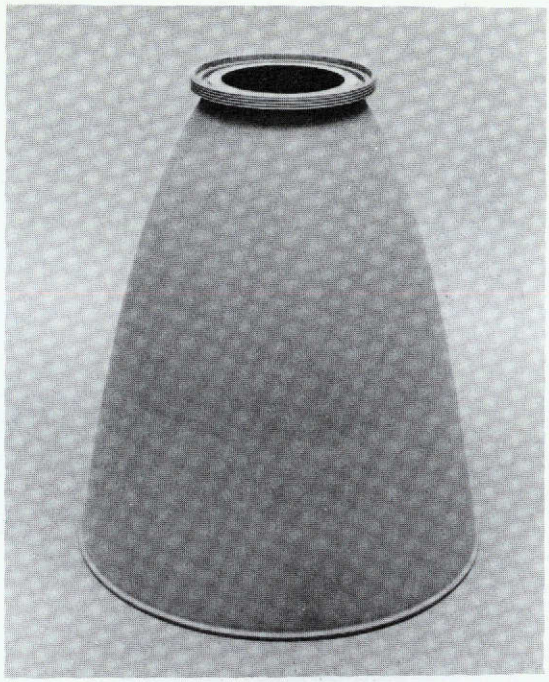

1SA22-12/14/73-C1F

L-605

1X232-1/2/74-C1

L-103

Figure 55. Fabricated Nozzles

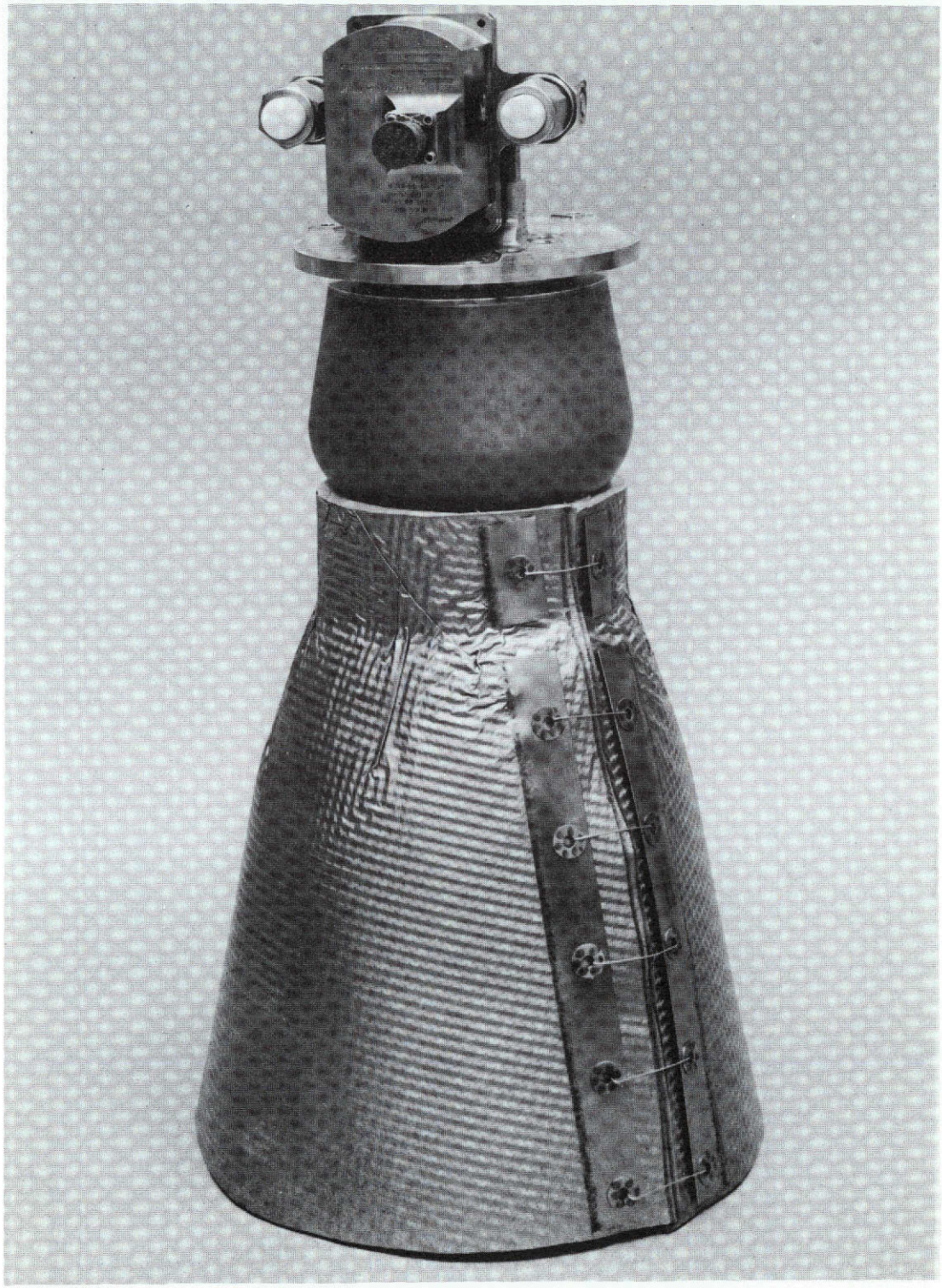

1SA22-12/14/73-C1A*

Figure 56. Durability Engine Test Hardware (With Insulation)

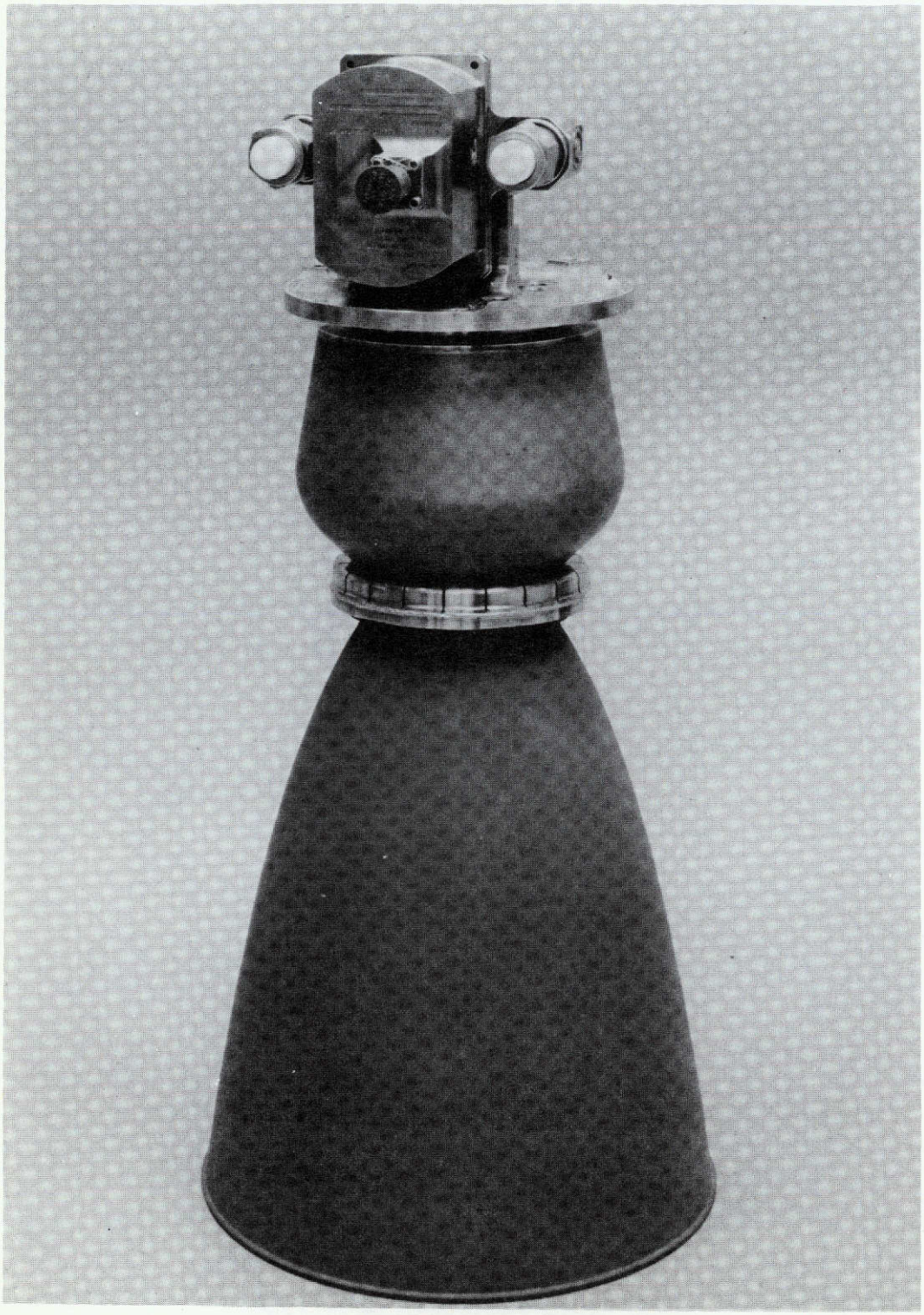

1SA22-12/14/73-C1C*

Figure 57. Durability Engine Test Hardware (Without Insulation)

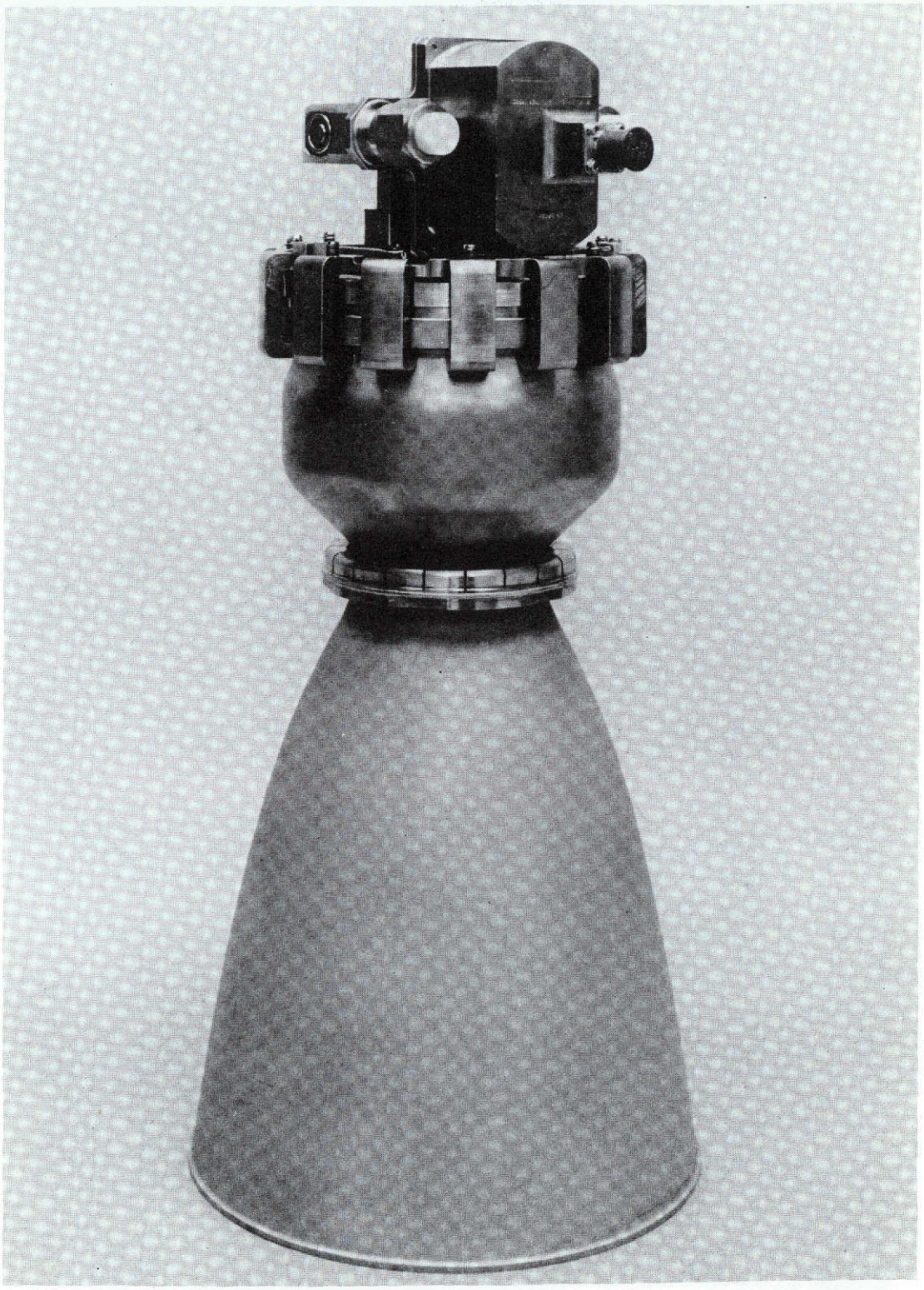

1XZ21-8/24/73-C1C*

Figure 58. Off-Limits Test Hardware

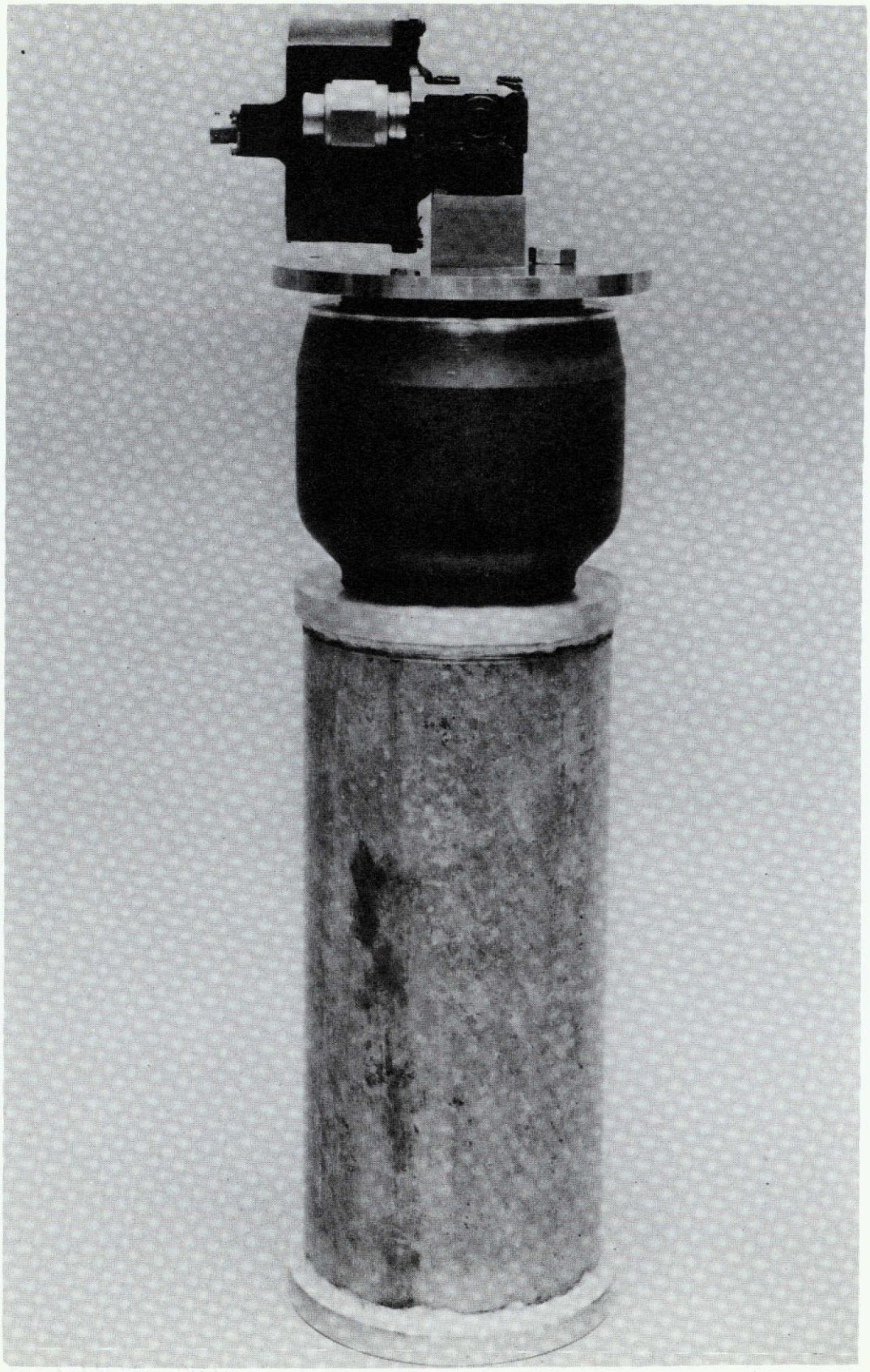

1SA22-12/14/73-C1E*

Figure 59. Vibration Simulator Test Hardware

PHASE III - ENGINE TESTING

During the test program, the Durability Engine was exposed to six environmental cycles interspersed with hot-fire tests where 500 starts and 1951 seconds were accumulated. The Off Limits Engine was run at extreme mixture ratio and chamber pressure levels, as well as with plugged primary and auxiliary film coolant orifices. Eighteen starts and 2615 seconds were accumulated during contract tests (test hardware which was previously used on a company-sponsored test program has accumulated 694 starts and 6033 seconds). The vibration simulator was exposed to 100 equivalent shuttle missions of X, Y, and Z axis random vibrations. Appendix A provides a description of the hot-fire and environmental test facilities employed during the test program.

DURABILITY ENGINE TEST PROGRAM

The purpose of the Durability Engine Test Program was to demonstrate the multiple reuse capability of beryllium engine without cleaning, service or maintenance. The environmental/endurance test sequence was originally to consist of five cycles of hot-fire and five cycles of environmental tests. Valve problems, however, resulted in a revision to the sequence where the scope of hot-fire testing was reduced and environmental tests increased to better assess valve sensitivity to rain, sand and dust, and vibration.

The Durability Engine was exposed to hot-fire and non-hot-fire environmental tests in the following sequence:

1. Acceptance hot-fire test
2. Baseline performance hot-fire test
3. First environmental test, sequence A
4. First hot-fire endurance test
5. Second environmental test, sequence A
6. Second hot-fire endurance test
7. Third environmental test, sequence A
8. Fourth environmental test, sequence B
9. Fifth environmental test, sequence B
10. Sixth environmental test, sequence B
11. Third hot-fire endurance test
12. Engine leak test and visual inspection

Table 23 provides the hot-fire test matrix. All tests, except the acceptance tests, were run with a coated columbium nozzle extension. A Haynes 25 nozzle was used during the acceptance tests.

During the course of the test program, two MOOG valves encountered excessive leakage problems. A detailed discussion of these failures is provided in the Phase IV section of this report. Throughout the above test sequence, the thrust chamber assembly was not decontaminated, even when servicing and installing valves.

TABLE 23. DURABILITY ENGINE TEST MATRIX

Sequence	Test No.	Test Dur.	Accum. Dur.	No. of Starts	Accum. Starts	Helium Sat.	Prop. Temp.	Mixture Ratio	Chamber Pressure
Acceptance Test	867	5	5	1	1	Yes	Ambient	1.55	197
	870	5	10	1	2			1.63	195
(Pulse train)	871-872	1.4	11.4	28	30			1.63	195
	873	100	111.4	1	31			1.63	194
Baseline Performance Test	45	10	121.4	1	32			1.56	194
	46	5	126.4	1	33			1.64	199
	52	600	726.4	1	34			1.66	190
(Pulse train)	53-68	30.65	760.05	130	164			1.62	179
Endurance Test No. 1	117	10	770.05	1	165			1.32	171
	118	5	775.05	1	166			1.34	174
	119	5	780.05	1	167			1.33	175
(Pulse train)	120-135	30.1	810.15	128	295			1.37	170
	136	5	815.15	1	296			1.34	179
	137	5	820.15	1	297			1.36	177
	138	5	825.15	1	298			1.50	178
	139	200	1025.15	1	299			1.58	184
Endurance Test No. 2	167	10	1035.15	1	300	No		1.46	191
	168	5	1040.15	1	301			1.82	208
	169	5	1045.15	1	302			1.65	198
(Pulse train)	170	139	1184.15	139	441			1.62	187
	171	200	1384.15	1	442			1.64	196
Endurance Test No. 3	296	10	1394.15	1	443	Yes		1.65	198
(Pulse Train)	297-353	57	1451.15	57	500			1.60	202

TABLE 24. PULSE PERFORMANCE SEQUENCE

On Time, (sec)	Off Time, (sec)	Cum Elapsed	No. of Pulses	Total on Time	Frequency Pulse/sec
0.050	2.950	30 10	10	0.1	0.33
0.050	0.950	10 10	10	0.1	1.0
0.050	0.450	5 10	10	0.1	2.0
0.050	0.150	2 10	10	0.1	5.0
0.100	2.900	30 10	10	1.0	0.33
0.100	0.900	10 10	10	1.0	1.0
0.100	0.400	5 10	10	1.0	2.0
0.100	0.100	2 10	10	1.0	5.0
0.250	2.750	30 10	10	2.5	0.33
0.250	0.750	10 10	10	2.5	1.0
0.250	0.250	5 10	10	2.5	2.0
0.500	2.500	15 10	5	2.5	0.33
0.500	1.000	7.5 10	5	2.5	0.67
0.500	0.500	5 10	5	2.5	1.0
1.00	3.00	20 10	5	5.0	0.25
1.00	1.00	5	5	5.0	0.50
Totals		341.5	135	31.0	

Acceptance Test

The acceptance test was conducted with ambient temperature and 100-percent helium saturated propellants at simulated altitude. Testing consisted of two 5-second tests to verify thrust and mixture ratio were properly set; a series of 8 pulses, 50 msec on/1000 msec off; a series of 20 pulses, 50 msec on/1000 msec off; and a 100-second burn. Some difficulty was encountered in opening the MOOG bipropellant valve, apparently due to a high valve pressure drop (64 psid), which resulted in a facility lockup pressure of 350 psia, at which level valve operation was marginal. This resulted in a loss of a majority of the planned pulses (20) in the first pulse sequence. Inlet pressure was adjusted downward to obtain better valve response for the second pulse series and the 100-second test. The resultant chamber pressure was 194 psia.

Baseline Performance Test

The baseline performance test was conducted with ambient temperature and 100-percent helium saturated propellants at simulated altitude. Testing consisted of two calibration tests to verify thrust and target mixture ratio (1.63 o/f), the pulse sequence specified in Table 24, and a 600-second steady-state duration test.

Difficulty was again encountered in opening the MOOG bipropellant valve (tests 47 through 51). Inlet pressures were adjusted downward and valve voltage was increased to 50 volts to obtain valve functioning. The resultant chamber pressures for the duration and pulsing test were $\approx$ 190 psia. Soakback data were recorded for 45 minutes subsequent to the pulse series.

Environmental Tests

All nonfiring environmental exposure tests were conducted at the Valley Division of AETL (Approved Engineering Test Laboratories) located at 9550 Canoga Avenue, Chatsworth, California.

The environmental tests (Fig. 60) were conducted according to MIL-STD-810B, the first three conducted to sequence A and the last three to sequence B. Environmental sequence A involved exposing the engine to: (1) rain, (2) humidity, (3) salt atmosphere, (4) sand and dust, and (5) vibration. Sequence B involved: (1) rain, (2) sand and dust, and (3) vibration. The order of Sequence A testing was selected on the basis of subjecting the engine to the worst possible case of environmental conditions prior to launch and during flight. The rain and humidity tests were performed first to provide a saturated condition, salt atmosphere to ensure a salt residue, sand and dust with a wet chamber to form mud adhering to the surface (all simulating pre-launch conditions) and finally vibration to simulate launch conditions.

The rain tests were conducted according to Method No. 506. The test program consisted of exposing the engine to simulated rain equivalent to 0.5 inches per hour for one-half hour. The water temperature was 75 ±20 F. The engine was mounted in the rain chamber in the nozzle up attitude with a protective plastic bag over the valve. The water collected in the engine was dumped subsequent to the test.

The humidity tests were conducted according to Method 507. The test procedure consisted of exposing the engine to a relative humidity of 100 percent at 100 F temperature for a period of 4 hours. The engine was installed in a nozzle up attitude in the humidity chamber and the valve was covered with a plastic bag during the test. The accumulation of moisture in the chamber was removed by turning the engine in the upright position.

The salt atmosphere tests were conducted according to Method 509. The test procedure consisted of exposing the engine to a simulated salt spray in a salt spray chamber. The spray was 1 percent salt solution at 75 ± 20 F and the exposure time was 4 hours. The engine was mounted at a 45 degree nozzle up attitude in the salt spray chamber and the excess salt spray solution accumulated in the chamber was dumped upon completion on the exposure test. The valve was covered with a plastic bag during this test.

The sand and dust tests were conducted in accordance to Method No. 510. The test procedure consisted of exposing the engine to a 140 mesh silica flour environment for 1 hour in a dust chamber. The dust concentration was 0.3 ± 0.2 gms per cubic foot, with temperature at 75 + 20 F at relative humidity of less than 22 percent, and with particle velocity up to 500 feet per minute. The engine was mounted in the nozzle up attitude. The engine was turned upright upon test completion to remove excess dust from inside the thrust chamber.

The vibration tests were conducted according to Method No. 514. The engine was instrumented with six accelerometers and four strain gages (strain gages installed for the first environmental sequence only) as shown in Fig. 61 and subjected in the three engine axes to the sinusoidal and random vibration inputs specified in Table 25. The engine was at ambient temperature, nonpressurized during Sequence A,

TABLE 25. VIBRATION REQUIREMENTS

RANDOM VIBRATION		SINUSOIDAL VIBRATION
20-100 Hz	+9 db/octave	5-23 Hz at 1.0 g peak
100-300 Hz	Constant at 0.70 G^2/Hz	23-40 Hz at 0.036 inch double amplitude
300-2000 Hz	-3 db/octave	Sweep of one actave/min from 5 Hz to 40 Hz and back to 5 Hz
70 seconds duration in each of three orthogonal axis		Dwell at each resonance for 30 seconds
		Total sweep time of six minutes plus dwell times

pressurized during Sequence B and all protective covers were removed with the exception of valve propellant inlet caps and plugs in the pressure sensing ports in the injector. The engine was visually inspected for physical damage due to the environmental tests prior to conducting the subsequent scheduled hot-fire tests.

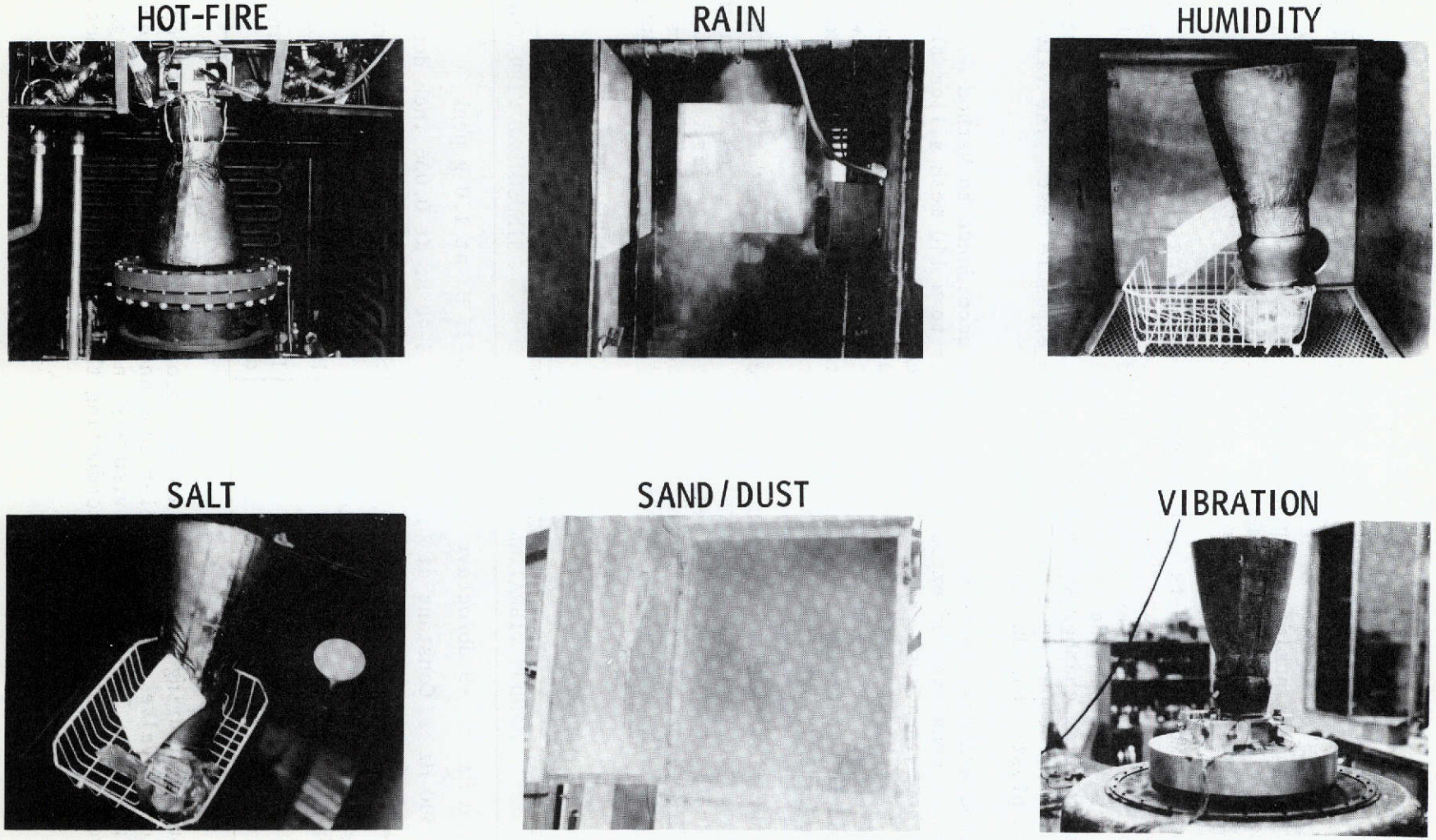

Figure 60. Durability Beryllium Engine Environmental Test Matrix (Sequence A)

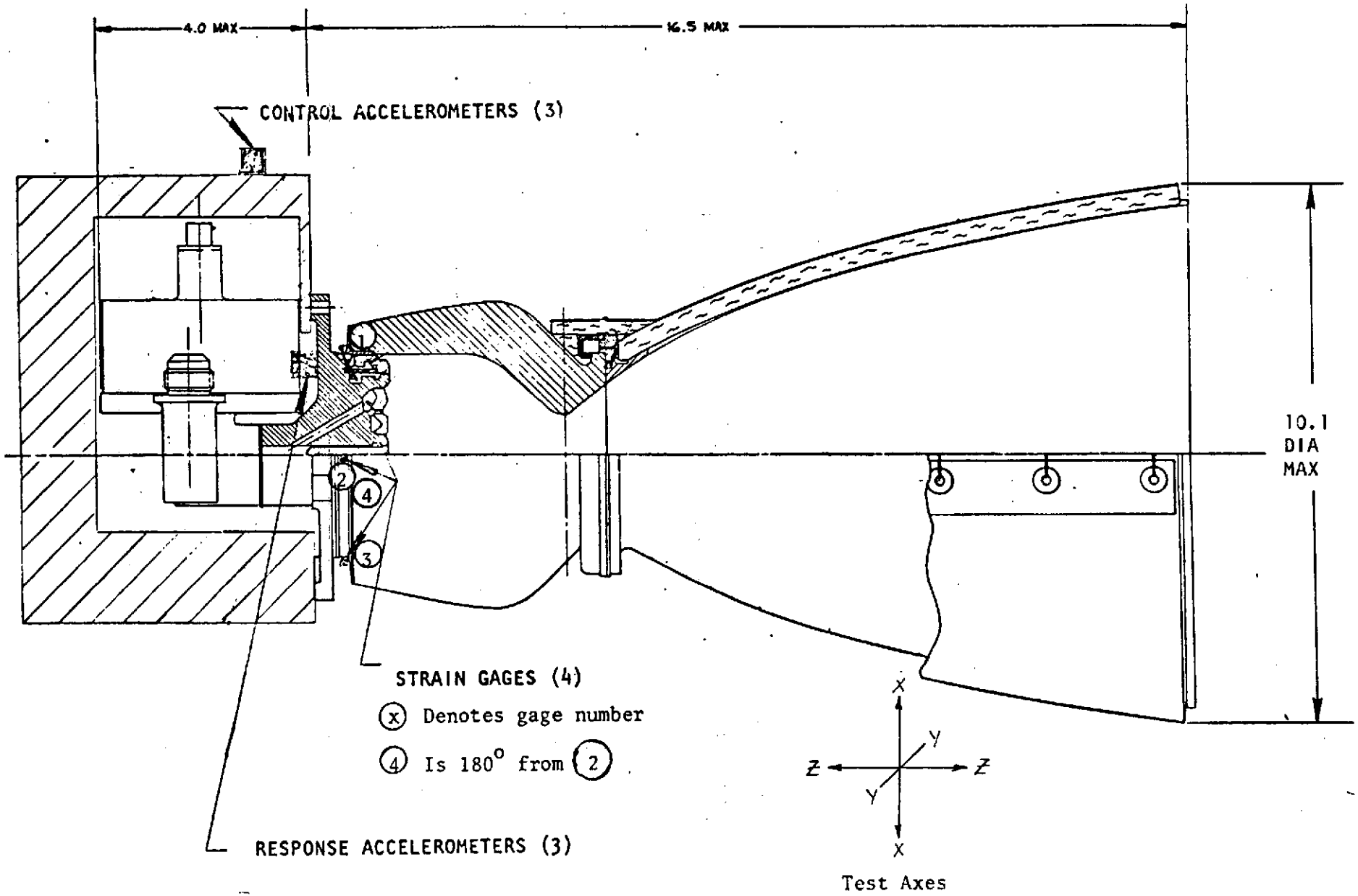

Figure 61. Location of Accelerometers and Strain Gages on RCE for Vibration Testing

Subsequent to environmental test No. 2, the MOOG Inc. bipropellant, Model 54X107A, S/N 003, valve was noted to have sustained seat damage which resulted in excessive leakage. A dummy valve was employed during environmental test No. 3. A new MOOG Inc. valve, Model 54X107A, S/N 005, was supplied by NASA/JSC for environmental tests No. 4, 5, and 6. The valve was pressurized during environmental tests No. 4, 5, and 6 with 300 psig GN_2 at both oxidizer and fuel inlets. The engine was purged through the valve subsequent to each of these tests to simulate the cleaning effects of hot fire. This valve also sustained seat damage.

Endurance Tests

Endurance test No. 1 was conducted per the test matrix shown in Table 23. The pulse sequence was accomplished per Table 24.

The 10-second steady-state test (test 117) was initiated with inlet conditions established from the baseline performance test. However, the nominal mixture ratio of 1.63 o/f was not achieved as shown in Table 23 and a marked shift in oxidizer side resistance occurred between the valve inlet and injector manifold. Because of the marginal opening condition of the valve, the remaining tests were conducted at the lower mixture ratio of $\approx$ 1.3 o/f.

The 200-second steady-state duration test was initiated at a mixture ratio of $\sim$ 1.4 o/f to open the valve and adjusted to the nominal value of 1.6 o/f during the run.

Endurance test No. 2 was conducted per the test matrix of Table 23 with Marotta PV-20 facility valves. The MOOG valve exhibited excessive leakage when attempting to initiate this test series and was, therefore, removed for failure analysis. The pulse sequence of Table 24 was replaced with 139 pulses of 1-second on and 2-seconds off.

The first test attempted (10-second steady-state test 167) revealed a restriction on the oxidizer side as evidenced by low mixture ratio with nominal inlet conditions. The inlet pressures were adjusted for the next test; however, the resultant mixture ratio was 1.8 o/f (restriction apparently came out). The inlet pressure was reset at the nominal conditions and nominal mixture ratio (163 o/f) was achieved.

Because a bipropellant valve was not available for hot-fire testing subsequent to the sixth environmental test series, the engine was refitted with Marotta PV-20 facility valves for the third endurance test. A 10-second steady-state burn (test 296) followed by 57 pulses (1 second on/2 seconds off) were performed with the engine as indicated in Table 23.

The 10-second steady-state test indicated a slightly higher than nominal mixture ratio with nominal inlet conditions, and mixture ratio decreased to near nominal during the pulse series.

The engine was removed from the test stand and decontaminated prior to posttest inspection.

OFF LIMITS ENGINE TEST PROGRAM

The Off Limits Engine was hot-fire tested at simulated altitude with ambient temperature 100-percent saturated propellants per the matrix of Table 26.

Test conditions were selected to simulate the off-limits operating capability of the engine. Specific objectives were to demonstrate:

1. Operation over a wide range of mixture ratio (1.45 to 1.85 o/f) and chamber pressure (150 to 230 psia)
2. Blowdown capability (reduce chamber pressure until pressure oscillations excessive)
3. Simulation of dual oxidizer regulator malfunction which can result in a mixture ratio of ~ 3 o/f and chamber pressure of ~ 235 psia
4. Operation with a plugged primary fuel orifice resulting in oxidizer impinging on the combustor wall causing localized high heat flux and oxidizer rich region
5. Operation with plugged film coolant orifices (1 to 4 adjacent orifices) resulting in localized high heat flux region

Eighteen tests were conducted, all at simulated altitude conditions. During the dual regulator malfunction simulation test the Haynes 25 nozzle extension reached equilibrium at 2300 F (Haynes 25 melts at approximately 2400 F). The resultant substantial loss in material strength resulted in nozzle damage. The nozzle was modified by removing the damaged section (at $E_n \sim 7{:}1$) and the test program was completed. This test established the limit for using Haynes 25 as a nozzle skirt material and resulted in the selection of a columbium nozzle for the Durability Engine tests. It is noted that the regulator malfunction test was repeated with a columbium nozzle during a company-sponsored program without incident (45-second test, nozzle reached equilibrium at 2300 F).

SIMULATED ENGINE TEST PROGRAM

The vibration simulator was subjected to 100 simulated random vibration space shuttle missions per Fig. 62. A total of 100 minutes of random vibration had been completed in the X-axis prior to a revision in the specification. The Y- and Z-axes were tested for 117 minutes each to the revised specification which reflects present shuttle orbiter launch levels. Posttest proof pressure at 500 psig and helium leak tests at 300 psig were performed after completion of the vibration testing.

The vibration simulator was installed on the shaker as shown in Fig. 63. The simulator was instrumented to obtain both accelerometer and strain data; however, the former were lost because of a data acquisition system malfunction.

During Y-axis testing, a TIG weld cracked in the aluminum tube assembly bolted to the beryllium chamber to simulate the nozzle extension. The weld was repaired and the vibration tests were completed. This failure had no bearing on the engine design since the aluminum structure was simply a low cost mass simulator whose purpose was to adequately load the braze joint.

TABLE 26. OFF-LIMITS ENGINE TEST SUMMARY

TEST SERIES	TEST NO. 870-	TEST DURATION SEC.	DATA POINT DUR. SEC.	ACCUM. DUR. SEC.	MIXTURE RATIO, o/F	CHAMBER PRESSURE, PSIA
1. Oxidizer Regulator Failed Simulation	768	210	200	200	1.65	200
			10	210	2.88	237
2. Mixture Ratio/ Chamber Pressure Survey	781	884	150	360	1.65	200
			100	460	1.63	230
			100	560	1.44	229
			100	660	1.43	200
			100	860	1.62	152
			100	960	1.83	202
			100	1060	1.82	230
			34	1094	2.04	184
	782	19	19	1113	1.90	153
	783	207	150	1263	1.66	201
			50	1313	1.86	201
			7	1320	1.96	184
	784	71	50	1370	1.65	201
			21	1391	2.04	202
	785	104	50	1441	1.67	201
			50	1491	2.01	230
			4	1495	2.12	223
	786	54	50	1545	1.65	201
			4	1549	2.39	216
	787	71	50	1599	1.65	201
			21	1620	1.99	160
Throttle Mode Operation	788	50	50	1670	1.67	152
	789	51	51	1721	1.69	128
	790	52	52	1773	1.70	102
	791	5	5	1778	1.58	66
	792	14	14	1792	2.08	204
3. Plugged Primary Fuel Hole	805	200	200	1992	1.68	202
4. One Plugged Coolant Hole	806	350	200	2192	1.59	201
			50	2242	1.79	153
			50	2292	1.83	153
			50	2342	1.81	179
5. Three Adjacent Plugged Coolant Holes	807	11	11	2353	1.65	201
	808	12	12	2365	1.64	201
	809	250	250	2615	1.64	200

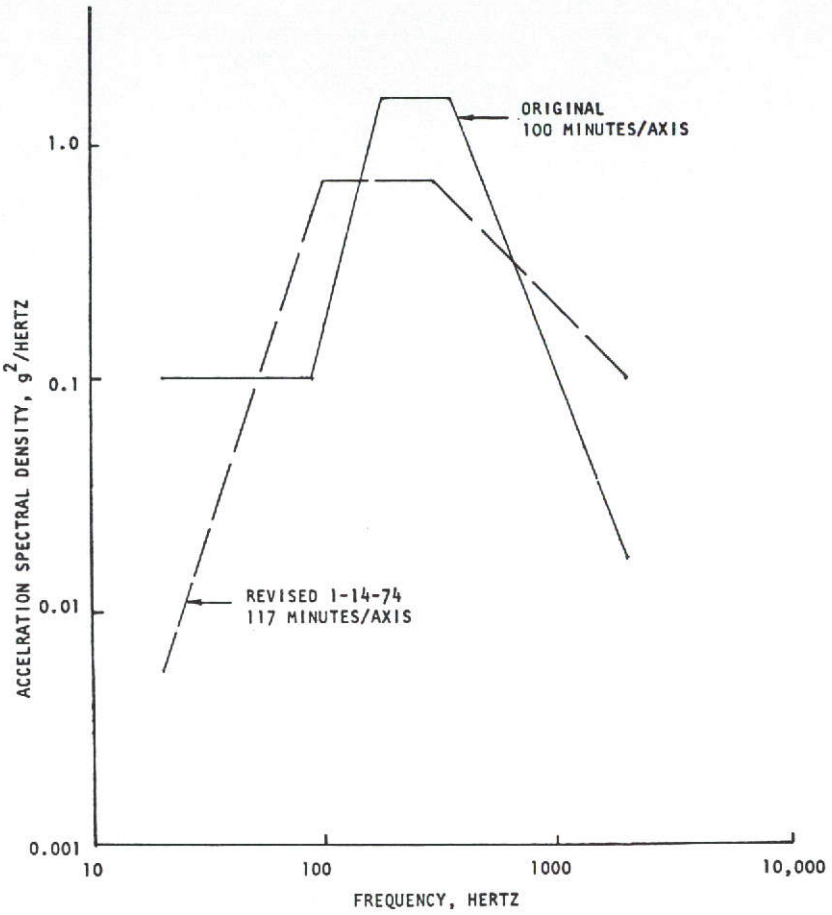

Figure 62. Random Vibration Specification

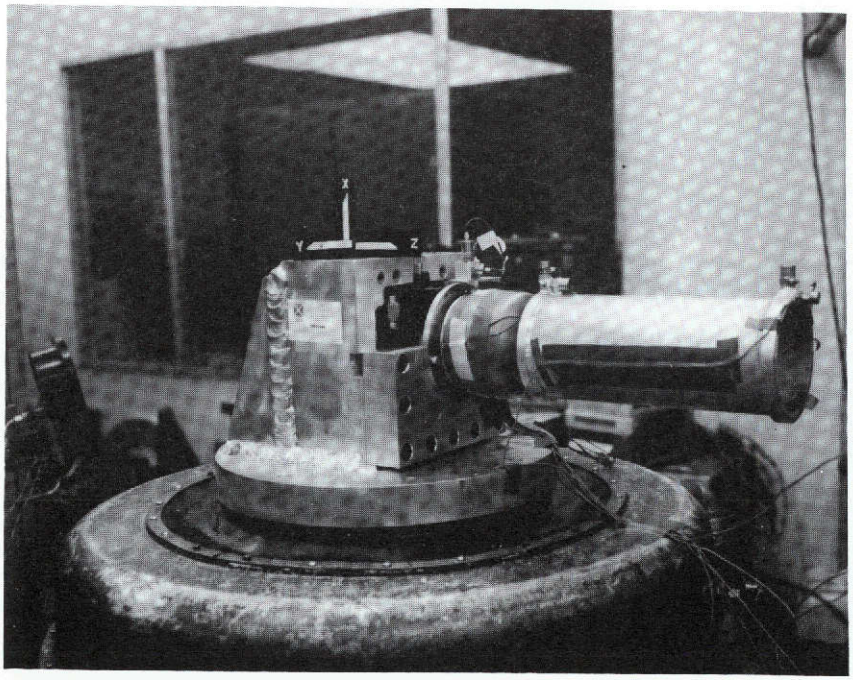

Figure 63. Vibration Simulator Mounted in Test Facility

PHASE IV - POSTTEST ANALYSIS AND DESIGN

Analyses of the Phase III test results is presented in this section along with a discussion of the impact of the test results on the projected flight configuration.

DURABILITY ENGINE TEST RESULTS

Steady-State Performance

The steady-state performance characteristics of the Durability Engine demonstrated throughout the test program are summarized in Table 27 and plotted in Fig. 64. All tests were conducted with ambient temperature propellants and at simulated altitude. All tests with the exception of endurance test No. 2 were conducted with 100-percent helium-saturated propellants. A vacuum specific impulse of 290 and 294 lbf-sec/lbm was demonstrated at nominal conditions (200-psia chamber pressure, 1.63 o/f mixture ratio) for saturated and unsaturated propellants, respectively.

The specific impulse achieved during the acceptance and baseline tests agrees with performance previously obtained with the three-ring design during a prior company-sponsored program. As discussed under Phase I an additional 1-second specific impulse could be obtained with an optimum 80-percent bell nozzle.

Several anomalies were encountered during tests performed subsequent to the environmental tests. During the endurance test No. 1, a high resistance was observed on the oxidizer side of the engine resulting in low mixture ratio. The engine assembly pressure drop had increased from 105 psid (prior to environmental tests) to 240 psid (after environmental tests). This pressure drop increase was isolated to the area between the valve inlet and injector manifold. Review of prior test data on the Moog, Inc., valve model 107A, S/N 003 indicated a history of increasing pressure drop during Rocketdyne hot-fire tests. This valve subsequently failed (excessive leakge on the oxidizer side). A detailed discussion of the valve problem is discussed later in this section.

Another increased resistance anomaly was experienced on the first short-duration test of endurance test No. 2. The oxidizer pressure drop had increased 20 psid, apparently due to blockage of several oxidizer orifices with sand and dust. Performance was low during this test, probably due to misimpingement of primary elements. The apparent blockage was removed by the subsequent engine start as indicated by nominal recorded pressure drops.

Blocked film coolant orifices were observed after the first (three adjacent orifices) and second (four adjacent orifices) endurance test series. In both cases 200-second duration tests were successfully run on the engine. The plugged orifices were not cleaned out; however, visual observations indicated the material to be sand and dust from the environmental test series. It is noted that the film coolant orifice diameter is 0.03 inch as are the main oxidizer orifices. The main fuel orifices, which have not appeared to plug, are 0.020 inch in diameter. These

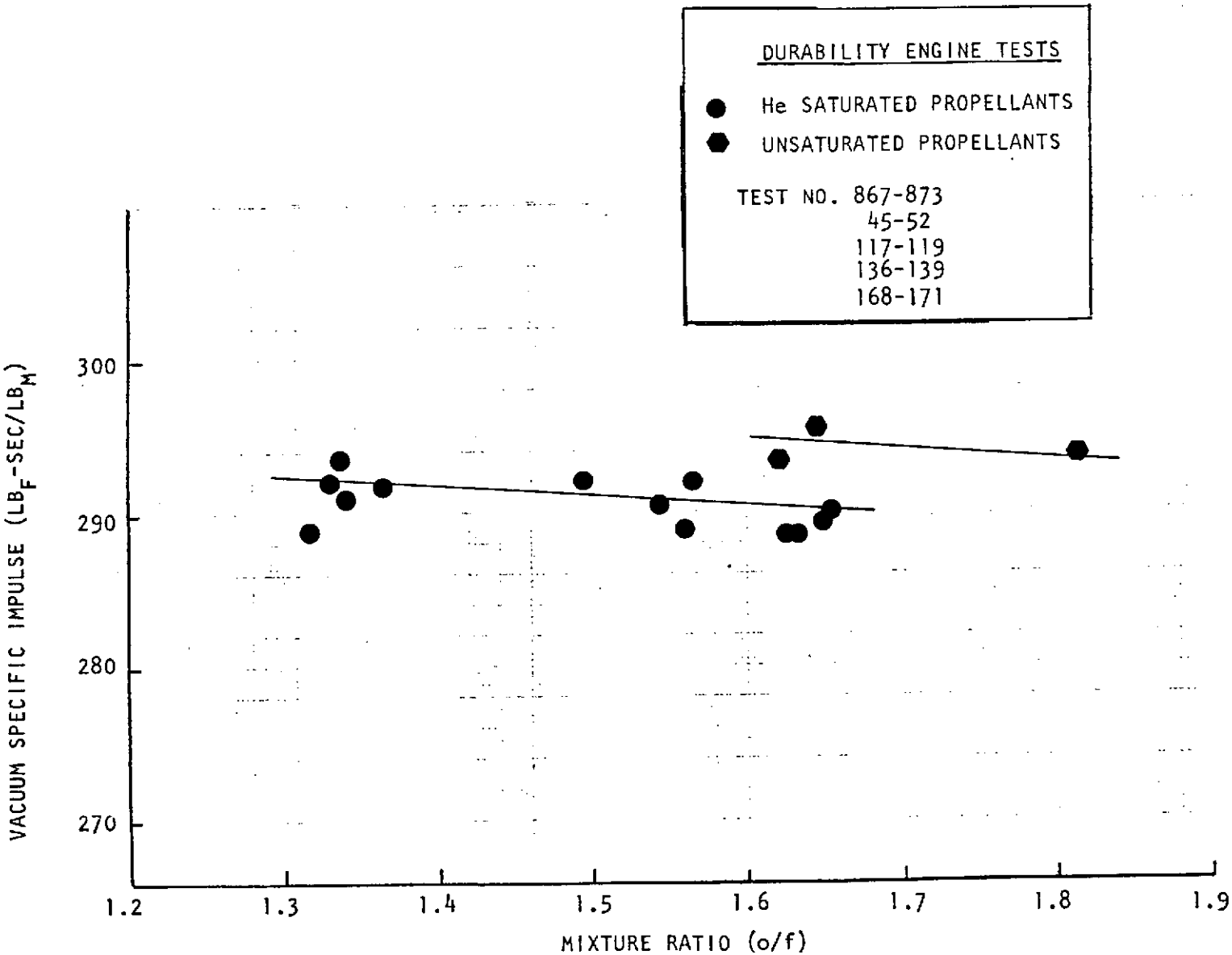

Figure 64. Durability Engine Steady-State Performance Specific Impulse vs Mixture Ratio, ϵ_N = 40:1

TABLE 27. DURABILITY ENGINE TESTS STEADY-STATE PERFORMANCE SUMMARY

ε = 40:1 NOZZLE

	Test No.	Test Duration (sec)	Slice Time (sec)	Vacuum Thrust (lb)	Chamber Pressure (psia),NS	Mixture Ratio (o/f)	Specific Impulse (lb_f-sec/lb_m)
Acceptance Test	867	5	5	596.1	196.9	1.55	290.2
	870	5	5	585.3	194.6	1.63	288.6
	873	100	5	585.3	194.3	1.63	288.6
			100	589.1	194.3	1.62	290.3
Baseline Performance	45	10	5	580.8	194.0	1.56	289.1
	46	5	5	595.4	198.6	1.64	289.5
	52	600	5	573.1	191.3	1.68	289.9
			100	573.9	190.6	1.67	290.9
			400	573.4	190.4	1.66	291.4
			600	571.7	190.2	1.66	290.8
Endurance Test No. 1	117	10	5	505.7	170.8	1.32	288.7
	118	5	5	517.7	174.4	1.34	290.8
	119	5	5	519.4	174.7	1.33	291.9
	136	5	5	534.9	179.2	1.34	293.4
	137	5	5	528.7	177.3	1.36	292.8
	138	5	5	532.5	178.1	1.50	292.0
	139	200	5	542.2	181.1	1.58	291.8
			100	559.5	186.3	1.62	291.0
			200	554.1	184.7	1.58	291.1
Endurance Test No. 2 Propellants Not Saturated	167	10	5	566.3	190.5	1.46	286.7
	168	5	5	620.0	207.7	1.82	293.8
	169	5	5	592.4	198.3	1.65	295.4
	171	200	5	592.1	196.9	1.62	293.3
			100	590.2	195.9	1.65	293.1
			200	589.8	196.3	1.65	293.2
Endurance Test No. 3	296	10	10	588.2	198.0	1.65	293.7

tests confirmed the susceptibility of a Space Shuttle RCS Engine to injector plugging when sequentially exposed to sand and dust and launch random vibration and the requirement that the engine be capable of safe operation under these conditions.

The engine pressure profile is shown in Table 28 as determined from the acceptance test data with the Moog, Inc., valve model 54-107A S/N 003. The profile is based on data taken at 100-second duration (test 873) at 194-psia chamber pressure with the valve inlet pressure on the oxidizer and fuel sides at 297 and 267 psia, respectively. At 200-psia chamber pressure, injector inlet pressures would be 246 and 250 psia such that in a flight configuration with a 30-psid valve and 10-psid calibration orifice, the engine inlet pressure requirement would be <290 psia.

TABLE 28. DURABILITY ENGINE PRESSURE PROFILE, ACCEPTANCE TEST NO. 873, MOOG INC. VALVE (54-107A S/N 003) AP73-110 INJECTOR

	Fuel		Oxidizer	
	Test	Nominal	Test	Nominal
Valve Inlet Pressure	266.8	277.1	296.9	309.4
Valve Outlet Pressure	241.2	249.5	237.4	245.8
Injector Manifold Pressure	236.3	244.6	234.9	243.2
Injector End Chamber Pressure	195.5	201.1	195.5	201.1
Nozzle Stagnation Chamber Pressure	194.3	200.0	194.3	200.0

Pulse Performance

The pulsing characteristics of the durability engine are summarized in Table 29. Figure 65 presents pulse performance measured during the baseline performance and endurance test series 1. Pulse data were not obtained during endurance tests 2 and 3 because of the use of facility valves in place of the malfunctioning Moog valve. Multiple 1-second pulses replaced the pulse sequence for these tests. The pulse data, as shown in Fig. 65, indicates the engine meets the pulse specific impulse goal of 220 lbf-sec/lbm at 30 lbf-sec pulse total impulse at a pulse frequency of 5 cycles/second. These data agree with that obtained during the company-sponsored program and previously presented in Fig. 21. Since the injector design was constrained by existing test facilities and valves which necessitated a large manifold volume, the 220 lbf-sec/lbm goal would be met at lower pulse frequencies with a flight design (Fig. 22).

Engine start times (valve signal to 90-percent thrust) of 40 msec were measured for 1/3-Hz pulses and 30 msec for 5-Hz pulses. Decreased start times with increased pulse frequency reflects the fact that the engine manifolds are not totally purged prior to each subsequent pulse. Cutoff time (valve signal to 10-percent thrust decay) of 20 msec was recorded.

TABLE 29. DURABILITY ENGINE TESTS
PULSING PERFORMANCE SUMMARY

Test No.	t_{on} (sec)	t_{off} (sec)	Frequency (cps)	Total Impulse (lb-sec)	Pulse Specific Impulse (lb_f-sec/lb_m)	Pulse Mixture Ratio (o/f)
871	0.050	2.95	1/3	16.0	153	1.43
872	0.050	2.95	1/3	16.4	155	1.42
53	0.050	2.95	1/3	14.8	132	1.39
54	0.050	0.95	1	15.5	139	1.44
55	0.050	0.45	2	17.4	159	1.52
56	0.050	0.15	5	18.4	178	1.65
57	0.10	2.90	1/3	43.3	191	1.50
58	0.10	0.90	1	45.0	203	1.59
59	0.10	0.40	2	46.1	210	1.63
60	0.10	0.10	5	53.4	258	1.60
61	0.25	2.75	1/3	127.5	239	1.58
62	0.25	0.75	1	131.2	250	1.61
63	0.25	0.25	2	136.3	263	1.63
64	0.50	2.50	1/3	272.9	264	1.61
65	0.50	1.00	2/3	274.5	267	1.61
66	0.50	0.50	1	275.9	270	1.62
67	1.0	2.0	1/3	558.4	275.5	1.61
68	1.0	1.0	1/2	561	277.4	1.61

TABLE 29. (Concluded)

Test No.	t_{on} (sec)	t_{off} (sec)	Frequency (cps)	Total Impulse (lb-sec)	Pulse Specific Impulse (lb_f-sec/lb_m)	Pulse Mixture Ratio (o/f)
120	0.050	2.95	1/3	17.5	146	1.18
121	0.050	0.95	1	18.6	147	1.31
122	0.050	0.45	2	20.7	169	1.40
123	0.050	0.15	5	20.4	170	1.43
124	0.10	1.90	1/2	44.5	192	1.36
125	0.10	0.90	1	46.3	205	1.41
126	0.10	0.40	2	50.1	227	1.47
127	0.10	0.10	5	52.1	253	1.41
128	0.25	2.75	1/3	124	243	1.38
129	0.25	0.75	1	125	250	1.40
130	0.25	0.25	2	129	264	1.41
131	0.50	2.50	1/3	255	263	1.38
132	0.50	1.50	2/3	256	265	1.38
133	0.50	0.50	1	258	269	1.39
134	1.0	2.0	1/3	524	276	1.37
135	1.0	1.0	1/2	524	278	1.37

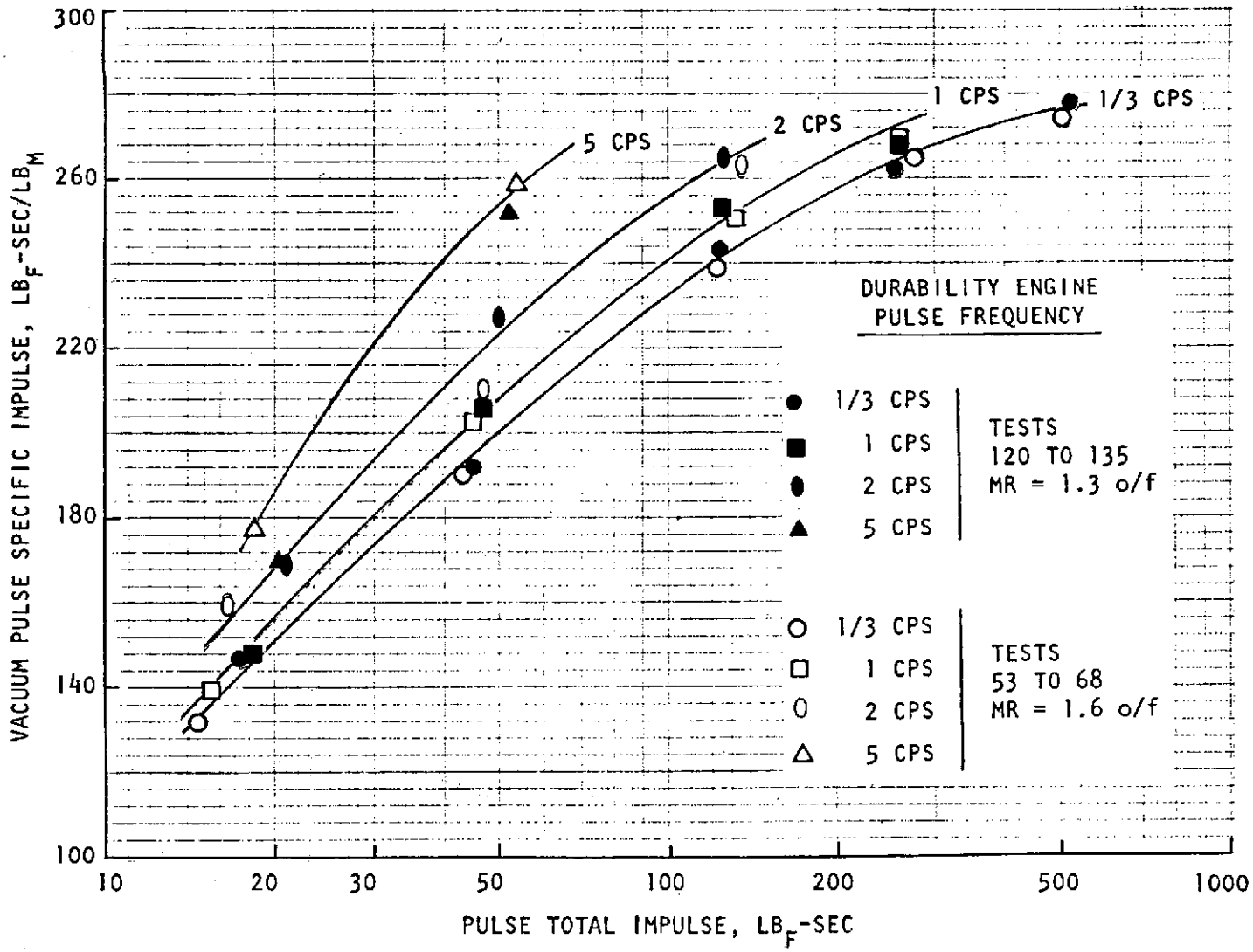

Figure 65. Durability Engine Pulse Performance Pulse Specific Impulse Vs Pulse Total Impulse, ε_N = 40:1

Thermal Characteristics

The Durability Engine was tested with both an uninsulated Haynes 25 nozzle extension (acceptance tests) and an insulated (Johns-Manville Dynaflex) coated columbium (C-103) nozzle extension (all subsequent tests).

Figure 66 provides temperature data recorded on the uninsulated temperature configuration. At the conclusion of the 100-second acceptance test (test 873), the Haynes-25 nozzle had reached a temperature of 1750 F. The beryllium at the injector end was at 190 F and at the throat was below 500 F. At the end of 100 seconds all temperatures, except the nozzle nut, had effectively reached thermal equilibrium conditions. Figure 68 provides temperature data for the 600-second baseline performance test (test 052) performed with the insulated configuration. All temperatures reached equilibrium in 200 seconds of on-time. Some temperatures (nozzle insulation OD) tend to decrease past the 200-second point and could be caused by changes in properties of the insulation and titanium (emissivity) due to heating and oxidation. The recorded beryllium temperatures were relatively unchanged, 500 F at the throat, from those measured during the test (test 873) without the nozzle insulation blanket. The measured peak nozzle temperature was 2000 F. The insulation outside temperature exceeded the 800 F requirement by 75 F at the end of the test. This can be explained by the unoxidized condition of the titanium insulation blanket.

Figure 70 shows the soakout temperatures after Test 068 and indicates a peak injector temperature of 190 F after 34 minutes of soak time. The valve thermocouple failed during testing prior to the soak period.

The temperature histories for duration tests 139 and 171 (200 seconds) and subsequent thermal soakouts for endurance tests 1 and 2 are presented in Fig. 71 through 74. The thermocouple locations are shown in Fig. 75.

The data of endurance test No. 1, test 139, indicate maximum nozzle and exit flange temperatures of 2025 F and 1630 F, respectively. The throat temperatures measured at locations 90, 180, and 270 degrees angular location indicate a mean outside surface temperature of 530 F. However, at 200 seconds into the run, a maximum throat outside surface temperature of 745 F was measured at the 0-degree angular location, which is an indication of fuel film plugging. Posttest inspection indicated that three film coolant holes were plugged. The two temperatures recorded at 0- and 180-degree angular locations at the head end of the combustor were 230 F and 190 F, respectively. A 180 F nominal temperature has previously been recorded for these positions; this indicates the influence of the three plugged film coolant holes. The injector back face and valve were indicated to be at their nominal values of 140 F and 80 F, respectively. The nozzle blanket temperature exceeds the requirement limit of 800 F by 70 F because of hotter wall temperatures due to fuel film orifice plugging. The thermal soakout data under vacuum conditions indicated beryllium combustor equilibration of 450 F occurred at approximately 100 seconds after engine cutoff and maximum beryllium head end temperature was 440 F. The peak valve temperature of 200 F was reached 30 minutes after engine cutoff.

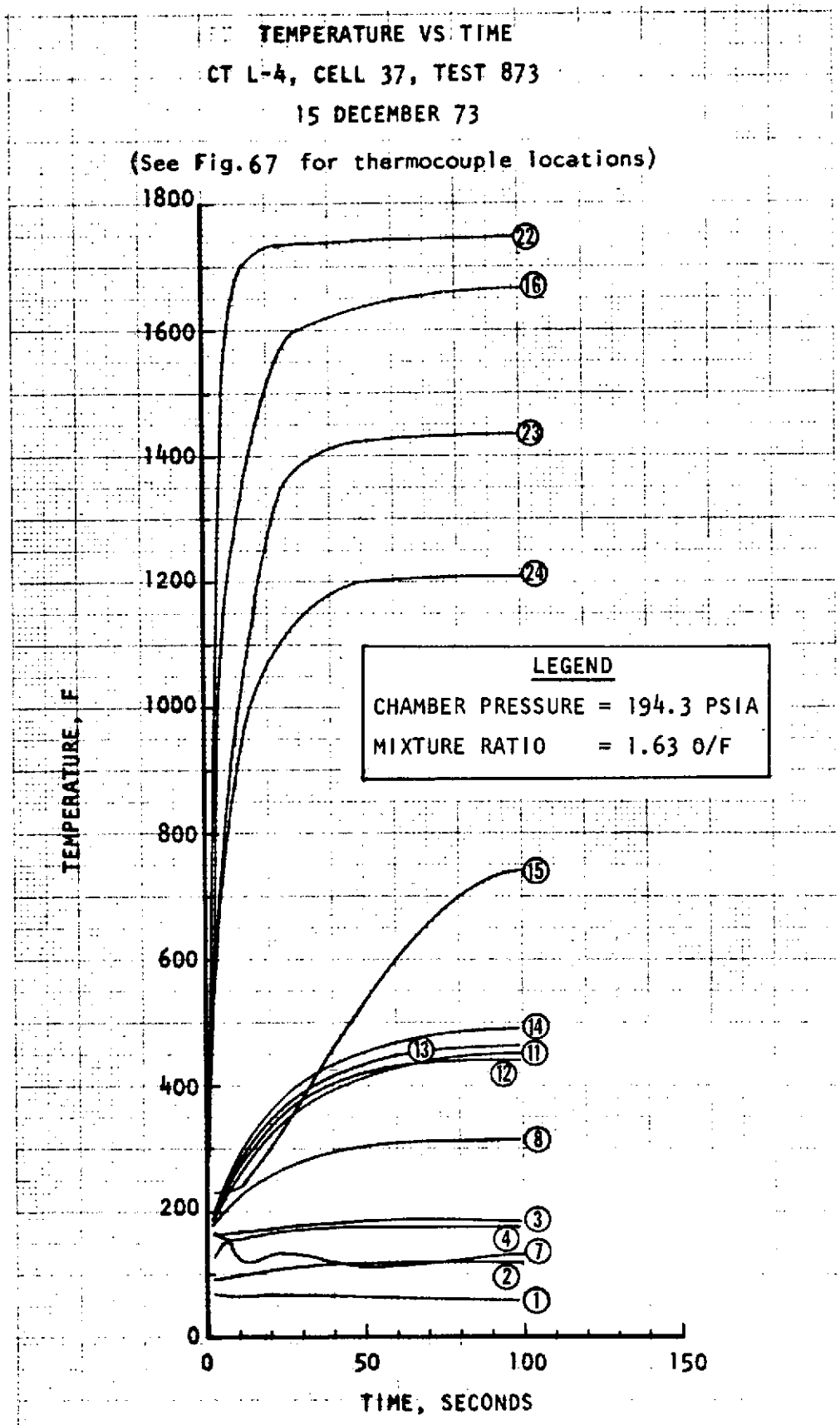

Figure 66. Acceptance Test 873

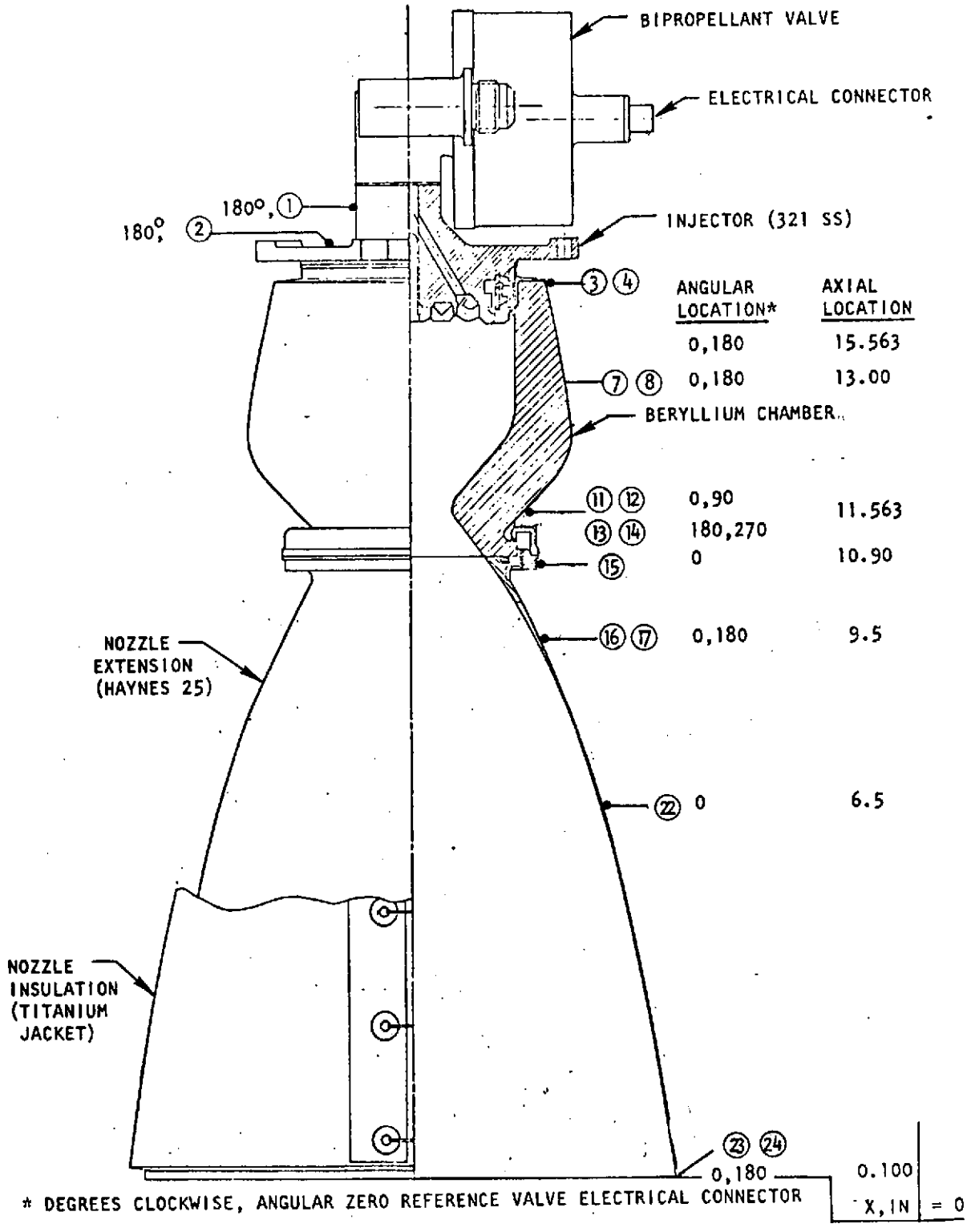

Figure 67. Rocket Engine Assembly Representative Thermocouple Installation

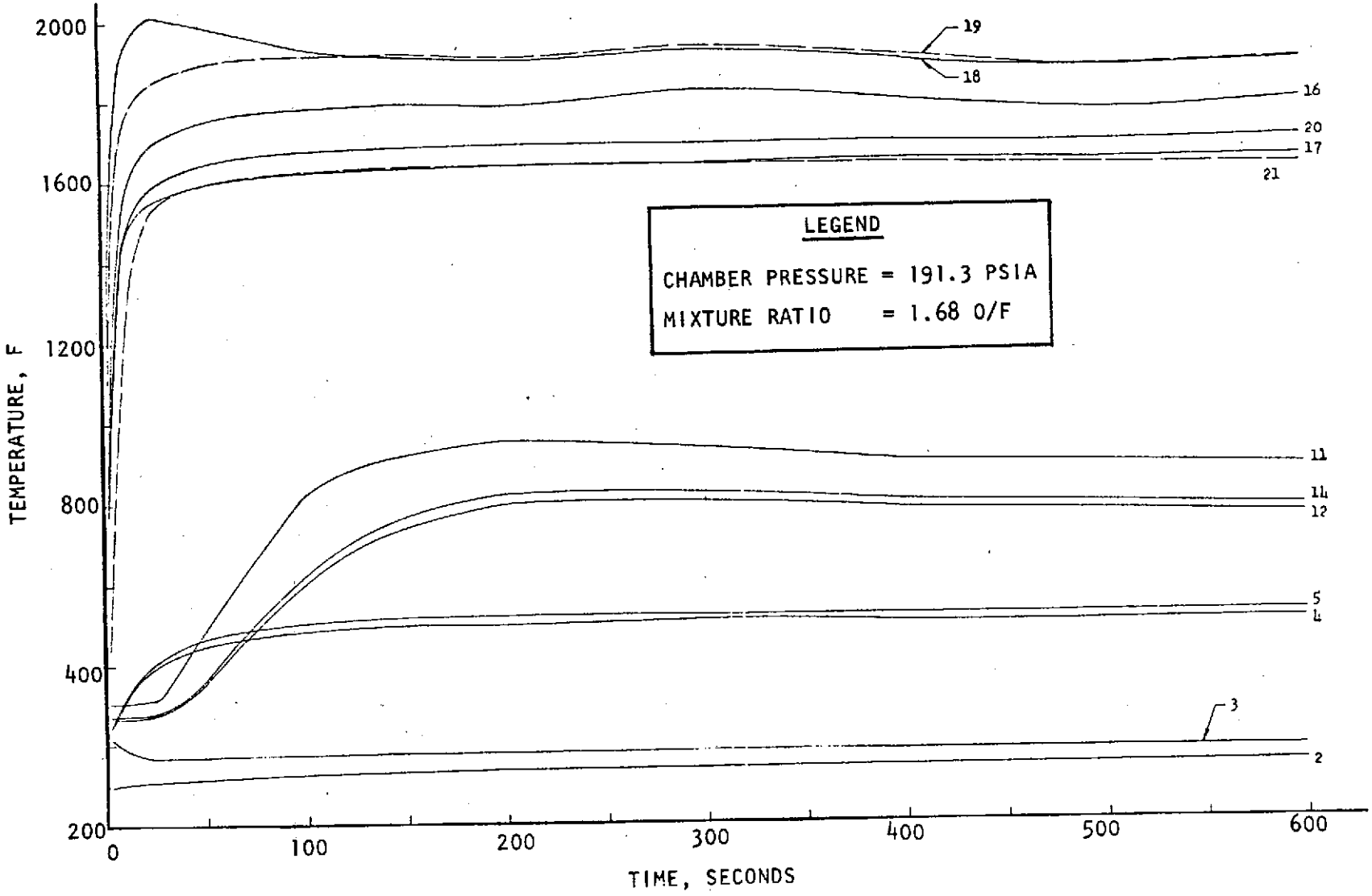

Figure 68. Temperature Vs Time, CTL-4, Cell 37, Test 870-052, 23 January 1974
(See Fig.69 for Thermocouple Locations)

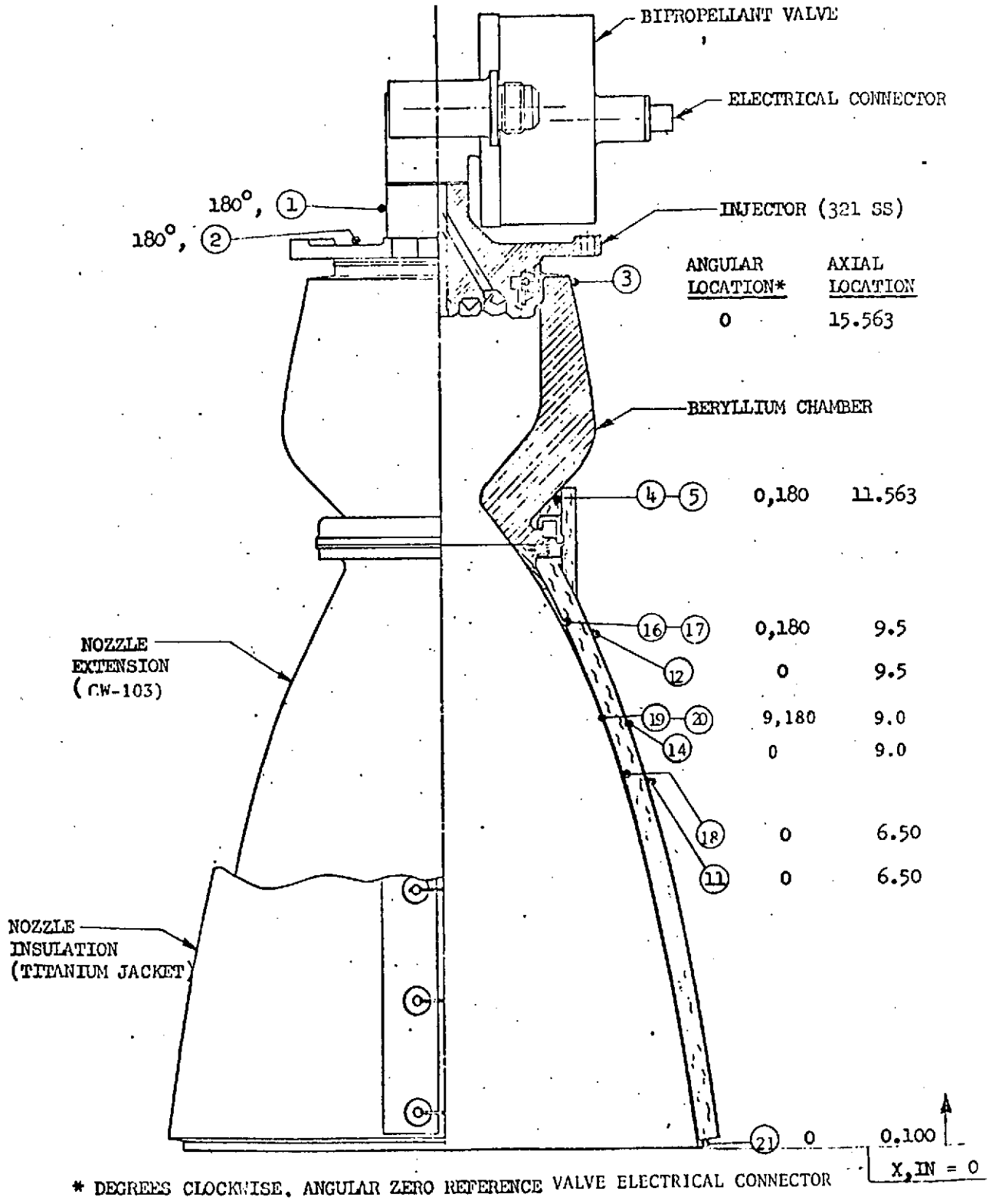

Figure 69. Rocket Engine Assembly Representative Thermocouple Installation

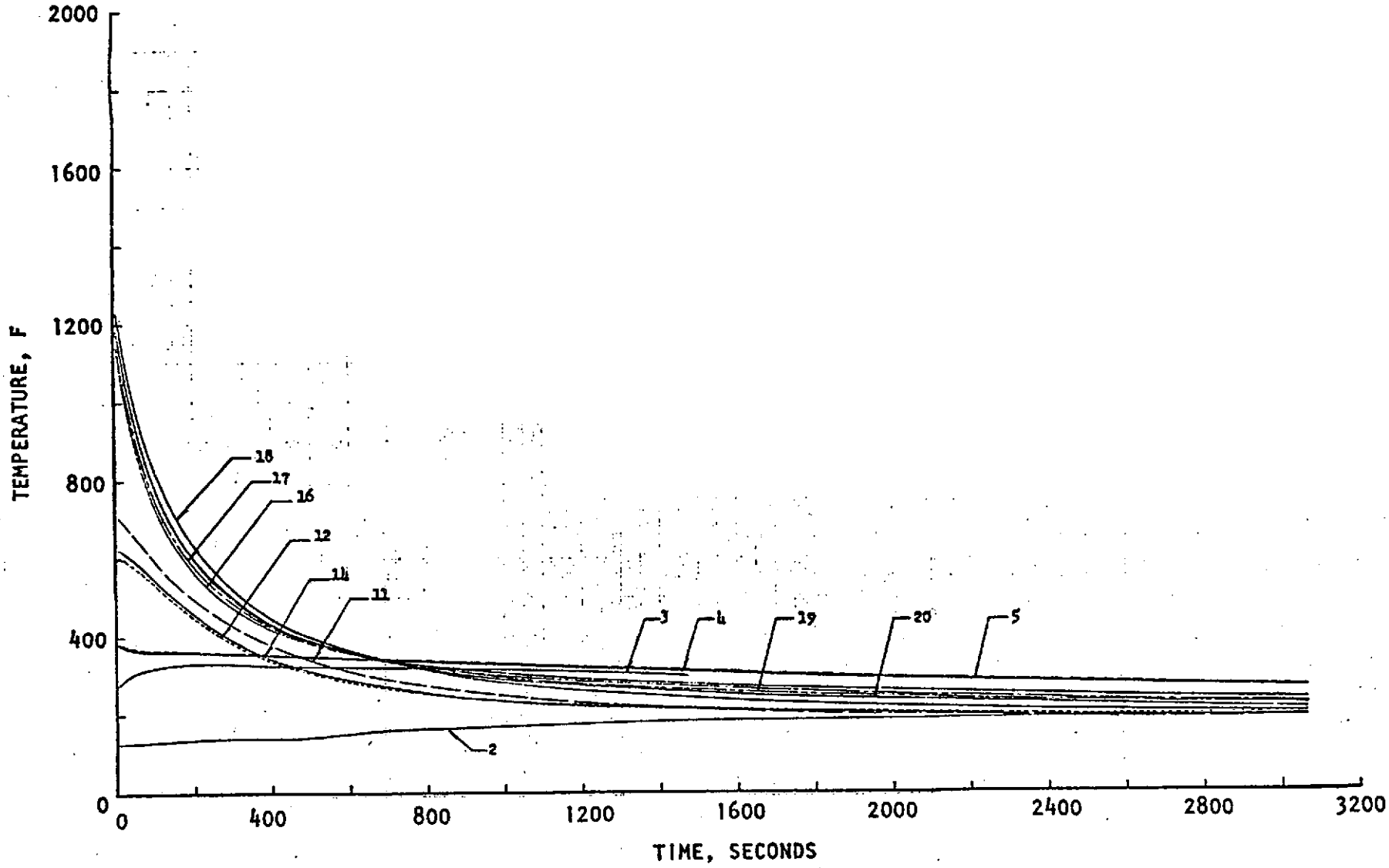

Figure 70. Temperature Vs. Time, CTL-4, Cell 37, Test 870-068 (Post Test Soak), 23 January 1974 (See Fig. 69 for Thermocouple Locations)

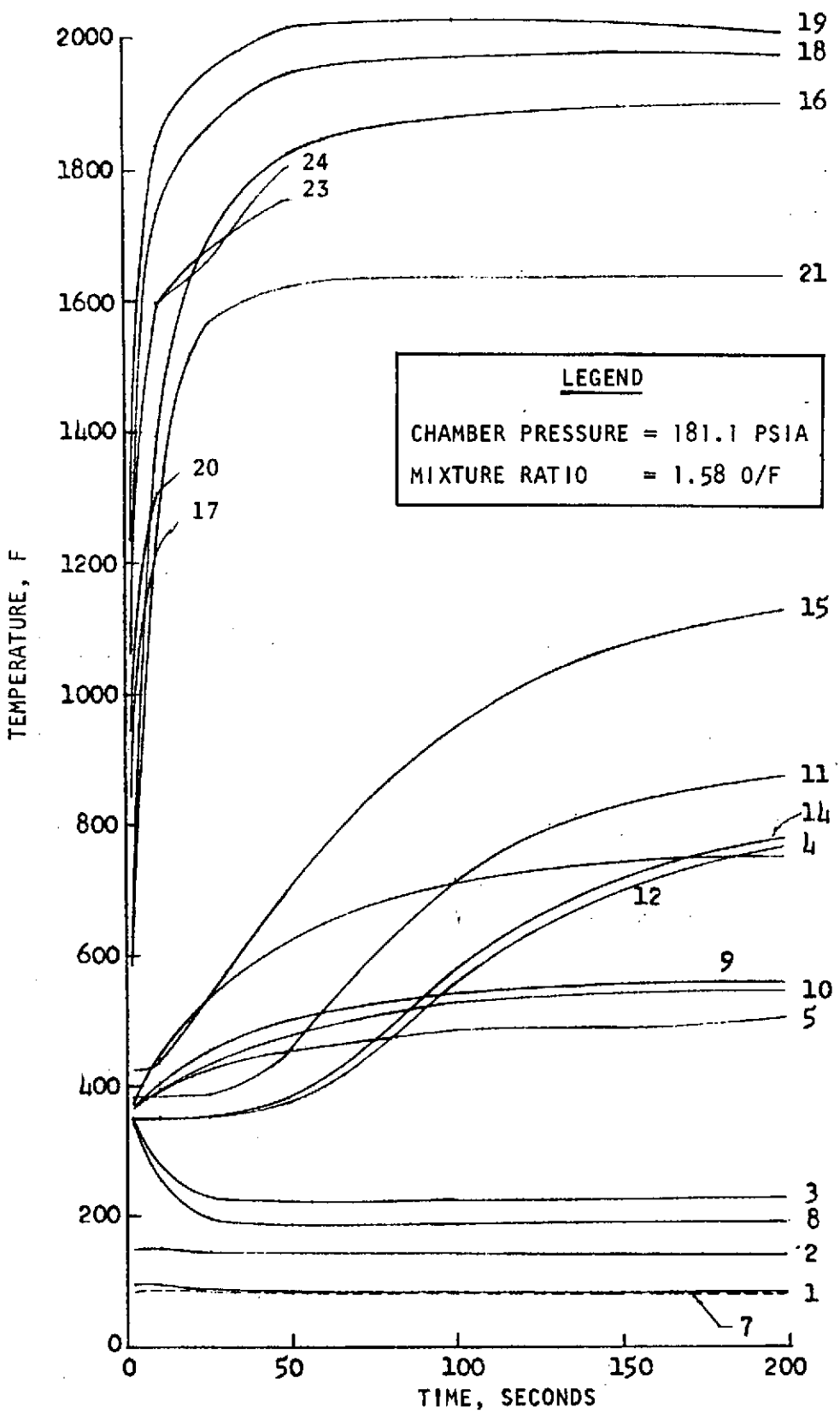

Figure 71. Durability Engine Temperature History Temperature vs Time, CTL-4, Cell 37 Test 870-139 (See Fig. 75 for thermocouple locations)

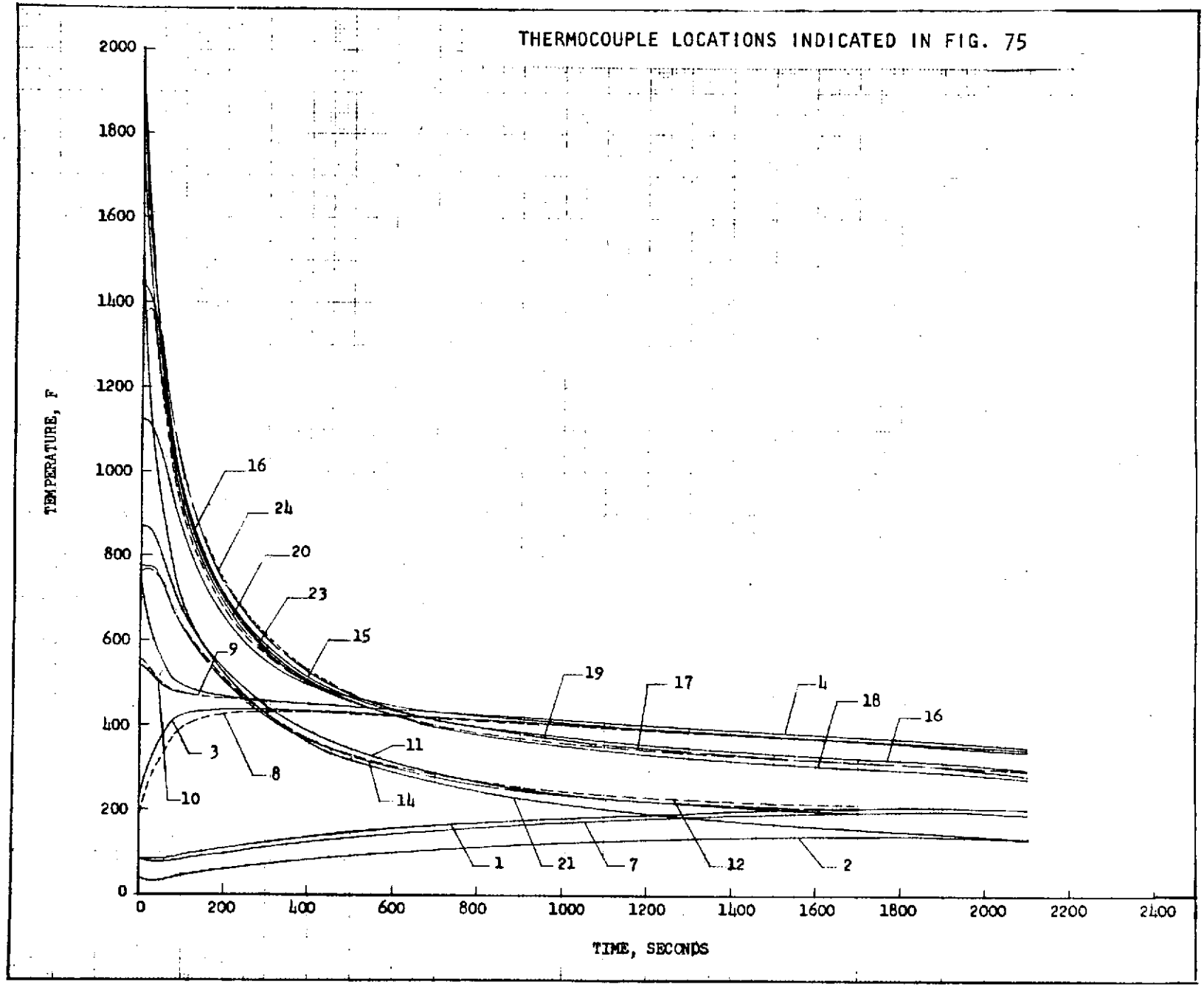

Figure 72. Durability Engine Thermal Soak Temperature Versus Time; CTL-4, Cell 37 Posttest 870-139

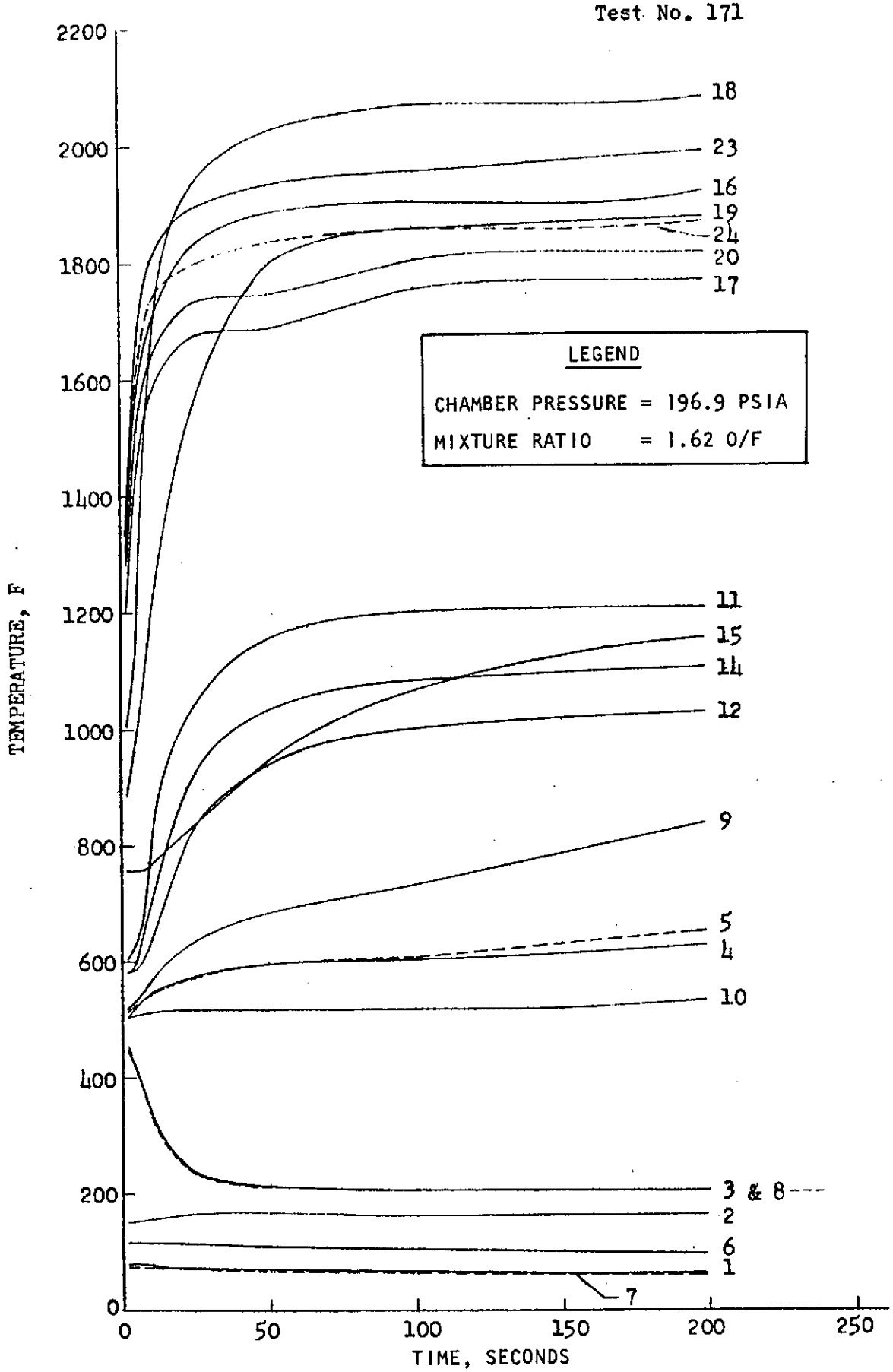

Figure 73. Durability Engine Temperature History Temperature vs Time, CTL-4, Cell 37, Test 870-171 (See Figure 74 for thermocouple locations)

R-9557

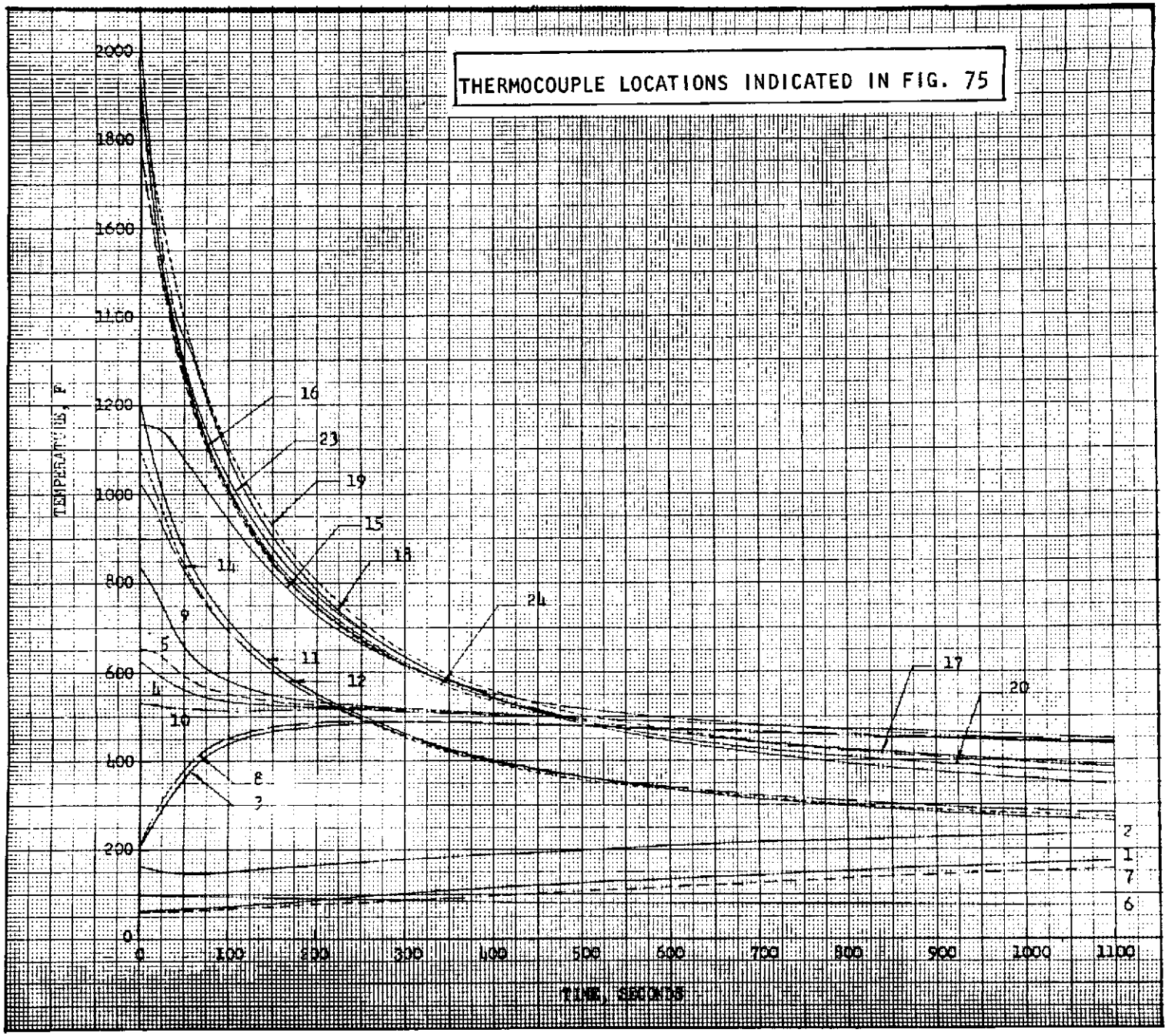

Figure 74. Durability Engine Thermal Soak Temperature Versus Time; CTL-4, Cell 37 Posttest 870-171

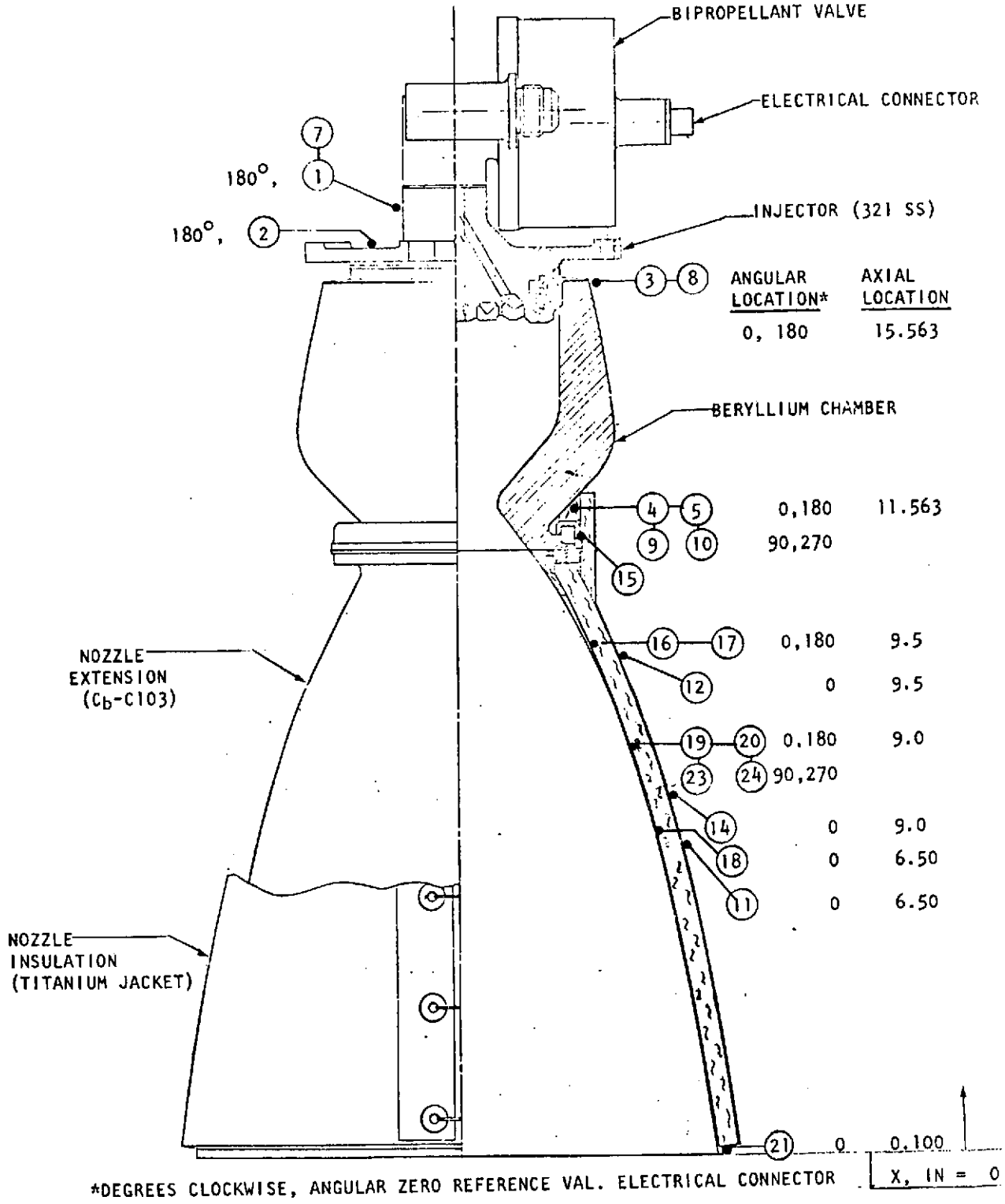

Figure 75. Rocket Engine Assembly Representative Thermocouple Installation

The data of endurance test No. 2, test 171, indicate a maximum nozzle temperature of 2000 F. The throat outside surface temperature of 600 F was recorded at 0, 180, and 270 degree angular locations. A throat outside surface temperature of 835 F was measured at a location of 90 degrees. Posttest inspection revealed four plugged film coolant holes at this location. The beryllium combustor head and temperature of 200 F was recorded on each side of the plugged film coolant region. Injector back side and valve adapter temperatures were nominal at 160 F and 60 F, respectively.

The thermal soakout results, Fig. 74, under vacuum conditions indicate 500 F equilibration beryllium combustor temperature in approximately 200 seconds after engine cutoff. A facility valve adapter was installed at the location indicated as the valve in Fig. 75; therefore, no meaningful results were obtained for a valve soakout temperature.

Throughout the test program the recorded temperature data agreed with the theoretical predictions presented in Fig. 24 and 25. The tests also demonstrated the ability of the engine to safely operate with multiple orifice plugging present because of environmental test conditions. Temperature levels are sufficiently low that further combustor optimization could result in engine weight reduction.

Environmental Tests

Excluding the propellant valve, the environmental tests had no adverse physical effect on the Durability Engine. Partial and total orifice blockage occurred due to sand and dust exposure on a wet engine from prior rain and humidity tests followed by vertical up and horizontal vibration. However, this did not result in engine malfunctions though shifts in mixture ratio did occur during the first hot-fire test in each series subsequent to environmental exposure and high heat input was recorded where fuel film coolant orifices were plugged. Some superficial pitting was noted on the beryllium after salt spray exposure, but this has no effect on engine operation or structural integrity.

Vibration Test Results. For the first vibration cycle, the durability engine was instrumented with six accelerometers and four strain gages as shown in Fig. 61 and subjected in the three engine axes to the sinusoidal and random vibration inputs specified in Table 1. No detrimental effects on the engine were noted as a result of these vibration tests.

No significant resonant response occurred during sinusoidal vibration testing since the maximum test frequency of 40 Hz is well below any engine resonant frequencies. The random vibration test data were recorded on FM magnetic tape and analyzed to obtain composite rms amplitudes as shown in Table 29 along with summarized frequency spectra listed in Table 30. Test data (frequency plots) are provided in the contract test report (Ref. 1).

The test results indicated that applied random vibration amplitudes were within specified tolerance bands, with the exception of the frequency range from 10 to 50 Hz where the amplitudes were above the tolerance range. However, since engine resonant modes occur at frequencies substantially higher than this frequency range, the degree of overtesting involved was insignificant.

TABLE 30. COMPOSITE GRMS AMPLITUDES OBTAINED FROM RCE RANDOM VIBRATION TESTS CONDUCTED DURING THE FIRST ENVIRONMENTAL TEST SERIES

Measurement Location	X-Axis Input	Y-Axis Input	Z-Axis Input
Input-On Fixture X-Axis	Control Accel. * 25.0 GRMS	18.0 GRMS	12.6 GRMS
Input-On Fixture Y-Axis	9.7 GRMS	Control Accel. *25.0 GRMS	3.8 GRMS
Input-On Fixture Z-Axis	27.2 GRMS	32.0 GRMS	Control Accel. 27.6 GRMS
RCE Injector Flange X-Axis	32.8 GRMS	21.2 GRMS	30.0 GRMS
RCE Injector Flange Y-Axis	16.3 GRMS	38.4 GRMS	16.6 GRMS
RCE Injector Flange Z-Axis	**32.8 GRMS	**28.3 GRMS	**18.2 GRMS
L605 Transition Piece Strain Gage No. 1	306 ERMS	132 ERMS	102 ERMS
L605 Transition Piece Strain Gage No. 2	107 ERMS	215 ERMS	162 ERMS
L605 Transition Piece Strain Gage No. 3	78 ERMS	55 ERMS	84 ERMS
L605 Transition Piece Strain Gage No. 4	36 ERMS (Questionable)	No Good	44 ERMS (Questionable)

Notes:
*1. Overdriven Data - Tape Recorder Dynamic Range Exceeded. Specified GRMS Amplitudes are From AETL Meter Readings Made During the Test.
**2. Intermittent Tape Recorder Signal.
3. ERMS Levels are in μ Inches/Inch RMS

TABLE 31. RCE RANDOM VIBRATION PREDOMINANT STRAIN AMPLITUDES AND FREQUENCIES

FIRST ENVIRONMENTAL TEST SERIES

Vibration Input Axis	Strain Gage No. 1		Strain Gage No. 2		Strain Gage No. 3		Strain Gage No. 4	
	Hz	ERMS	Hz	ERMS	Hz	ERMS	Hz	ERMS
X	220	50	110	3	110	13	110	* 5
	270	38	220	7	200	21	200	7
	410	25	400	1	430	3	410	5
	500	24	620	3	600	4	630	6
	600	24	920	7	770	4	920	6
	920	58	1250	13	920	16	1250	8
	1250	25	1450	8	1250	9	1450	8
	1450	44	1900	7	1500	9	1900	7
Y	110	8	120	14	120	7	No Good (High Noise Level)	
	175	18	175	33	210	8		
	580	11	620	7	410	5		
	700	17	880	13	550	5		
	950	22	1020	6	620	7		
	1350	21	1280	17	920	7		
	1500	15	1450	5	1280	17		
	1700	19	1650	8	1450	5		
Z	140	10	115	4	185	5	110	* 2
	170	12	185	8	220	5	200	2
	450	5	300/360	6	250	5	380	1
	550	5	410	7	430	4	450	2
	920	40	450	7	550	4	600	4
	1280	5	550	9	920	38	920	7
	1500	5	920	38	1280	5	1500	1
	1900	5	1250	5	1500	4	1900	2

Notes: * 1. Strain Gage No. 4 is questionable due to low signal level in all axex.

2. Strain amplitudes obtained from power spectral density plots with a 16 Hz analysis band width as follows: $\varepsilon_{RMS} = \left[\left[\text{RMS Microstrain}\right]^2 \text{ Filter}\right]^{1/2}$

Strain gage data indicated that low-frequency resonant modes were present in the 150- to 250-Hz frequency range. High-frequency strain response were noted, particularly in the 900- to 1500-Hz frequency range. The maximum strain amplitude of 58 μin./in. rms (174 μin./in. peak) was measured in the Haynes-25 transition ring (braze joint between injector and chamber). The joint was designed for a load that would result in a peak strain of 1000 μin./in. Therefore, the joint is capable of inertial loads on the order of 5.7 times that measured in the engine vibration test.

During the second through sixth vibration cycles, the durability engine was instrumented with six accelerometers as shown in Fig. 61 and subjected in the three engine axes to the sinusoidal and random vibration input specified in Table 1. The random vibration test data for the second through sixth cycles were recorded on FM magnetic tape and analyzed to obtain composite rms amplitudes as shown in Tables 32 through 36. The applied random vibration amplitudes over the specified frequency range for each of the three axes for all the cycles are included in the contract test report.

The vibration test setup was modified for the fourth, fifth, and sixth environmental series. Flex lines were routed to the bipropellant valve to allow pressurization of the valve during vibration testing. The engine was subjected to the three environmental test series consecutively with GN_2 purging between series to simulate engine firing effects.

The test spectra for these final three tests were within specified tolerance bands for the random vibration tests with some minor deviations, the most noticeable deviation being an adjacent peak and notch at 1500 Hz during the X-axis random vibration portion of the fourth environmental test series. None of these deviations significantly affected the test results.

Propellant Valve Failures

Two Moog, Inc. Model 54-107A bipropellant valves were supplied to Rocketdyne to support the program. During the course of the program, both valves exhibited failure modes.

Both valves S/N 003 and S/N 005 consist of two sets of staggered seats, one set for oxidizer sealing and one set for fuel sealing. Both valves were fabricated using valve bodies from Model 103A used on the Minuteman III PBPS axial engine. The added flowrates required for a 600-pound thrust engine was provided for by staggered seats, larger seat diameters, and longer strokes.

Valve S/N 003. This valve was supplied to Rocketdyne by NASA/JSC as residual hardware from NASA Contract NAS9-12996. Prior to delivery to Rocketdyne the valve had undergone a hot-fire and environmental test program. During eleven hot-fire test series, 1976 starts and 1230 seconds were accumulated. Ten environmental tests (salt spray, sand and dust, sinusoidal vibration, temperature/humidity, hot-fire) were conducted with the valve. This was followed by 23 minutes of X-axis random vibration (horizontal axis only). Reported nominal pressure drops were 38 psid on the oxidizer side and 26 psid on the fuel side. No leakage was detected with this valve.

TABLE 32. COMPOSITE GRMS AMPLITUDES OBTAINED FROM RCE RANDOM VIBRATION TESTS CONDUCTED DURING THE SECOND ENVIRONMENTAL TEST SERIES

Measurement Location	X - Axis Input	Y - Axis Input	Z - Axis Input
Input - On Fixture X-Axis	Control Accel. 23.5 GRMS	6.5 GRMS	5.2 GRMS
Input - On Fixture Y-Axis	4.5 GRMS	Control Accel. 24.1 GRMS	2.6 GRMS
Input - On Fixture Z-Axis	12.2 GRMS	14.1 GRMS	Control Accel. 23.0 GRMS
RCE Injector Flange X-Axis	38.7 GRMS	27.4 GRMS	37.1 GRMS
RGE Injector Flange Y-Axis	24.5 GRMS	36.7 GRMS	23.0 GRMS
RCE Injector Flange Z-Axis	29.2 GRMS	23.5 GRMS	39.1 GRMS

TABLE 33. COMPOSITE GRMS AMPLITUDES OBTAINED FROM RCE RANDOM VIBRATION TESTS CONDUCTED DURING THE THIRD ENVIRONMENTAL TEST SERIES

Measurement Location	X-Axis Input	Y-Axis Input	Z-Axis Input
Input - On Fixture X-Axis	Control Accel. 24.9 GRMS	5.8 GRMS	7.7 GRMS
Input - On Fixture Y-Axis	No Good	Control Accel. 26.1 GRMS	No Good
Input - On Fixture Z-Axis	21.2 GRMS	24.5 GRMS	Control Accel. 24.5 GRMS
RCE Injector Flange X-Axis	35.0 GRMS	21.9 GRMS	36.1 GRMS
RCE Injector Flange Y-Axis	23.5 GRMS	43.3 GRMS	22.1 GRMS
RCE Injector Flange Z-Axis	39.7 GRMS	30.4 GRMS	40.6 GRMS

TABLE 34. DURABILITY ENGINE FOURTH ENVIRONMENTAL TEST SERIES
COMPOSITE GRMS AMPLITUDES OBTAINED
FROM RANDOM VIBRATION TESTS

Measurement Location	X-Axis Input	Y-Axis Input	Z-Axis Input
Input - On Fixture X-Axis	Control Accel. 25.5 GRMS	5.7 GRMS	9.7 GRMS
Input - On Fixture Y-Axis	2.9 GRMS	Control Accel. 25.5 GRMS	7.9 GRMS
Input - On Fixture Z-Axis	24.5 GRMS	21.0 GRMS	Control Accel. 27.0 GRMS
RCE Injector Flange X-Axis	44.2 GRMS	25.5 GRMS	59.2 GRMS
RCE Injector Flange Y-Axis	30.0 GRMS	No Good	38.1 GRMS
RCE Injector Flange Z-Axis	40.9 GRMS	28.3 GRMS	54.8 GRMS

TABLE 35. DURABILITY ENGINE FIFTH ENVIRONMENTAL TEST SERIES COMPOSITE GRMS AMPLITUDES OBTAINED FROM RANDOM VIBRATION TESTS

Measurement Location	X-Axis Input	Y-Axis Input	Z-Axis Input
Input - On Fixture X-Axis	Control Accel. 26.0 GRMS	7.0 GRMS	8.8 GRMS
Input - On Fixture Y-Axis	5.8 GRMS	Control Accel. 25.5 GRMS	11.0 GRMS
Input - On Fixture Z-Axis	17.3 GRMS	13.2 GRMS	Control Accel. 26.0 GRMS
RCE Injector Flange X-Axis	42.4 GRMS	27.8 GRMS	57.0 GRMS
RCE Injector Flange Y-Axis	33.2 GRMS	57.7 GRMS	26.8 GRMS
RCE Injector Flange Z-Axis	37.1 GRMS	28.3 GRMS	58.3 GRMS

TABLE 36. DURABILITY ENGINE SIXTH ENVIRONMENTAL TEST SERIES COMPOSITE GRMS AMPLITUDES OBTAINED FROM RANDOM VIBRATION TESTS

Measurement Location	X-Axis Input	Y-Axis Input	Z-Axis Input
Input - On Fixture X-Axis	Control Accel. 26.0 GRMS	7.4 GRMS	8.7 GRMS
Input - On Fixture Y-Axis	12.4 GRMS	Control Accel. 26.0 GRMS	3.6 GRMS
Input - On Fixture Z-Axis	15.5 GRMS	14.5 GRMS	Control Accel. 26.0 GRMS
RCE Injector Flange X-Axis	51.5 GRMS	30.4 GRMS	60.4 GRMS
RCE Injector Flange Y-Axis	28.8 GRMS	54.3 GRMS	27.4 GRMS
RCE Injector Flange Z-Axis	46.4 GRMS	31.6 GRMS	59.2 GRMS

The chronological test history at Rocketdyne is presented in Table 37 and is discussed in some detail in the following paragraphs.

Engine tests showed propellant pressure drops to increase in the oxidizer side with time. Pressure drops were measured during a number of steady-state runs at each test sequence and adjusted to nominal flowrates for comparison. Pressure drops were measured from valve inlet to injector manifold just upstream of injector orifices. Acceptance test values were 62 psid (oxidizer) and 27 psid (fuel). Subsequent baseline tests were 83 psid (oxidizer) and 27 psid (fuel). The engine was exposed to the Environmental Test Series No. 1. Subsequent Endurance Test No. 1 hot-fire steady-state tests resulted in oxidizer pressure drops of 172 to 199 psid with a constant fuel-side pressure drop of 28 psid.

Subsequent to Endurance Test No. 1 and Environmental Test No. 2 rain, humidity, salt spray, and sand and dust exposure, the valve was removed from the engine. Freon flow tests were conducted at Rocketdyne and it was determined that the valve pressure drops were oxidizer 51 psid and fuel 31 psid. After the valve was reinstalled on the engine, the engine was vibration tested, completing Environmental Test No. 2.

During preparation for Endurance Test No. 2, hot-fire tests gross oxidizer leakage was encountered through the valve. The valve was removed from the engine assembly, decontaminated and shipped to Moog, Inc., for analysis.

Effort at Moog consisted of helium leakage tests, disassembly, and visual inspection. The helium leakage tests verified gross leakage through the oxidizer side. The manifold assembly was removed, and visual inspection revealed the presence of gross amounts of fine-textured sand. The bottom of the sealing grooves in both oxidizer Teflon button seals were covered with the noted contaminant and it was observed that both oxidizer sealing grooves were excessively deep (Fig. 76). It was also noted that minor amounts of the contaminant were present in the seal grooves of the fuel side of the valve, however, no leakage was observed during the previous helium leakage tests. Samples of the contaminant were analyzed at Rocketdyne and determined to be predominantly silicon. The valve oxidizer inlet filter appeared to have been deformed outward, radially; no significant contamination was observed in the filter.

It was concluded that the sand, dust and salt spray introduced into the engine nozzle during the environmental tests, migrated through the engine injector into the valve outlets during random vibration tests (particularly Z-axis tests--nozzle up) and abraded the oxidizer-side Teflon seal sealing groove during vibration test to a depth sufficient to unload the sealing force between the nozzle tips and Teflon button seals. This, together with the sand particles in, around, and on Teflon seal areas, resulted in the observed oxidizer seat leakage.

It was learned from Moog, Inc. that in the Model 54-107A valve that Rocketdyne used (S/N 003), the flapper just barely contacts the flapper stop pin minimizing flapper "wind up." In a typical valve concept, the flapper normally hits the flapper stop

TABLE 37. ENGINE TEST HISTORY USING BIPROPELLANT VALVE MODEL 54-107A, S/N 003

Test Date	No. of Starts	Duration (seconds)	Remarks
12-15-73	31	.050 to 100	Acceptance Test
1-23-74	135	.050 to 600	Baseline Performance
			Environmental Test No. 1
1-25-74	--	--	Rain
1-28-74	--	--	Humidity
	--	--	Salt Spray
	--	--	Sand and Dust
2-6-74	--	--	Random and Sinusoidal Vibration (X, Y, and Z Axes)
2-14-74	135	.050 to 200	Endurance Test No. 1
			Environmental Test No. 2
2-15-74	--	--	Rain
2-18-74	--	--	Humidity
2-19-74	--	--	Salt Spray
	--	--	Sand and Dust
2-20-74	--	--	Valve removed from engine for Freon flow test
2-22-74	--	--	Valve reinstalled on engine
2-25-74	--	--	Random and sinusoidal vibration (X, Y, and Z Axes)
2-27-74	--	--	Endurance Test No. 2 aborted because of high oxidizer leakage through valve. Valve removed from engine, decontaminated and shipped to MOOG, Inc. for analysis.

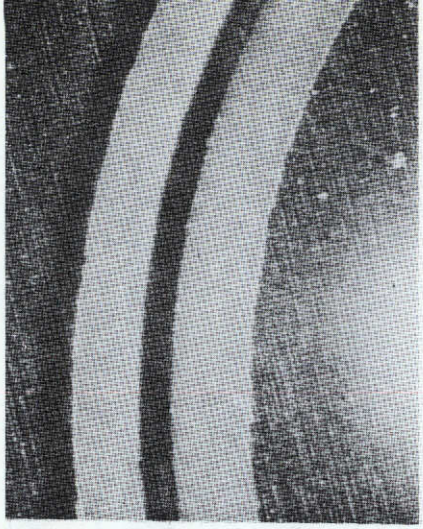

Lower
Oxidizer
Button
Seal

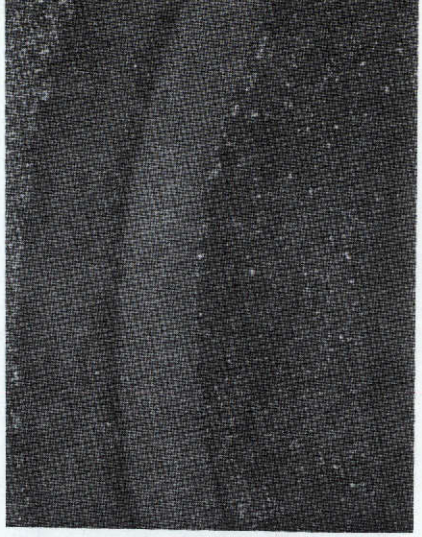

Side light

Low light

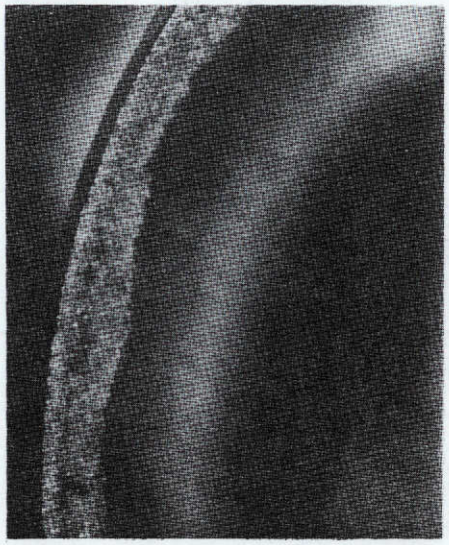

Lower Oxidizer Nozzle Tip

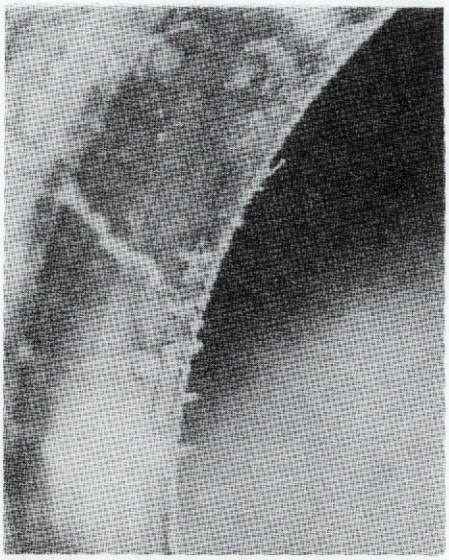

Upper
Oxidizer
Nozzle
Tip

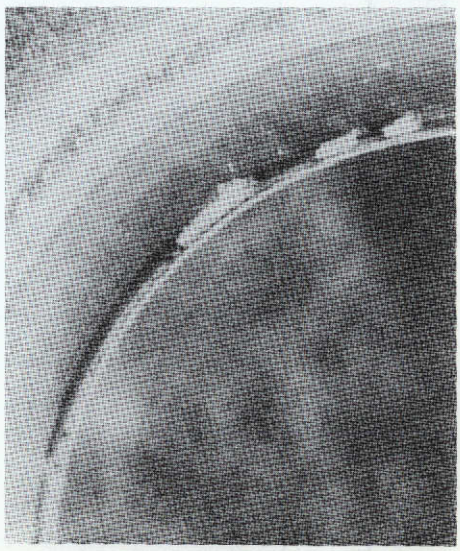

Figure 76. Model 54-107A, S/N 003 Bipropellant Valve

pin first and the armature continues to travel, winding up the flapper holding the buttons in a stationary open position. Without flapper wind up, the poppet is subject to dynamic pressure forces of the flow stream tending to force the energized valve poppet toward a closed position which results in valve flutter (poppet pulsing closed and open) and increased pressure drop. Model 54-107A S/N 003 valve exhibited increasing pressure drop and Model 54-107B (tested on another program) exhibited flutter.

Valve Model 54-107B was assembled without valve windup to minimize valve pressure drop; that is, the flapper stop pin was installed so that the flapper would not contact it in the open position. Without the flapper windup, the dynamic flow forces required to drive the buttons closed is greatly reduced. During engine tests, valve flutter at a 40-millisecond pulse rate was observed.

It is thought that the large increase in oxidizer-side pressure drop experienced during Endurance Test No. 1 could have been caused by the flow forces driving the oxidizer button toward the closed position, reducing the flow area. Since the component tests conducted on the valve when it was removed from the engine to check pressure drop shift were conducted at Moog acceptance test conditions and not engine test conditions, the flow forces were not sufficient to drive the buttons toward the closed position.

Since (1) no contamination was observed in the oxidizer valve inlet and (2) the posttest Freon pressure drops were normal, the cause of the deformed filter was unknown. Oxidizer pressure drop appeared to be due to a gradual degradation rather than a sudden jump.

Valve S/N 005. The chronological test history for this unit is presented in Table 38. This unit was not hot fired on the engine. Moog, Inc. informed Rocketdyne that the flapper stop pins on this unit were installed sufficiently to cause a definite decrease in flow area, ensuring at least some flapper windup. Moog, Inc. also stated that one of the diameters on the valve seats had been held to the minimum side of the tolerance to permit actuation at higher inlet pressures. Flow test on this valve at Rocketdyne as a component, using engine flowrates, resulted in steady-state pressure differentials of 30 psid fuel and 50 psid oxidizer indicating that the flow forces were not driving the buttons closed. Open response time tests were also conducted at Rocketdyne using 28 vdc and increasing inlet pressures. The valve actuated at 360 psig in 51 milliseconds and would not actuate at 370 psig with voltages up to 36.5 vdc.

As shown on Table 38, the engine was not hot fired with this valve installed. Environmental tests 4, 5, and 6 were modified to exclude humidity and salt spray, maintain 300-psig inlet pressure on the valve during vibration and add a GN_2 purge subsequent to vibration. Valve leakage got increasingly worse as environmental testing progressed. The valve exhibited zero leakage on the first leakage test following Environmental Test No. 6; however, the oxidizer leakage increased to 393 cc/min subsequent to actuation. Additional actuations did not decrease the oxidizer leakage.

TABLE 38. ENGINE TEST HISTORY USING BIPROPELLANT VALVE MODEL 54-107A, S/N 005

Test Date	Remarks
4-17-74	ENVIRONMENTAL TEST NO. 4 Rain Sand and Dust Random and Sinusoidal Vibration (valve inlets pressurized - 300 psig) GN_2 Purge No Valve Leakage
4-18-74	ENVIRONMENTAL TEST NO. 5 Rain Sand and Dust Random and Sinusoidal Vibration (valve inlets pressurized - 300 psig) GN_2 Purge Previbration Test Leakage - 19 cc/min During Vibration Test Leakage 48 cc/min
4-19-74	ENVIRONMENTAL TEST NO. 6 Rain Sand and Dust Random and Sinusoidal Vibration (valve inlets pressurized - 300 psig) GN_2 Purge Previbration Test Leakage - 19 cc/min During Vibration Test Leakage 76 cc/min
4-22-74	Internal Leakage Test at 300 psig inlet pressure Results fuel 0/12 min oxid 0/12 min Cycle valve 4 times with 300 psig inlet pressure Repeat internal leakage test Results fuel 0/12 min oxid 393 cc/min Cycle valve 24 times with 300 psig inlet pressure Repeat internal leakage test Results fuel 0/12 min oxid 393 cc/min

The valve was submitted to Moog, Inc. for disassembly and inspection. Some sand and contamination was found on the downstream side of the fuel side; otherwise the fuel valve was fairly clean and looked in good condition. The oxidizer side was contaminated. The metal portion of the downstream seat looked sand-blasted. The seat was wet and contained many black particles in the groove. The downstream and upstream nozzles were covered with a dark congealed material. The upstream seat had black material in the groove.

It was concluded oxidizer side valve seat leakage was caused by sand in, around, and on the seat seal. Pressurizing the valve was sufficient to eliminate particle migration onto the seat during vibration after sand and dust exposure, but subsequent cycling allowed the sand to migrate from the downstream side up onto the seat seal. Dark material is probably propellant decomposition and/or reaction products in the valve seat area.

OFF-LIMITS ENGINE TEST RESULTS

Performance and Thermal Characteristics

Eighteen steady-state altitude tests were conducted with the Off-Limits Engine. A summary of performance and thermal data obtained during these tests is presented in Table 39. The tests consisted of demonstrating beryllium engine operation under extreme off-limit conditions; namely, simulated oxidizer regulator failure (2.88 o/f mixture ratio with 237-psia chamber pressure), mixture ratio ranges of 1.43 through 2.88 o/f with throttling which resulted in chamber pressures of from 66 through 230 psia, and discrete tests with one plugged primary fuel hole (oxidizer stream sprayed directly on wall), and one and three adjacent plugged coolant holes. The engine accumulated a total of 2615 seconds of burn time during the 18 starts.

The result of the chamber pressure/mixture ratio excursions defined engine operating regimes. The data points describe an operating map (Fig. 77) where the engine can safely operate with a Haynes-25 nozzle extension. If actual shuttle RCS operational requirements exceed this envelope, the beryllium engine will be able to meet thse conditions by using a coated columbium nozzle extension. The Haynes-25 has a useful temperature limit of approximately 2200 F. Mixture ratio/chamber pressure conditions in excess of approximately 2.0/230 psia, 1.9/150 psia produce nozzle extension temperatures in excess of the useful limit of Haynes-25 which could result in nozzle extension damage. This occurred on Test 768 which was run at a mixture ratio of 2.9 o/f and chamber pressure of 237 psia to simulate dual oxidizer regulator malfunction (full open) resulting in the engine running at an inlet pressure equivalent to a relief valve setting of 435 psia. Prior to running this condition a 200-second firing was made during which the engine reached thermal equilibrium. Through a servo system in the test facility the test condition was changed to the 2.9 o/f. The nozzle reached equilibrium at 2300 F (Haynes-25 melts at approximately 2400 F). The resultant substantial loss in material strength resulted in Haynes-25 nozzle extension damage. The nozzle was modified by removing the damaged nozzle section ($\varepsilon \sim 7{:}1$) and the test program completed. This test condition was successfully demonstrated with a columbium nozzle under a company-sponsored program where a 45-second test was performed. Temperatures reached during this test are provided in Fig. 78.

TABLE 39. OFF-LIMITS ENGINE TEST DATA

Date	Test No.	Total Duration, seconds	Data Point Duration	Mixture Ratio,* o/f	Chamber Pressure (NS), psia	Characteristic Velocity, ft/sec	Specific Impulse,** lbf-sec/lbm	Engine Temperatures, F		
								MID Chamber	Throat Maximum	Nozzle Maximum
11/6/73	768	210	200	1.65	200.2	4954	--	337	511	1770
			10	2.88	237.0	5001	--	352	601	2300
11/14/73	781	884	150	1.65	200.4	4983	283.4	320	539	1462
			100	1.63	229.9	4929	279.5	331	582	1473
			100	1.44	229.3	5049	286.0	331	586	1525
			100	1.43	199.7	5091	289.2	327	570	1536
			100	1.44	150.2	5114	292.2	295	444	1280
			100	1.62	152.3	5133	293.2	299	468	1402
			100	1.83	201.5	4958	281.3	328	582	1526
			100	1.81	229.5	4829	273.4	329	570	1413
			34	2.04	184.3	5201	293.8	340	693	2017
	782	19	19	1.90	153.4	5174	289.3	368	611	1907
11/16/73	783	207	150	1.66	200.5	4980	281.0	324	567	1661
			50	1.86	201.1	4964	280.0	332	619	1697
			7	1.96	184.0	5101	286.0	333	628	2025
	784	71	50	1.65	200.5	4990	281.8	329	557	1666
			21	2.04	202.4	5030	283.0	341	686	1847
	785	104	150	1.67	201.1	4997	282.4	332	559	1487
			50	2.01	230.2	4890	276.7	361	737	1719
			4	2.12	222.6	5011	282.5	364	744	1842
	786	54	50	1.67	200.8	4995	283.8	336	568	1494
			4	2.39	215.8	5141	291.2	335	569	1717
	787	71	50	1.65	201.1	5017	283.2	328	558	1476
			21	1.99	160.1	5260	293.7	326	598	1868
	788	50	50	1.67	151.8	5099	291.3	312	492	1425
	789	51	51	1.69	127.9	5231	--	296	470	1548
	790	52	52	1.70	101.5	5148	--	273	396	1707
	791	5	5	1.58	66.2	4532	--	278	299	748
	792	14	14	2.08	203.7	5062	283.9	290	485	1782
11/21/73	805	200	200	1.68	201.7	5043	284.7	377	605	1764
11/28/73	806	350	200	1.59	200.9	5117	288.5	363	568	1614
			50	1.79	152.7	5290	294.5	360	633	1900
			50	1.83	153.1	5298	295.4	399	742	1986
			50	1.81	178.5	5176	290.7	392	692	1831
11/29/73	807	11	11	1.65	200.5	5121	287.4	174	297	1969
	808	12	12	1.64	200.5	5103	286.6	258	384	2020
	809	250	280	1.64	200.2	5084	287.1	443	726	2211

*Percent of total flowrate
**Corrected to expansion ratio of 40:1

NOTES:

1. All tests conducted with propellants saturated with helium
2. All tests conducted with propellant temperatures within the ranges of 50 to 70 F
3. Facility valves used to conduct all tests

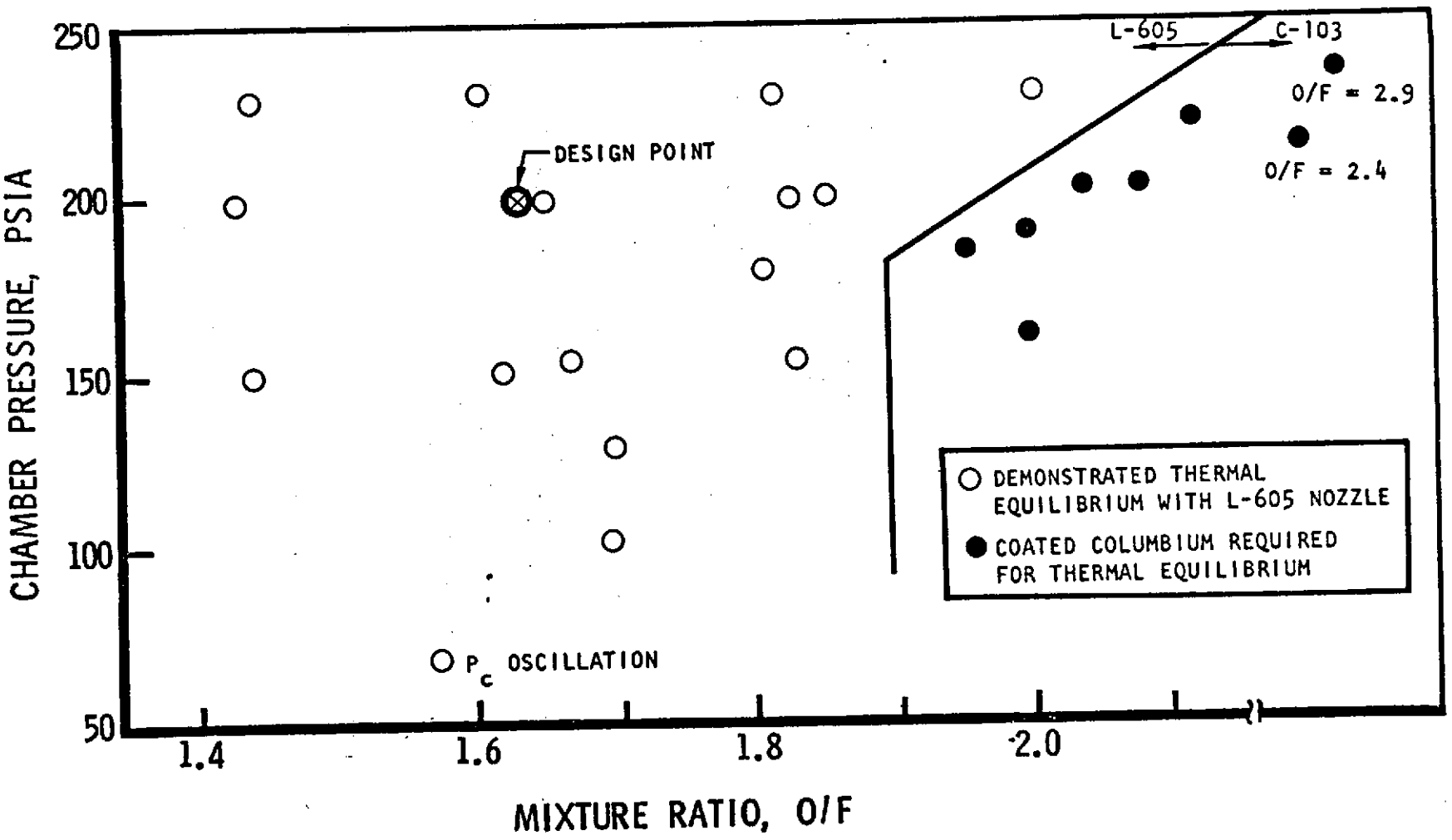

Figure 77. Demonstrated 600 Lb RCS Engine Operating Map

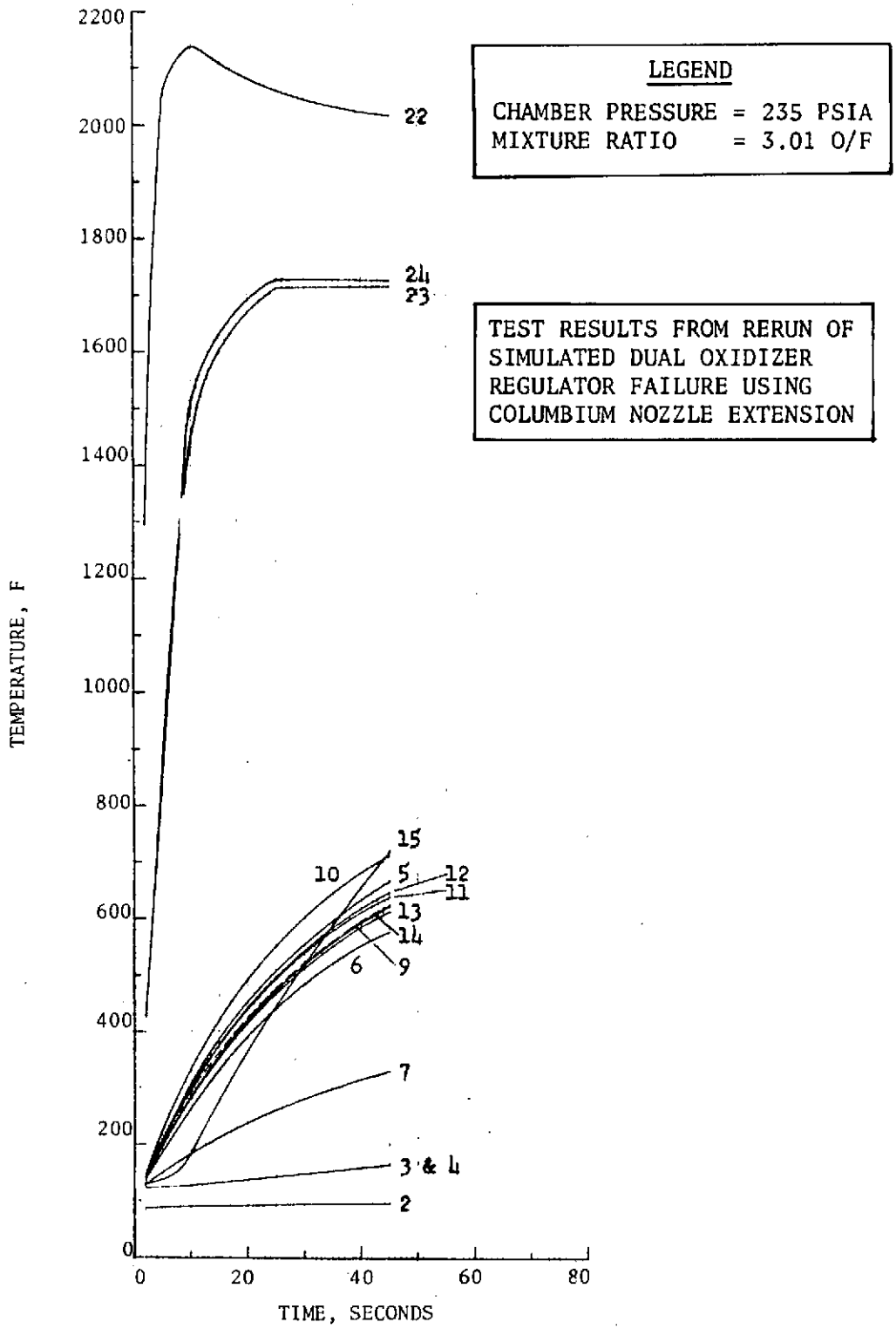

Figure 78. Advanced Beryllium Reaction Control Thrust Chamber, Test 870-2 9 January 1974, CTL-4, Cell 37. (See Fig. 79 for Thermocouple Locations)

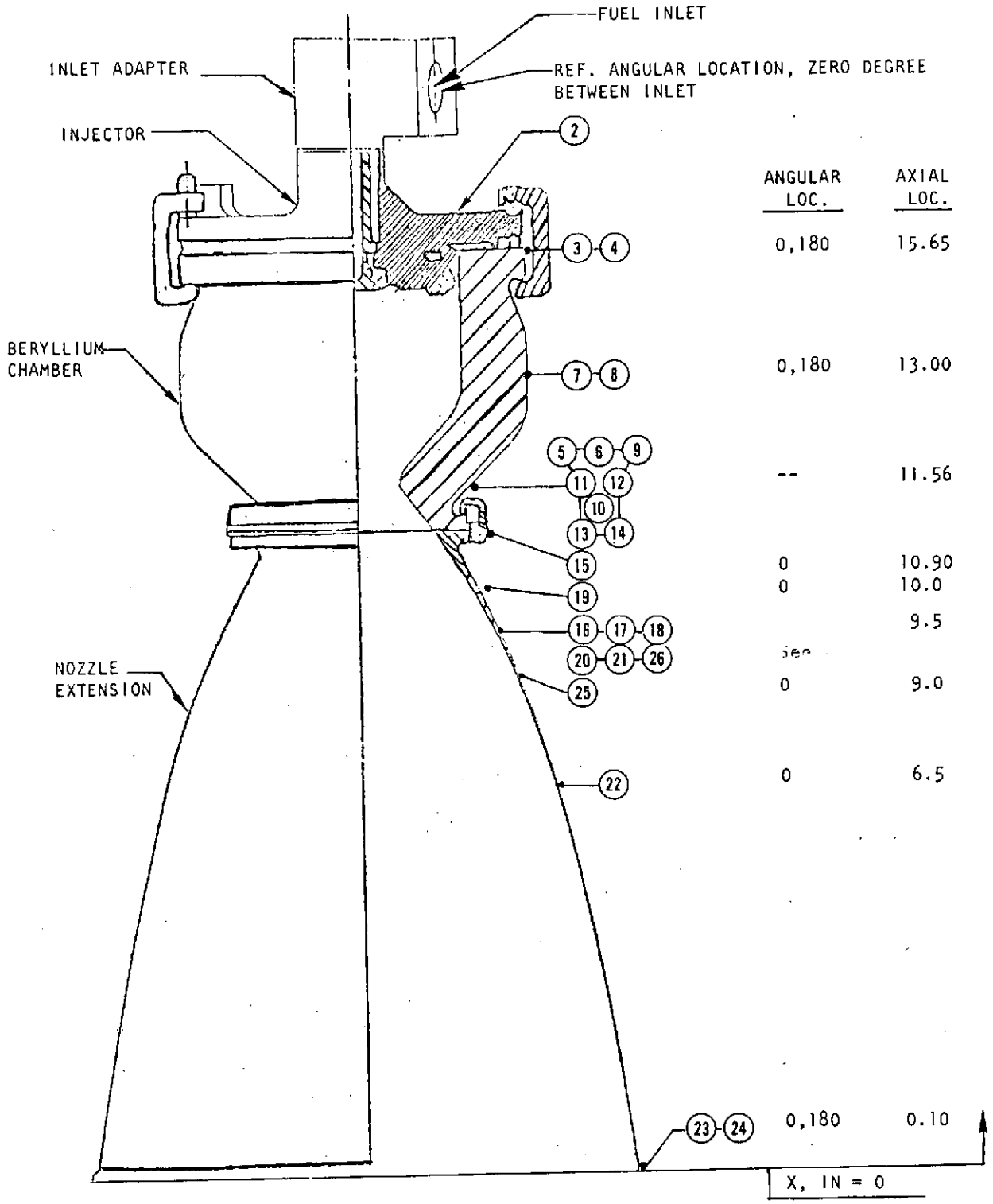

Figure 79. Thermocouple Locations for Tests 870- 2 and 5

Five tests were conducted with various injector plugged orifice conditions. Test 805 was conducted with one primary fuel hole located adjacent to the chamber wall being plugged; this resulted in the direct impingement of the oxidizer onto the beryllium chamber wall. Test 806 was conducted with one coolant hole plugged. Tests 807, 808, and 809 were conducted with three adjacent coolant holes plugged. The thermal profiles showing the temperature gradients caused by the orifice plugging of these five tests are depicted in Fig. 80. All temperatures were at thermal equilibrium during these tests. The beryllium chamber was in excellent condition after these tests; this correlates with the extremely low recorded hot streak temperature of 726 F. Under a company-sponsored program a test was performed with four adjacent film coolant holes plugged and a columbium nozzle installed. As shown in Fig. 81 the nozzle reached an equilibrium temperature below 2200 F.

Throttle mode tests were conducted with the engine operated at the nominal 200-psia chamber pressure through a low of 67-psia chamber pressure. The test results are summarized in Table 40. Stable operation was achieved between 200 to 102 psia chamber pressure. Intermittent pressure oscillations at 110 Hz and magnitudes of ±15 psi were observed at the 102-psia level (50 percent throttle with helium-saturated propellants). Chamber oscillations of ±40 psi were observed at the 67-psia operating level.

At the completion of the off-limits test program, the beryllium chamber was in excellent condition as was the chamber/nozzle extension joint and the nozzle extension section not damaged during the test at a mixture ratio of 2.9 o/f.

Vibration Simulator Test Results

The simulator was designed to evaluate the brazed joint of the engine and to obtain the same frequency response as the engine in the 20-Hz to 2000-Hz frequency range by replacing the nozzle extension with an aluminum tube and using a dummy valve. Input control PSD plots are shown in Fig. 82, 83, and 84 for the X, Y, and Z axes. The simulator was tested in the X-axis for 100 minutes to the vibration levels of Fig. 62 specified in the initial contract work statement, and in the Y and Z axes for 117 minutes each to the revised vibration levels of Fig. 62 to simulate shuttle launch loads.

Nine accelerometers and four strain gages were installed on the simulator and recorded on magnetic tape. For greater detail on instrumentation, see Appendix A. As noted previously, accelerometer data were invalid.

Analysis of the strain gage data indicated that the primary resonant frequency of the simulator was a lateral bending mode at 150 to 200 Hz. A maximum strain amplitude of ~125 μin./in. rms (350 μin./in. peak) was measured. The injector/chamber braze joint was designed for a load that would result in 1000 μin./in. peak strain. Therefore, the joint is designed to withstand inertial loads of approximately 2.5 times that measured in the test.

Examples of strain amplitude versus frequency plots are included in Fig. 85 through 87 for the Y axis testing. Strain amplitudes observed in each axis are included in Table 41.

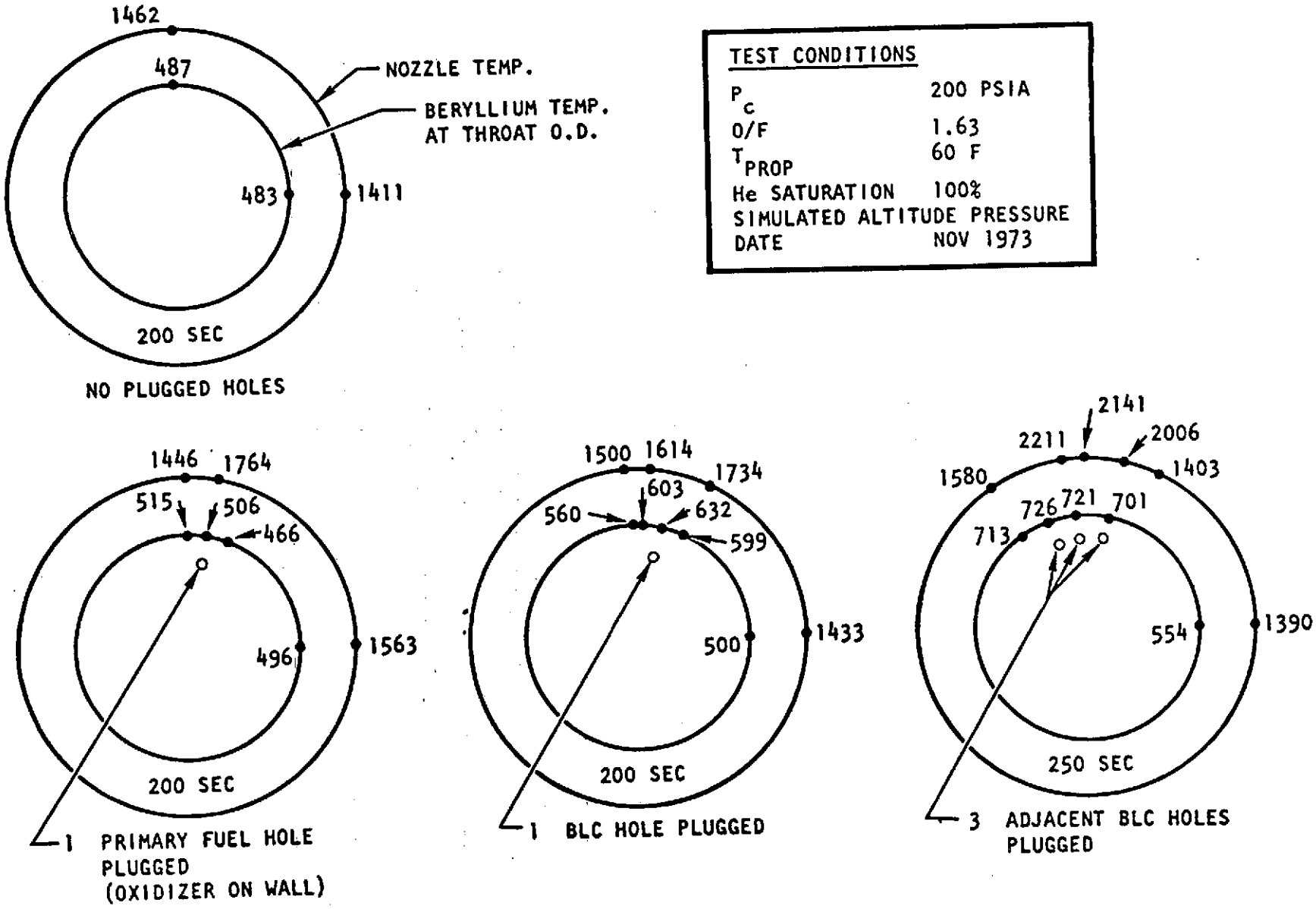

Figure 80. Off-Limits Engine Plugged Injector Hole Test Results

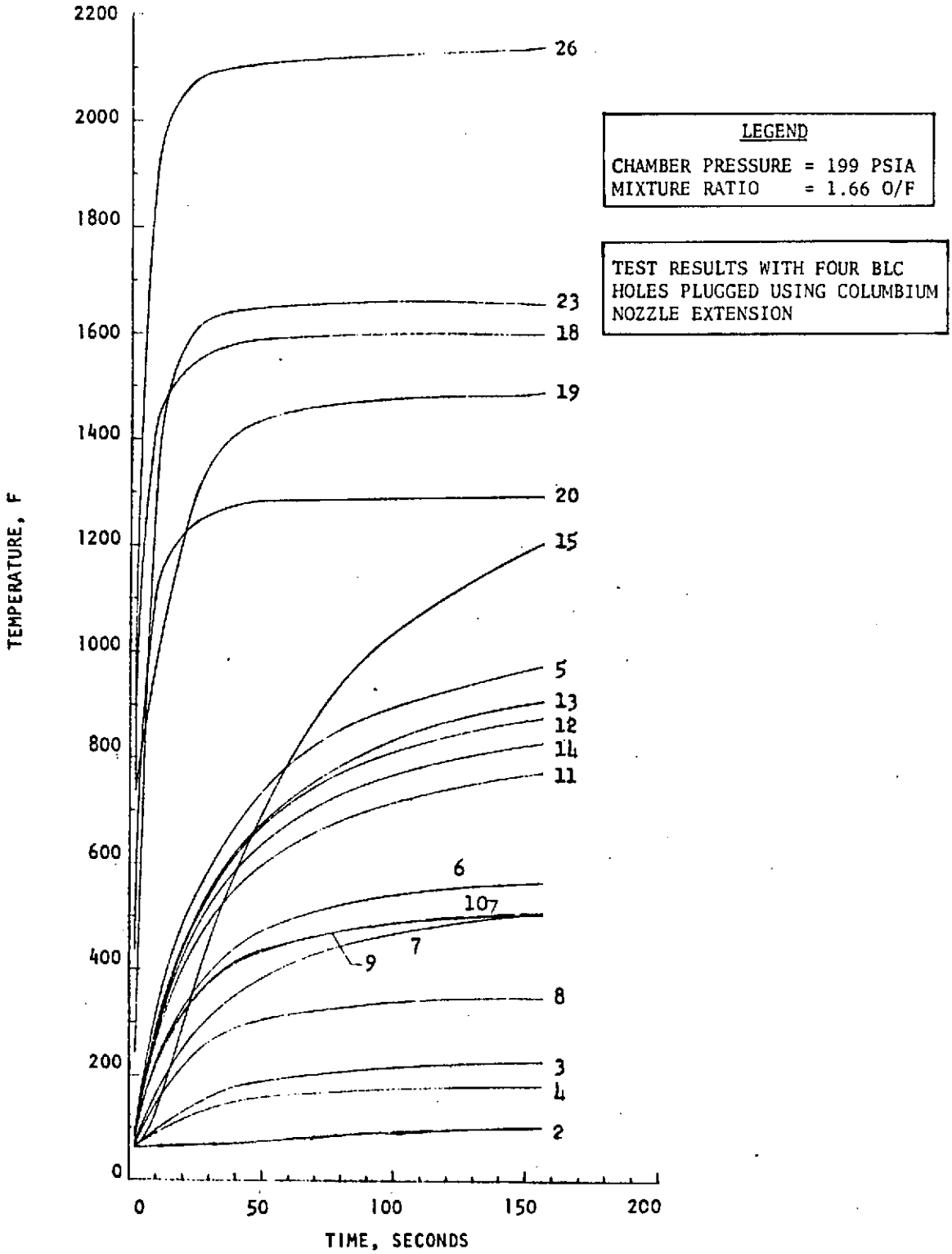

Figure 81. Advanced Beryllium Reaction Control Thrust Chamber, Test 870-5, 11 January 1974, CTL-4, Cell 37 (See Fig. 79 for Thermocouple Locations)

TABLE 40. RCE THROTTLE TEST RESULTS

P_c Nozzle Stagnation (psia)	MR (o/f)	ΔP_{OX} Injector Oxidizer (psid)	ΔP_{Fuel} Injector Orifice (psid)	$\left(\frac{\Delta P}{P_{c_{OX}}}\right)$ (percent)	$\left(\frac{\Delta P}{P_{c_{Fuel}}}\right)$ (percent)	Stable
201	1.65	49.8	40.6	24.8	20.2	Yes
152	1.67	26.4	20.5	17.3	13.5	Yes
128	1.69	17.5	12.6	13.7	9.8	Yes
102	1.70	10.9	7.9	10.7	7.7	±15 psi Oscillation
67	1.57	5.8	4.9	8.9	7.3	±40 psi Oscillation

Propellant Temperatures - 60 F

Helium Saturation Level - 100 percent

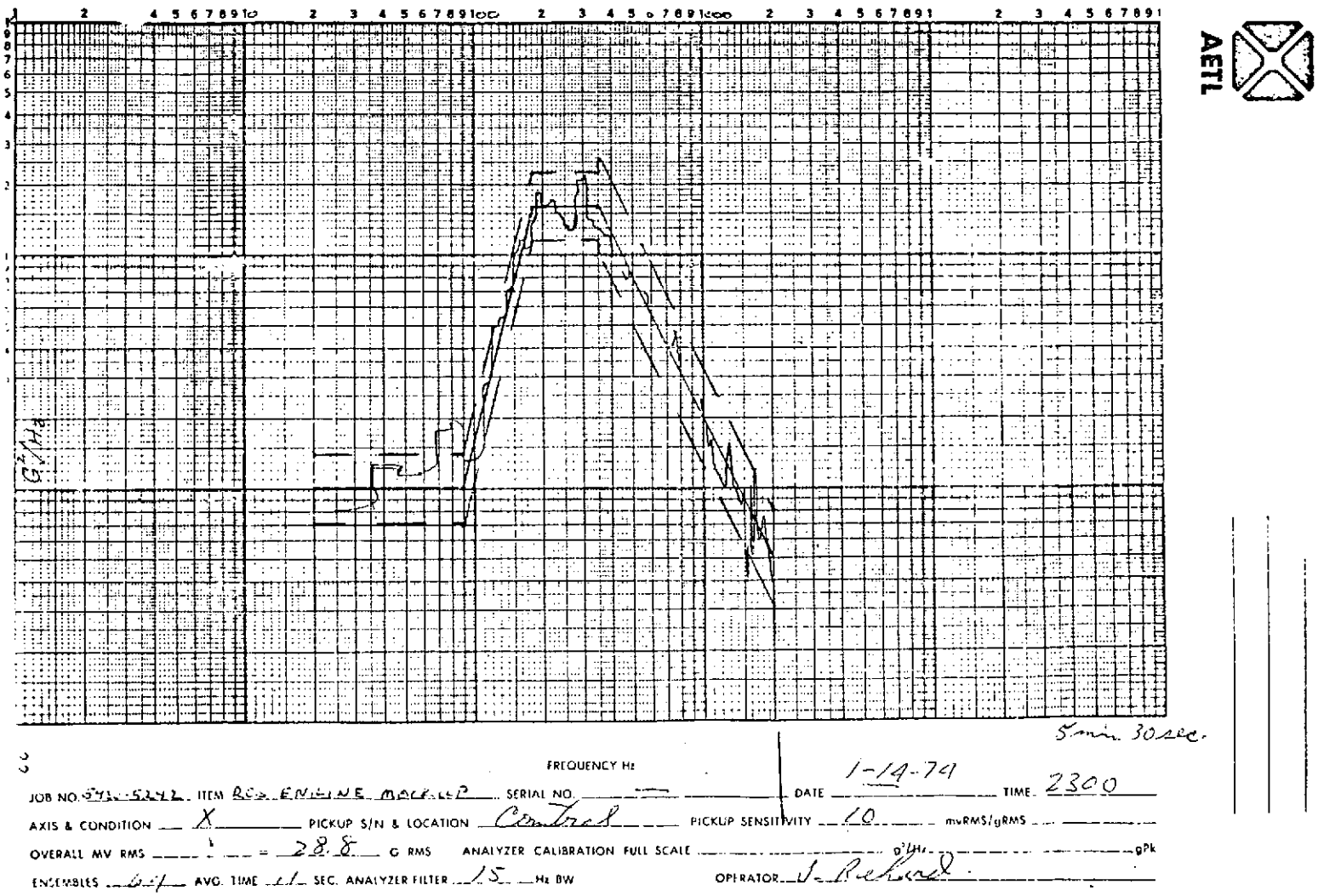

Figure 82. Engine Simulator X-Axis Random - 100 Minute Run

AETL

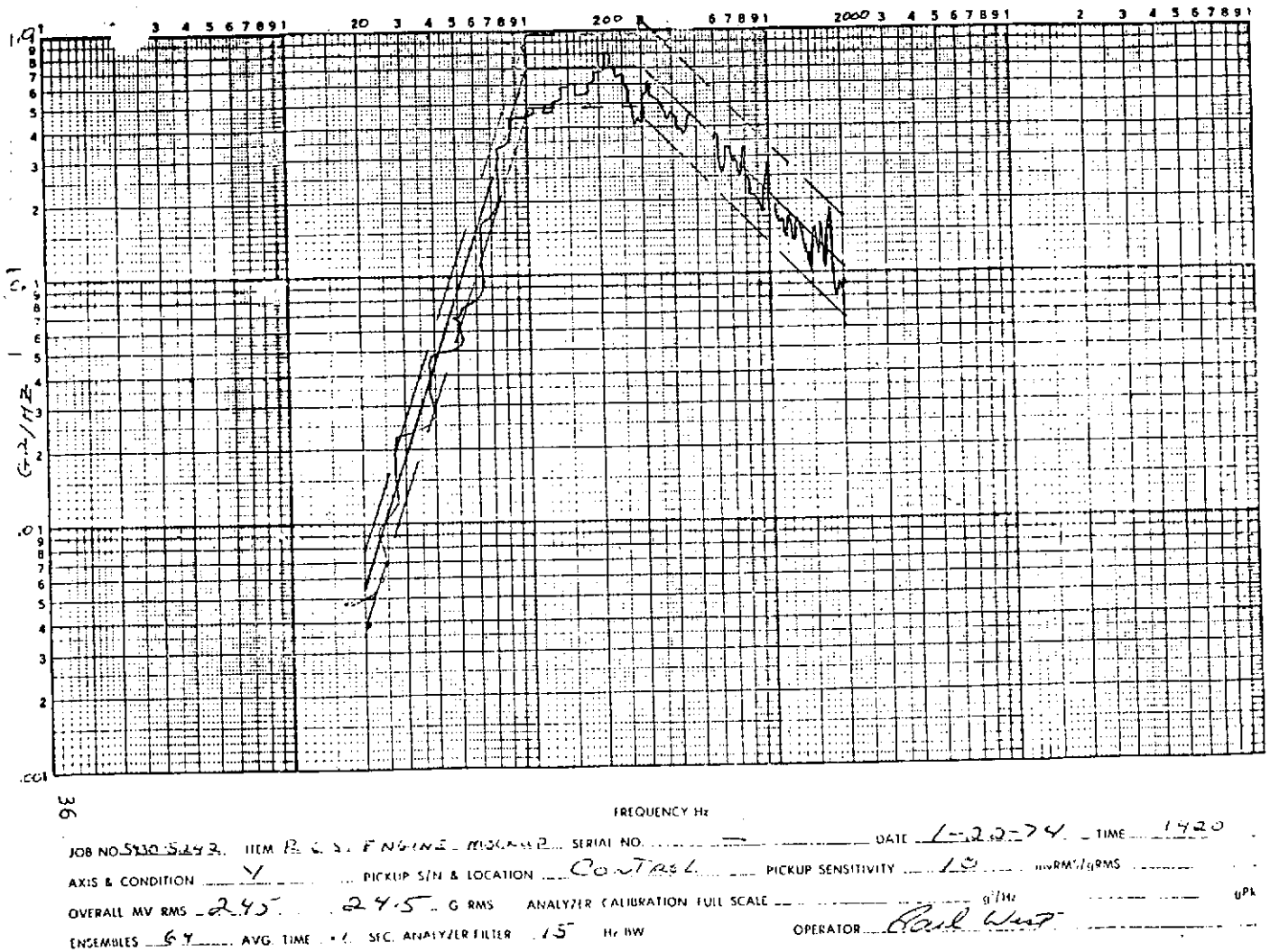

Figure 83. Engine Simulator Y-Axis Random - 117 Minute Run

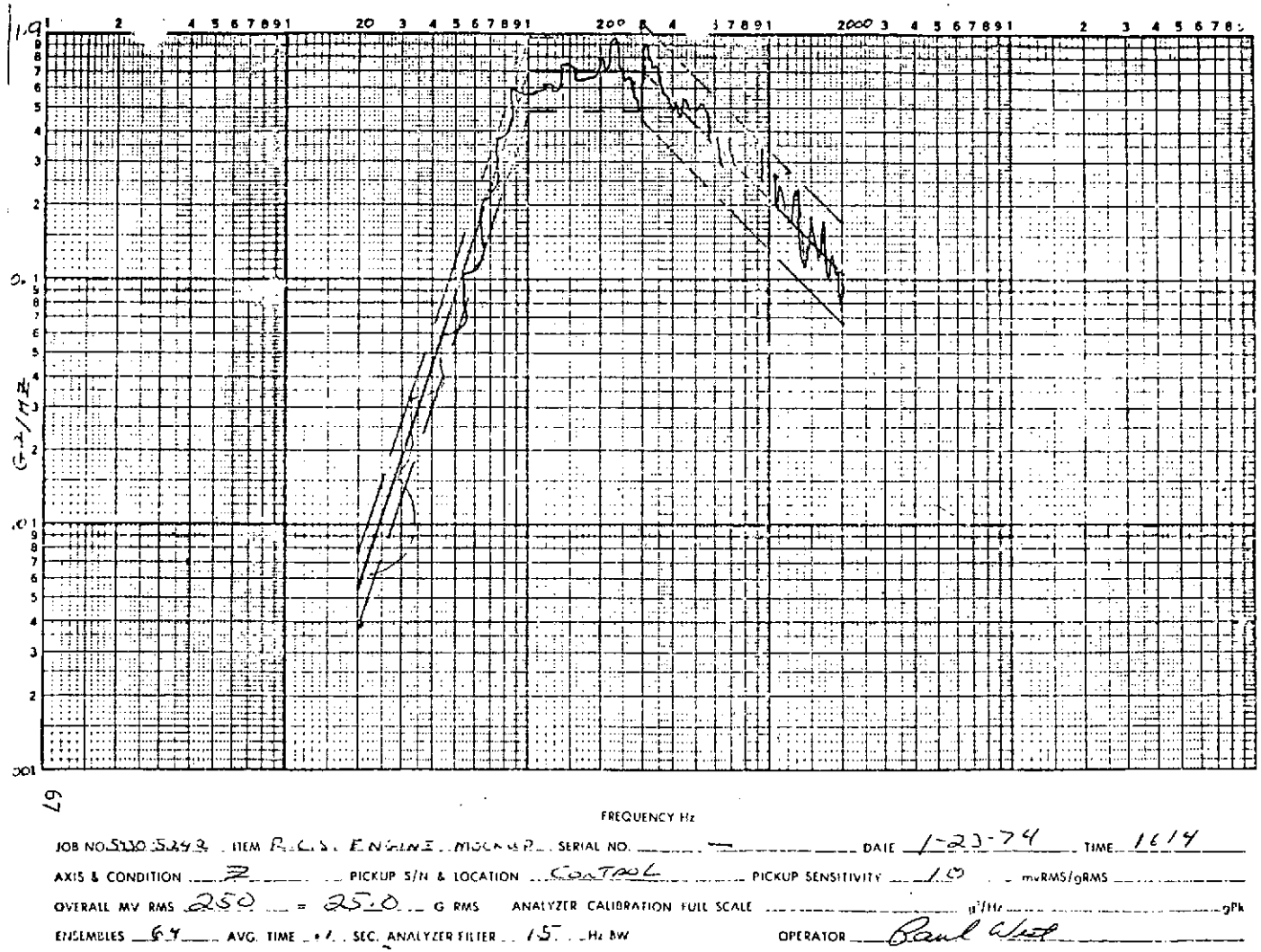

Figure 84. Engine Simulator Z-Axis Random - 117 Minute Run

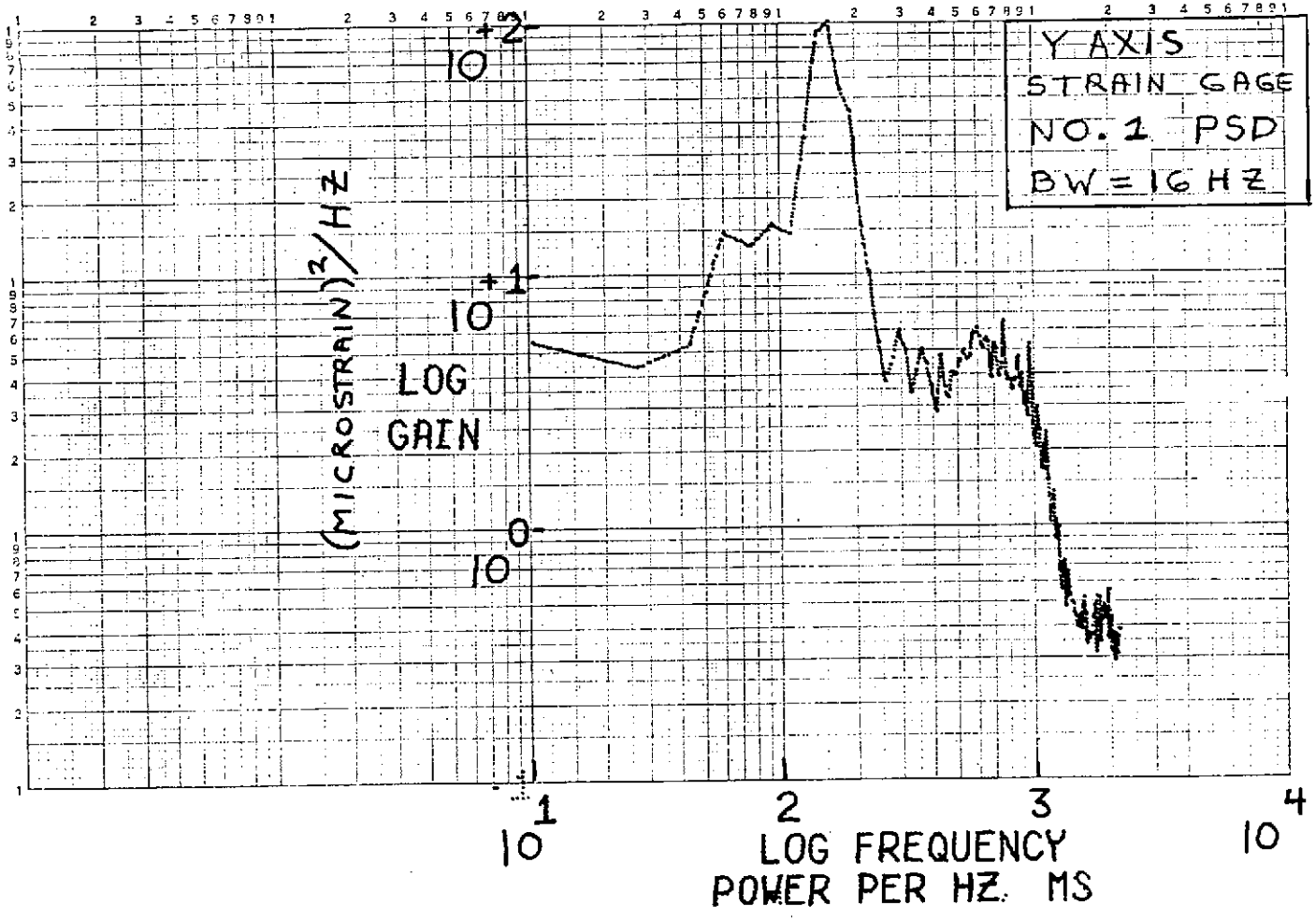

Figure 85. Simulator Test, Strain Amplitude Data Strain Guage No. 1

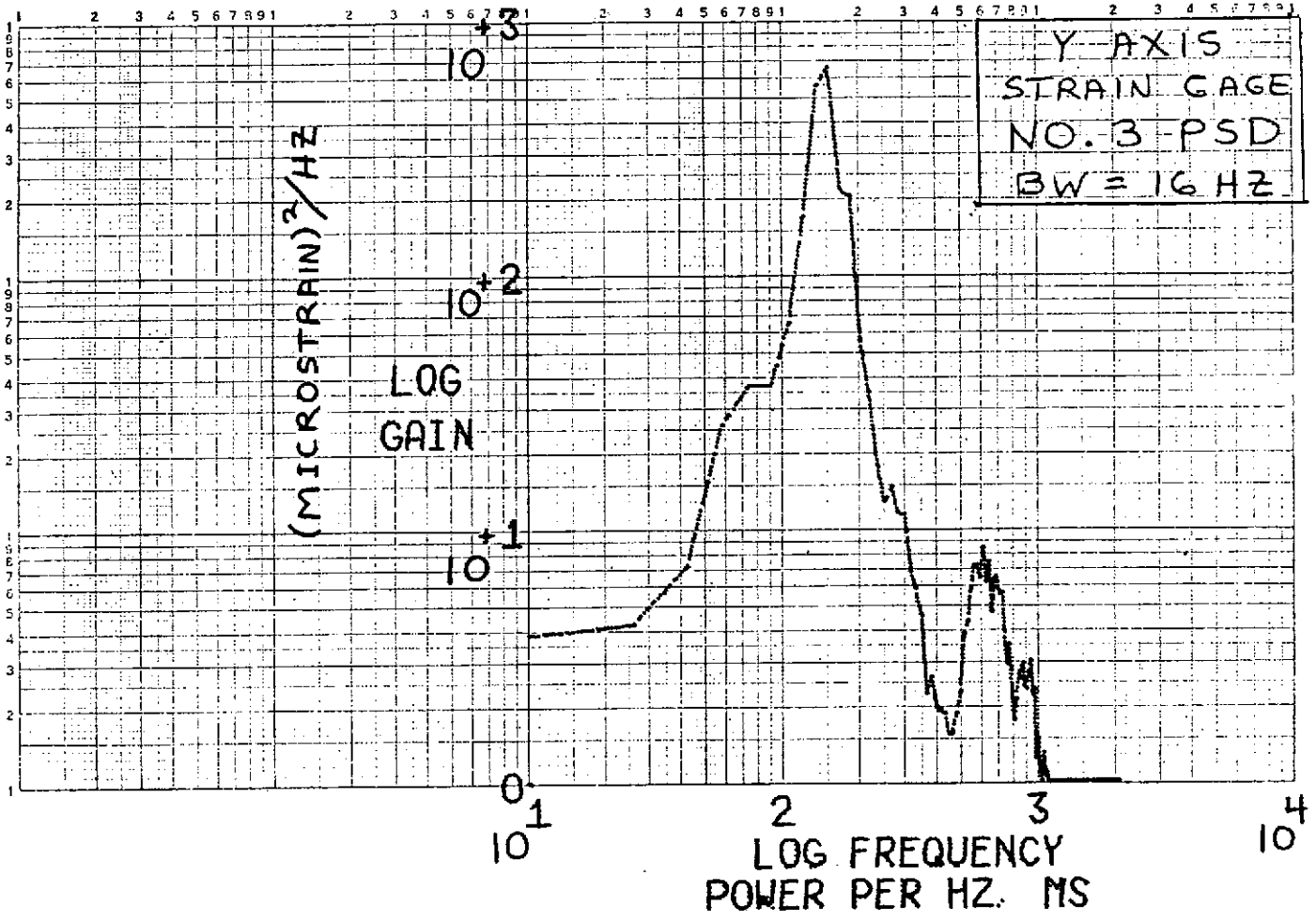

Figure 86. Simulator Test, Strain Amplitude Data Strain Guage No. 3

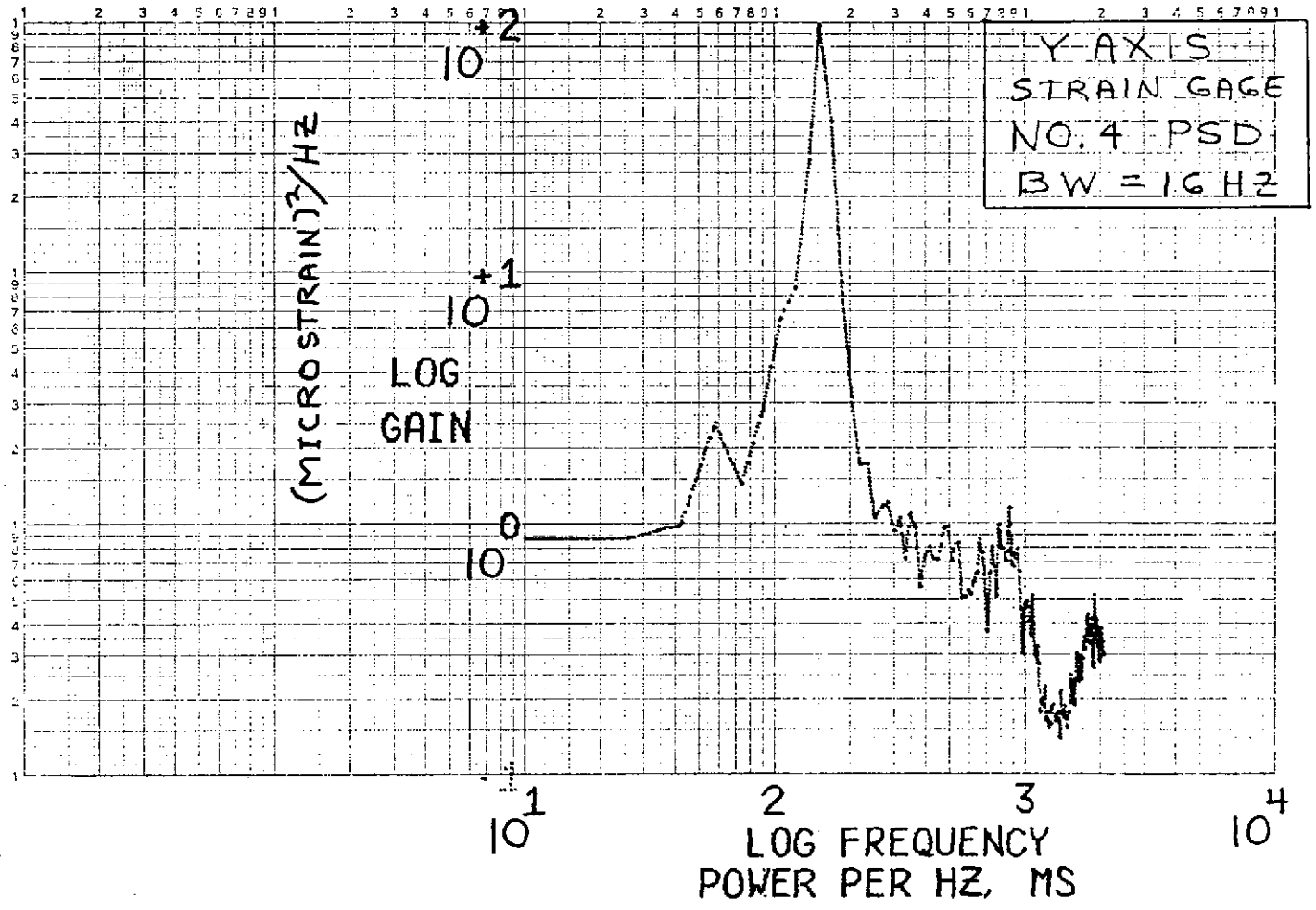

Figure 87. Simulator Test, Strain Amplitude Data Strain Guage No. 4

TABLE 41. SIMULATOR VIBRATION TEST STRAIN AMPLITUDES

Input Vibration Axis	Strain Gage No. 1		Strain Gage No. 3		Strain Gage No. 4	
	Freq. hz	Microstrain in/in RMS	Freq. hz	Microstrain in/in RMS	Freq. hz	Microstrain in/in RMS
x*	190	25	190	94	190	63
y**	180	89	180	125	180	75
y***	150	40	150	105	150	40
z***	190	35	190	18	No	--
	900	21	500	19	Good	--
			900	28		--

NOTES:
1. Strain gage No. 2 failed prior to first test.
*2. Test conducted after fixture modification with input per original requirement.
**3. Test conducted prior to simulator tube weld joint failure with input per revised requirement (failure not applicable to engine).
***4. Test conducted after weld joint repair and final fixture modification with input per revised requirements.
5. RMS microstrain determined from power spectral density plots as:

$$\text{RMS Microstrain} = \left[\frac{(\text{Microstrain})^2}{\text{h2}} \times \text{Filter Band Width}\right]^{1/2}$$

TABLE 42. ENGINE DECONTAMINATION PROCEDURE

Step	Procedure
1	Purge engine in test stand with GN_2
2	Purge engine in Clean Room with GN_2 120 seconds on/2 seconds off; repeat three times
3	Purge engine with alcohol on fuel side, GN_2 on oxidizer side for 2 minutes followed by 25 cycles of 10 seconds on and 2 seconds off
4	Repeat step 3 above with GN_2 on fuel side, Freon on oxidizer side
5	Purge engine with 160 F GN_2 for 10 minutes
6	Oven dry engine at 160 F for 4 hours

POSTTEST INSPECTION

Durability Engine

The Durability Engine was visually inspected and dimensionally checked after completing the post hot-fire decontamination procedure and leak test. The pretest throat and nozzle extension average dimensions were D_t = 1.469 and D_{ex} = 9.280 inch, respectively; while posttest average dimensions were D_t = 1.463 and D_{ex} = 9.267 inch. The decontamination procedure (Table 42) followed the third endurance test. The engine was neither decontaminated nor cleaned before or after previous tests.

No leakage was detected at the valve simulator interface or injector/chamber braze joint. However, 0.12 cu in./sec at 6 psig GN_2 leakage was detected at the chamber to nozzle joint which is well within Mars Mariner requirements.

Review of movies taken during test indicate no nozzle leakage during hot fire. It is evident that the nozzle joint seals because of differential thermal expansion. Up to four film coolant holes were plugged during each of the endurance tests. In the nozzle leak test, the leakage was predominantly in the region downstream of the plugged region. Since the nozzle is spun and the threaded flange is welded to the nozzle, the nozzle when fabricated in one piece would not have the residual stresses the welded configuration has and therefore should not sustain the slight change in form which occurs here. The nozzle joint was leak checked prior to the first hot-fire test and zero leakage was measured.

Figures 88, 89, and 90 show the posttest condition of the engine. In Fig. 88 black marks on the external surface of the nozzle, which are in line with the plugged film coolant holes, are evidence of charring of RTV 90 and 106 glues used to bond the insulation to the external shell. The Dynaflex insulation blanket posttest condition was good, but does show evidence of the charring glues in matching areas with the nozzle extension. The internal view of the nozzle, Fig. 89, showed no effect of the film hole plugging.

Figure 90 shows a closeup view through the nozzle exit into the throat region and a section of the injector face. The camera light against the injector face casts a reflective light on the throat plane on the left side and reveals a clean sharp line which is an indication of the excellent condition of the chamber. On the right side, which is downstream of the plugged film coolant holes, a slight amount of oxide is evident which was predictable from the external throat temperatures measured during the plugged coolant hole tests. No attempt has been made to remove this material from the throat region since further hot-test firings are anticipated.

Off-Limits Engine

The posttest condition of the beryllium chamber was excellent as was the chamber/nozzle extension joint and Haynes/nozzle extension section not damaged during the simulated regulator failure test (MR = 2.9 o/f, P_c = 237 psia). The engine and two-ring injector were completely disassembled and were later reassembled with a

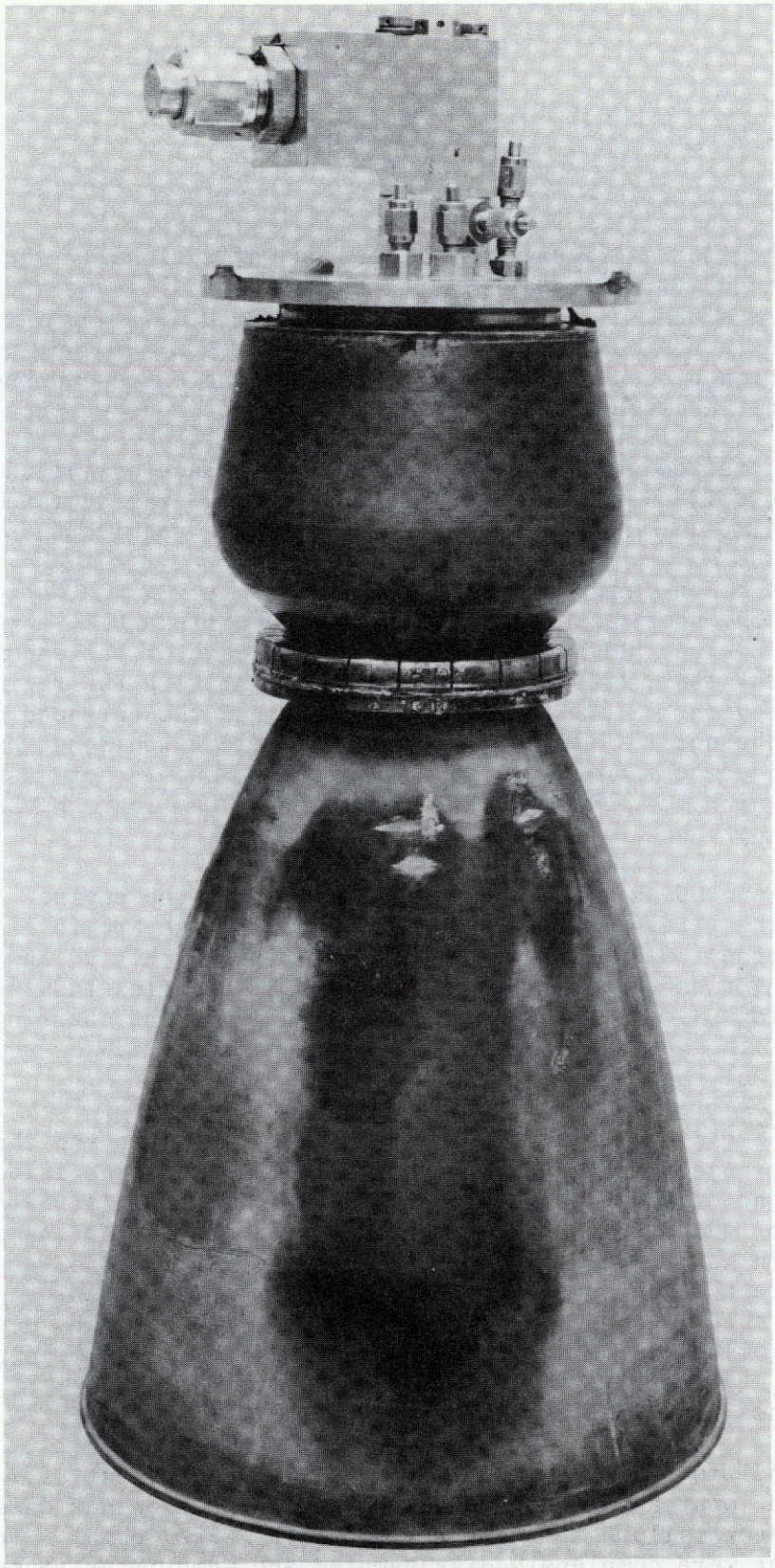

1SA25-5/7/74-C2F*

Figure 88. Durability Engine Assembly Posttest

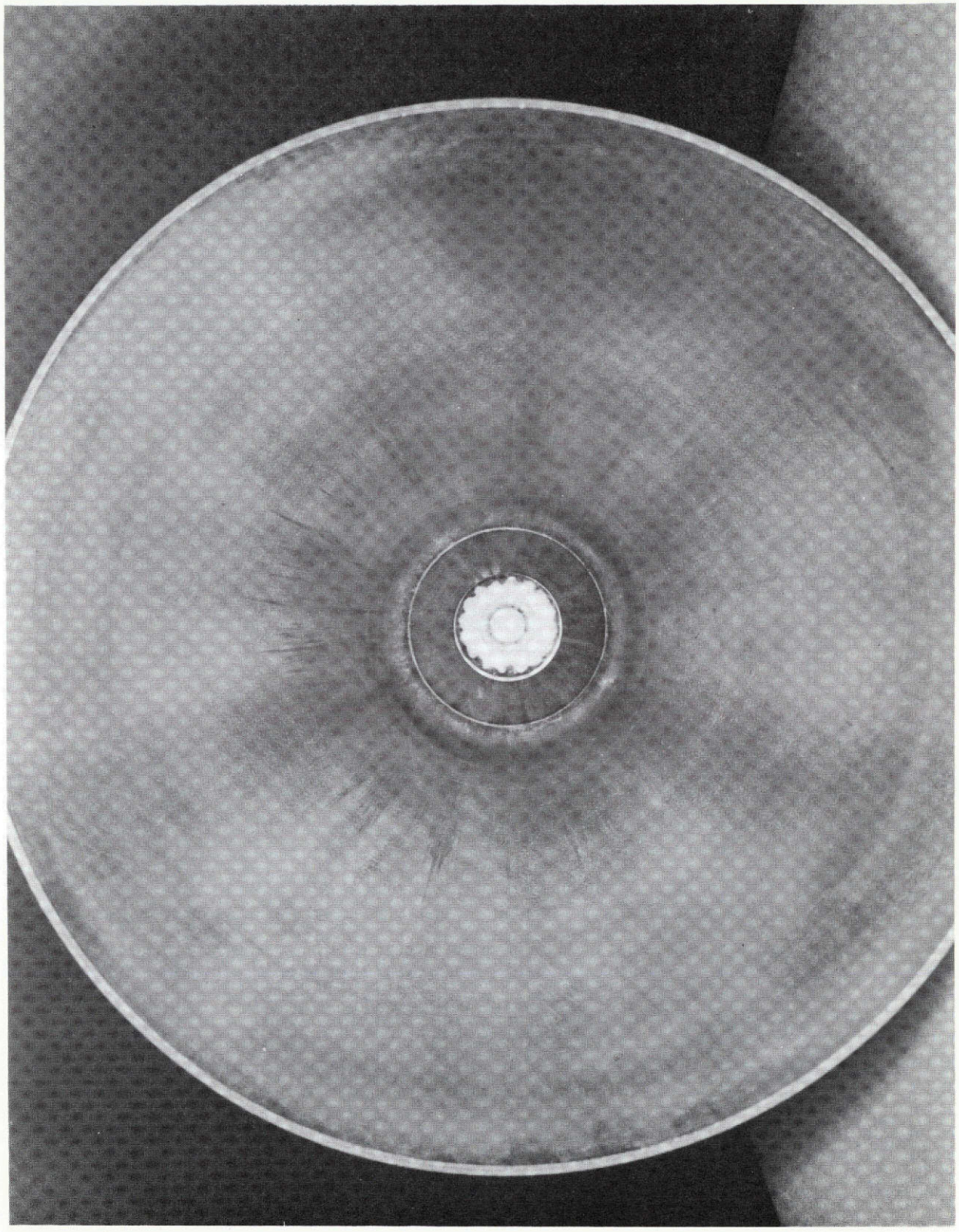

1SA25-5/7/74-C2B*

Figure 89. Durability Engine Exit View Posttest

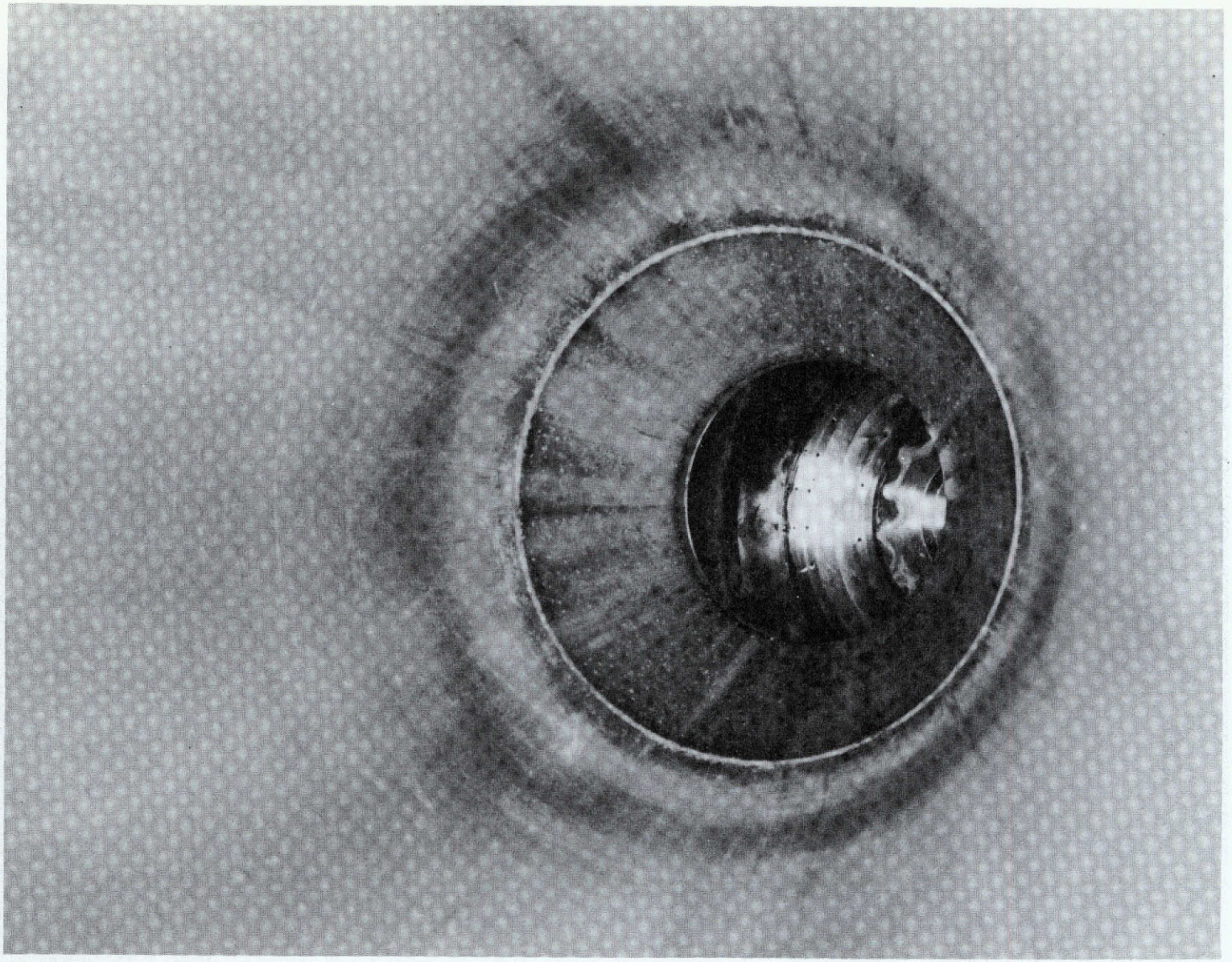

1SA25-5/7/74-C2A*

Figure 90. Durability Engine Exit Through Throat-to-Injector

a columbium nozzle extention (ε = 40:1) and the off-limit tests were repeated on a company-sponsored program. The final condition of the engine assembly was excellent except for slight oxidation of the throat ID downstream of the plugged film coolant region.

Vibration Simulator

Posttest examination of the vibration simulator revealed it to be in excellent condition. Posttest proof pressure at 500 psig and helium leak tests at 300 psig verified the structural integrity of the simulator and qualified the injector to beryllium braze joint.

ENGINE DESIGN UPDATE

During this program, the ability of a beryllium INTEREGEN cooled engine with a columbium nozzle to meet the severe operating requirements of the Space Shuttle RCS with large thermal margins was demonstrated through analysis and experimental programs. The problems encountered, valve failure and injector orifice plugging, are independent of the cooling process. Both of these problems were associated with environmental exposure tests, more specifically exposure to large quantities of sand and dust with a set engine prior to random vibration testing. Orifice plugging was demonstrated not to be a problem relative to safe engine function; however, mixture ratio shifts could occur which would affect propellant consumption. Since the largest injector hole in the injector was more susceptible than the smaller ones, reducing the number of elements does not appear to be a solution to obviating orifice plugging. The migration of particles to the valve could be a severe problem, however. Unless a valve is developed which does not degrade in the environment, the engine will have to be protected from sand and dust and/or purged prior to each mission.

The large thermal margin demonstrated on the engine indicates that substantial weight reduction could be made by reducing the mass of the beryllium. In addition, a lower contraction ratio configuration is feasible which would result in both lower combustion and injector weight.

Thermal predictions were made for the Durability Engine operating at nominal conditions. The temperatures measured during baseline performance tests (test 052) are indicated on the predicted isotherm and temperature history plots in Fig. 91 and 92 and show the agreement of test with predicted results. The correlation with test data of test 052 was used to perform a beryllium chamber weight reduction analysis. The results of this analysis are presented in Fig. 93 and 94. They indicate the chamber can be reduced in weight by 0.5 pound while maintaining INTEREGEN operation at only slightly higher temperature lvels than measured with the existing design. These temperature levels are well within the operating capability of the material. Additional weight savings can be gained by going to a lower contraction ratio configuration; that is, reduce contraction ratio from 6:1 to 4:1. The greatest savings would be in the injector since it is stainless steel. The existing injector weighs 6.0 lbm and could be reduced by 2.8 lbm.

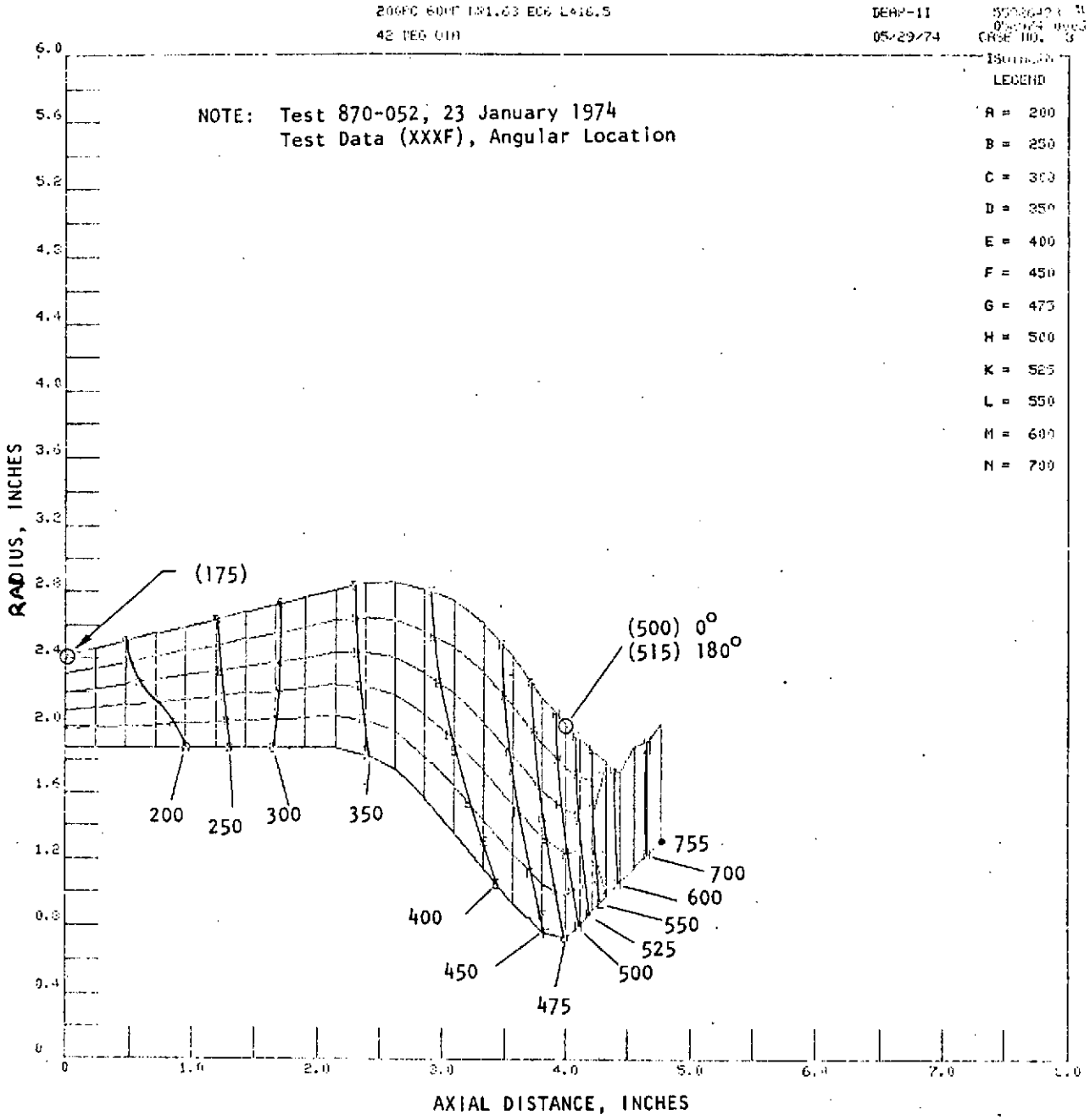

Figure 91. Durability Engine - Thermal Analysis Isotherms Data Correlation

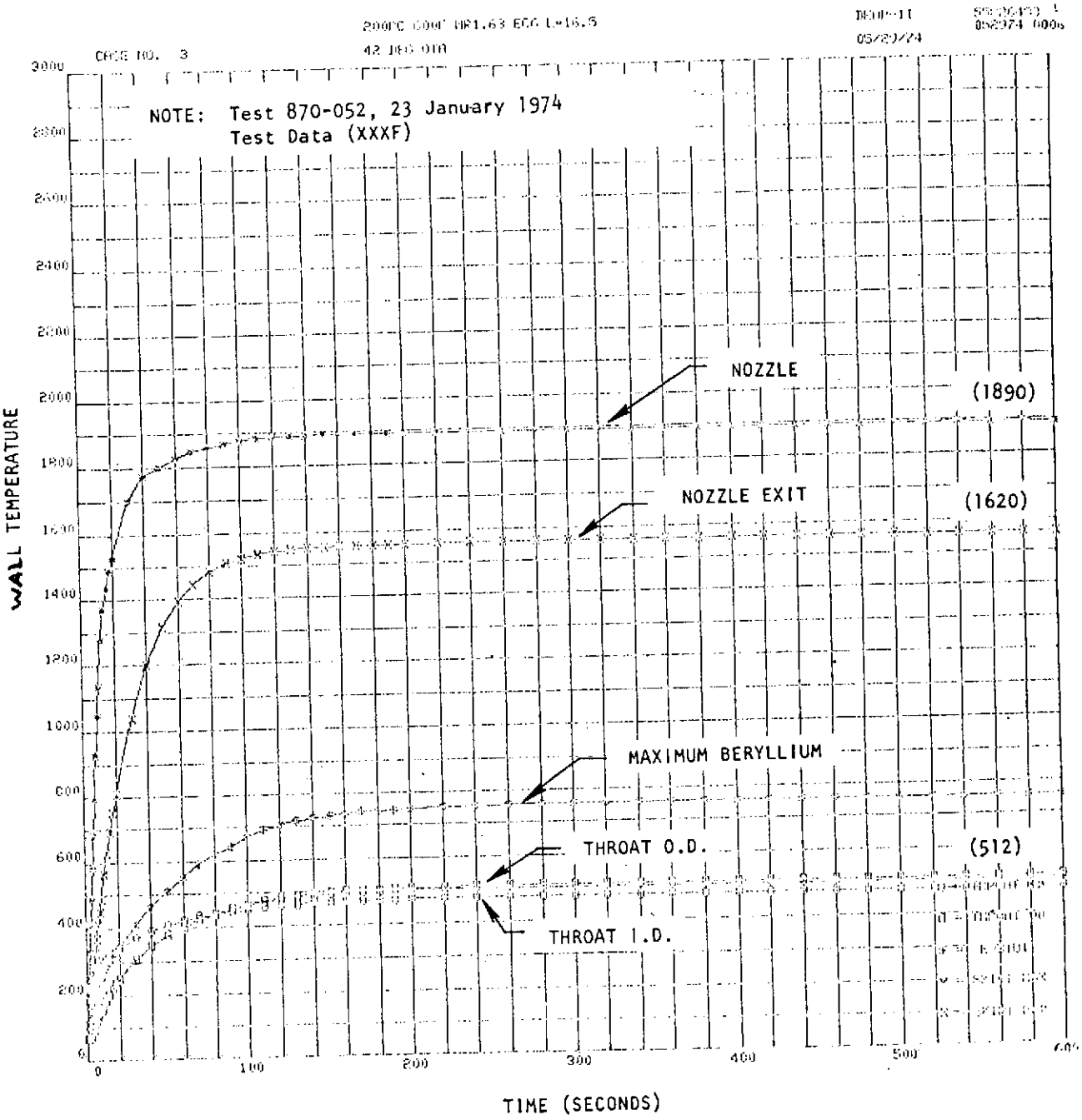

Figure 92. Durability Engine - Thermal Analysis Temperature History Data Correlation

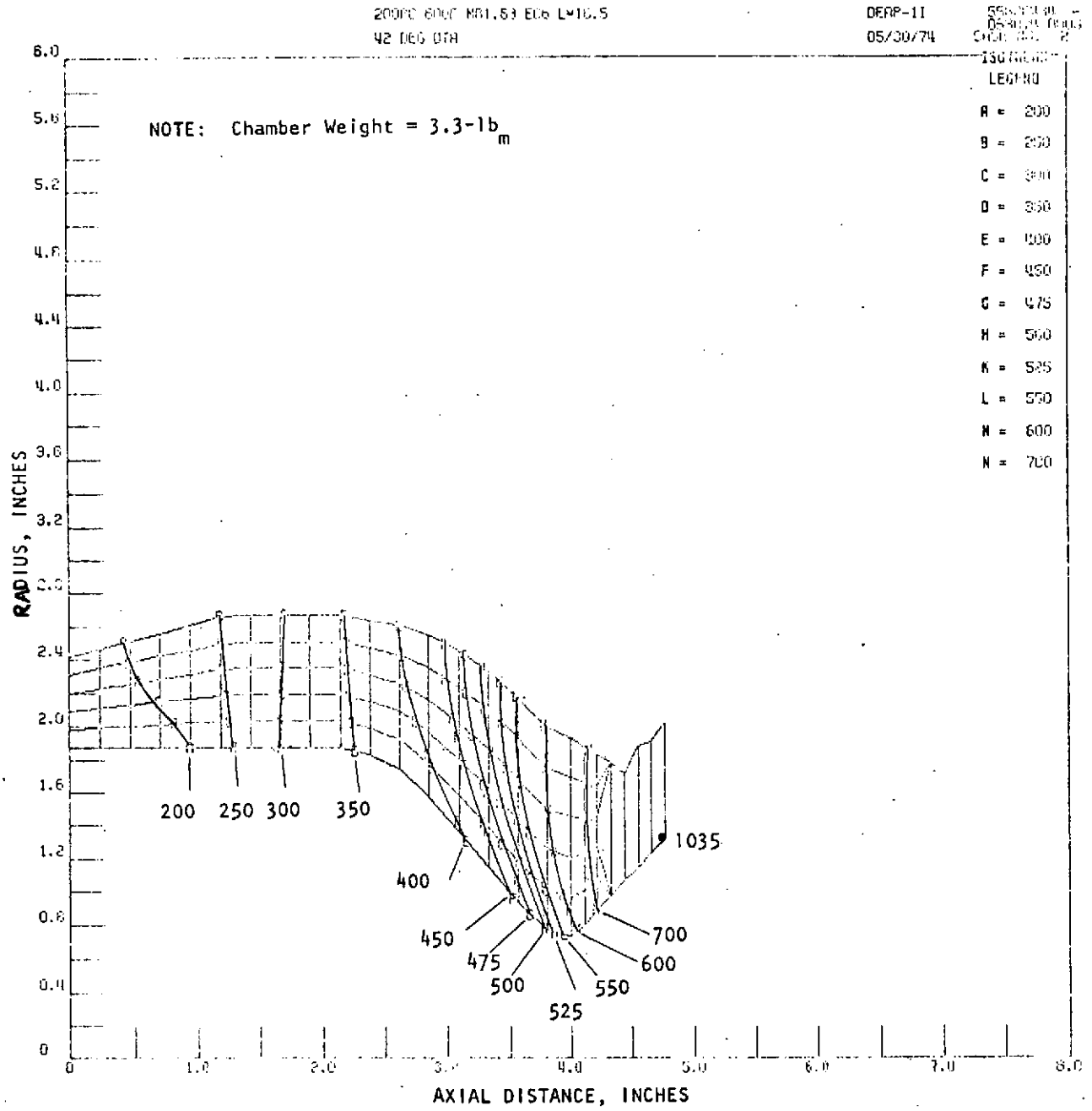

Figure 93. Durability Engine - Predicted Isotherms Weight Reduction Thermal Analysis

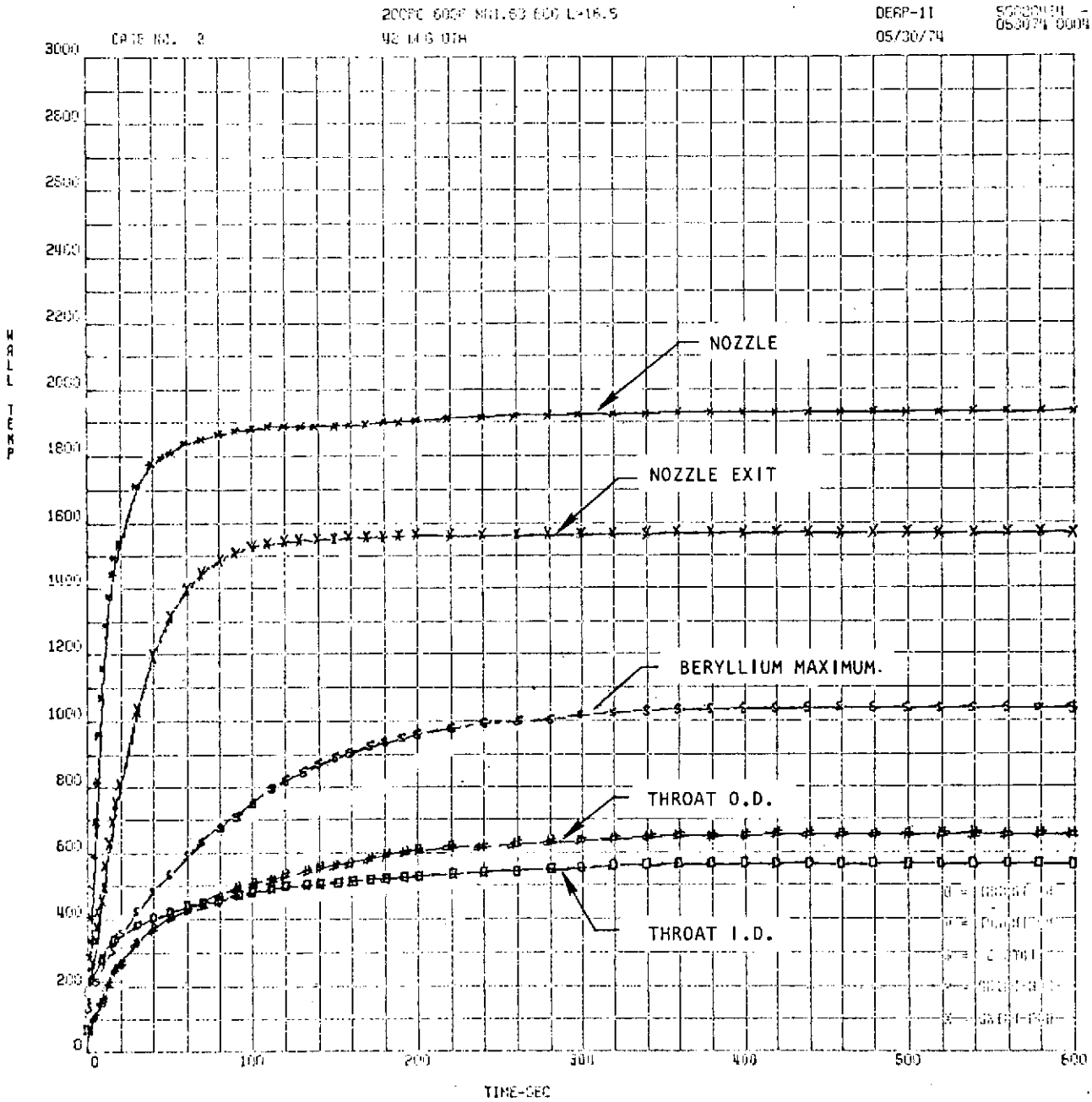

Figure 94. Durability Engine Predicted Temperature History Weight Reduction Thermal Analysis

The lower contraction ratio would result in a higher integrated heat load to the chamber, but since the engine shows thermal margin, the increased heat load could be accommodated by increased beryllium wall thickness (improved conduction path to head end liquid film) while still effecting a weight reduction in the beryllium chamber.

A comparison of projected weight reduction with the Durability Engine configuration is shown in Table 43. As noted in this report, the Durability Engine injector weight was not optimized (designed to mate with existing valve and test facility, excess external material not machined to reduce fabrication cost). The weight of the two flight configurations reflect optimized injector weight with a flush mounted valve and scalloped exterior. This weight reflects that of a two-piece thrust chamber where the nozzle extension is adaptable to any vehicle interface scarfing requirement.

TABLE 43. BERYLLIUM INTEREGEN ENGINE WEIGHT COMPARISON

	Test Configuration	Optimized Flight Configuration ($\xi_c = 6$)	Optimized Flight Configuration ($\xi_c = 4$)
Valve*	4.55	4.55	4.55
Injector	6.04	3.31	2.21
Combustor	3.86	3.33	2.62
Nozzle	2.81	2.81	2.81
Nozzle Nut	0.86	0.86	0.86
Total	19.00	15.74	13.93

*Mechanically linked, single stage, bipropellant valve

CONCLUSIONS

The beryllium INTEREGEN engine has successfully completed a rigorous hot-fire and environmental test program. The results of testing have indicated that performance, thermal characteristics and durability are consistent with space shuttle application requirements. The following conclusions can be drawn from the test program:

1. The engine has demonstrated 294.4 lbf-sec/lbm steady-state specific impulse with unsaturated propellants at the nominal design point. Specific impulse is projected to 295.8 lbf-sec/lbm by incorporating an optimum nozzle contour. Further performance gains can be made by reduction in film coolant and adjustment in propellant outer row momentum angle.

2. The pulse specific impulse goal of 220 lbf-sec/lbm was demonstrated for a minimum impulse bit of 30 lbf-sec at a pulse frequency of 5 Hz. The pulse specific impulse goal can be met at lower pulse frequencies with reduced injector volumes. The propellant injection volumes were compromised by valve mounting configuration and the fact that downstream of the seat, valve volumes were large. Reconfiguration of the valve seating to reduce volume and design to allow valve mounting directly on the back face of the injector is recommended.

3. An engine start time of 0.040 second and cutoff time of 0.020 second was demonstrated with the MOOG inc. valve.

4. Chamber pressure overshoot associated with start transient was a maximum of 20 percent which is no compromise to engine life or performance.

5. The engine demonstrated very broad off-limits operation capability (1.43 to 2.88 o/f mixture ratio and 66 through 230 psia chamber pressure) without sustaining damage. However, the worst case simulated dual oxidizer regulator failure (2.88 o/f mixture ratio with 237 psia chamber pressure) mode of operation, high temperatures in the Haynes 25 nozzle extension caused a failure of the material. This test was repeated successfully with this engine with a columbium nozzle extension on a company sponsored program. Discrete tests with one plugged primary fuel hole and one and three-adjacent plugged coolant holes were conducted to steady state at nominal conditions with the Off-Limits Engine. The engine throat outside surface temperatures reached predictable values which demonstrated the feasibility of reliable engine shutdown devices to allow for subsequent engine operation. The plugged coolant orifices caused only slight oxidation of the throat ID downstream of the plugging.

6. At nominal operating conditions (200 psia chamber pressure, 1.63 o/f mixture ratio) with a 30 psid valve and allowing 10 psid calibration orifice, the inlet pressure is 290 psia which meets the design requirement.

7. The maximum single burn requirement of 600 seconds was demonstrated with steady-state performance and thermal equilibrium conditions achieved. Lower than steady-state mean operating temperatures were demonstrated for pulse operation over a pulse frequency range of from 1/3 to 5 Hz with pulse widths of 0.050 to 1.0 second with no degradation to performance or engine integrity.

8. Thermal equilibrium was demonstrated: with and without a nozzle extension insulation blanket, with and without helium saturated propellants, with one primary fuel hole plugged (oxidizer on wall), with one coolant hole plugged and with four adjacent coolant holes plugged.

9. High cycle life capability was demonstrated by the attainment of low beryllium chamber operating temperatures and thermal gradients. The low operating temperatures at nominal conditions provided large thermal margin which allows for operation over a wide range of inlet conditions.

10. The valve seat maximum soakout temperature from engine operation was well within limits to allow for engine restart and not impose restrictions on life or performance.

11. The nozzle extension thermal insulation exceeded the maximum specified temperature requirement of 800 F by approximately 75 F. However, the external titanium shell can be painted with emissivity control paint or a slight increase in Dynaflex blanket thickness will provide the required effect with better reliability.

12. The Durability Engine while subjected to six environmental cycles did not encounter adverse effects other than slight superficial staining and minor pitting of the beryllium chamber. The engine successfully completed the sinusoidal vibration testing with no evidence of detrimental effects. During random vibration testing, strain gage data indicated that low frequency resonant modes were present in the 150 to 250 Hz frequency range. Strain values recorded in the braze transition joint between the injector and chamber were on the order of one half that allowed for in the design. Therefore, the design is capable of withstanding inertial loads greater than twice those experienced in test.

13. The Vibration Simulator demonstrated successful completion of random vibration test equivalent to 100 space shuttle missions. The measured peak strain applitude was less than one-half the design value. Therefore, the injector/chamber braze joint was designed to withstand inertial loads greater than those experienced in test.

14. The MOOG Inc. bipropellant valve was used for acceptance and baseline performance testing. Due to its inlet pressure limitations and marginal operating characteristics, facility valves were required for the off-limits testing. Also, severe damage was sustained by the valve seats

during environmental testing due to migration of sand/dust particles between the poppet and seat during vibration sequence even under specification lockup inlet pressures. It is obvious from this testing that redesign of the valve seat is required and/or precautions must be taken to preclude the admittance of sand and dust into the engine whenever possible. The precautions could be taken in the form of inexpensive blow out throat plugs or nozzle exit covers.

15. Posttest analyses indicate that lower weight designs are feasible by recontouring the beryllium chamber and scalloping the injector. Also, additional weight reductions are possible by incorporating designs of lower contraction ratio. Thermal predictions using correlations with test data acquired in this program indicate adequate cooling is available to effect the lower contraction ratio designs.

16. The results of this program suggest that the beryllium INTEREGEN cooling concept is capable of application to higher thrust and chamber pressure regimes.

REFERENCES

1. R-9556, Final Test Report, A study of the Durability of Beryllium Rocket Engines, NASA Contract NAS9-13475, dated June 1974, Rocketdyne Division, Rockwell International.

APPENDIX A

TEST FACILITIES

ROCKETDYNE FACILITY

Hot-fire testing of the Durability Engine was performed in Cell 37 at the CTL-4 facility located in Area III of the Santa Susana Field Laboratory. This facility is composed of a control center encompassed by four test modules and is primarily used for space engine, component development, and production testing. Included in its capabilities are temperature and altitude environmental facilities. One Class B (per RA0615-003) clean room (trailer) is located at CTL-4 to provide the required cleanliness environment for assembly, disassembly, and cleaning of the engine hardware.

Cell 37 has an altitude chamber 7 feet in diameter and 12-1/2 feet long. It is capable of maintaining a simulated altitude of 120,000 feet for 3000 seconds while firing a 600-pound-thrust engine, using NTO and MMH as propellants. Altitude is maintained with a two-stage steam ejector and diffuser. The chamber has one vertical position firing downward with thrust measuring capabilities.

The control center has teletype service to the Canoga Complex computer center where data input was computed on an IBM 370 for fast reduction. The total control center instrumentation capability includes: oscillograph (72 channels--2-36 channel recorders); DIGRs (54 channels--Foxboro); high-frequency recorders (28 channels); event recorders (80 channels); digital recorders (100 channels); digital display meters (20) and Brush recorders (40 channels). Primary measurement parameters are recorded utilizing Astrodata Model 4024 digital acquisition system.

Engine and Facility Parameter Measurements

The parameters monitored during hot-fire testing at simulated altitude are as shown in Table A-1 and Fig. A-1.

Description of Sensors Used During Hot-Fire Testing

The description of the force, pressure, and temperature sensing devices that were used to monitor engine and facility parameters are as described in Table A-2.

Steady-State Data Acquisition

Steady-state parameters such as thrust, pressure, temperature, current, and voltage were directly converted to d-c signals, and were recorded on magnetic tape in digital format. Frequency determinations were accomplished by a pulse-rate integrator which amplifies and clips an a-c voltage signal, converting each cycle into a square wave d-c pulse. These pulses were fed into a capacitor which discharges at a rate proportional to the d-c pulse rate. The Analog to Digital Converter converts the analog output to a digital output (counts) which were recorded directly on magnetic tape. The flowmeter output frequency was also established in this manner.

TABLE A-1. ADVANCED BERYLLIUM REACTION CONTROL THRUST CHAMBER INSTRUMENTATION REQUIREMENTS, CELL 37, CTL-4

MEASUREMENT	RANGE	REQUIRED	MAX RANGE PRE-CISION	DYNA-LOG	ASTRO-DATA	FREQ. RESP
THRUST, AXIAL, LB	0-1000	2	±1/2%	X	X	500 Hz
CHAMBER PRESSURE, PSIA	0-400	1	±1/2%	X	X	500 Hz
OX. VALVE INLET PRESSURE, PSIG	0-400	1	1.0%	X	X	350 Hz
FUEL VALVE INLET PRESSURE, PSIG	0-400	1	1.0%	X	X	350 Hz
OX. INJECTOR INLET PRESSURE, PSIG	0-400	1	1.0%	X	X	350 Hz
FUEL INJECTOR INLET PRESSURE, PSIG	0-400	1	1.0%	X	X	350 Hz
OX. INJECTOR MANIFOLD PRESSURE, PSIG	0-400	1	1.0%	X	X	350 Hz
FUEL INJECTOR MANIFOLD PRESSURE, PSIG	0-400	1	1.0%	X	X	350 Hz
OXIDIZER FLOWRATE (TURBINE), LB/SEC	1.0-1.5	1	±1/2%	X	X	
FUEL FLOWRATE (TURBINE), LB/SEC	0.5-1.0	1	±1/2%	X	X	
OXIDIZER FLOWRATE (DRAG), LB/SEC	1.0-1.5	1	±1/2%	X	X	500 Hz
FUEL FLOWRATE (DRAG), LB/SEC	0.5-1.0	1	±1/2%	X	X	500 Hz
OXIDIZER INLET TEMPERATURE, F	0-150	1	±2F	X	X	
FUEL INLET TEMPERATURE, F	0-150	1	±2F	X	X	
VALVE VOLTAGE, VDC	0-35	1	2.0%	X	X	
VALVE CURRENT, AMP	0-1	1	2.0%	X	X	
AXIAL ACCELEROMETER, g P-P	0-500	1	-	X	X	10K Hz
ENVIRONMENTAL PRESSURE, PSIA	0-0.5	2	1.0%	X	X	
TIME (IRIG B), SEC	-	1	±0.1	X	X	
AMBIENT PRESSURE, IN. HG	0-30	1	1.0%	X	X	
AMBIENT TEMPERATURE, F	0-150	1	±5F	X	X	
OXIDIZER TANK PRESSURE, PSIA	0-400	1	1%	X	X	350 Hz
FUEL TANK PRESSURE, PSIA	0-400	1	1%	X	X	350 Hz
VALVE SEAT TEMPERATURE, F (1)*	0-500	1	±5F	X	X	
INJECTOR FLANGE TEMPERATURE, F (2)*	0-500	1	±5F	X	X	

*SEE LOCATIONS INDICATED IN FIGURE A-1

TABLE A-1. (Concluded)

MEASUREMENT	RANGE	REQUIRED	MAX RANGE PRE-CISION	DYNA-LOG	ASTRO-DATA	FREQ. RESP
CHAMBER TEMPERATURE, F (3)*	0-1000	4	±5F		X	
THROAT TEMPERATURE, F (4) (5)*	0-1000	2	±5F	X	X	
NOZZLE EXTENSION, F (6) (7)*	0-2000	1	±5F		X	
NOZZLE EXTENSION, F (8)*	0-2000	1	±5F	X	X	
NOZZLE EXTENSION, F (9)*	0-2000	5	±5F		X	
THERMAL INSULATION, F (10) (11)*	0-1000	4	±5F		X	

*SEE LOCATIONS INDICATED IN FIGURE A-1

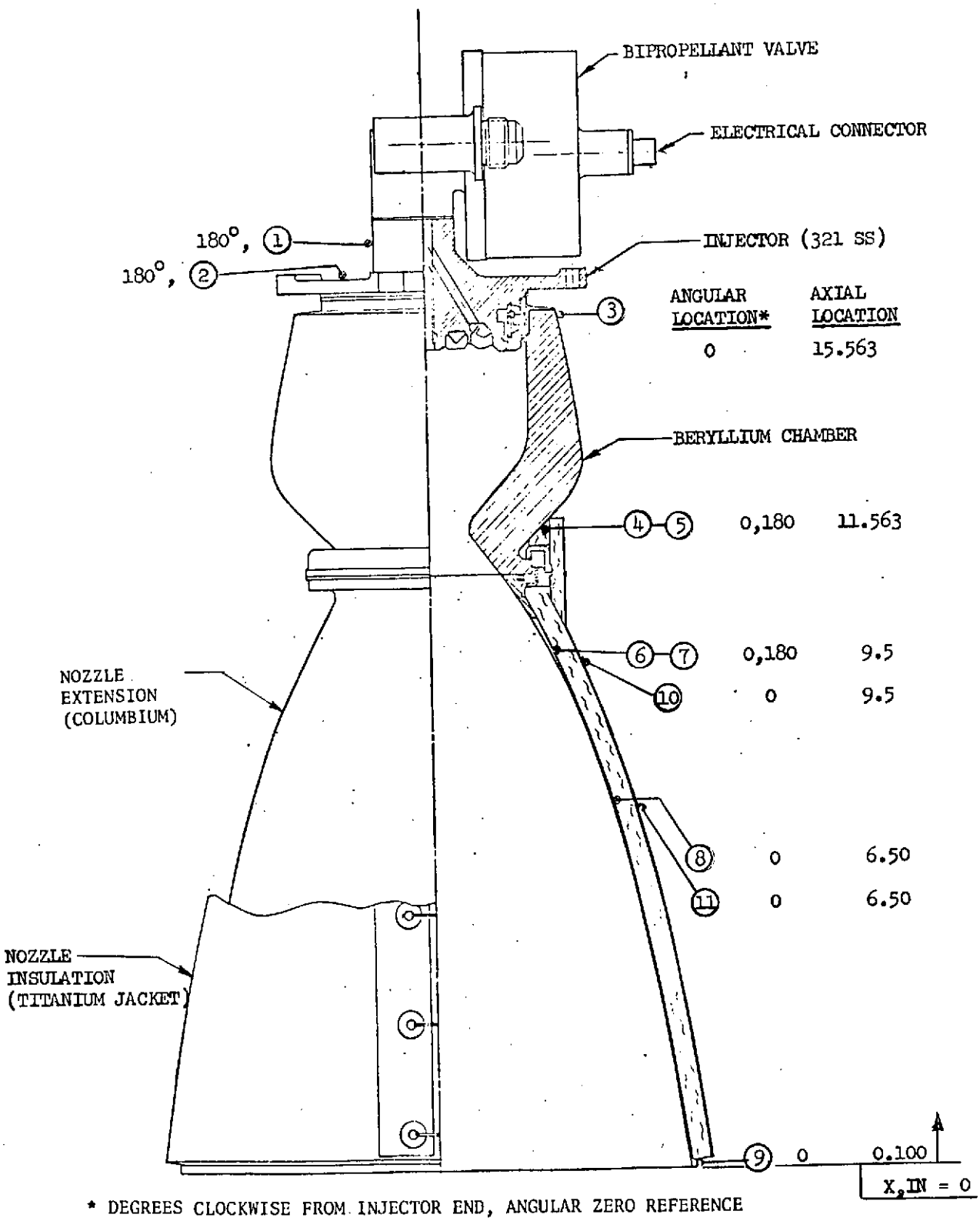

Figure A-1. Rocket Engine Assembly Representative Thermocouple Installation

C-3

TABLE A-2. SENSORS USED DURING ENGINE TEST

		Test Range	Sensor Range	No Reqd	Recording Precision, %		
Axial Thrust	lb_f	0-1000	5K	2	0.5	Bonded Strain Gage	Shaevitz-Bytrex
Chamber Pressure	psia	0-300	0-350	2	0.5	Diaphragm Strain Gage	Taber
Inj Man Pressure	psia	0-500	0-500	2	0.5	Diaphragm Strain Gage	Taber
Prop Inlet Pressure	psia	0-500	0-500	2	0.5	Diaphragm Strain Gage	Taber
Ox Flowrate	lb_m/sec	0-1.5	-	1	0.5	Turbine Flowmeter	Foxboro
Ox Flowrate	lb_m/sec	0-1.5	-	1	0.5	Drag Body Strain Gage	Ramapo W/RD Mod
Fuel Flowrate	lb_m/sec	0-1.0	-	1	0.5	Turbine Flowmeter	Foxboro
Fuel Flowrate	lb_m/sec	0-1.0	-	1	0.5	Drag Body Strain Gage	Ramapo W/RD Mod
Propellant Temp	F	0-120	-	2	1.0	Platinum Resistance Bulb	Rosemount
Acceleration	G, P-P	0-1500	-	2	1.0	Piezoelectric Crystal	ElectroScientific
Altitude Press	psia	0-.5	-	2	1.0	Variable Capacitance	Data Metric
Engine Temp	F	0-2000	-	As Reqd	1.0	Iron Con, Chromel Al	-

The components of each measurement system are illustrated in block diagram in Fig. A-2. The CTL-4 test facility data acquisition system consists of an Astrodata Model 4020 digital system supplemented with direct inking graphic recorders (DIGR's) and FM magnetic tape recorders. The FM tape and DIGR data were provided as backup information in the event of a failure of the digital acquisition system.

Transient Data Acquisition

Transient performance parameters were recorded on the digital data acquisition system identical to the steady-state parameters discussed above, with the exeption that thrust chamber pressure, flowrate (Ramapo) and propellant valve supply voltage are multiple sampled to obtain the response required to define the transient characteristics.

In addition to digital acquisition, high-frequency data were also recorded on FM magnetic tape using a Model FM-7211 Ampex Tape Recorder. The axial acceleration (g-level) of the engine was monitored by an accelerometer mounted on the injector. The accelerometer output was recorded on FM tape to verify combustion stability during engine firings.

Temperature Data Acquisition

Thermocouple data were recorded on the digital system and on Foxboro Dynalog Direct Inking Graphic Recorders (DIGR). The DIGR temperature recording system was calibrated by applying standard voltages to simulate the thermocouple output by at least two points. These data determine the slope and intercept of the calibration line, and give recorder units as a function of voltage. The relationship was converted to obtain voltage as a function of recorder units. Thermocouple tables published by the National Bureau of Standards were used for reducing the indicated voltage output of the thermocouple to degrees.

"Redline" Conditions

The engine test was terminated when the following test parameters exceed their redline valve.

Parameter	Redline Valve
Simulated Altitude	1.0 psia (60,000 ft)
Chamber Pressure	220 psia (for nominal conditions)
Throat Temperature	1000 F
Nozzle Temperature	2200 F
Valve Temperature	300 F

Helium Saturation

Helium saturation of both the NTO and MMH propellants was accomplished using the existing helium ingestion system in Cell 37. The existing system provided a 5-6 gpm pump recirculation system, propellant supply tanks, and a helium injectiom

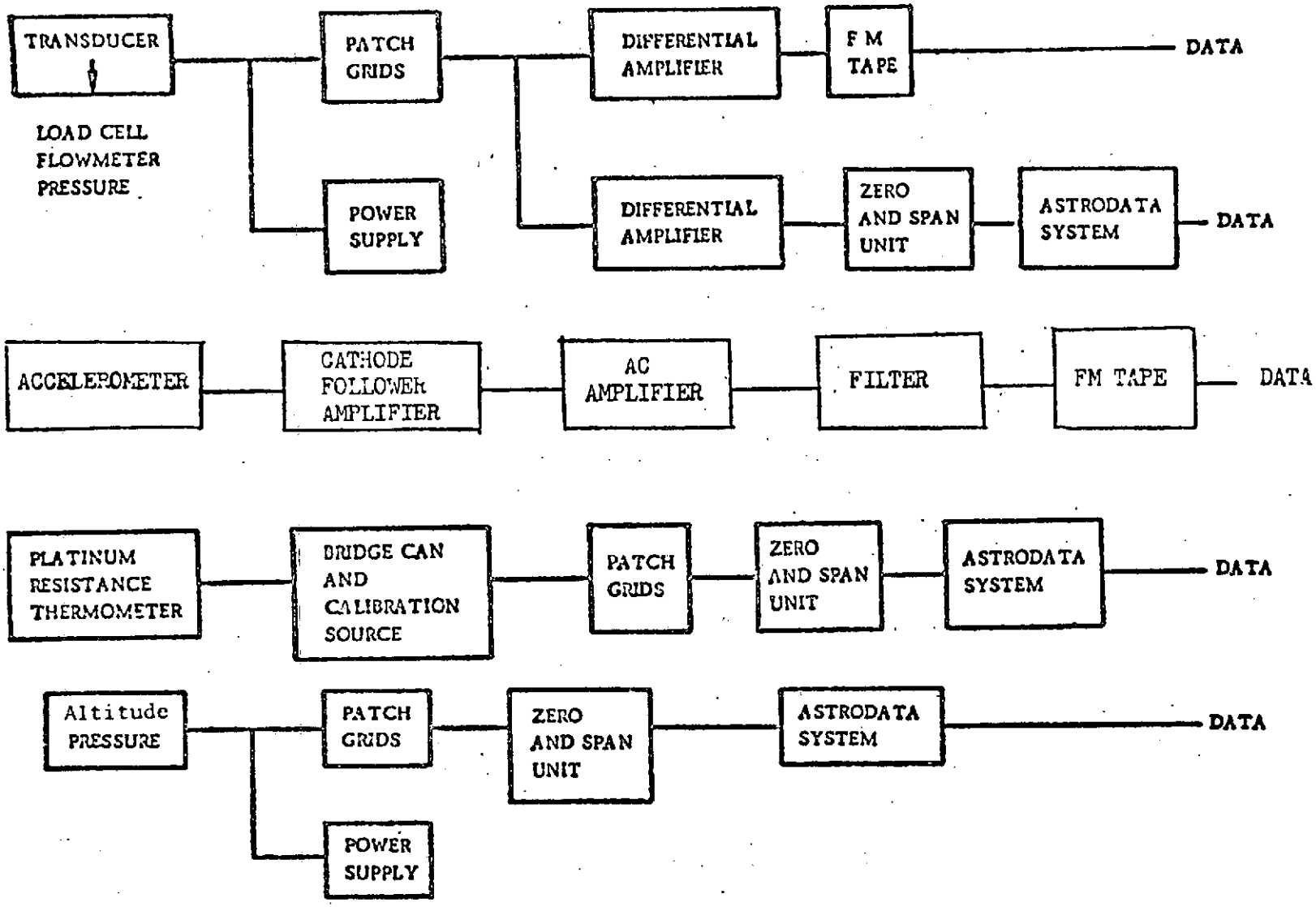

Figure A-2. Measurement Systems, Rocketdyne Test Facility

system, along with the necessary filters, valving and gages to clean, control and monitor the ingestion process. The helium saturation system is shown schematically in Fig. A-3.

A representative sample of propellant was removed and an "on-site" analysis conducted to verify saturation level prior to conducting each test series requiring propellants saturated with helium.

Sample removal was accomplished by first evacuating the sample container (bomb) with a vacuum pump, and then sealing this vacuum in the bomb by closing the vacuum-side hand valve. The facility sample valve was opened and the propellant allowed to flow into the bomb until a positive pressure of 35 to 65 psia was obtained. The bomb valves were then closed, facility secured, and sample bomb removed from the sampling point.

The sample bomb temperature was stabilized in a water bath, the final pressure recorded, and the bomb weighed. This data, in conjunction with the bomb dry weight, internal volume, and the density of the unsaturated propellant was unsaturated propellant was utilized to calculate the degree of saturation by using the "perfect" gas laws to determine the volume of gas and propellant in the sample bomb.

The accuracy of the "on-site" method of analysis has been adequately verified and correlated by a more accurate laboratory method of separating the gases by a vacuum line distillation procedure followed by a mass spectrometric analysis of the collected non-condensable gases.

APPROVED ENGINEERING TESTING LABORATORY

Environmental testing of the Durability Engine was conducted at Approved Engineering Test Laboratories (AETL) located in Chatsworth, California.

AETL is experienced in testing sophisticated products for the aircraft and aerospace industry and has been actively engaged in all forms of testing for private and commercial applications. AETL is staffed with professional engineers, chemists, and technical specialists of many disciplines and registered inspectors. All facilities have approval of NASA and all prime contractors.

Included in AETL test capabilities are: vibration--Random sine to 10,000 force pounds superimposed sine on random or random on random and simulated environment, and chambers of all descriptions for thermal vacuum, salt spray, fungus, extremes of temperature, altitude including a 512 cubic foot temperature-altitude-humidity chamber capable of more than 200,000 feet. Instrumentation is traceable to NBS for the measuring and recording of all laboratory phenomena including random vibration analysis, 1 inch magnetic tape recording analysis, shock spectrum analysis, strain guage output, high speed color photography, and recording and analysis of noise.

Engine Parameter Measurements

The parameters monitored during environmental testing are shown in Table A-3 and Fig. A-4.

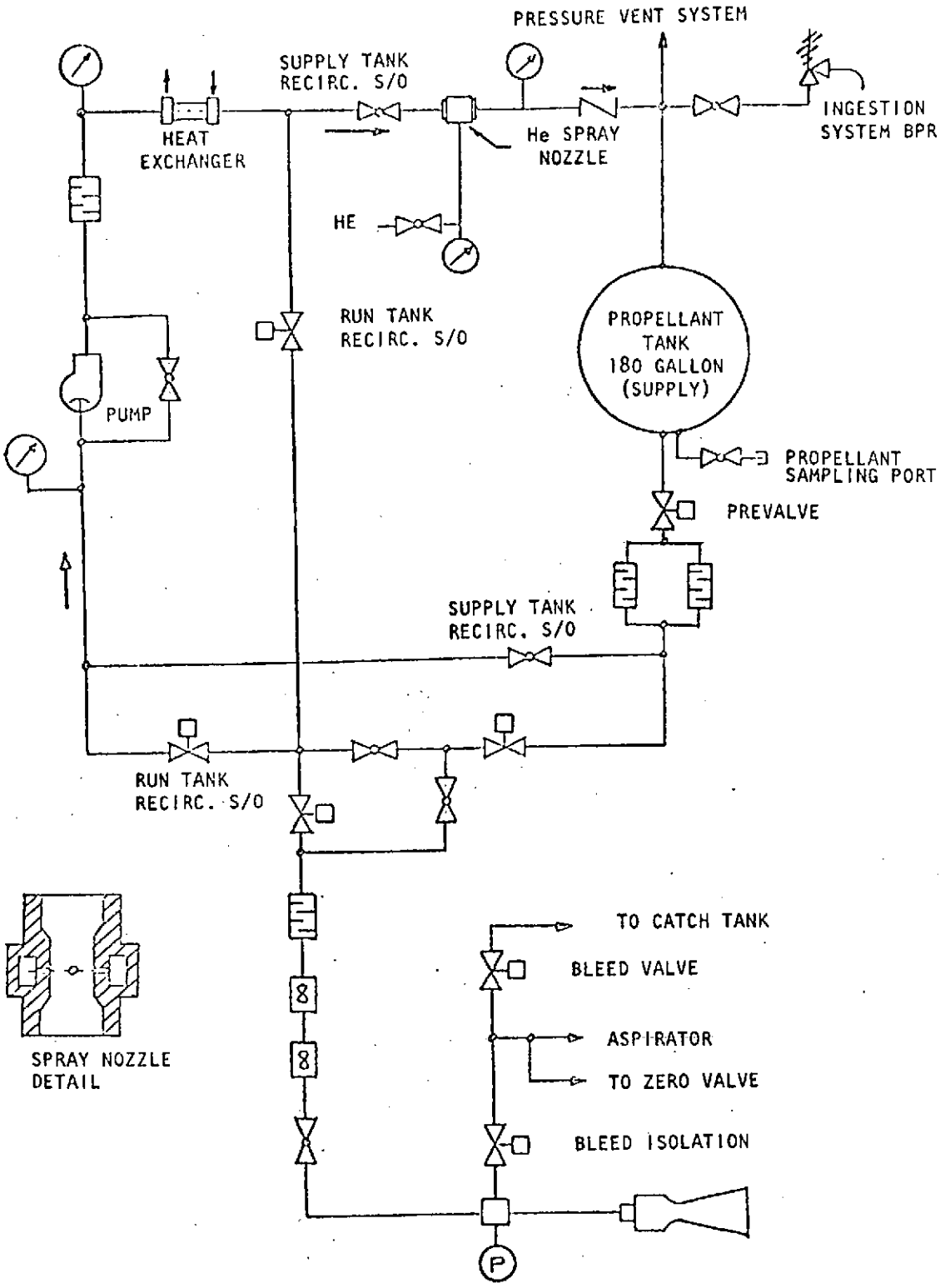

Figure A-3. Simplified Facility Ingestion System Schematic, Typical for Fuel and Oxidizer Systems

TABLE A-3. ACCELEROMETER AND STRAIN GAGE LOCATIONS FOR VIBRATION TESTING

	ACCELEROMETERS		
Axis	Accel. No.	Location	Response Axis
X	1 *	On Fixture	X
	2	On Fixture	Z
	3	On Fixture	Y
	4	On Flange	X
	5	On Flange	Y
	6	On Flange	Z
Y	1 *	On Fixture	Y
	2	On Fixture	Z
	3	On Fixture	X
	4	On Flange	X
	5	On Flange	Y
	6	On Flange	Z
Z	1 *	On Fixture	Z
	2	On Fixture	X
	3	On Fixture	Y
	4	On Flange	X
	5	On Flange	Y
	6	On Flange	Z

* Control Accelerometer

Strain Gages

Along X axis looking from nozzle end

No. 1 - on Top
No. 2 - On Left
No. 3 - On Bottom
No. 4 - On Right
(all gages 90° apart)

NOTE: See locations indicated in Fig. A-4

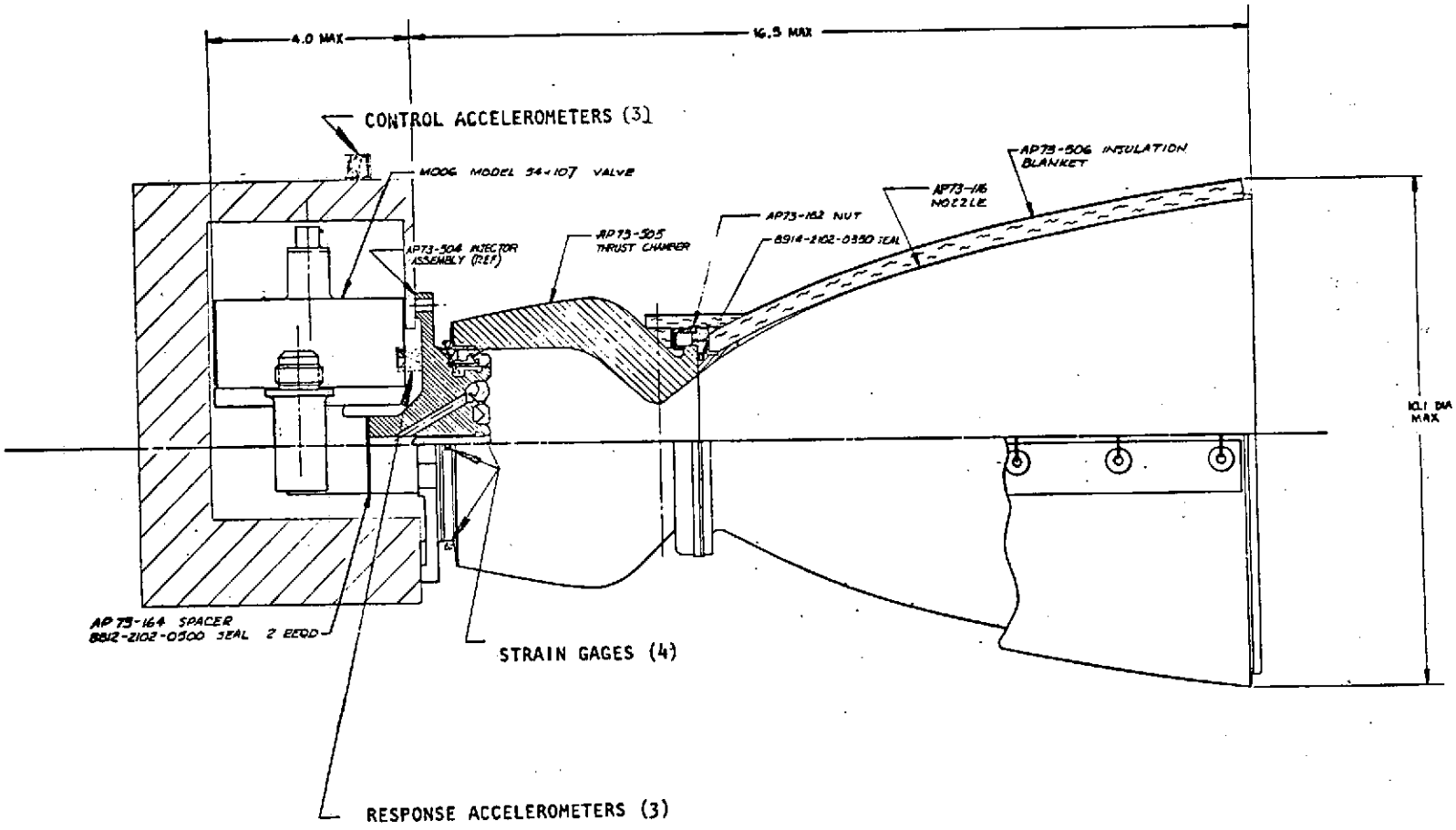

Figure A-4. Location of Accelerometers and Strain Gages on RCE for Vibration Testing

Simulated Engine Parameter Measurements

The parameters monitored during the simulator vibration testing are shown in Fig. A-5. Nine stud mounted accelerometers were attached to the test specimen; namely, three to the test fixture near the vibration input for control, three at the the simulated nozzle attachment, and three at the simulated nozzle exit.

Description of Sensors and Test Equipment Used During Engine Environmental Testing

The description of the environmental test chambers and sensing devices that were used to monitor engine and facility parameters are as described in Table A-4.

Description of Test Equipment and Sensors Used During Simulated Engine Vibration Testing

The description of the sensing devices that were used to monitor simulated engine parameters are as described in Table A-5.

Test Data Acquisition

The data record included the actual test sequence used and test conditions, including the output of the control and control monitor transducers. The test record contained a signature and date block for certification of the test data by the test engineer. Sinusoidal vibration accelerometer data were recorded on analog FM tape. The control accelerometer and the signal generator sweep frequency were recorded. Random vibration test data were recorded on analog FM tape. The control and control monitor channels and the engine response channels were recorded. The test records of the control or control monitor transducers were reviewed to verify conformance with the test requirements.

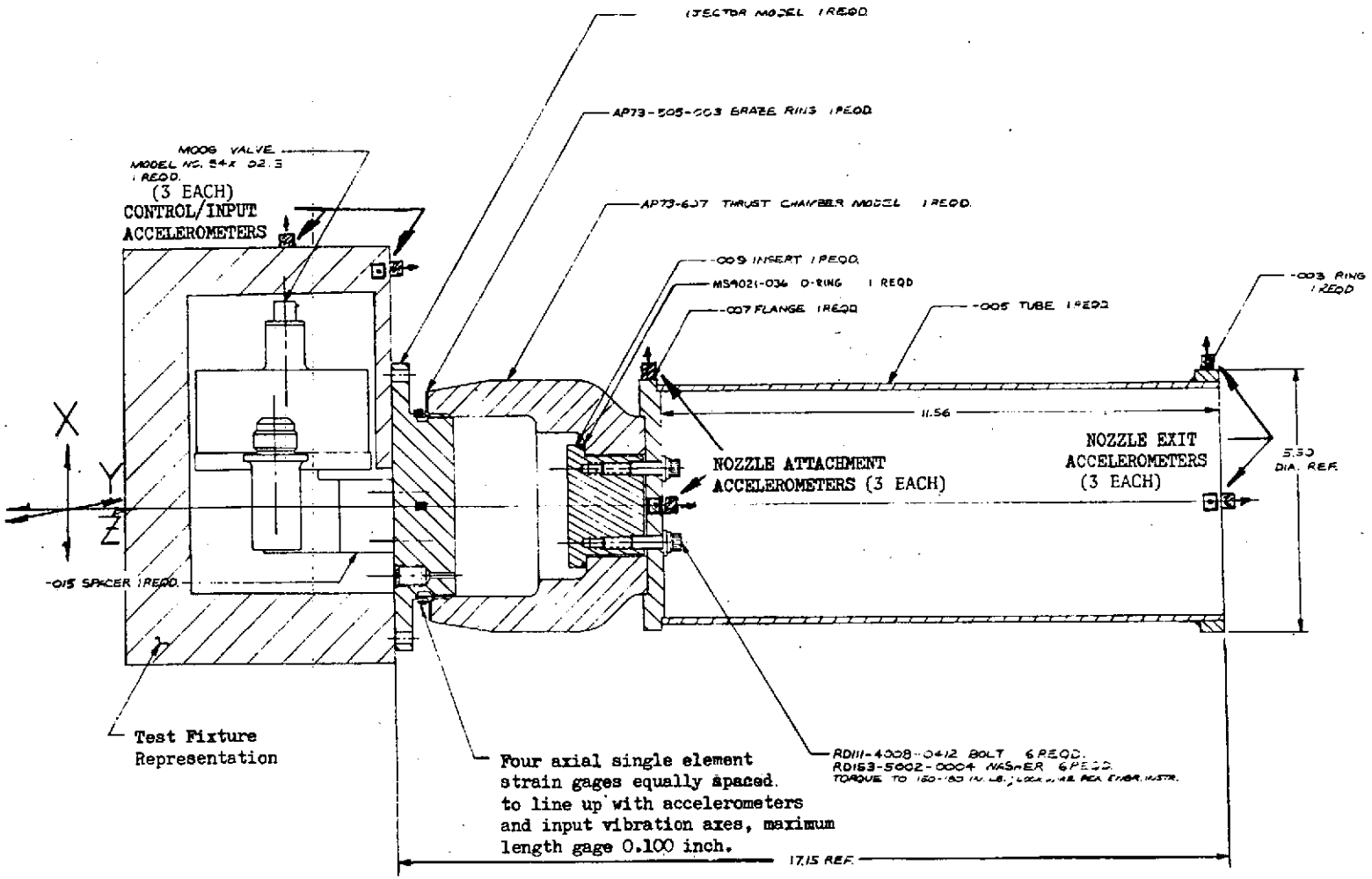

Figure A-5. 600 Pound-Thrust RCE Vibration Simulator With Accelerometer and Strain Gage Locations

TABLE A-4. TEST EQUIPMENT

Environmental Test

AETL Number	ENV502V
Instrument	Temperature Humidity Chamber
Manufacturer	Conrad, Inc.
Model Number	FD-27-3-3
Serial Number	703
Calibration Period	N/A
Range and Accuracy	-125 to +325°F, 15 to 100% RH

AETL Number	ENV561V
Instrument	Electro Hygrometer
Manufacturer	Labline Instruments, Inc.
Model Number	2200
Serial Number	0765
Calibration Period	Six months (Cal. Due 6-20-74)
Range and Accuracy	30 to 100% RH

AETL Number	ENV562V
Instrument	Temperature Recorder Controller
Manufacturer	Minneapolis Honeywell
Model Number	152C15-P-239-E-91
Serial Number	936074
Calibration Period	Six months (Cal. Due 6-20-74)
Range and Accuracy	-125 to +325°F; ±0.5%

AETL Number	ENV620V
Instrument	Salt Spray Chamber
Manufacturer	Industrial Filter
Model Number	CA1
Serial Number	S2578
Calibration Period	N/A
Range and Accuracy	Meets requirements of Federal Test Method Standard Number 151

TABLE A-4. (Continued)

AETL Number	G583V
Instrument	Salt Spray Chamber
Manufacturer	New York Blower
Model Number	L11436
Serial Number	None
Calibration Period	N/A
Range and Accuracy	--

AETL Number	P525V
Instrument	Pressure Gauge
Manufacturer	Helicoid
Model Number	None
Serial Number	None
Calibration Period	Three months (Cal. Due 5-6-74)
Range and Accuracy	0 to 60 psig; ±0.5%

AETL Number	F11L
Instrument	Flowrator
Manufacturer	Fischer & Porter
Model Number	None
Serial Number	6005C1208B1
Calibration Period	One year (Cal. Due 4-29-75)
Range and Accuracy	1.36 to 10.26 gpm; ±1.0%

4.2.2 Vibration Test

AETL Number	D512V
Instrument	Accelerometer
Manufacturer	Bruel & Kjaer
Model Number	4334
Serial Number	None
Calibration Period	Six months (Cal. Due 7-29-74)
Range and Accuracy	--

TABLE A-4. (Continued)

Vibration Test (Cont.)

AETL Number	D519V
Instrument	Servo Oscillator
Manufacturer	Spectral Dynamics
Model Number	SD114A
Serial Number	225
Calibration Period	Six months (Cal. Due
Range and Accuracy	--

AETL Number	D528V
Instrument	Accelerometer
Manufacturer	Endevco Corp.
Model Number	2246
Serial Number	None
Calibration Period	Six months (Cal. Due 5-26-74)
Range and Accuracy	--

AETL Number	D540V
Instrument	Accelerometer
Manufacturer	Endevco Corp.
Model Number	2224C
Serial Number	CP15
Calibration Period	Six months (Cal. Due 7-24-74)
Range and Accuracy	0 to 1,000 g; ±2.0%

AETL Number	D545V
Instrument	Accelerometer
Manufacturer	Endevco Corp.
Model Number	2220C
Serial Number	PA82
Calibration Period	Six months (Cal. Due 5-26-74)
Range and Accuracy	2 to 10 KHz; ±3.0%

TABLE A-4. (Continued)

Vibration Test (Cont.)

AETL Number	D597V
Instrument	Vibration Exciter
Manufacturer	M. B. Electronics
Model Number	C-126
Serial Number	1A1
Calibration Period	N/A
Range and Accuracy	10,000 force pounds

AETL Number	D623V
Instrument	Amplifier
Manufacturer	M. B. Electronics
Model Number	N4450MB
Serial Number	206
Calibration Period	N/A
Range and Accuracy	125 KVA

AETL Number	D633V
Instrument	Real Time Analyzer
Manufacturer	Spectral Dynamics
Model Number	SD301B
Serial Number	None
Calibration Period	Six months (Cal. Due 8-15-74)
Range and Accuracy	--

AETL Number	D634V
Instrument	Ensemble Averager
Manufacturer	Spectral Dynamics
Model Number	SD302B
Serial Number	None
Calibration Period	Six months (Cal. Due 8-15-74)
Range and Accuracy	--

TABLE A-4. (Continued)

Vibration Test (Cont.)

AETL Number	D651V
Instrument	Accelerometer
Manufacturer	Endevco Corp.
Model Number	2217M2
Serial Number	2809
Calibration Period	Six months (Cal. Due 3-24-74)
Range and Accuracy	±100 g; ±2.0%

AETL Number	D635V
Instrument	Accelerometer
Manufacturer	Bruel & Kjaer
Model Number	4333
Serial Number	288644
Calibration Period	Six months (Cal. Due 4-5-74)
Range and Accuracy	2 to 9 KHz; ±2.0%

AETL Number	D652V
Instrument	Accelerometer
Manufacturer	Endevco Corp.
Model Number	2224M20
Serial Number	WA08
Calibration Period	Six months (Cal. Due 3-24-74)
Range and Accuracy	±1,000 g; ±2.0%

AETL Number	D686V
Instrument	Accelerometer
Manufacturer	Bruel & Kjaer
Model Number	4333
Serial Number	401204
Calibration Period	Six months (Cal. Due 9-22-74)
Range and Accuracy	2 to 9 KHz; ±2.0%

TABLE A-4. (Continued)

Vibration Test (Cont.)

AETL Number	D3066E
Instrument	Accelerometer
Manufacturer	Bruel & Kjaer
Model Number	4335
Serial Number	177180
Calibration Period	Six months (Cal.Due 5-26-74)
Range and Accuracy	50 to 4 KHz; ±1.0%

AETL Number	D3067E
Instrument	Charge Amplifier
Manufacturer	Endevco Corp.
Model Number	2720
Serial Number	AE02
Calibration Period	Six months (Cal. Due 5-29-74)
Range and Accuracy	0 to 5,000 g; ±1.5%

AETL Number	D3069E
Instrument	Charge Amplifier
Manufacturer	Endevco Corp.
Model Number	2720
Serial Number	AE04
Calibration Period	Six months (Cal. Due 5-29-74)
Range and Accuracy	0 to 5,000 g; ±1.5%

AETL Number	D3071E
Instrument	Charge Amplifier
Manufacturer	Endevco Corp.
Model Number	2720
Serial Number	AE07
Calibration Period	Six months (Cal. Due 5-29-74)
Range and Accuracy	0 to 5,000 g; ±1.5%

TABLE A-4. (Continued)

AETL Number	D3072E
Instrument	Charge Amplifier
Manufacturer	Endevco Corp.
Model Number	2720
Serial Number	AE08
Calibration Period	Six months (Cal. Due 5-29-74)
Range and Accuracy	0 to 5,000 g; ±1.5%

AETL Number	D3074E
Instrument	Charge Amplifier
Manufacturer	Endevco Corp.
Model Number	2720
Serial Number	AE09
Calibration Period	Six months (Cal. Due 5-29-74)
Range and Accuracy	0 to 5,000 g; ±1.5%

AETL Number	D3076E
Instrument	Charge Amplifier
Manufacturer	Endevco Corp.
Model Number	2720
Serial Number	13
Calibration Period	Six months (Cal. Due 5-29-74)
Range and Accuracy	0 to 5,000 g; ±1.5%

AETL Number	D3078E
Instrument	Charge Amplifier
Manufacturer	Endevco Corp.
Model Number	2720
Serial Number	AE0-14
Calibration Period	Six months (Cal. Due 5-29-74)
Range and Accuracy	0 to 5,000 g; ±1.5%

TABLE A-4. (Continued)

Vibration Test (Cont.)

AETL Number	D3079E
Instrument	Charge Amplifier
Manufacturer	Endevco Corp.
Model Number	2720
Serial Number	AE0-15
Calibration Period	Six months (Cal. Due 5-29-74)
Range and Accuracy	0 to 5,000 g; ±1.5%

AETL Number	D3080E
Instrument	Charge Amplifier
Manufacturer	Endevco Corp.
Model Number	2720
Serial Number	AE0-16
Calibration Period	Six months (Cal. Due 5-29-74)
Range and Accuracy	0 to 5,000 g; ±1.5%

AETL Number	D3084E
Instrument	Charge Amplifier
Manufacturer	Endevco Corp.
Model Number	2720
Serial Number	AE01
Calibration Period	Six months (Cal. Due 5-29-74)
Range and Accuracy	0 to 5,000 g; ±1.5%

AETL Number	D3089E
Instrument	Accelerometer
Manufacturer	Bruel & Kjaer
Model Number	4333
Serial Number	328092
Calibration Period	Three months (Cal. Due 5-29-74)
Range and Accuracy	20 to 3 KHz; +0,-4%

TABLE A-4. (Concluded)

Vibration Test (Cont.)

AETL Number	D3094E
Instrument	Accelerometer
Manufacturer	Bruel & Kjaer
Model Number	4333
Serial Number	401195
Calibration Period	Three months (Cal. Due 4-8-74)
Range and Accuracy	20 to 3 KHz; +0,-4%

AETL Number	D3108E
Instrument	Accelerometer
Manufacturer	Bruel & Kjaer
Model Number	4333
Serial Number	401204
Calibration Period	Three months (Cal. Due 4-16-74)
Range and Accuracy	20 to 3 KHz; +1.5,-0%

AETL Number	E896V
Instrument	True RMS Voltmeter
Manufacturer	Ballantine Labs
Model Number	320A
Serial Number	6963
Calibration Period	Six months (Cal. Due 5-14-74)
Range and Accuracy	0 to 320 vrms; ±2.0%

AETL Number	E898V
Instrument	X-Y Recorder
Manufacturer	Moseley
Model Number	135
Serial Number	2231
Calibration Period	Six months (Cal. Due 7-9-74)
Range and Accuracy	--

AETL Number	None
Instrument	Control Console
Manufacturer	M. B. Electronics
Model Number	T388
Serial Number	G2656-1
Calibration Period	Prior to use
Range and Accuracy	--

TABLE A-5. SIMULATED ENGINE TEST
EQUIPMENT AND SENSORS

AETL No.	Manufacturer	Instrument
D528V	Endevco Corp.	Accelerometer, M/N 2246
D540V	Endevco Corp.	Accelerometer, M/N 2224
D545V	Endevco Corp.	Accelerometer, M/N 2246
D565V	Endevco Corp.	Accelerometer, M/N 2224
D597V	M. B. Electronics	Vibration Exciter, M/N C-126
D623V	M. B. Electronics	Amplifier, M/N 4450
D633V	Spectral Dynamics	Real Time Analyzer, M/N SD301B
D634V	Spectral Dynamics	Ensemble Averager, M/N SD302B
D635V	Bruel and Kjaer	Accelerometer, M/N 4333
D651V	Endevco Corp.	Accelerometer, M/N 2217M2
D652V	Endevco Corp.	Accelerometer, M/N 2224M20
D3067E	Endevco Corp.	Charge Amplifier, M/N 2720
D3069E	Endevco Corp.	Charge Amplifier, M/N 2720
D3071E	Endevco Corp.	Charge Amplifier, M/N 2720
D3072E	Endevco Corp.	Charge Amplifier, M/N 2720
D3075E	Endevco Corp.	Charge Amplifier, M/N 2720
D3079E	Endevco Corp.	Charge Amplifier, M/N 2720
D3083E	Endevco Corp.	Charge Amplifier, M/N 2720
D3085E	Endevco Corp.	Charge Amplifier, M/N 2720
D3094E	Bruel and Kjaer	Accelerometer, M/N 4333
D3108E	Bruel and Kjaer	Accelerometer, M/N 4333
E896V	Ballantine Labs	True RMS Voltmeter, M/N N122
E898V	Moseley	X-Y Plotter, M/N 135